

## Durham E-Theses

---

### *The application of non-linear optimisation techniques in geophysics*

Al-Chalabi, Mahboub

#### How to cite:

---

Al-Chalabi, Mahboub (1970) *The application of non-linear optimisation techniques in geophysics*, Durham theses, Durham University. Available at Durham E-Theses Online:  
<http://etheses.dur.ac.uk/8870/>

#### Use policy

---

The full-text may be used and/or reproduced, and given to third parties in any format or medium, without prior permission or charge, for personal research or study, educational, or not-for-profit purposes provided that:

- a full bibliographic reference is made to the original source
- a [link](#) is made to the metadata record in Durham E-Theses
- the full-text is not changed in any way

The full-text must not be sold in any format or medium without the formal permission of the copyright holders.

Please consult the [full Durham E-Theses policy](#) for further details.

THE APPLICATION OF NON-LINEAR OPTIMISATION  
TECHNIQUES IN GEOPHYSICS

BY

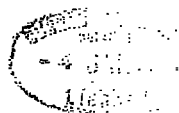
MAHBOUB AL-CHALABI

A thesis submitted for the degree  
of Doctor of Philosophy in  
the University of Durham

The copyright of this thesis rests with the author.  
No quotation from it should be published without  
his prior written consent and information derived  
from it should be acknowledged.

Graduate Society

November 1970



## C O N T E N T S

CHAPTER 1	INTRODUCTION	
1.1.	General Remarks on Programming Techniques	1
1.2.	Optimisation Techniques in Geophysics	3
1.3.	Scope of the Present Work	4
CHAPTER 2	BASIC CONCEPTS AND DEFINITIONS	
2.1.	The Concept of Optimisation in Geophysics	6
2.2.	The Objective Function	6
2.2.1.	General remarks	6
2.2.2.	Choice of the objective function	8
2.2.3.	Representation of the objective function	11
2.3.	Solutions and Minima	13
2.4.	General Procedures in Optimisation	16
2.5.	Scaling of the Problem	17
2.6.	Univariate Search	18
2.7.	Convergence	20
2.8.	Accuracy of Optimum Parameters	21
CHAPTER 3	A REVIEW OF OPTIMISATION METHODS	
3.1.	General Remarks	23
3.2.	Direct Search Methods	24
3.2.1.	Tabulation methods	24
3.2.2.	Sequential methods	25
3.2.3.	Linear methods	28
3.3.	Gradient Methods	34
3.4.	Constrained Optimisation	42
3.5.	Conclusions	49

## CHAPTER 4

AN INVESTIGATION OF NON-  
UNIQUENESS IN GRAVITY AND MAGNETIC  
INVERSE PROBLEMS

4.1.	Introduction	51
4.2.	The Case of Exact Models	53
4.3.	Influence of Anomaly Length and Number of Points	58
4.4.	Model Approximation	59
	4.4.1. Adequate models	59
	4.4.2. Inadequate models	59
4.5.	Presence of Observational Errors	66
4.6.	The Regional Background	67
4.7.	The Question of Uniqueness	68
4.8.	Discussion of Some Examples	70

## CHAPTER 5

## GRAVITY INTERPRETATION

5.1.	Introduction	75
5.2.	The Auxiliary Procedure	77
	5.2.1. Calculating the anomaly	77
	5.2.2. The objective function	79
5.3.	Available Programmes	81
5.4.	Nature of the Objective Function	83
5.5.	Method of Application	85
5.6.	Advantages and Limitations of Optimisation Methods in Gravity Interpretation	88
	5.6.1. Advantages	88
	5.6.2. Limitations	89
5.7.	Examples	89
	5.7.1. The Weardale anomaly	89
	5.7.2. Gravity "low" C - North of Scotland	91
	5.7.3. The gravity high in southeastern Minnesota	93

## CHAPTER 6

## MAGNETIC INTERPRETATION

6.1.	Introduction	95
6.2.	The Auxiliary Procedure	97
6.2.1.	Calculating the anomaly	97
6.2.2.	The objective function	99
6.3.	Available Programmes	102
6.4.	Nature of the Objective Function	103
6.5.	Method of Application	105
6.6.	Advantages and Limitations of Optimisation Methods in Magnetic Interpretation	106
6.7.	Examples	107
6.7.1.	The Solway Firth and Southern Uplands	108
6.7.2.	The English Channel anomalies	111
6.7.3.	The Moray Firth	112

## CHAPTER 7

SEISMIC AND ELECTRICAL RESISTIVITY  
EXAMPLES

## PART I

## INTERPRETATION OF SURFACE WAVE DISPERSION

7.1.	Introduction	115
7.2.	Interpretation Using Optimisation Techniques	116

## PART II

## INTERPRETATION OF APPARENT RESISTIVITY

## CURVES OVER LAYERED MEDIA

7.3.	Introduction	121
7.4.	Interpretation Using Optimisation Techniques	122

CHAPTER 8	THE FITTING OF CONTINENTAL EDGES	
8.1.	Evolution of the Concept of Continental Drift	127
8.2.	The Significance of the Fit	129
8.3.	Fitting Procedures	130
	8.3.1. General remarks	130
	8.3.2. Bases of the method	131
8.4.	Description of Programme	136
8.5.	Significance of the Position of the Pole of Rotation	138
8.6.	Examples	140
	8.6.1. The fit of Greenland to Northern Europe	140
	8.6.2. Movement between the Arabian, Nubian and Somalian plates	143
SUMMARY AND CONCLUSIONS		149
APPENDIX 1		153
APPENDIX 2		155
APPENDIX 3		160
APPENDIX 4		163
APPENDIX 5		164
PROGRAMME SPECIFICATIONS		166
REFERENCES		185

## A C K N O W L E D G E M E N T S

I would like to thank Professor G.M. Brown for providing departmental facilities. I am grateful to the Iraqi Ministry of Education and the Calouste Gulbenkian Foundation for granting me a research fellowship.

I am deeply indebted to Professor M.H.P. Bott for his kind supervision and for his concern and encouragement at all stages of the work.

I am grateful to Dr. R.A. Smith for many useful discussions and to Dr. G.M. Greig for her help and advice. I am grateful to my colleagues M.A. Hutton, A.G. McKay and K. Sundaralingam for their help and for many useful discussions and criticisms.

I wish to thank Mr. C. Moffat for the provision of many resistivity field curves. A number of optimisation subroutines were kindly provided by I.C.I. Ltd.; I am particularly grateful to Dr. D. Davies, Dr. J.A. Payne and Mr. A.K. Datta for their interest and cooperation.

All computations were carried out using the NUMAC IBM 360/67 computer.

## ABSTRACT ..

Non-linear optimisation techniques form an important subject in non-linear programming. They work by searching for an optimum of a function in the hyperspace of its variable parameters. The purpose of the present work is to test the applicability of the techniques to solving non-linear geophysical problems. A problem from each of the major branches of geophysics is considered. The problem of fitting continental edges is also considered. Direct search methods are slow but are robust and, therefore, useful in the early stages of the search. Gradient methods are fast and are efficient in the proximity of the optimum.

A gravity or magnetic anomaly due to a two-dimensional polygonal model has a unique solution in theory. In practice, ambiguity arises from the presence of several factors and takes the form of a scatter of local minima and elongated 'valleys', in the hyperspace. The solution becomes less ambiguous as the influence of these factors gets less and as more parameters in the model are specified.

The techniques are used successfully to interpret two-dimensional gravity and magnetic anomalies. Their efficiency, and flexibility make it possible to tackle a wide range of gravity and magnetic problems. The required computer time can be reduced by careful programming. The techniques are useful in interpreting surface wave dispersion data; the large degree of ambiguity associated with the problem may be overcome by specifying several parameters. A fast curve matching process is devised for interpreting apparent



resistivity curves. The method of outputting the results reduces the effect of equivalence. A method of fitting continental edges, by minimising the gaps and overlaps between them, is given. The ambiguity in the precise position of the pole of rotation is illustrated using the same concept adopted in the gravity, magnetic and seismic problems.

## C H A P T E R 1

## INTRODUCTION

1.1. General Remarks on Programming Techniques

An optimisation problem is any problem which involves the determination of the maximum or the minimum of a function of one or more variables. Such problems have been of interest to scientists since the eighteenth century and their solution was usually sought through techniques based on differential calculus. In the early 1950's, however, optimisation techniques started being developed as a major subject within the newly evolving field of operational research. Their application to meet the increasing demands of industry and commerce led to the formulation of several computational disciplines which, being accompanied by the advent of digital computers, were based on numerical methods. These are usually referred to as programming techniques.

Linear and quadratic functions subject to linear constraints are handled by techniques classed under linear programming and quadratic programming respectively. Programming techniques are not required when these functions are unconstrained since the solution of such problems is directly obtainable by straight-forward methods of differential calculus and matrix algebra.

Non-linear programming applies to problems involving non-linear functions. A formal solution to an unconstrained non-linear problem can be formulated by equating the partial derivatives of the function to zero and solving the resulting

equations. However, the use of such a procedure is not usually helpful because the resulting equations are often very difficult to solve and, if the solution can be obtained, it may represent a local optimum or a saddle point. Hence, there are several numerical algorithms to treat the unconstrained non-linear problem.

Non-linear programming further includes multi-stage decision processes known as dynamic programming. It also includes the treatment of problems with linear or quadratic functions subject to non-linear constraints (Fig. 1.1)

Many linear and non-linear problems require the additional constraint that the variables should only assume integer values. Techniques dealing with these problems are covered by integer programming. When only some of the variables must be integers, the problem is a mixed programming problem.

However, the classification of programming techniques tends to vary with usage. Fig. 1.1 does not, therefore, bear a relation to a specific author. It represents a summary of the foregoing account and illustrates the relation of non-linear optimisation techniques to the other programming techniques.

The term non-linear optimisation techniques refers to the methods of treating problems with non-linear functions, constrained or unconstrained. It constitutes our subject matter and must not be confused with the wider and more general problem of non-linear programming.

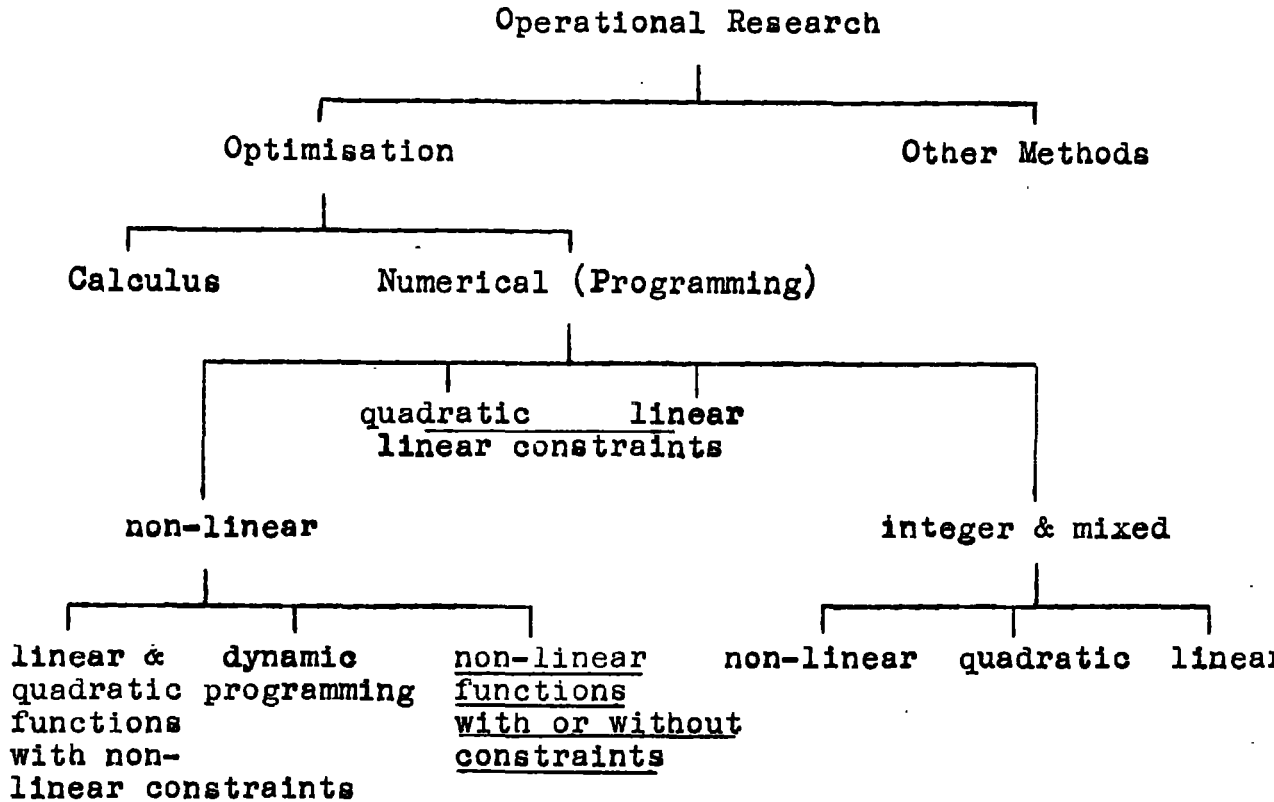


Fig. 1.1. A general sketch illustrating the place of non-linear optimisation techniques (underlined) in relation to other programming methods.

1.2. Optimisation Techniques in Geophysics

Optimisation techniques are currently employed in the mineral industry in various chemical, economic and management problems (Klimpel, 1969). However, their use in geophysics has been limited to individual methods, such as that of steepest descent and the method of alternating variables (see Chapter 3), rather than their application as a whole integrated group of programming disciplines. The work of Stacey (1965) was the first real application of non-linear optimisation techniques in geophysics. He employed them to interpret gravity and magnetic anomalies although progress

was limited by the low speed of available computers and by difficulties caused by local minima. This was followed by the work of Butler (1968) who successfully applied the techniques to the interpretation of magnetic anomalies due to dykes.

The importance of non-linear optimisation techniques in geophysics is due to the very large number of non-linear geophysical problems; the high efficiency of these techniques makes it now possible to tackle problems which have proved intractable in the past. The demand for linear programming techniques appears to be less pronounced, since most problems tend to have simple or no constraints so that linear problems become amenable to treatment by simple algebraic methods.

There are many problems demanding the use of other types of optimisation techniques. For example, integer or mixed programming would be desirable to determine layer thicknesses in resistivity problems where thicknesses are usually given as integer multiples of the thickness of the top layer. However, the treatment of such problems falls outside the scope of our present topic and are not pursued further. We shall, therefore, use the term optimisation to imply non-linear optimisation, unless otherwise indicated.

### 1.3. Scope of the Present Work

The present work deals with the application of optimisation techniques to selected problems in gravity, magnetic, seismic, and electric methods, thus obtaining a general coverage of the main methods in applied geophysics. The problem of fitting

continental edges is used as an example of a subject not directly related to applied geophysics. The work also deals with the use of optimisation techniques for investigating the non-uniqueness problem in gravity and magnetic interpretation.

The work on the seismic and the electric problems was somewhat less thorough than in the case of the other problems. The entire work, however, provides a general guide to the method of utilising and applying optimisation techniques in geophysics and also demonstrates the potentialities of these techniques as a tool for tackling many geophysical problems.

The direct concern of the work was to use rather than to devise methods of optimisation. It was, therefore, necessary to rely on external sources for optimisation subroutines. The use of any optimisation method was, hence, subject to the availability of the relevant computer subroutine. Although this was occasionally undesirable, it did not present any problem. A good variety of subroutines were actually available, all of which were among the most efficient methods of optimisation.

The problems treated in this work are essentially interpretational. It is clear, however, that programming techniques have an equally promising field of application in various design, processing, planning and other problems in geophysics. Future work will, undoubtedly, show increasing signs of such application as the importance of optimisation techniques become more generally realised.

## CHAPTER 2

## BASIC CONCEPTS AND DEFINITIONS

2.1. The Concept of Optimisation in Geophysics

The use of optimisation techniques in geophysics may be described in the following manner: Given a set of geophysical data that may be attributed to certain properties of a particular system defined by  $m$  adjustable parameters ( $m = 1, 2, \dots$ ) and  $u$  unadjustable parameters ( $u = 0, 1, 2, \dots$ ), it is required to modify the adjustable parameters until the relevant output data of the system agree with the input geophysical data within certain requirements. No change in the system topology is allowed during the adjusting process.

The input data may take the form of an observed anomaly or some ideal behaviour or performance. The output data are the corresponding calculated anomaly or behaviour of the system. The system is usually in the form of a model. The requirements frequently include the condition that the data must be satisfied within the range of observational errors. Other requirements vary according to individual problems but usually include a number of constraints to ensure the physical or geological feasibility of the optimum model.

2.2. The Objective Function

## 2.2.1. General remarks

All optimisation procedures work by minimising or maximising a single scalar quantity called the objective function (or the function). The objective function depends upon the adjustable parameters  $\underline{x}$  defined by

$$\underline{x} = \begin{bmatrix} x_1 \\ x_2 \\ \cdot \\ \cdot \\ x_m \end{bmatrix} \quad (2.1)$$

At any particular  $\underline{x}$ , the objective function gives a measure of the agreement between the input and output data, i.e. the degree of optimality of the system.

In geophysical work, it is usually more convenient to express the objective function in terms of the discrepancy between the input and output data. The discrepancy in each of the values being compared is measured using a discrepancy function  $\phi(\underline{x}, \xi)$ , where  $\xi$  is a parameter along which the input data are distributed. Hence, the objective function is defined by

$$f(\underline{x}) = \int_b \phi(\underline{x}, \xi) \cdot w(\xi) \, d\xi \quad (2.2)$$

where  $b$  is the range along which the input data are given and  $w$  is an appropriate weighting function which makes it possible to lay different emphasis on different parts of the data.

Input geophysical data are normally given as a set of discrete observations. The objective function is, therefore, more conveniently represented by

$$f(\underline{x}) = \sum_{i=1}^n \phi(\underline{x}, \xi_i) \cdot w(\xi_i) \quad (2.3)$$

where  $n$  is the number of input data points. In order to obtain a representative optimum system,  $n$  must be larger than  $m$ .

Because one is generally dealing with discrepancies optimisation of a system requires the minimisation of the objective function. For this reason the term optimisation will be used synonymously with minimisation throughout the text. Individual cases requiring maximisation can be



readily dealt with by changing the appropriate signs in the optimisation procedure.

To illustrate the above scheme, consider an observed gravity anomaly,  $A$ , attributed to a subsurface anomalous mass system represented by a model. Suppose that the depth to the top of the mass is known as well as the regional background associated with the anomaly. These are the unadjustable parameters. The other coordinate points defining the model and the density contrast are the adjustable parameters  $\underline{x}$ . If  $n$  observation points have been made along the profile, all of which are equally good, then each point could be given an equal weight. Suppose now that a trial model, having its top at the known depth, be used to represent the anomalous mass. The discrepancy function at the  $i^{\text{th}}$  observation point may be defined by the absolute difference between the calculated anomaly,  $c$ , due to the model and the observed anomaly, i.e.

$$\phi(\underline{x}, \xi_i) = |A_i - C_i| \quad (2.4)$$

where  $\xi_i$  is the distance of the  $i^{\text{th}}$  point along the profile from some arbitrary origin.

The objective function  $f(\underline{x})$  for that trial model is the sum of the  $n$  discrepancy functions defined by equation (2.4). The optimisation procedure attempts to generate a model which yields the lowest possible value of  $f(\underline{x})$  by adjusting the  $m$  adjustable parameters under certain constraints that ensure its geological feasibility.

### 2.2.2. Choice of the objective function

A fully adequate objective function is essential for

obtaining a good solution. Maximum care should, therefore, be taken when choosing the objective function. Because a correct choice of the objective function is dependant upon a suitable choice of the discrepancy function, an effective measure of discrepancy must be first established. However, this is normally quite straight-forward and assumes forms similar to that of equation (2.4).

In some problems the discrepancy function may not be immediately obvious. Suppose in the above example that we wish to optimise the function independently of the regional background (assuming that it is horizontal). This could be achieved by basing the objective function on

$$\phi(\underline{x}, \xi_1) = |(A_1 - A_0) - (C_1 - C_0)| \quad (2.5)$$

where  $A_0$  and  $C_0$  are the observed and calculated anomaly values at an arbitrary point.

In some optimisation problems more than one acceptable discrepancy criteria can be used. The choice of the criterion to be used will usually depend upon the form of the data, the main purpose of the problem, the computation time available, etc. An example of this is given in Chapter 8 where the misfit between continental edges may be measured by the area of gaps and overlaps or, alternatively, by the difference in longitude between equivalent points on both edges.

The relation between the objective function and the discrepancy criterion has to be defined. The choice is usually between expressing the objective function as the sum of squares of discrepancies or expressing it as the sum of absolute values of discrepancies. The first of these is more

widely used and is particularly useful when the distribution of observational errors is normal.

However, the distribution of errors may not, in some cases, be normal. To test how critical the choice of the objective function was, some experimentation was carried out. The gravity anomaly due to a polygonal model was computed and pseudo-random errors were superimposed on the anomaly. Different solutions were obtained by optimising three different objective functions defined by the following

$$f_1 = \sum_{i=1}^n (|A_i - C_i|)^{\frac{1}{2}} \quad (2.6a)$$

$$f_2 = \sum_{i=1}^n |A_i - C_i| \quad (2.6b)$$

$$f_3 = \sum_{i=1}^n (A_i - C_i)^2 \quad (2.6c)$$

In terms of approximating the original model, and in producing minimum residuals, procedures using  $f_1$  were invariably inferior to those using  $f_2$  or  $f_3$ . However, there was no significant difference between using  $f_2$  and  $f_3$ .

In view of the limited amount of experimentation, the above results are by no means conclusive; they were accepted as being only provisionally true. Moreover, functions in the form of  $f_3$  lend themselves readily to a linear treatment of the density and magnetisation contrasts and the regional background, as will be demonstrated later. For these reasons, objective functions expressed as the sum of squares of residuals were employed in most interpretations presented in this work.

Several other rules concerning the correct choice of an objective function may be found in the literature.

Two relevant rules given by Wilde (1964, p.6) are:

1. Prefer a representation which can be approximated by a low degree Taylor series expansion in the vicinity of the optimum.

2. Prefer a representation in which the variable parameters do not interact, i.e. they can be separated in different terms.

A further rule concerning scaling will be discussed in section 2.5.

### 2.2.3. Representation of the Objective function

#### 2.2.3.1. Geometric representation

The objective function may be represented geometrically in an  $m$  - dimensional space by constructing a Euclidean hyperspace in which each of the  $m$  mutually orthogonal axes represents one variable parameter. In such a hyperspace the objective function is then completely representable by means of contours of equal value. The geometrical representation is important in studying and understanding the behaviour of the objective function qualitatively in order to adopt an appropriate strategy for tackling a given problem. These geometrical studies also proved important in demonstrating a number of phenomena relating to the ambiguity of gravity and magnetic fields as will be shown in Chapter 4.

The contour surfaces of the objective function may be conceived as behaving in the same manner as topographical contours. The use of topographic terms like peaks, troughs

and valleys will, therefore, be extended into the multi-dimensional space. Two-dimensional cross-sections (or maps) of these contours provide a convenient method for a direct visual inspection of the hyperspace (e.g. Figs. 4.1, 5.2, etc.).

Geometrical intuition will usually help to pass the cross-section through the required points in the hyperspace. Only plane cross-sections were used in the present work but other forms of sectioning can be used if required. When the objective function depends upon two variables only, a two-dimensional map of the function in the space of the two variables provides a complete representation in the mapped range. The solution(s) may then be located and their validity assessed visually.

### 2.2.3.2. Mathematical representation

The local behaviour of the objective function is best studied with the aid of an  $m$  - dimensional Taylor series expansion

$$f(\underline{x} + \underline{\delta}) = f(\underline{x}) + \sum_{j=1}^m \frac{\partial f}{\partial x_j} \delta_j + \frac{1}{2} \sum_{j=1}^m \sum_{k=1}^m \frac{\partial^2 f}{\partial x_j \partial x_k} \delta_j \delta_k + \dots \quad (2.7)$$

where  $\delta_1, \delta_2, \dots, \delta_m$  are the components of parameter changes along each of the  $m$  mutually orthogonal axes  $x_1, x_2, \dots, x_m$ , respectively.  $\underline{\delta}$  is thus an  $m$  - dimensional vector given by

$$\underline{\delta} = \begin{bmatrix} \delta_1 \\ \delta_2 \\ \vdots \\ \delta_m \end{bmatrix} \quad (2.8)$$

In the vicinity of the optimum, where the objective function

can be usually approximated by a quadratic, higher terms in equation (2.7) can be neglected. Adopting a matrix notation the truncated Taylor series is given by

$$f = f_0 + \underline{G}' \underline{\delta} + \frac{1}{2} \underline{\delta}' H \underline{\delta} \quad (2.9)$$

where the prime indicates matrix transposition and

$$\underline{G} = \begin{bmatrix} \partial f / \partial x_1 \\ \partial f / \partial x_2 \\ \vdots \\ \partial f / \partial x_m \end{bmatrix} \quad (2.10)$$

$$H = \begin{bmatrix} \partial^2 f / \partial x_1 \partial x_1 & \dots & \partial^2 f / \partial x_1 \partial x_m \\ \vdots & & \vdots \\ \partial^2 f / \partial x_m \partial x_1 & \dots & \partial^2 f / \partial x_m \partial x_m \end{bmatrix} \quad (2.11)$$

H is also known as the Hessian matrix.

Equation (2.9) is the basis for many optimisation procedures. It often gives a sufficiently accurate description of the behaviour of the objective function in regions which are not necessarily close to the optimum.

### 2.3. Solutions and minima

An ideal optimum solution is obtained when the optimum parameters define a system which is an exact solution to the problem. Equation (2.2) becomes

$$f(\underline{x}) = \int_b \phi(\underline{x}, \xi) \cdot w(\xi) d\xi = 0 \quad (2.12)$$

Such conditions are rarely realised in practice. The problem becomes that of searching for the minimum of  $f(\underline{x})$  in the  $\underline{x}$  hyperspace.

Formally, the minimum in an unconstrained problem must satisfy

$$\frac{\partial f}{\partial x_1} = \frac{\partial f}{\partial x_2} = \dots = \frac{\partial f}{\partial x_m} = 0 \quad (2.13)$$

A sufficient condition when equations (2.13) are satisfied is that the principal minors of the Hessian matrix must all be positive (Box et al, 1969, p.5).

When the problem is constrained the necessary condition for a minimum can be found by the method of Lagrangian multipliers.

A more useful definition for the present work is that a minimum exists at  $\underline{X}$  if it satisfies

$$f(\underline{X}) \leq f(\underline{X} + h\underline{x}) \quad (2.14)$$

in the neighbourhood of  $\underline{X}$ , for all sufficiently small values of  $h$ .

Before a minimum can be regarded as a solution it must satisfy the requirement that it falls within a feasible region. Other requirements usually include the condition

$$f(\underline{X}) < \epsilon \quad (2.15)$$

where  $\epsilon$  is a specific tolerance determined by the magnitude of observational errors.

Definitions of the relevant terms used in this work are as follows:

1. The coordinates of the solution point  $\underline{X}$ , in the  $\underline{x}$  hyperspace, define the parameters of an optimum system. The terms solution, minimum and optimum model will, therefore, be used synonymously when appropriate.

2. A global minimum in a given feasible region  $R$  is the required overall solution in  $R$ .

3. A local minimum is any minimum other than the global minimum.

4. If only one minimum exists in  $R$  then  $f(\underline{x})$  is unimodal in  $R$ . If more minima exist then  $f(\underline{x})$  is multimodal in  $R$ . Therefore, if a global minimum and one or more local minima exist, the solution is unique in  $R$  although  $f(\underline{x})$  is multimodal.

5. The contours defining some minima do not close in all directions. These minima are not true minima and will only behave as such in some directions. They are called ill-defined minima. The term may also be extended to describe minima which are extremely shallow. Clearly, the distinction between an ill-defined and a well-defined minimum is gradational.

The following rules were used throughout:

1. Although a solution exists, a global minimum may not exist. Solutions are then given by two or more local minima in the feasible region. Therefore, if  $R$  includes the entire feasible region, the solution in  $R$  is not unique. This situation arises in many geophysical problems, e.g. in gravity and magnetic interpretations. In these cases, it is more convenient to refer to all points in a region (or regions) bounded by a contour of magnitude  $e$  as possible solutions.

2. In the absence of a global minimum, not every local minimum in  $R$  is necessarily a possible solution, as the requirements for a solution may not be satisfied.

3. A minimum possessing a lower function value than another minimum is not necessarily a better solution. A minimum possessing the least function value is not necessarily a global minimum.



## 2.4. General Procedures in Optimisation

All optimisation procedures (except tabulation methods) start the search for a minimum by evaluating the objective function at a given initial point,  $\underline{x}_0$ . The adjustment of parameters is carried out iteratively by generating the points  $\underline{x}_1, \underline{x}_2, \dots$  such that

$$f(\underline{x}_{i+1}) < f(\underline{x}_i) \quad i = 0, 1, 2, \dots \quad (2.16)$$

with

$$\underline{x}_{i+1} = \underline{x}_i + h_i \underline{d}_i \quad (2.17)$$

where  $h_i$  is the distance moved along the  $m$ -dimensional direction vector,  $\underline{d}_i$ .

The choice of  $h_i \underline{d}_i$  at each iteration, i.e. the manner in which the successive  $\underline{x}$  points are generated, is the feature that distinguishes the various optimisation methods from each other. It also influences the efficiency of each method in adapting its strategy to meet certain situations.

To comply with the iterative rule of equations (2.16) and (2.17), the optimisation process must consist of two essential parts. The first part is a procedure which furnishes the value of the objective function for a given set of parameters  $\underline{x}_i$ . This part is usually in the form of an auxiliary programme which computes  $f(\underline{x}_i)$  using, generally, a method based on equation (2.3). The second part is the optimisation subroutine or procedure which, given  $f(\underline{x}_i)$  and  $\underline{x}_i$ , will search to locate the point  $\underline{x}_{i+1}$  that satisfies equation (2.16). In doing so, it may pass the current  $\underline{x}$  parameters to the auxiliary procedure a number of times.

The process of generating new points according to

equation (2.17) continues using, possibly, many previous informations about the behaviour of the function. The two parts of the optimisation process are thus enclosed in a major feedback loop until the search is terminated by some convergence criterion.

Fig. 2.1 shows a simplified flow chart summary of this process.

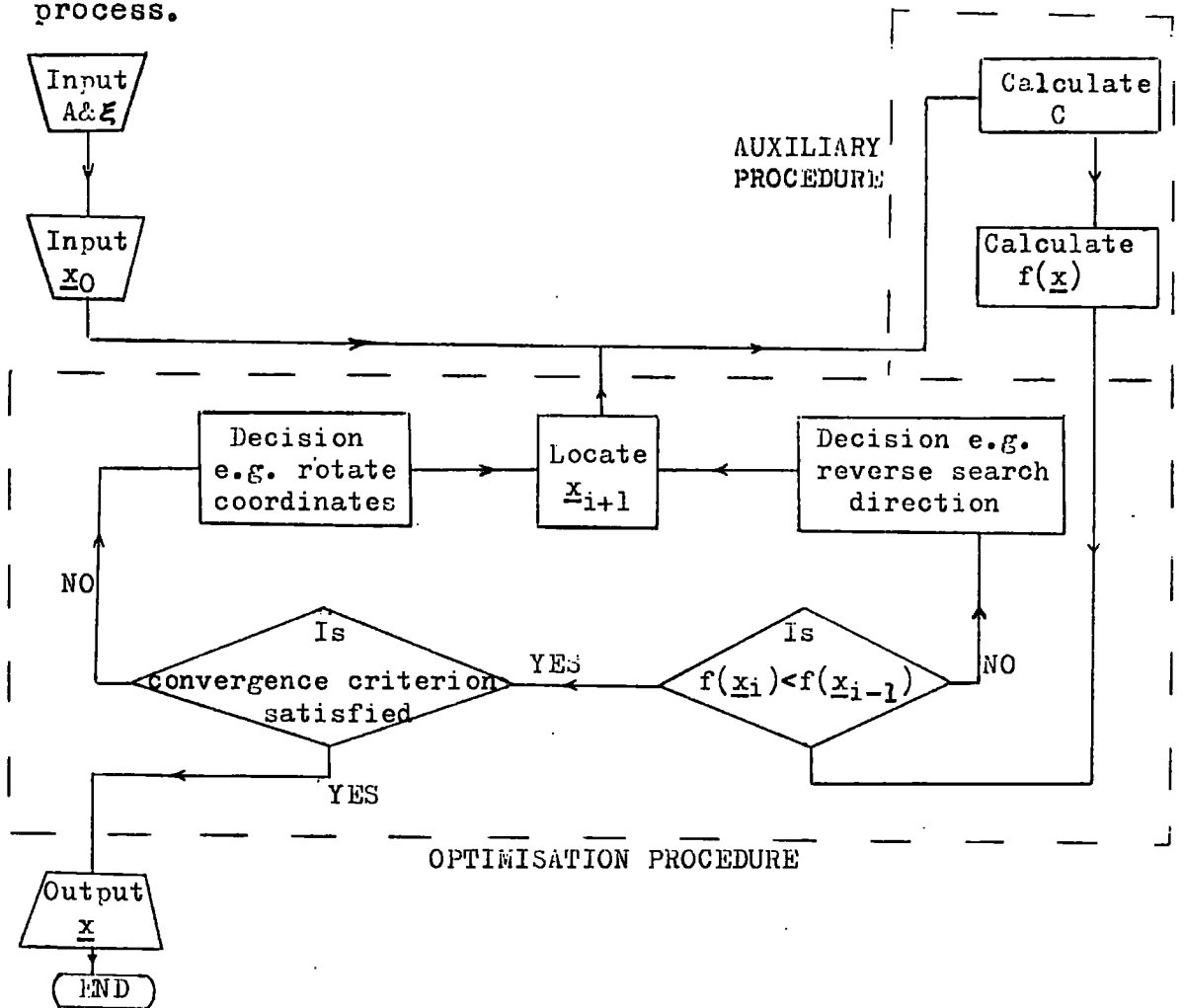


Fig. 2.1. A schematic representation of the general iterative optimisation procedure.

## 2.5. Scaling the Problem

A well scaled problem is one in which the contours of the objective function are approximately hyper-spherical or they are elongated parallel to most search directions. Good scaling is desirable in all problems because it enables most

optimisation methods to obtain a solution rapidly and accurately.

The change of scale implies a change in the measurement units of individual parameters. However, when the contours of the objective function are elongated in directions which are inclined to the parameter axes (Fig. 2.2.B), a change in the units will only change the angle at which these directions are inclined. This may improve the conditioning of some problems but requires a detailed study of the behavior of the function. Experiments on gravity problems, where the objective function is usually very curved, showed that changes in the measurement units were incapable of improving the scaling of the problem.

A better strategy would be to do the inverse, i.e. to transform the search axes so that they lie favourably with respect to the objective function in the hyperspace (Fig. 2.2). Some optimisation methods are based on this transformation. The success of Rosenbrock's method (section 3.4.3) in dealing with gravity and magnetic methods is due mainly to its capability to rotate the search axes according to the general trend of the objective function.

## 2.6. Univariate Search

In order to carry out the optimisation process in accordance with equation (2.17) many optimisation methods work by locating a minimum along each of a series of directions in the hyperspace of the variable parameters. Each of these searches is equivalent to a univariate search, i.e. to

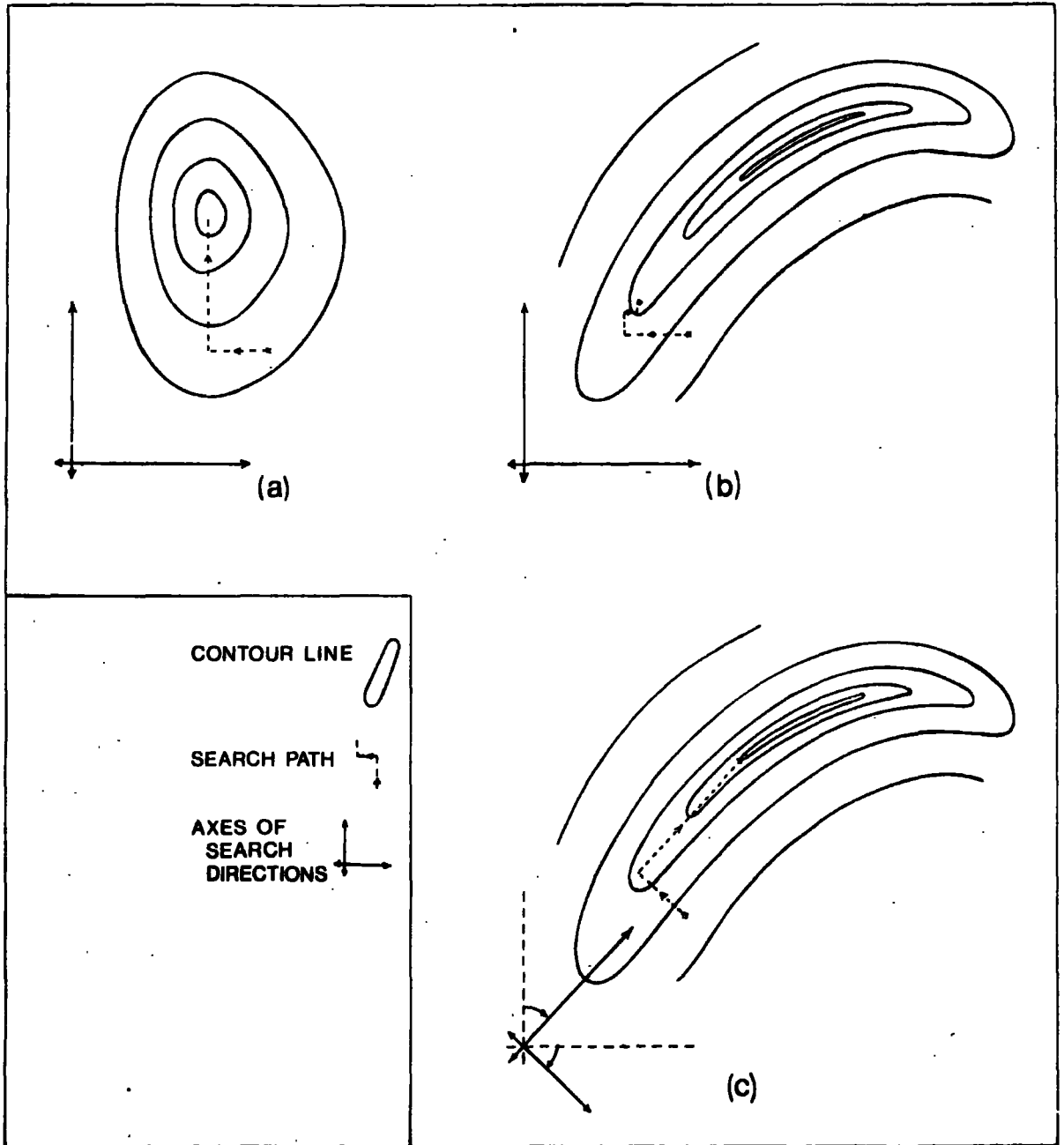


Fig. 2.2. A two-dimensional illustration of the scaling problem.

(a) A well-scaled problem.

(b) A badly-scaled problem.

(c) Rotating the search axes to improve effective scaling.

searching for the optimum of a function of a single variable. Univariate search methods are, therefore, basic to most optimisation techniques. The fundamental procedures involved in them are given below.

The older types of univariate search attempt to obtain the minimum to a certain accuracy after a specific number of iterations. The dichotomous search involves the reduction of a large interval,  $T$ , which is known to contain the minimum, by successive function evaluations at points placed symmetrically inside each new  $T$ . Fibonacci search depends upon the use of Fibonacci numbers to decide the manner in which the successive  $T$  intervals are reduced. Search by golden section selects the searching intervals symmetrically inside  $T$  in a manner known geometrically as a golden section. These methods are described fully by Wilde and Beightler (1967, p.215-267).

In recent methods, the minimum is found by processes involving the fitting of low order polynomials through a number of points. These methods, being more efficient, are gradually replacing the older types. However, they lack the advantage of being able to guarantee to locate the minimum in a given number of iterations. They depend basically upon evaluating the function at several points along a given direction and use some criterion to indicate that the minimum has been straddled. The points straddling the minimum are then used either for quadratic interpolation, as in the algorithm of Powell and that of Davies, Swann and Campey or for cubic interpolation, as in Davidon's method

(Box et al, 1969, p.14 and 39). There are many other methods both old and recent but the bases are similar to those described above.

The transition from a univariate search to an actual problem involving many variables is not just one of degree. Difficulties resulting from the use of a large number of variables have become popularly known as the "curse of dimensionality" (Wilde and Beightler, 1967, p.279). In geophysics, this curse takes several forms. For example, as the number of variables is increased, many ill-defined local minima begin to appear in a complex fashion causing the problem to be ill-conditioned. The vastness of the hyper-volume of a multi-dimensional space is another difficulty which causes a thorough search of even a small fraction of the hyperspace to be a formidable task.

## 2.7. Convergence

Most optimisation methods gradually reduce the step  $h_1$  (equation 2.17) in the vicinity of the minimum until some conditions, called the convergence criteria, are satisfied. The search is then said to have converged at the minimum. Depending on the method, the convergence criteria may usually be satisfied when either  $f(\underline{x}_{i+1}) - f(\underline{x}_i)$  or  $f(\underline{x}_i)$  falls below some specific value or after a given number of iterations. Convergence will therefore refer to locating the minimum within these conditions.

If the problem is rather ill-conditioned, and particularly when using a method which is unsuitable for the objective function being handled, a rapid reduction in  $h_1$  can take place

without necessarily being in the vicinity of any minimum. This causes an erroneous termination of the search and will, here, be called local convergence. It must not be confused with converging at a local minimum.

A large number of optimisation methods are based on the quadratic approximation of equation (2.9) and will, therefore, locate the minimum of a quadratic function in a specified number of iterations. Such methods are described as quadratically convergent. Because most functions closely approximate a quadratic in the vicinity of the minimum (Box et al, 1969 p.28), quadratically convergent methods are of particular interest in optimisation techniques.

## 2.8. Accuracy of Optimum Parameters

It may be sometimes desirable to obtain an estimate of the possible error in each variable parameter, at the optimum, in terms of the residuals between the observed and the calculated data. However, a very low value of the objective function at the optimum is not necessarily an indication that the values of optimum parameters are accurate since the observed data are themselves subject to many sources of error. To obtain an estimate for the parameter accuracy, in terms of observational errors and the residuals, is a very difficult task. To simplify the procedure, we assume that the observational errors are wholly accounted for by the residuals at the optimum. This is usually only partially true. Furthermore, we assume that the system being optimised is fully defined by the parameters. This is again frequently untrue. For example, in gravity and

magnetic interpretations, the number of parameters required to represent the anomalous body fully is far too large to be handled practically. Moreover, the corner points of the representative polygonal model are dummy parameters which do not have an actual physical standing. In view of these gross assumptions plus the many approximations made by the model itself, the estimates of parameter accuracy are sometimes of limited significance.

The parameter accuracy may be obtained as follows:

The variance of parameter  $x_i$  is  $\bar{\sigma}^2 p_{ii}$  Hence,

$$x_i = \bar{x}_i \pm a \bar{\sigma} \sqrt{p_{ii}} \quad (2.18)$$

where

$\bar{x}_i$  is the value of parameter  $x_i$  at the optimum,

$a$  is the confidence factor (= 1.96 for 95% confidence),

$p_{ij}$  is the element of the inverse matrix of second partial derivatives of the objective function with respect to the variable parameters,

$\bar{\sigma}^2$  is the estimate of the residual variance,

i.e.  $\bar{\sigma}^2 = s^2 / (n-m)$  where  $s^2$  is the sum of squares of residuals at the optimum. The term  $n-m$  represent the degrees of freedom of the problem.

The covariance of parameters  $x_i$  and  $x_j$  is  $\bar{\sigma}^2 p_{ij}$ . The method of derivation and the procedures involved in computing these estimates are given in Appendix 1.



## C H A P T E R 3

## A REVIEW OF OPTIMISATION METHODS

3.1. General Remarks

This review discusses the general suitability of various optimisation methods for solving geophysical problems. Only those methods which have a direct relevance or were actually used in the present work are described in some detail. A fuller account of optimisation methods may be found in several books (e.g. Wilde and Beightler, 1967; Box et al, 1969).

A large number of optimisation methods have been introduced during the past fifteen years. Nomenclature and classification of these methods vary according to whatever criteria are considered appropriate by different authors. For example, Box et al (1969, p.16) call tabulation methods what Wilde and Beightler (1967, p.222-230) class as simultaneous methods. Rosenbrock and Storey (1966, p.58) regard the method of steepest descent as distinct from gradient methods while Wilde (1964, p.107) regards them as synonymous.

The classification of Box et al (1969) is the most consistent for the purpose of the present work and is, therefore, adopted throughout the text. It appears to be a modification of an older classification introduced by Spang (1962). Accordingly, optimisation methods are divided into two major categories:

(1) Direct search methods are methods which do not require the explicit evaluation of any partial derivatives of

the objective function in carrying out the search for an optimum. They are divided into three classes: (a) tabulation methods, (b) sequential methods and (c) linear search methods.

(2) Gradient methods include a whole series of methods which use first order or higher partial derivatives of the objective function with respect to the independent variables, in selecting the direction of search  $\underline{d}_1$  as defined by equation (2.17).

Several of these methods may be adapted so that the search is carried out subject to  $s$  inequality constraints in the form

$$t_i(\underline{x}) \geq 0 \quad i = 1, 2, \dots, s \quad (3.1)$$

or  $r$  equality constraints in the form

$$q_j(\underline{x}) = 0 \quad j = 1, 2, \dots, r \quad (3.2)$$

### 3.2. Direct Search Methods

#### 3.2.1. Tabulation methods

These methods proceed by evaluating the objective function at a pre-determined set of points at various intervals in the hyperspace of the variable parameters. These points define a region within which the minimum  $\underline{x}$  is assumed to lie so that

$$L_i \leq x_i \leq U_i \quad i = 1, 2, \dots, m \quad (3.3)$$

where  $L_i$  and  $U_i$  are, respectively, the lower and upper bounds of the  $i^{\text{th}}$  parameter. The point giving the lowest function value is assumed to be the minimum.

Tabulation methods require a large number of function evaluations so that their use must be restricted to special circumstances. Among methods included are:

##### 3.2.1.1. Grid method

The minimum is approximately located by dividing each variable parameter into  $B_1 = (U_1 - L_1) / b$  intervals where  $b$  is chosen to give an acceptable spacing. The objective function is then evaluated at each of the

$$M = (B_1 + 1) (B_2 + 1) \dots (B_m + 1) \quad (3.4)$$

nodes of the resulting "hyper-grid".

The grid method becomes very useful if the problem can be transformed so that the number of variables is reduced to two or three. The method of fitting continental edges (Chapter 8) makes use of a two-dimensional grid. It was also found that the method provides an efficient way for curve matching. The method has, therefore, many possible applications in geophysics and has already proved valuable in interpreting electric resistivity data (Chapter 7).

#### 3.2.1.2. Random search methods

The objective function is evaluated at points whose coordinates in the  $x$  hyperspace are chosen at random. These methods have had some geophysical applications in the past, usually by generating a series of models by Monte Carlo procedure (e.g. Press, 1968). However, statistical considerations show them to be less efficient than the grid method (Spang, 1962).

#### 3.2.2. Sequential methods

In its strict sense, the term applies to those methods which are based on the evaluation of the objective function at the vertices of some geometric configuration in the hyperspace of the variable parameters, with an eventual shrinkage of the configuration about the minimum.

With these configurations, sequential methods enjoy a powerful strategy in being able to move out of local minima that possess higher function values than neighbouring ones. They are, therefore, suited to problems involving a large number of local minima.

Sequential methods may appear to be an obvious choice for many geophysical problems because of their multi-modal nature. However, a local minimum with a higher function value than a neighbouring one is not necessarily a worse solution. Moreover, undulations in the contours of the objective function caused by observational errors may be largely smoothed out when a form similar to equation (2.6c) is used. Sequential methods are much slower than many linear methods and their choice should, therefore, depend on the merit of each individual problem.

3.2.2.1. The simplex method (Spendly, Hext and Himsworth, 1962), modified by Campey and Nickols (1961) and by Nelder and Mead (1965).

It is a popular sequential method owing to its adaptability to suit difficult conditions such as progress along narrow valleys.

Minimisation starts by evaluating the objective function  $F_1$  at the vertices  $V_i$  ( $i = 0, 1, 2, \dots, m$ ) of a regular simplex in the hyperspace of the  $m$  variable parameters.<sup>1</sup> Denoting those vertices with the highest, next highest and lowest

---

1. A simplex is a higher dimensional equivalent of a tetrahedron.

function values by  $V_h$ ,  $V_g$  and  $V_l$  respectively,  $V_h$  is reflected in the centroid  $V$  of the remaining vertices to give the new vertex  $V_r$  such that

$$\overline{V_r V} / \overline{V V_h} = \alpha \quad (\alpha > 0) \quad (3.5)$$

where  $\alpha$  is the reflection coefficient. Subsequent operations are decided upon in the following manner:

- i) If  $F_l < F_r < F_g$ ,  $V_r$  replaces  $V_h$  and the procedure is repeated.
- ii) If  $F_r < F_l < F_g$ , the search is expanded in the direction  $V_h V_r$  to the point  $V_e$  which is given by the expansion coefficient  $\gamma$  ( $\gamma > 1$ ) such that

$$\overline{V_e V_h} / \overline{V_r V_h} = \gamma \quad (3.6)$$

$V_h$  is then replaced by whichever of  $V_r$  and  $V_e$  possessing a smaller function value.

- iii) If  $F < F_r$  then  $V_r$  replaces  $V_h$  only if  $F_r < F_h$ . In either case, a point  $V_c$  is located between  $V_h$  and  $V$  such that

$$\overline{V_c V} / \overline{V_h V} = \beta \quad (0 < \beta < 1) \quad (3.7)$$

where  $\beta$  is the contraction coefficient. The simplex is then modified according to:

-If  $F_c < F_h$ ,  $V_c$  replaces  $V_h$  and the procedure is re-started from this new simplex.

-If  $F_c > F_h$ , the mid point between  $V_l$  and the remaining vertices are taken to be the vertices of the new simplex. The whole procedure is then re-started.

Appropriate values of  $\alpha$ ,  $\beta$  and  $\gamma$  are suggested to be 1, 0.5 and 2 respectively (Nelder and Mead, 1965). The process is terminated when the standard deviation of the function values at the  $(n+1)$  vertices falls below a pre-assigned value.

### 3.2.3. Linear Methods

These methods carry out the search along a set of linear directions. The class includes a large variety of procedures, each procedure being more suitable for one type of problem than for another although some of them exhibit an ingenious adaptability to suit a broad range of problems.

#### 3.2.3.1. The alternating variable method: Friedman and Savage (1947).

This is the simplest form of linear methods. A univariate search is carried out parallel to each variable parameter axis in turn; a change to the next axis is not made until a minimum has been located along the current axis.

Unless the problem happens to be well-scaled, the progress towards the minimum, after the first few iterations, follows a slow zig-zag path and the method usually breaks down by local convergence. It cannot, therefore, be recommended for general geophysical purposes although its simplicity has attracted some geophysical applications in the past (e.g. Bullard et al, 1965)

#### 3.2.3.2. Pattern search method (Hooke and Jeeves 1961) with subsequent modification by Wood (1962).

This method attempts to align the direction of search with the general trend of the objective function. The search starts at some initial point  $B_1$  by changing the parameters one at a time, the parameter  $x_1$  being perturbed by an amount  $d_1$ . If this results in a lower function value the new point replaces the current point and the parameter  $x_{i+1}$  is then considered. Otherwise,  $-d_1$  replaces  $d_1$  and the function is evaluated again. If this move also fails, the current point is unchanged and the

parameter  $x_{i+1}$  is considered. When all parameters have been considered a stage of exploratory moves is completed and the final point  $B_2$  becomes the new base. In general, if a move from  $B_j$  to  $B_{j+1}$  results in a lower function value, a pattern move is made to the point  $2B_{j+1} - B_j$  from which another set of exploratory moves is made to give the new base point  $B_{j+2}$ . If the exploration fails to find a lower function value at  $B_{j+2}$ , the exploration is re-started from  $B_{j+1}$  itself. When all explorations about a base  $B_k$  fail to find a lower function value,  $d_1$  is reduced and the process is re-started from  $B_k$ . Convergence is assumed when  $d_1$  have been reduced to a pre-assigned value.

The method is speedy and efficient when the minimum lies in a valley with only slight curvature. Its efficiency stems from its ability to treat straight valleys as a one-dimensional case, thus reducing the effective dimensionality of the problem (Wilde, p.145). It has many possible applications in geophysical interpretation particularly in cases where the function is not very complicated.

### 3.2.3.3. The method of rotating coordinates (Rosenbrock, 1960)

The search is carried out parallel to a series of mutually orthogonal directions which are rotated at the end of each search stage so that the first of the new directions lies in the direction of total progress made during that stage. This rotation renders the method extremely flexible in following the general trend of the objective function in a fashion similar to, but much more powerful than that of the pattern search.

Starting from some initial point  $\underline{x}_0$ , each variable is usually perturbed independently so that the search directions of the first stage are parallel to the coordinate axes of the variables. Denoting the  $i^{\text{th}}$  direction vector at the  $j^{\text{th}}$  stage by  $\underline{D}_i^j$  and its respective step-length by  $e_i$ , the search starts from the current point by perturbing along each direction by  $e_k$  ( $k=1,2,\dots,m$ ). If the perturbation succeeds in finding a function value which is not larger than the current value, the current point is replaced by the new point,  $e_k$  is multiplied by a ( $a > 1$ ) and the direction  $k+1$  is considered. Otherwise, the perturbation is a failure, the current point remains unchanged,  $e_k$  is multiplied by  $-b$  ( $b < 1$ ) and the  $k+1^{\text{th}}$  direction is also considered. When all  $m$  directions have been perturbed the cycle is repeated starting from the first direction. The process goes on until a success followed by a failure has occurred along all  $m$  directions. This marks the end of a stage. The next stage is started by defining new direction vectors in the following manner:

The vectors  $\underline{A}_1, \underline{A}_2, \dots, \underline{A}_m$  are defined by

$$\underline{A}_1 = \sum_{k=1}^m u_k \underline{D}_k \quad (3.7)$$

where  $u_k$  is the algebraic sum of all successful  $e_k$  steps during the  $j^{\text{th}}$  stage. Thus  $\underline{A}_1$  represents the total progress made during the  $j^{\text{th}}$  stage. The direction vector is obtained by normalisation. Thus,

$$\underline{D}_1^{j+1} = \underline{A}_1 / |\underline{A}_1| \quad (3.8)$$



The mutual orthogonality of the remaining directions is re-established using the Gram-Schmidt orthogonalisation procedure (Wilde, 1964, p.155) which is summarised in the equations.

$$\underline{B}_k = \underline{A}_k - \sum_{i=1}^{k-1} (\underline{A}_k \cdot \underline{D}_i^{j+1}) \underline{D}_i^{j+1} \quad (3.9)$$

$$\underline{D}_k^{j+1} = \underline{B}_k / |\underline{B}_k| \quad (3.10)$$

The search starts now along the new directions from the current point and the whole process is repeated. Convergence is assumed when  $A_1$  falls below a specified limit for several consecutive stages. The search may also be terminated after a certain number of function evaluations.

Since its introduction by Rosenbrock (1960) the method has claimed wide popularity in various fields of industry. It is robust and will successfully handle many ill-conditioned problems. The rotation of coordinates attempts to orientate the search directions so that they are locally the most favourable both for following very curved valleys and for reducing the difficulties from badly scaled problems. It also enables the search to move out of ill-defined local minima.

These properties give the method a wide field of application in geophysics. The main disadvantage in the method is that it is, on the whole, slower than methods which make a direct use of equation (2.9).

#### 3.2.3.4. The modification of Davies, Swann and Campey

Box et al (1969, p.27) describe a modification of

Rosenbrock's method aiming at speeding up the computation and overcoming certain orthogonalisation difficulties.

The first aim is achieved by carrying out a linear search, equivalent to the univariate search of Davies, Swann and Campey (section 2.6), only once along each direction instead of perturbing cyclically several times at each stage.

Difficulties with orthogonalisation arise when some of the  $u_k$  in equation (3.7) happen to be zero resulting in linear dependence between the search directions. These conditions are very unlikely to occur (Rosenbrock, 1960) but if they did then the orthogonalisation process would fail. The procedure is therefore modified so that only those vectors associated with non-zero  $u_k$ 's are orthogonalised. Box et al then show that the orthogonality of the system remains unimpaired and the second aim is thus fulfilled.

### 3.2.3.5. Poor man's optimiser

This method is fully described by Wilde (1964, p.155). It is based on techniques similar to the method of alternating variables (section 3.2.3.1) but the current base point is found by averaging or interpolating between two points possessing the lowest function values.

It is claimed to be well suited for curved valleys and may, therefore, be of some use in geophysics. However, its sluggish progress makes it a poor substitute for the method of rotating coordinates.

### 3.2.3.6. Powell's method (Powell, 1964). Procedure P 303.

Methods which are based on the quadratic behaviour of

the objective function are of considerable interest because, as soon as the search reaches a region where the behaviour is essentially quadratic, the minimum is attained rapidly by quadratic convergence. Most of these methods, however, are gradient methods. The conjugate directions method of Powell is, therefore, very useful in that it does not require the evaluation of any derivatives, yet it enjoys most of the basic advantages in these methods.

In its simplest form the method starts by setting  $m$  search directions in the hyperspace of  $m$  variable parameters, the  $i^{\text{th}}$  direction of the  $j^{\text{th}}$  stage being denoted by  $\underline{D}_i^j$  and with the direction of the first stage parallel to the original mutually orthogonal coordinate axes.

At stage  $j$  and starting from a base point  $\underline{x}_0$ , a linear search using Powell's algorithm (section 2.6) is carried out along each search direction in turn. When a minimum is located at point  $\underline{x}_1$  along  $\underline{D}_1^j$ ,  $\underline{x}_1$  becomes the starting point for the search along  $\underline{D}_2^j$  and so on until all  $m$  directions have been searched and  $\underline{x}_m$  located. The direction  $\underline{D}$  is now defined by  $\underline{x}_m - \underline{x}_0$  and a linear search along it locates the new base point  $\underline{x}_0^{j+1}$  from which the search starts at the  $(j+1)^{\text{th}}$  stage.  $\underline{D}$  is added to the end of the list of directions and the first direction is discarded so that

$$\underline{D}_1^{j+1}, \underline{D}_2^{j+1}, \dots, \underline{D}_m^{j+1} = \underline{D}_2^j, \underline{D}_3^j, \dots, \underline{D}_m^j, \underline{D} \quad (3.11)$$

For a quadratic function, Powell demonstrates that, by choosing  $\underline{D}$  in this manner, the  $m$  search directions become mutually conjugate<sup>1</sup> after  $m$  stages. The method is, therefore, quadratically convergent.

---

1. Two directions  $\underline{D}_i$  and  $\underline{D}_j$  are said to be conjugate with respect to the linear operator  $H$  if  $\underline{D}_i^T H \underline{D}_j = 0$ , ( $i \neq j$ ).

This simple procedure may occasionally choose nearly dependant directions. In extreme cases, some directions could become permanently lost and the resulting directions do not span the whole space. Powell's method incorporates further modifications to overcome these problems.

Convergence is assumed when the change in every variable at successive stages has fallen below 10% of the required accuracy. The method does not have provisions for the use of constraints. Therefore, its use in multi-modal problems may not always be desirable.

### 3.3. Gradient Methods

These methods are based on approximating the behaviour of the objective function by the first few terms in equation (2.7). Hence, they use the first or higher order partial derivatives of  $f(\underline{x})$  with respect to  $x_i (i=1,2,\dots,m)$  to determine the search direction. In comparison with direct search methods they are generally much faster and can also handle many more variables. However, they are quite sensitive to curvatures and local gradients so that the search could terminate by local convergence when the particular function happens to have many ill-defined local minima. Moreover, approximating the behaviour of the function by a truncated Taylor series may be very unrepresentative especially in regions which are far from the solution(s). These features, combined with the frequent difficulty in providing the derivatives analytically, can reduce the extent to which gradient methods may be recommended to solve a given geophysical problem.

### 3.3.1.1. The method of steepest descent (Cauchy, 1847)

This is the simplest gradient method and is based on a local linearisation of the objective function by neglecting the second order and higher terms in equation (2.7). Thus,

$$f(\underline{x} + \underline{\delta}) = f(\underline{x}) + \sum_{j=1}^m \frac{\partial f(\underline{x})}{\partial x_j} \delta_j \quad (3.12)$$

which in our matrix notation becomes

$$f - f_0 = \underline{G}'\underline{\delta} \quad (3.13)$$

where the prime indicates matrix transposition

Equation (3.13) shows that, for a fixed magnitude of  $\underline{\delta}$ , the greatest reduction in the function value takes place in the direction of  $-\underline{G}$ , hence the name steepest descent. This direction is locally orthogonal to the contours since  $f - f_0 = 0$  when  $\underline{\delta}$  is orthogonal to  $\underline{G}$ .

The search direction  $\underline{D}_1$  at the  $i^{\text{th}}$  iteration is obtained from the normalised gradient vector at the current point  $\underline{x}_1$ . The search for a minimum  $\underline{x}_{1+1}$  in this direction is then carried out linearly or by using a constant steplength.  $\underline{x}_{1+1}$  then becomes the current point and the process is repeated until a minimum is located with the required accuracy.

The neglect of the higher terms in equation (2.7) imposes severe drawbacks and, although the vector  $\underline{G}$  provides the direction with the greatest function change, this effect is only local and the direction of steepest descent does not in general coincide with that leading to the minimum. Consequently, although the initial stages may attain large reductions in the function value the progress towards a solution would generally take a zig-zag form, becoming gradually slower or terminating

by local convergence.

This situation has inspired the design of several variations from the basic scheme. Booth (1957) has suggested starting each new iteration from some point other than the minimum in the current direction. Marquardt (1963), on the other hand, starts the search in the direction of steepest descent but gradually changes to that given by the least squares procedure (see section 3.3.1.4). However, owing to the linearisation of the Taylor series expansion, steepest descent and its modifications remain essentially of little promise in tackling but the simplest forms of functions. Several alternatives are now available (e.g. Davidon's method) for solving geophysical problems.

### 3.3.1.2. Newton-Raphson method

It is clear that the next step in gradient methods is to include the second order terms of equation (2.7). The inclusion of the second order derivatives is quite basic since all informations relating to the curvature of the function are usually essential in leading to the optimum.

All first and second order partial derivatives of the objective function are assumed to be available at the current point  $\underline{x}$ . If the minimum is at  $\underline{x} + \underline{\delta}$  then differentiating the objective function with respect to  $\delta_k$  and equating that to zero, we obtain from the truncated equation (2.7)

$$\frac{\partial f(\underline{x} + \underline{\delta})}{\partial \delta_k} = 0 = \frac{\partial f(\underline{x})}{\partial x_k} + \frac{1}{2} \sum_{i=1}^m \frac{\partial^2 f(\underline{x})}{\partial x_i \partial x_k} \delta_i + \frac{1}{2} \sum_{k=1}^m \frac{\partial^2 f(\underline{x})}{\partial x_i \partial x_k} \delta_k$$

$$k = 1, 2, \dots, m \quad (3.14)$$

which, in view of the symmetry of the Hessian matrix, may be simplified to give

$$\frac{\partial f(\underline{x})}{\partial x_k} = - \sum_{i=1}^m \frac{\partial^2 f(\underline{x})}{\partial x_i \partial x_k} \delta_i, \quad k = 1, 2, \dots, m \quad (3.15)$$

or in our matrix notation

$$\underline{\delta} = - H^{-1} \underline{G} . \quad (3.16)$$

$\underline{\delta}$  is obtained by solving the  $m$  linear equations for the  $m$  unknown  $\delta_i$ 's and the iterative move

$$\underline{x}_{p+1} = \underline{x}_p + \underline{\delta} \quad (3.17)$$

is then made.

The method is quadratically convergent since if  $f$  were quadratic, equation (2.9) would be an exact representation and the minimum would be attained in one move. Obviously, this is seldom the case and an iterative process is usually necessary for locating the solution.

The progress towards a minimum is only ensured if the matrix of the second order derivatives,  $H$  is positive definite and if the quadratic approximation is not grossly violated. These conditions are, generally, satisfied in the vicinity of the minimum but are not guaranteed if the initial estimates happened to be far from the solution.

Further obstacles are presented by the frequent difficulty in providing the second order partial derivatives of the objective function analytically and by the necessity to solve the  $m$  linear equations at each iteration.

Past geophysical applications of the method are not uncommon (e.g. Vosoff, 1958). However, it is not recommended for general use in geophysics owing to its many drawbacks.

3.3.1.3. Davidon's method (Davidon, 1959), refined by Fletcher and Powell (1963). Procedure P306

We have seen that, away from the minimum, the method of steepest descent usually achieves a rapid reduction in function value whereas the efficiency of Newton-Raphson's method is restricted to the neighbourhood of the minimum. The success of Davidon's method has largely depended upon making use of both features, starting initially as steepest descent and changing gradually to Newton-Raphson, as the optimum is approached.

The basic iterative procedure of Davidon's method is

$$\underline{x}_{p+1} = \underline{x}_p - h_p \underline{M}_p \underline{G}_p \quad (3.18)$$

where  $\underline{M}_p$  is a symmetric matrix which must be positive definite and where  $h_p$  is the required step-length, from the current point, to locate the minimum along the direction

$$\underline{D}_p = \underline{M}_p \underline{G}_p \quad (3.19)$$

Starting with a unit matrix so that the first move is in the direction of steepest descent,  $\underline{M}$  is updated at every iteration such that it would continually and increasingly tend to  $\underline{H}$ .  $\underline{M}$  is updated using values and first derivatives of the objective function and, as  $\underline{H}$  is approached, the later stages become essentially a Newton-Raphson procedure. In the essentially quadratic neighbourhood of the minimum, the latter is attained in one move, i.e. the method is quadratically convergent. In this way, not only the main objectives of the method are realised but, also, the need for providing a matrix of second derivatives is completely avoided.



At the end of the  $p^{\text{th}}$  iteration when  $\underline{x}_{p+1}$  has been located,  $f(\underline{x}_{p+1})$  and  $\underline{G}_{p+1}$  are evaluated.  $M$  is then updated by setting the matrix

$$M_{p+1} = M_p + A_p + B_p \quad (3.20)$$

where, if we denote  $\underline{G}_{p+1} - \underline{G}_p$  by  $\underline{Y}_p$  and  $-h_p M_p \underline{G}_p$  by  $\underline{d}_p$  then

$$A_p = \frac{\underline{Y}_p \underline{Y}'_p}{\underline{Y}'_p \underline{Y}_p} / \frac{\underline{Y}'_p \underline{d}_p}{\underline{Y}_p \underline{d}_p} \quad (3.21)$$

and

$$B_p = - \frac{M_p \underline{Y}_p \underline{Y}'_p}{\underline{Y}'_p \underline{Y}_p} \frac{M_p \underline{Y}_p \underline{Y}'_p}{\underline{Y}'_p \underline{Y}_p} \quad (3.22)$$

Fletcher and Powell (1963) demonstrate that  $A_p$  ensures that the successive  $M_p$  matrices converge to  $H^{-1}$  while  $B_p$  ensures that the successive  $M_{p+1}$  remain positive definite. Consequently, this form of updating results into an extremely effective matrix which adapts itself to suit various situations. The process is repeated until convergence.

The difficulty of providing first order partial derivatives of the objective function analytically can be a major task. However, Stewart (1967) has presented a method for use in conjunction with Davidon's method whereby the first order partial derivatives are calculated numerically. Stewart's method is claimed to be very successful and should provide a much needed sophistication to an already powerful optimisation method.

Davidon's method is one of the most efficient optimisation methods but, suffers from the drawbacks of gradient methods mentioned earlier. This causes many difficulties in the general use of the method. Its application in many magnetic

and gravity problems fails when the initial estimates in the  $\underline{x}$  hyperspace are far from the region containing satisfactory solutions. The failure is usually due to the vanishing of all the first partial derivatives of the objective function at an ill-defined local minimum (A.K. Datta, private communication). On the other hand, its progress in the relative absence of ill-defined minima or when the initial estimates are close to a solution, is extremely rapid. In general, however, if the objective function is not essentially unimodal, an efficient use of the method may have to be restricted to the later stages of the search.

#### 3.3.1.4. The method of least squares

The formulation of the method is attributed to Gauss (Wilde and Beightler, 1967 p.299). As the name indicates, the method is only applicable to functions of the form

$$f(\underline{x}) = \sum_{i=1}^n e_i^2(\underline{x}) \quad (3.23)$$

where  $e(\underline{x})$  is a non-linear function of  $\underline{x}$ .

$$\text{Let } P_{ij} = \frac{\partial e_i}{\partial x_j} \quad \begin{array}{l} i=1,2,\dots,n \\ j=1,2,\dots,m \end{array} \quad (3.24)$$

and define the  $n \times m$  matrix

$$P = [P_{ij}] \quad (3.25)$$

and the vector

$$\underline{E} = \begin{bmatrix} e_1 \\ e_2 \\ \cdot \\ \cdot \\ e_n \end{bmatrix} \quad (3.26)$$

Differentiating  $f(\underline{x})$  with respect to  $x_j$  gives

$$\frac{\partial f(\underline{x})}{\partial x_j} = 2 \sum_{i=1}^n e_i \frac{\partial e_i}{\partial x_j} \quad (3.27)$$

which in matrix notation becomes

$$\underline{G} = 2\underline{P}'\underline{E} \quad (3.28)$$

Gauss noticed that if  $e_i(\underline{x})$  were all linear functions of  $\underline{x}$  then the matrix  $\underline{P}$  does not change from one point to another. The gradient at the minimum  $\underline{x} + \underline{\delta}$  is then approximated by

$$\underline{G}(\underline{x} + \underline{\delta}) \approx 2 \underline{P}(\underline{x})\underline{E}(\underline{x} + \underline{\delta}) \quad (3.29)$$

An approximation for  $\underline{E}$  is obtained from the truncated Taylor expansion about  $\underline{x}$

$$\begin{aligned} \underline{E}(\underline{x} + \underline{\delta}) &\approx \underline{E}(\underline{x}) + \frac{\partial \underline{E}'(\underline{x})}{\partial \underline{x}} \underline{\delta} \\ &\approx \underline{E}(\underline{x}) + \underline{P} \underline{\delta} \end{aligned} \quad (3.30)$$

Since the gradient vanishes at the minimum, equation (3.29) becomes

$$0 = 2 \underline{P}' (\underline{E} + \underline{P} \underline{\delta}) \quad (3.31)$$

which gives

$$\underline{\delta} = -[\underline{P}' \underline{P}]^{-1} \underline{P}' \underline{E} \quad (3.32)$$

When  $e_i(\underline{x})$  are linear in  $\underline{x}$  the procedure is exact and the minimum is attained in one move. This is equivalent to a linear regression in statistics. However, for non-linear functions, an iterative procedure where  $\underline{x}_{k+1}$  replaces  $\underline{x}_k + \underline{\delta}_k$ , is usually necessary.

The method is widely used in various application including geophysics (e.g. Corbato, 1965).

However, the linear approximations involved in the assumptions render the method rather inefficient. When the initial point is remote from a solution and the quadratic approximation is poor, the procedure behaves erratically and the search will usually fail altogether (Wilde and Beightler, 1967, p.302).

Marquardt (1963) suggested a method which modifies equation (3.32) to

$$\underline{\delta} = - [P'P - \lambda I]^{-1} P' \underline{E} \quad (3.33)$$

where  $I$  is an  $m \times m$  unit matrix and  $\lambda$  is an arbitrary constant ( $\lambda \geq 0$ ). When  $\lambda = 0$ , equation (3.33) reduces to the Gauss procedure. For very large  $\lambda$ , equation (3.33) becomes

$$\underline{\delta} = - \lambda^{-1} P' \underline{E} = - \frac{1}{2} \lambda^{-1} \underline{G} \quad (3.34)$$

so that the required excursion is in the direction of steepest descent.

Marquardt suggests using a large  $\lambda$  at the initial stages where steepest descent achieves a rapid reduction in the function value. The changeover to Gauss method is achieved by progressively reducing  $\lambda$  as the solution is approached.

Johnson (1969) used Marquardt procedure to interpret linear and non-linear magnetic problems.

This procedure is probably the best modification of steepest descent and least squares but appears to be inferior to Davidon's method which makes use of the second order properties of the objective function.

#### 3.4. Constrained Optimisation

The description is now extended to problems subject to constraints in the form of equations (3.1) or (3.2). Both  $t(\underline{x})$  and  $q(\underline{x})$  may be linear or non-linear in  $\underline{x}$ . However,

constraints in geophysical work are usually some upper or lower bound on each variable parameter serving as a guard against geological or physical unfeasibility. The constraints will, therefore, be of a very simple form.

For illustration, consider an example where the depth, defined by  $x_k$ , to some magnetically anomalous body is known to be greater than  $z$  kms. Expressing this as

$$x_k - z > 0 \quad (3.35)$$

gives the inequality constraint  $t_k(x_k) > 0$ .

In view of this simplicity, it is more useful to briefly discuss the broad outline of the general case, which is usually non-linear, and to detail only those points which are of direct interest.

#### 3.4.1. Variable transformation (Box, 1966).

The simplest approach to constrained optimisation is to transform the variable such that the constraints are removed from the formulation of the problem. An unconstrained optimisation may then be carried out. The general method is to express the variable  $x_k$  in terms of a second variable which, when used unconstrained, will not violate the conditions imposed on the problem.

Consider, for instance, the example given in equation (3.35). Writing

$$\begin{aligned} x_k &= z + |y_k| \\ \text{or} \\ x_k &= z + y_k^2 \\ \text{or} \\ x_k &= z + e^{y_k} \end{aligned} \quad (3.36)$$

reduces the problem to finding the optimum with respect to the new variable  $y_k$ . Suppose that it was further required that the depth  $x_k$  should not exceed  $Z$  kms, i.e.

$$Z > x_k > z$$

The transformation may then be achieved by

$$x_k = z + (Z - z)\sin^2 y_k \quad (3.37)$$

with  $y_k$ , in equations (3.36 and 3.37) being completely unconstrained.

There are several methods for transforming variables, following the same general idea. The principal advantage of variable transformation is that it is directly applicable to the type of simple constraint usually encountered in geophysical work. However, it becomes of little use when the constraints are more complex in which case one of the methods considered below would become necessary. The method has also other disadvantages. The transformation is often tedious and introduces the risk of human error. The increased complexity of the new variables causes a further disadvantage where the derivatives with respect to the variable parameters are to be furnished.

For geophysical purposes, however, the method of variable transformation is, probably, the best first aid treatment of constraints and is often also one of the best final treatments.

#### 3.4.2. Direction Modification

The constrained problem may also be treated by changing the direction of search when a constraint is encountered. The main disadvantage of such methods is that when the

constraint is highly non-linear, many direction modifications may become necessary, involving a large number of computations.

#### 3.4.2.1. Riding the constraint : Roberts and Lyvers (1961).

This method assumes that when a constraint is violated along the direction of search the true minimum for a unimodal function must lie on the unfeasible side of the constraint. The search will, therefore, follow that constraint and not leave it at any subsequent stage. The increments chosen in following the constraint depend upon the partial derivatives of the constrained function with respect to the variables. The progress can be very slow for very non-linear constraints.

#### 3.4.2.2. Hemstitching : Roberts and Lyvers (1961).

In its original form, the method is only applicable to search by steepest descent. When a constraint is violated, a step is taken back into the feasible region in a direction locally orthogonal to the constraint. Thus, by moving into and back from the unfeasible region, the progress assumes a pattern that justifies the name.

Difficulties arise in relocating the feasible region when more than one constraint is violated. Certain modifications succeed in overcoming such difficulties but the method still suffers from the poor convergence properties of search by steepest descent (Box et al 1969 p.47)

#### 3.4.2.3. Davidon's method with constraints

Davidon (1959) suggested that his method is applicable to problems involving linear equality constraints by reducing the rank of the matrix  $M$  defined in equation (3.20) by the

number of active equality constraints. If during the optimisation process it happens that better progress will be made by relaxing a certain constraint, the rank of  $M$  must be increased by 1 using a certain recurrence formula. When inequality constraints are involved, the search is carried out unconstrained until an inequality constraint is violated. This is then treated as an active equality constraint and the process continues as before.

Non-linear constraints in Davidon's procedure may be treated using the method of created response surface (section 3.4.3.). Davies (1968) also extends the method of handling linear constraints described above to treat functions subject to inequality constraints by incorporating techniques based on hemstitching.

#### 3.4.2.4. The "Complex" method (Box, 1965). Procedure 301

This is a modification of the simplex method described in section (3.2.2.1.) where the term "complex" refers to a simplex in a constrained problem. The complex is constructed as follows:

An initial point is given in the feasible region, i.e. it satisfies

$$l_i \leq x_i \leq u_i \quad i=1,2,\dots,m,m+1,\dots,L \quad (3.38)$$

where the implicit variables  $x_{m+1}, \dots, x_L$  are functions of the independent variables  $x_1, x_2, \dots, x_m$ .  $l_i$  and  $u_i$  are lower and upper limits respectively and can be constants or functions of  $x_1, \dots, x_m$ .



The remaining  $k-1$  ( $k \geq m$ ) vertices of the complex are constructed in the following manner. A point is generated with coordinates

$$\mathbf{x}_j = \mathbf{l}_j + r_j (\mathbf{u}_j - \mathbf{l}_j) \quad j = 1, 2, \dots, m \quad (3.39)$$

where the random numbers  $r_j$  lie in the interval 0-1 so that the explicit constraints cannot be violated. If this point violates an implicit constraint, it is contracted towards the centroid of the points already selected. The process is repeated until all vertices have been generated. The search is then carried out by methods similar to those described in section (3.2.2.1.). Whenever a constraint is violated the relevant vertex is moved back into the feasible region along the same expansion line.

$k = 2m$  is recommended but may be too large for  $m > 10$  (Box et al, 1969, p.53).

### 3.4.3. Function modification

With this technique, the function is modified at the constraints such that a minimum can always be found within the feasible region. Consider, for example, a modification of  $f(\underline{x})$  so that the problem is to minimise

$$F(\underline{x}) = f(\underline{x}) + \sum W_i t_i^2(\underline{x}) \quad (3.40)$$

where the summation involves only those constraints that have been violated and where  $W_i$  is an appropriate weight and  $t_i$  is defined in equation (3.1). The constraint is then effectively replaced by a 'hill' whose sides get steeper away from the feasible region. The particular form of equation

(3.40) is not convenient since it could involve function evaluations outside the feasible region. Using the same concept, Rosenbrock (1960) and Carroll (1961) suggest methods which overcome these difficulties.

#### 3.4.3.1. Rosenbrock's method: Procedure P300

A boundary zone of width  $(u_1 - l_1) 10^{-4}$  is assumed on the feasible side of each of the constraints. The search is carried out as in the unconstrained case until a constraint is violated in which case the trial is deemed a failure equivalent to  $f_{i+1} > f_i$ . The basic search procedure is then resumed.

When at any stage, a point falls within a boundary zone the function  $f$  is modified by replacing it by

$$F = f - (f - f_0)(3b - 4b^2 + 2b^3) \quad (3.41)$$

where  $f_0$  is the lowest function value obtained thus far outside the boundary zone and where  $b$  is the fractional depth of penetration of the boundary zone.

At the edge of the boundary,  $b = 0$  and  $F = f$  while at the constraint,  $b = 1$  and  $F = f_0$ . Rosenbrock (1960) shows that for a function which decreases as the constraint is approached, this modification creates a minimum within the boundary zone. Thus, an unconstrained minimum exists for some  $b$  between 0 and 1.

While this method of treating constraints is very successful in conjunction with the method of rotating coordinates (section 3.2.3.3.) it has generally proved less effective with other methods (Box et al, 1969, p.50).

### 3.4.3.2. Carroll's method

The constrained problem is replaced by an unconstrained procedure using

$$F(\underline{x}, W) = f(\underline{x}) + W \sum_{i=1}^L \frac{w_i}{t_i(\underline{x})} \quad (3.42)$$

where  $W$  and  $w_i$  are positive constants.

As the constraint is approached,  $t_i$  tends to zero and the function becomes extremely large. Thus, an unconstrained minimum of  $F(\underline{x}, W)$  is produced in the feasible region. In the actual application, each  $w_i$  is initialised to zero until the respective constraint is violated when  $w_i$  assumes its specified value.  $W$  is reduced at each of the successive optimisation stages. This finally results in convergence to the true minimum of the feasible region (Davies, 1968).

Carroll's created response surface technique has been applied successfully to many unconstrained algorithms, particularly in conjunction with Davidon's method (Davies, 1968).

### 3.5. Conclusions

The use of the methods of steepest descent, Newton-Raphson and least squares has been traditional in the solution of non-linear problems, in various branches of science including geophysics. This is because they have had an unrivalled monopoly from the time of their introduction until the advent of digital computers. The methods of alternating variables and random search have also had a wide range of application. However, all these methods are

relatively slow and suffer from severe drawbacks which make them unsuitable to meet the demands of geophysical problems except on a limited scale.

More recent elaborations, e.g. Davidon's method, use a combination of the good features of some of these methods and have generally proved quite successful. However, gradient methods are very powerful only in an essentially unimodal region and seem to break down when applied to problems which are rather ill-conditioned. The slower but more robust direct search methods enjoy a superior strategy with multimodal functions.

The rule in treating most geophysical problems is to start the initial search stages using a direct search method and to change to a gradient method at the later stages when the search has converged to an essentially unimodal region. This usually corresponds to equation (2.9) becoming a closer representation of the behaviour of the objective function. The objective functions encountered in gravity and magnetic problems are typical of the functions which qualify for this kind of approach.

However, within the general principles outlined above, the choice of the particular optimisation method is not very critical. Fleischer (1965) comments on this by quoting J.D. Williams in the book *The Complacent Strategist* "As with all models of performance, the shoe has to be tried on each time an application comes along to see whether the fit is tolerable; but, it is well known, in the Military Establishment for instance, that a lot of ground can be covered in shoes that do not fit properly."

## C H A P T E R 4

AN INVESTIGATION OF NON-UNIQUENESS IN GRAVITY AND  
MAGNETIC INVERSE PROBLEMS4.1. Introduction

Ambiguity in the solution of gravity and magnetic problems is a well established fact. We shall, in this work, view the problem of ambiguity through a number of factors which most significantly contribute to it. Each factor is dealt with separately since a combined treatment would tend to confuse the picture. These factors are:

I) Potential theory considerations show that a given gravity (or magnetic) anomaly on some plane  $H$  may be produced by an infinite number of possible solutions below  $H$ , down to a certain depth (see, for example, Skeels, 1947; Parasnis, 1962, p.46). The solutions usually involve non-uniform density distributions and no particular restrictions regarding the shape of the anomalous body. This factor imposes an inherent non-uniqueness but may be severely limited by using certain restrictive conditions which we shall give later.

II) Incomplete knowledge of the full length of the anomaly is a factor which is a direct result of our practical limitations.

III) The geological setting is invariably represented by models which are substantially simpler. This factor results into a number of models, all satisfying the observed anomaly to within an acceptable range but each, individually, emphasising a certain aspect of the anomalous feature.

A further related point is the lack of adherence to the

conditions assumed by the model. A familiar example is the use of two-dimensional models to interpret anomalies which are only approximately two-dimensional.

IV) Observational errors resulting from measurement, reduction etc. are always present on field anomalies. This factor causes a multitude of possible but widely differing solutions that approximate the observed anomaly within the amplitude of the errors.

Other factors in ambiguity are less general and will be dealt with when encountered, as appropriate.

For the sake of simplicity, all investigated cases are two-dimensional but an extension of the results to three-dimensional cases should follow in a general way. It is also more convenient to present the problem using mostly gravity anomalies although most cases below have been verified to be true for magnetic problems as well.

The anomaly is assumed measurable at each point  $(x,0)$  along the horizontal  $x$ -axis in a Cartesian system with the  $z$ -axis pointing vertically downwards.

The following conditions have been assumed for the anomalous body and for the model representing it throughout this investigation:

1. They are bounded by a finite number of straight sides so that they are both of a polygonal cross-section.
2. They have a uniform, not necessarily known, density (or magnetisation) contrast with a uniform surrounding medium.
3. Any line vertical to the  $x$ -axis will not meet the bounding surface more than twice. The absence of cavities is

an important implication of this condition.

These conditions are usually quite adequate geologically. The use of polygonal models has been adopted in most interpretational procedures since the introduction of the general method by Talwani, Worzel and Landisman (1959). The conditions imposed here do not, therefore, represent any deviation from an established routine. They have, for our purpose, the further advantage of completely overcoming the effect of factor I as will be shown in the next section.

#### 4.2. The Case of Exact Models

A hypothetical case is now considered where factors III and IV are assumed absent. The N-sided anomalous body can, therefore, be exactly represented by a model.

Consider the case where the anomalous polygon has a density contrast  $\rho_1$  with the surrounding medium. Using a formula given by Heiland (1940, p.153) for a semi-infinite step-model, the gravity anomaly at the k th point is then given by

$$\begin{aligned}
 A_k = & \sum_{j=1}^N (2G\rho_1 \left\{ z_{2j} \tan^{-1} \frac{x_{2j} - \xi_k}{z_{2j}} - z_{1j} \tan^{-1} \frac{x_{1j} - \xi_k}{z_{1j}} \right\} \\
 & - \left\{ x_{1j} \sin i + z_{1j} \cos i \right\} \left[ \frac{1}{2} \sin i \log \frac{(x_{2j} - \xi_k)^2 + z_{2j}^2}{(x_{1j} - \xi_k)^2 + z_{1j}^2} \right. \\
 & \left. + \cos i \left( \tan^{-1} \frac{x_{2j} - \xi_k}{z_{2j}} - \tan^{-1} \frac{x_{1j} - \xi_k}{z_{1j}} \right) \right] \quad (4.1)
 \end{aligned}$$

where G is the gravitational constant,  $x_{1j}$ ,  $z_{1j}$ ,  $x_{2j}$ ,  $z_{2j}$  are the coordinates defining respectively the top and bottom

corners of the  $j$  th semi-infinite step-model.  $\xi_k$  is the  $x$ -coordinate of the  $k$  th anomaly point and may assume any value between  $-\infty$  and  $+\infty$ , and

$$i = \sin^{-1} [ (x_{2j} - x_{1j}) / \{ (z_{2j} - z_{1j})^2 + (x_{2j} - x_{1j})^2 \}^{\frac{1}{2}} ]$$

Simplifying we write

$$A_k = 2G\rho_1 \sum_{j=1}^N T_{jk} \quad (k = 1, 2, \dots, \infty) \quad (4.2)$$

A second  $N'$  - sided polygon of density contrast  $\rho_2$  will produce

$$A'_k = 2G\rho_2 \sum_{j=1}^{N'} T'_{jk} \quad (4.3)$$

The values of  $\xi_k$  which will satisfy  $A_k = A'_k$  are given by the roots of the equation

$$\rho_2 / \rho_1 = \sum_{j=1}^N T_{jk} / \sum_{j=1}^{N'} T'_{jk} \quad (4.4)$$

For any particular ratio  $\rho_2 / \rho_1 = R$ , equation (4.4) is reduced to

$$\sum_{j=1}^N T_{jk} - R \sum_{j=1}^{N'} T'_{jk} = 0 \quad (4.5)$$

In order that  $A = A'$  for each and every  $\xi_k$ , equation (4.5) has to be similarly satisfied for each and every  $\xi_k$ . A sufficient condition is the trivial case where

$$N = N', \quad \rho_1 = \rho_2,$$

$$x_{1j} = x_{1'j}, \quad x_{2j} = x_{2'j}, \quad z_{1j} = z_{1'j}, \quad z_{2j} = z_{2'j} \quad (j=1, 2, \dots, N) \quad (4.6)$$



By referring to equation (4.1), it may be readily conjectured that equation (4.5) will not be otherwise satisfied for all possible values of  $\xi$  and the implied geometrical considerations lead to the conclusion that the solution is unique.

However, a rigorous mathematical proof that equations (4.6) are the only conditions that satisfy equation (4.5) for all possible values of  $\xi$ , is obtainable by showing that the harmonic continuation of the second derivative of some complex function of the external gravity field is singular at each corner of the  $N$ -sided polygon (R.A. Smith, private communication). This means that a second  $N$ -sided polygon producing exactly the same external field will necessarily have all its corners coincident with those of the first polygon.

For  $N' > N$ , the above results are still obtainable since this simply implies that the extra  $N' - N$  sides will define co-linear segments on one or more of the sides and no extra corners will appear. However, an exact solution of an anomaly caused by an  $N$ -sided polygon is unobtainable if the solution is represented by an  $N'$ -sided polygon, when  $N' < N$ . This is the main cause of factor III and is discussed more fully in section 4.4.

The applicability of our conclusions were tested using non-linear optimisation techniques. We set up a Euclidean hyperspace defined by  $M$  mutually orthogonal axes where  $M$  is the number of parameters (including density contrast) that represent the polygon. The objective function is then defined

by

$$F(\underline{c}) = \sum_{k=1}^n (A_k - S_k)^2 \quad (4.7)$$

where  $\underline{c}$  is an  $M$ -dimensional vector representing the parameters defining the model,  $n$  is the number of observation points and  $S_k$  is the calculated anomaly of a polygon defined by  $\underline{c}$ .

The search is carried out using an anomaly  $A$  due to a polygon defined by  $\underline{c}_0$ . When starting from an arbitrary initial point  $\underline{c}_1$  the search ends either at  $\underline{c}_0$  or at some local minimum for which  $F(\underline{c}) > 0$ . The practical aspect of the facts established above is hence verified.

Therefore, under the conditions imposed in section 4.1, factor I is entirely removed and, in the hypothetical absence of the other factors, the solution is unique. No coordinate or density parameter need be specified.

The case of regular polygons is of particular interest. Let us start by considering the gravity anomaly  $A$  due to an equilateral triangle with radius  $r_0$  and density contrast  $\rho_0$  and with its centre<sup>1</sup> at the point  $x_0, z_0$ . One apex is made to point vertically upwards in order to unify the system of orientation when compared with other regular polygons.

The objective function is

$$F(r, \rho) = \sum_{k=1}^n (A_k - S_k)^2 \quad (4.8)$$

where  $S_k$  is the calculated anomaly due to a regular triangle with the same orientation and with its centre at  $x_0, z_0$ .

$F(r, \rho)$  is mapped for the range  $0 < r < z_0$  and for the

---

1. The radius and centre of a regular polygon refer to those of the escribing circle.

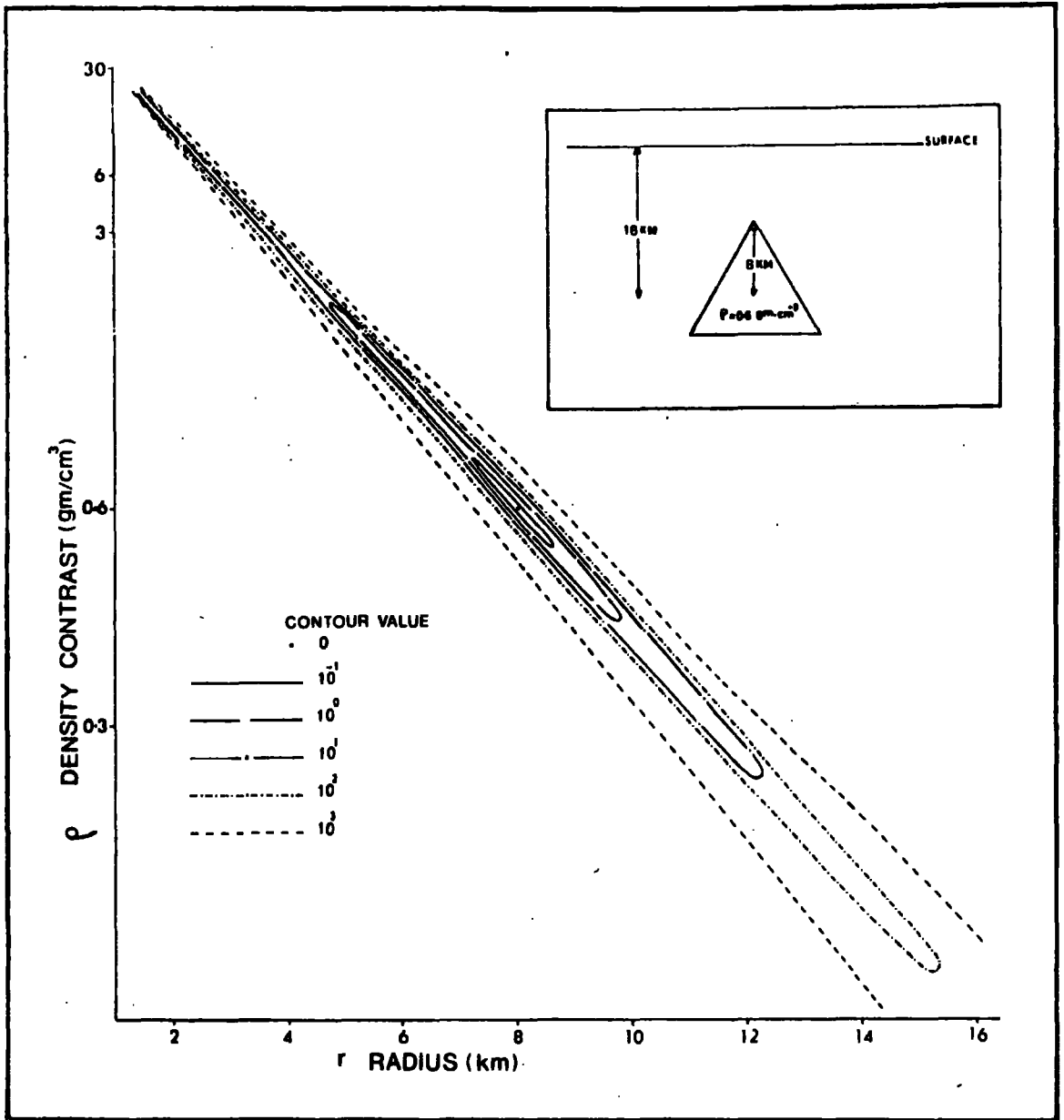


Fig. 4.1. The radius and density contrast as the only variables of an objective function defined by equation (4.8). The observed anomaly is due to a regular triangle of radius 8 km and density contrast  $0.6 \text{ gm/cm}^3$ . The uniqueness of solution is clearly demonstrated.

corresponding range of  $\rho$  that would result in the same mass/unit length as the triangle at  $r_0, \rho_0$ , (Fig. 4.1). This range of mapping is sufficient to show the behaviour of the objective function over all feasible possibilities. Fig. 4.1 shows the unique solution at  $r_0, \rho_0$  distinctly situated along an axis of low values or a 'trough'. All points along the middle of this trough have the same mass/unit length as the triangle at  $r_0, \rho_0$ .

$F(r, \rho)$  is similarly mapped for a square (Fig 4.2) and a hexagon (Fig 4.3). The uniqueness of solutions is again clearly demonstrated in both cases. However, the increase in the number of sides is accompanied by a rapid increase in the length of every contour in the trough containing the solution. As  $N$  continues to increase and the body asymptotically approaches a circular cross-section, the trough stretches further and uniqueness becomes acceptable only if computer truncation errors are allowed for. At  $N = \infty$ , it is clear that, even down to zero tolerance, all points  $(r, \rho)$  having the correct mass/unit length provide a solution and the case becomes completely non-unique.

Similar experiments on other geometrical shapes, such as ellipses, do not show any ambiguity as  $N$  is increased. The observation is, therefore, not related to employing a large number of sides to define the model, a factor whose role will be explained more fully in section 4.4.

These results are of fundamental importance for they show that the widely advocated use of a horizontal cylinder (or a sphere) to illustrate basic ambiguity is unrepresentative since

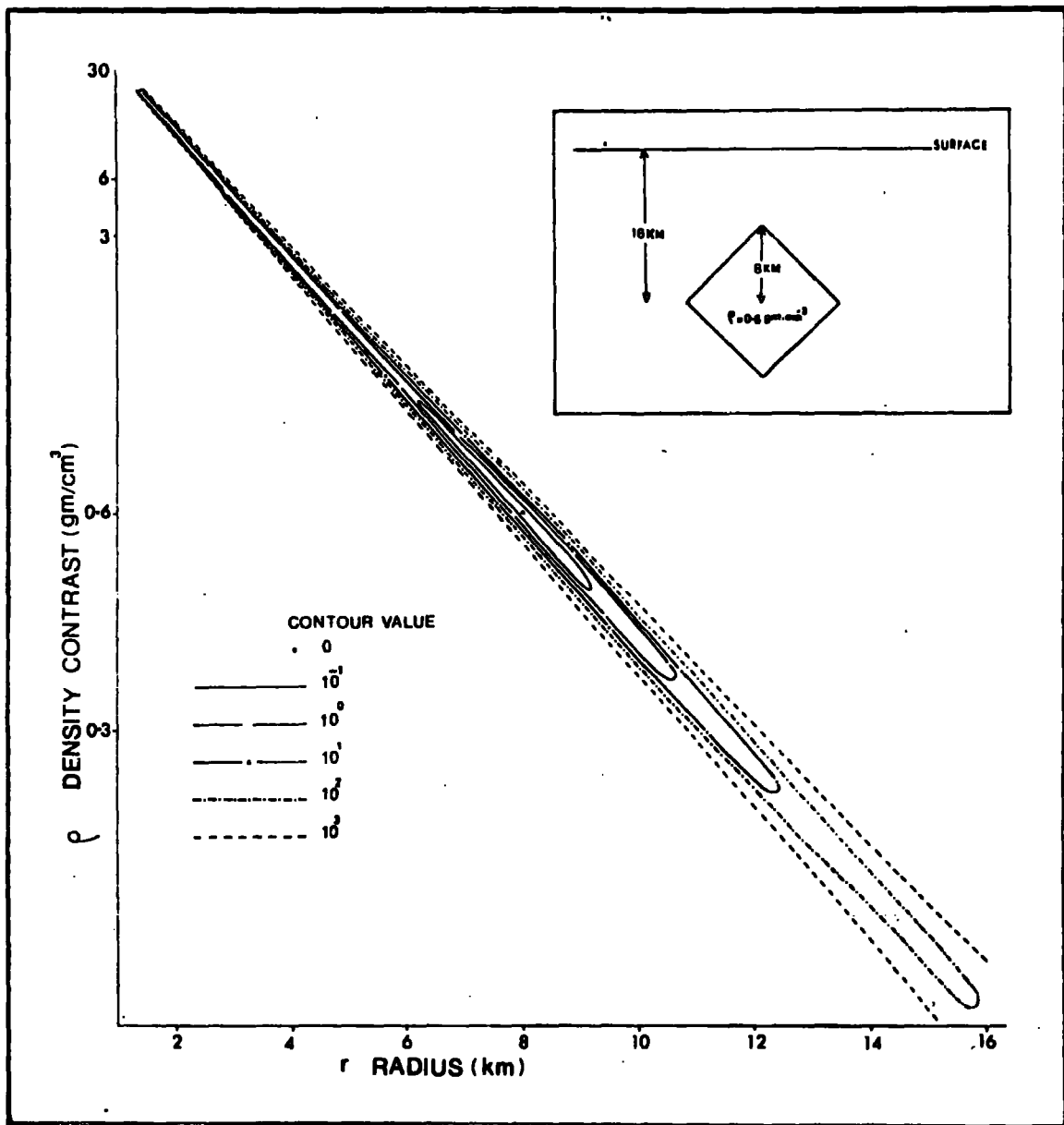


Fig. 4.2. A map of the same function as in Fig. 4.1 for a square of radius 8 km and density contrast  $0.6 \text{ gm/cm}^3$ . The uniqueness of solution is still obvious but is less well established than in the case of a regular triangle.

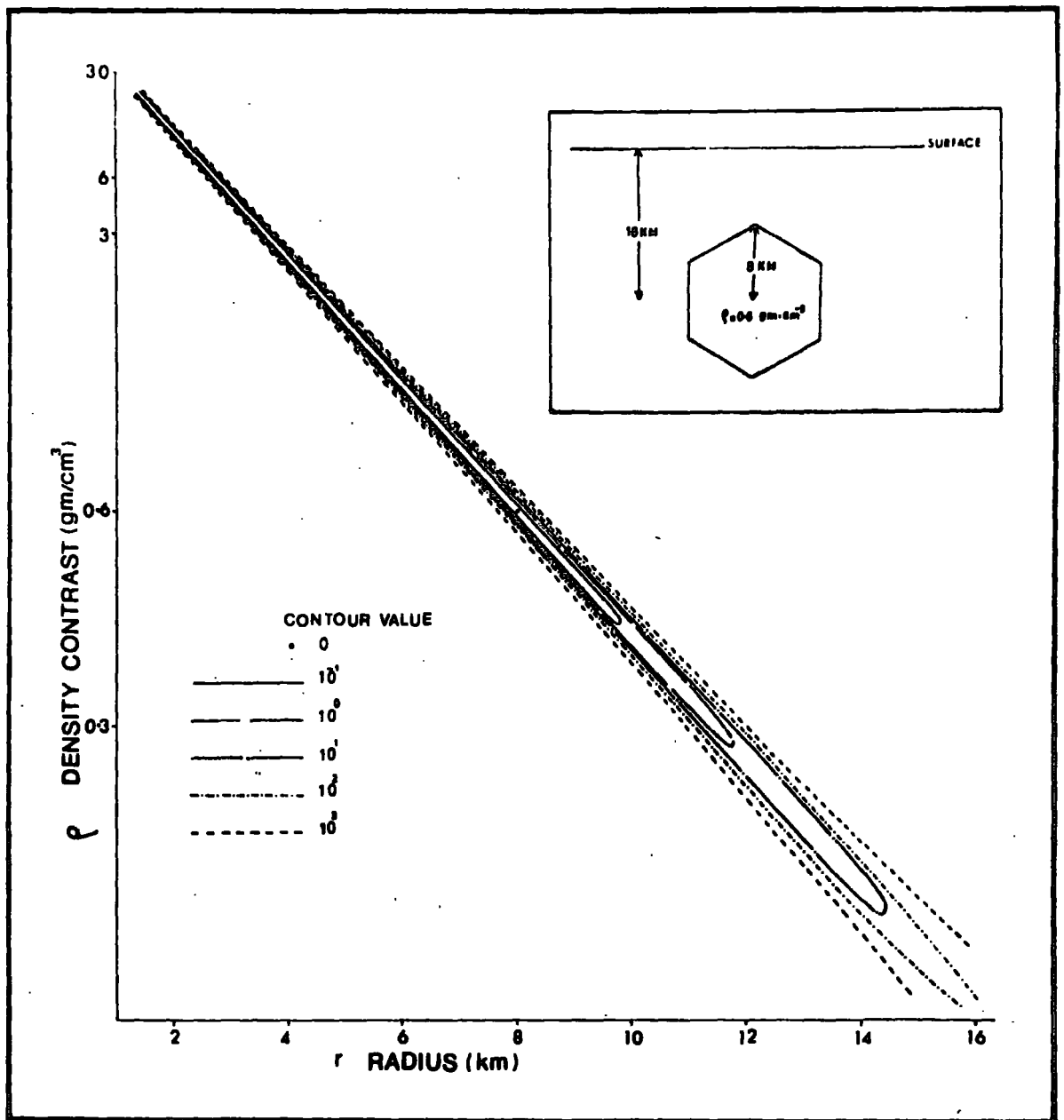


Fig. 4.3. A map of the same function as in Fig. 4.1 for a regular hexagon. The uniqueness of solution is still apparent but the trough containing the solution is very elongated

as we have seen, a circular cross-section is a singular case in a problem in which the solution for a polygon is unique.

However, for practical purposes, where exact representation and measurement are not possible, this would show that bodies which approximate a circle in cross-section cause more ambiguity than those which deviate from such shapes. It is possible that other shapes causing a similar ambiguity may exist although our limited investigation of this possibility was inconclusive.

#### 4.3. Influence of Anomaly Length and Number of Points

The range of  $n$  in a given objective function should, in theory, include all points  $(\xi, 0)$  and should extend to infinity on both sides of the model. In practice, the limitation is two-fold.

1. The anomaly is usually known only for a finite range because of the influence of neighbouring anomalies.
2. The measurements are usually made or digitised at a finite number of discrete points.

The effect of the two limitations was studied by mapping the objective function in the parameter hyperspace.

When the length of the profile gets smaller but is still sufficient to extend on both sides of the model, only the sharpness of definition of the solution at  $\underline{c}_0$  is reduced;  $\underline{c}_0$  is now a vector defining a general polygon which causes the anomaly, i.e. the global solution. As the profile is shortened further, new minima in the hyperspace begin to appear rapidly and new solutions become, therefore, acceptable within some tolerance.

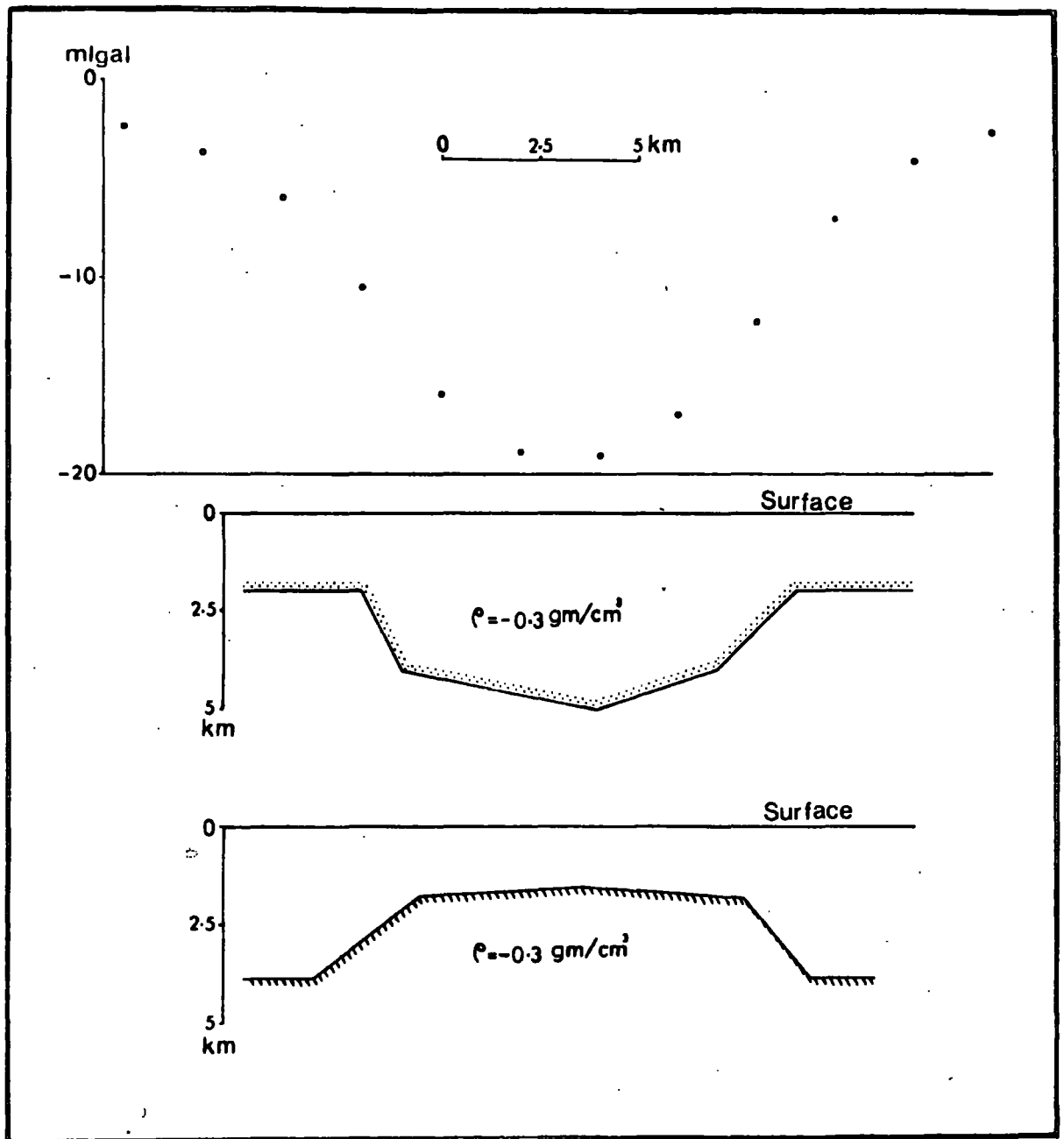


Fig. 4.4. The basin-like model and the batholith-like model both satisfy the negative gravity anomaly shown by the black circles within 0.04 milligal. This is a consequence of using widely spaced observation points.  $\rho$  = density contrast.



The second limitation similarly influences the sharpness of definition of the solution at  $\underline{c}_0$  when the density of the observation points is still sufficient to describe the anomaly adequately. When the density of points decreases further, new solutions also appear but, generally, less rapidly than in the first case. However, the appearance of new solutions is such that many of them develop in feasible regions quite remote from that containing  $\underline{c}_0$ . Hence, a batholith-like structure may satisfy an anomaly caused by a basin-like structure (Fig. 4.4). This is probably related to the inaccurate definition of the higher derivatives of the gravity profile as the density of points decreases; the second derivative has already been suggested as a criterion to distinguish basin-like structures from batholith-like structures (Bott, 1962)

Unless otherwise suggested, it will be assumed in the subsequent text that a finite but sufficient length of the profile, with a sufficient number of points, is being considered.

#### 4.4. Model Approximation

##### 4.4.1. Adequate models

An adequately representative model is defined as one which gives a concise 'summary' of the anomalous feature, outlining all its essential aspects. Thus, a model, at its best, can be no more than a fairly adequate representation. The number of sides defining the anomalous feature,  $N$ , is never actually known and is frequently prohibitively large for an exactly representing model. Moreover, the model

assumes straight and well defined contrast boundaries and a homogeneously distributed density (or magnetisation). Whilst these assumptions are sometimes closely approximated when the overall anomalous feature is considered on the surface, deviations from such assumptions are common in practice. Two-dimensional work suffers from the additional drawback that conditions along the y-axis are seldom as uniform as assumed. These and other familiar causes combine to give rise to the ambiguity discussed below.

Assuming that the number of parameters defining the anomalous feature and the model representing it are  $M$  and  $M'$  respectively, an exact solution was shown in section 4.2 to be unique for  $N' \geq N$  and unobtainable for  $N' < N$ . In practice, one is faced with the problem where  $N' \ll N$  and it is strictly this situation that we shall discuss now ( $M = 2(N+1)+1$  if we include the density contrast).

The absence of an exact solution results into the development of a number of approximate solutions. This is more easily visualised by constructing an  $M'$  - dimensional hyperspace, each of its mutually orthogonal axes representing a model parameter. Each solution is then a local minimum for which

$$0 < F(\underline{c}) < \sigma \quad (4.9)$$

where  $\sigma$  is a tolerance limit and  $F(\underline{c})$  is defined by

$$F(\underline{c}) = \sum_{k=1}^n (A_k - S_k)^2 \quad (4.10)$$

$\underline{c}$  being now an  $M'$  - dimensional vector representing the

parameters of the model.  $S$  is the anomaly caused by the model while  $A$  is the observed anomaly.  $\sigma$  is determined in practice by the amplitude of observational errors to be presented in section 4.5 but, for the sake of clarity, we shall treat them separately.

There are two distinct roles played by  $M'$ . Firstly, a large number of parameters on the model is sometimes necessary in order to represent those anomalous features which do not behave as simple bodies. Secondly, when the  $M'$  dimensional hyperspace is considered, a large  $M'$  causes the development of a large number of possible solutions. This is due to the increased number of possible combinations that would give a reasonable fit between  $A$  and  $S$ . Hence, while a large number of parameters can increase representation it can also increase ambiguity. The relative contribution to either factor depends upon the particular problem being solved. However, the situation is usually simpler in practice due to the decrease of the resolving power of gravity and magnetic methods with depth.

A large number of local minima may appear in regions that are geologically unfeasible. We shall assume, however, that the hyperspace could be constrained so that we may exclusively deal with geologically feasible regions.

The solution minima in the feasible region are generally clustered within a region which would have contained the unique global solution had the anomalous body been simple enough so that  $M = M'$ . The parameters defining these solutions are, therefore, of the right order of magnitude,

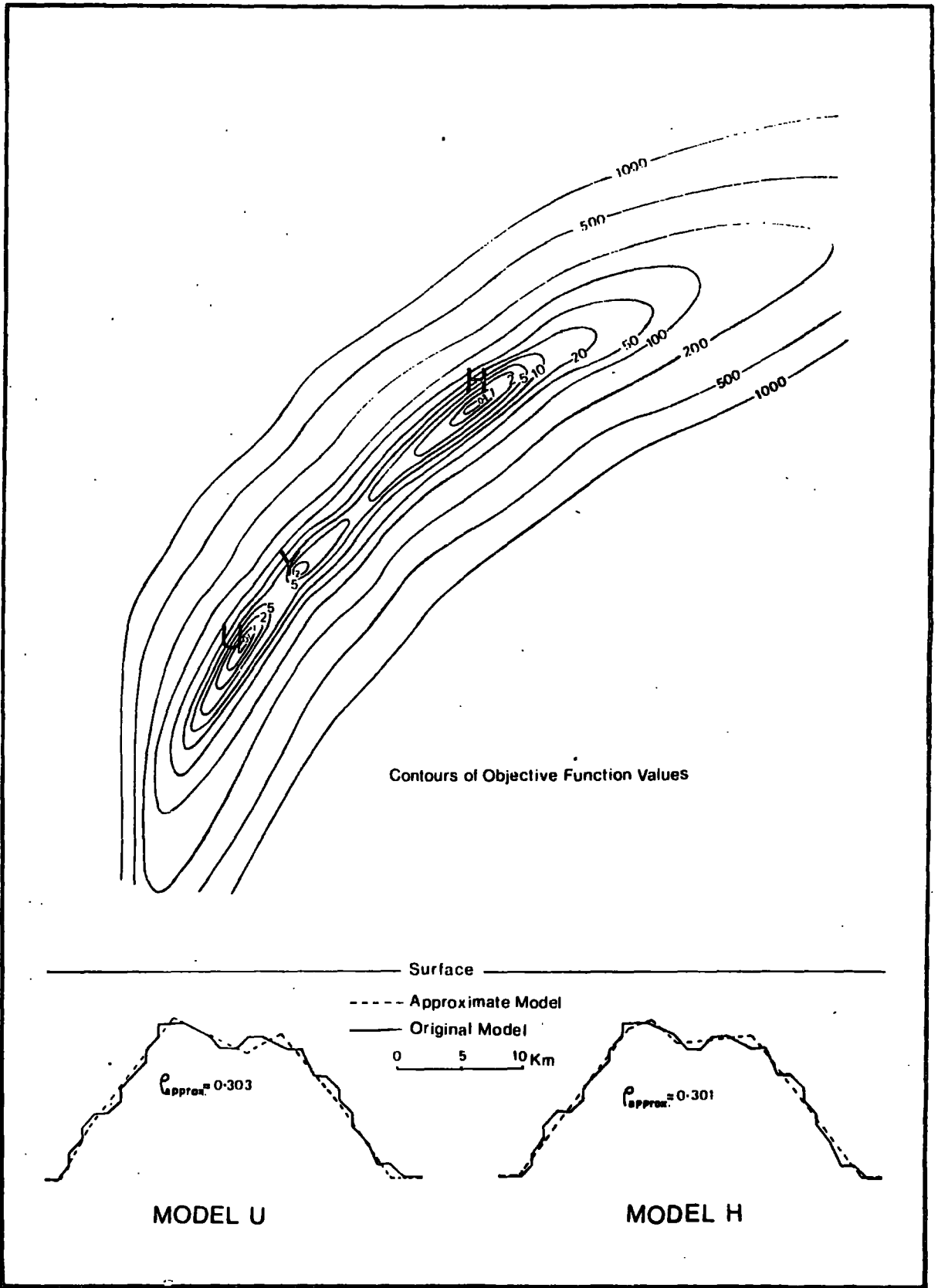


Fig. 4.5. A cross-section in the hyperspace of an objective function corresponding to a gravity anomaly caused by a 30-sided polygon and interpreted using a six-sided model. Each of solutions U and H emphasises a different aspect of the original polygon.

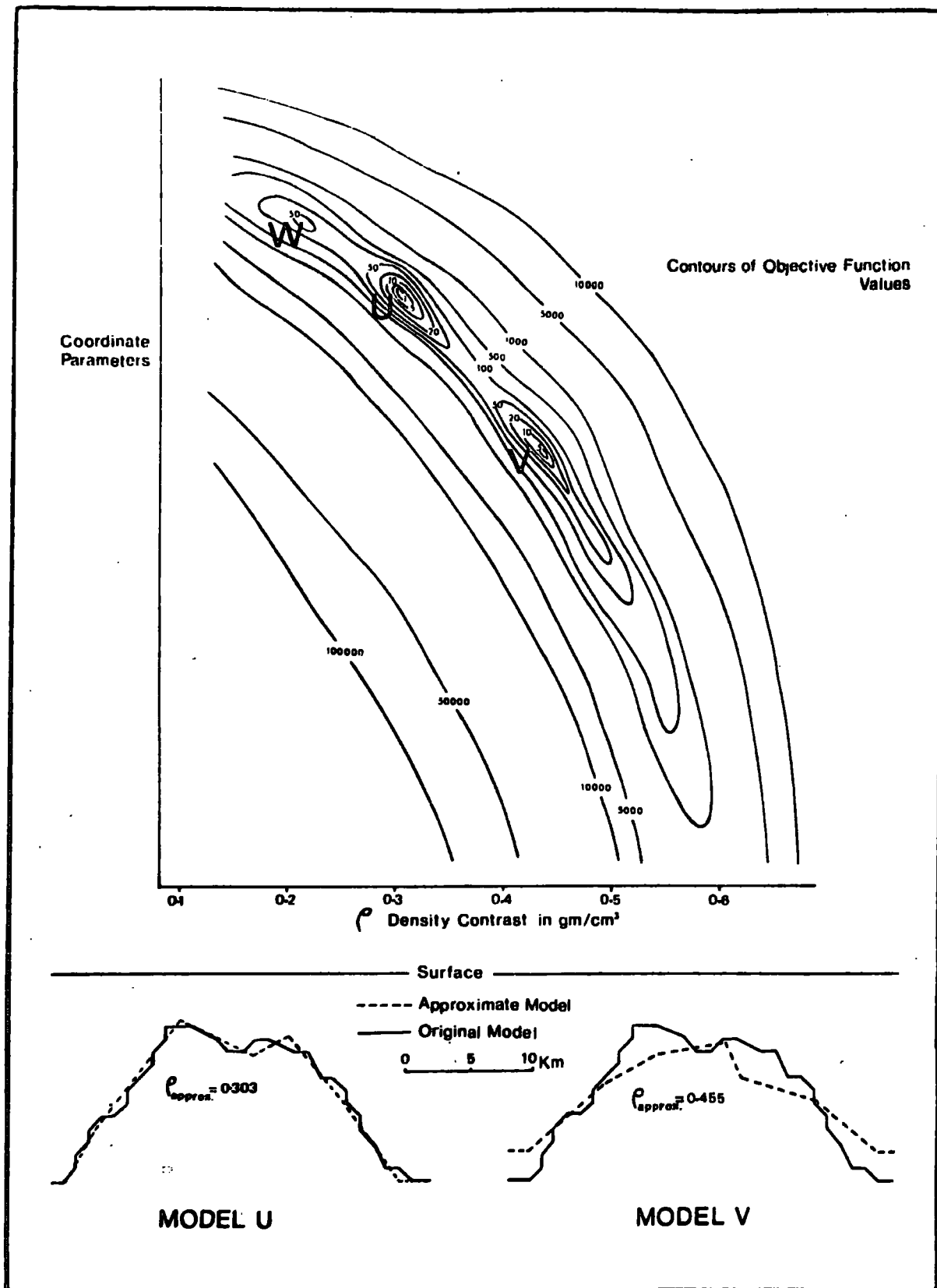


Fig. 4.6. A cross-section in the  $\underline{c}$  hyperspace of the same objective function as in Fig. 4.5, parallel to the density contrast axis. The trough containing U and V (not wholly in the plane of the section) is a 'valley of ambiguity' for a function value  $< 10$ .

an important statement which will be more accurately qualified when the region containing the cluster of minima is discussed more fully.

Figs. 4.5 and 4.6 show a hypothetical case (only factor III being effective) where an anomalous 30-sided body is represented by a six-sided model. The orientation of Fig. 4.6, parallel to the density contrast axis, is adopted to show the effect of not specifying the density contrast and will help later discussions.

The behaviour of the objective function, as revealed in Figs 4.5 and 4.6 is typical of its general behaviour in the multi-dimensional space. A similar study of a large number of such problems, both real and hypothetical has helped to formulate the following:

i) Minima satisfying  $F < \sigma$  are all good solutions. Depending on its particular coordinate in the hyperspace, each solution emphasises certain aspects of the anomalous feature. Minima H and U in Fig 4.5 are examples of such different emphases both of which represent satisfactory solutions.

ii) The value of  $\sigma$  determines the extent of the region containing acceptable solutions. For example, minimum V (Fig 4.6) is regarded as a good solution for quite a low value of  $\sigma$  while minimum W would also become an acceptable solution if  $\sigma$  is increased proportionately. In this sense a solution can no longer be represented by a single point in the hyperspace but has to refer to a neighbourhood of this point bounded by a contour of magnitude  $\sigma$ . Therefore, the trough containing U and H (Fig. 4.5) and that containing U and V

(Fig. 4.6) are each a 'valley of ambiguity' because for some reasonable value of  $\sigma$ , all points along these valleys, not necessarily in the plane of the diagram, would provide a solution.

The range of acceptable solutions can only extend between certain limits determined by the boundaries  $F = \sigma$ . Viewed inversely, this means that for each parameter there exists a certain range beyond which no acceptable solution is obtainable. For example, tests using optimisation techniques show that the value of density contrast for solution V (Fig. 4.6) is about the limit which an acceptable solution could give within that particular  $\sigma$ . Figs. 4.5 and 4.6 also show that increasing  $\sigma$  would rapidly increase the extent of the region containing acceptable solutions.

A familiar predecessor is the work on limiting depth estimation (e.g. Bott and Smith, 1958; Smith, 1959, 1960). We have used a hyperspace illustration to show that there is in fact a limiting range (increasing with increased tolerance) not only for the depth parameters but for every parameter defining the polygonal model.

iii) For a given  $\sigma$ , the range limiting each parameter increases rapidly as the extent and interaction of the factors causing ambiguity increase.

iv.) Specifying any parameter prior to the procedure of obtaining the solution is merely equivalent to confining the search to a space orthogonal to that particular axis at the specified value. Any uniqueness thus obtained is only relative

for there are always solutions that would emphasise a certain aspect of the body even if the specified parameters happened to be extremely representative. Fig. 4.7 shows a hypothetical example of a magnetic anomaly caused by a seven-sided body for which a solution is sought in terms of a four-sided model. Although the bottom of the model and the magnetisation contrast are specified at their actual value, there are several possible solutions. Two of these solutions are shown in Fig. 4.7.

v. The ill-conditioning of a problem may develop for a number of reasons such as using a very large number of parameters to define the model (Fleischer, 1965). Many gravity and magnetic problems are, in fact, ill-conditioned. The distribution of local minima in these problems is such that groups of solutions would cluster into a number of almost isolated regions in the hyperspace. Hence, extensive ambiguity exists when the entire feasible region is considered. However, within each region, some relative uniqueness may be attained. Which of these regions would give a solution depends, primarily, on the position of the initial search point in the hyperspace. This is a definite advantage because one has generally some idea, from the regional geology, about the anomalous feature being investigated such as its approximate depth or shape. The initial point can, therefore, be placed at a favourable position. This effectively limits the search to the desirable region and the ambiguity in the hyperspace, as a whole, is thus largely eliminated. However, in the complete absence of information about the feature, the case



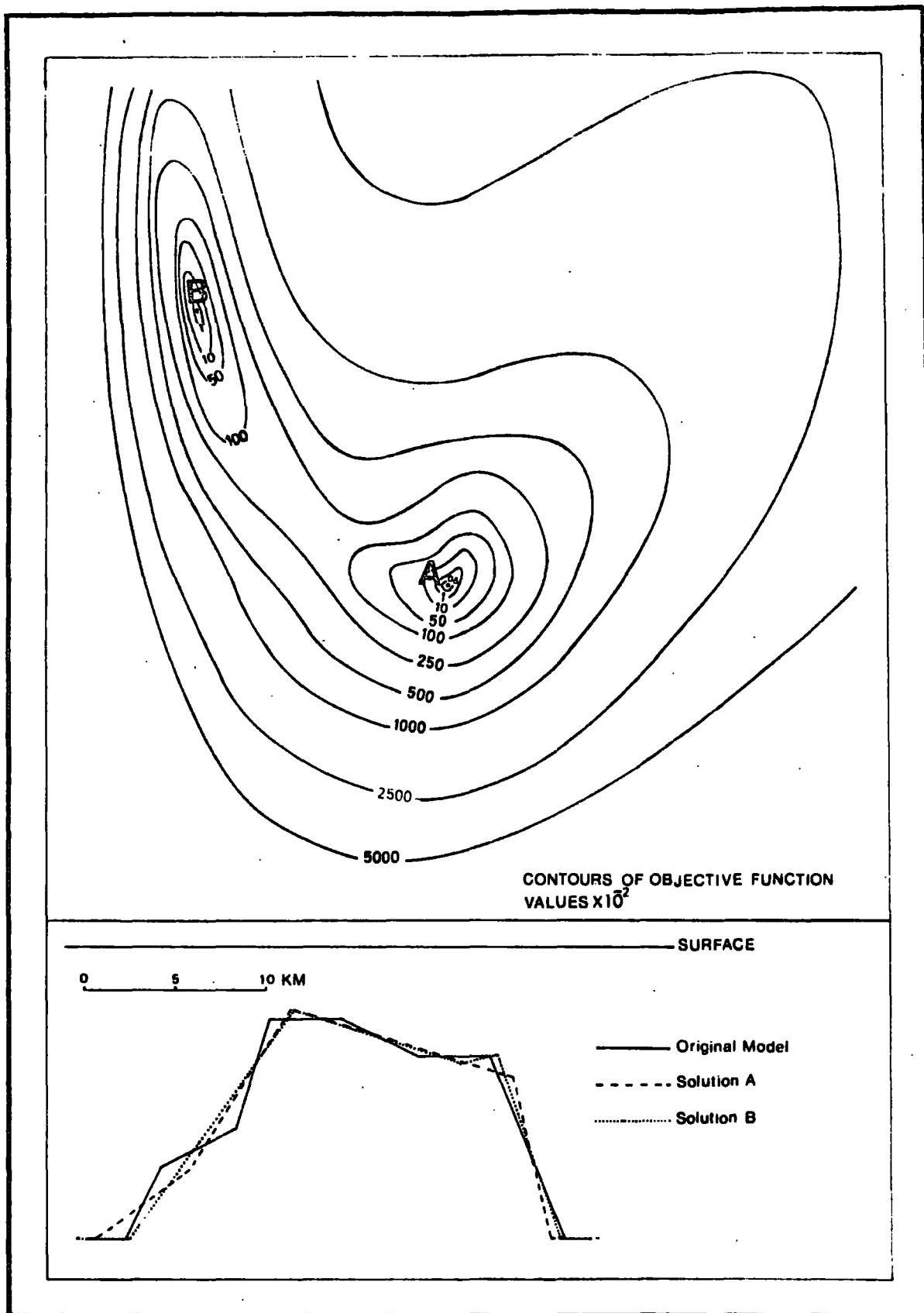


Fig. 4.7. A cross-section in the  $c$  hyperspace of an objective function corresponding to a magnetic anomaly caused by a seven-sided model and interpreted using a four-sided model. The section demonstrates that a unique solution is unobtainable even if the lower (or upper) boundary and the magnetisation contrast are fixed at their precise values.

can become extremely ambiguous (see, for example, Skeels, 1947, Fig. 5).

The position of the initial point is also important in determining, within a given region, the minimum to which the search will converge. This gives the possibility of biasing the solution towards certain aspects of the anomalous feature, if desired.

vi. From an extension of ii - iv, it follows that methods which search for a solution by setting a parameter hyperspace may be effectively employed for range estimation of the parameters. The estimation of the possible range of the basic parameters (see section 4.7) is particularly useful.

#### 4.4.2. Inadequate models

When the number of parameters is not sufficient to define an adequately representative model or when the position of the initial search point in the hyperspace is such that an adequately representative solution would not be obtained, the outcome of the interpretation procedure varies widely. There is a complete gradation from an adequate hyperspace setting to an inadequate one. As the hyperspace setting becomes less adequately representative, solutions ( $F < \sigma$ ) pass from being an actual description of the essential features of the anomalous body to a mere averaging out of such features. When the setting becomes completely inadequate, a solution with  $F < \sigma$  is very difficult to obtain and would, anyway, be usually so unrepresentative that it is often discarded on geological bases.

#### 4.5. Presence of Observational Errors

The consequences of the presence of observational errors, up to a magnitude  $e_{\max}$ , can be illustrated by investigating the objective function

$$F(\underline{c}) = \sum_{k=1}^n (A_k - S_k)^2 \lambda_k \quad (4.11)$$

where  $\lambda_k = 0$  if  $|A_k - S_k| \leq e_{\max}$

and  $\lambda_k = 1$  if  $|A_k - S_k| < e_{\max}$

The presence of  $e_{\max}$  imposes, on the objective function, a tolerance  $E$  which is equivalent to  $\sigma$  discussed in the previous section. Therefore, the statements made in i - vi in the previous section follow in exactly the same way. In particular, a solution, defined as any point in the feasible region satisfying  $F < E$ , refers to a domain bounded by a contour of value  $E$ . Fig. 4.8 illustrates the effect of assuming  $e_{\max} = 1.5$  milligals on the behaviour of the objective function shown in Fig 4.6. It is clear that several solutions would become acceptable even for quite a low value of  $E$  and that the problem as a whole has become less well-conditioned. The value of  $e_{\max}$  is not low but it serves to compensate for the fact that other factors have been largely suppressed. The magnitude of  $e_{\max}$  is perhaps the most vital of all factors, in practice, as it has a direct bearing on  $E$  and  $\sigma$ . When other factors are present on a more tangible scale, a small increase in  $e_{\max}$  causes the development of a

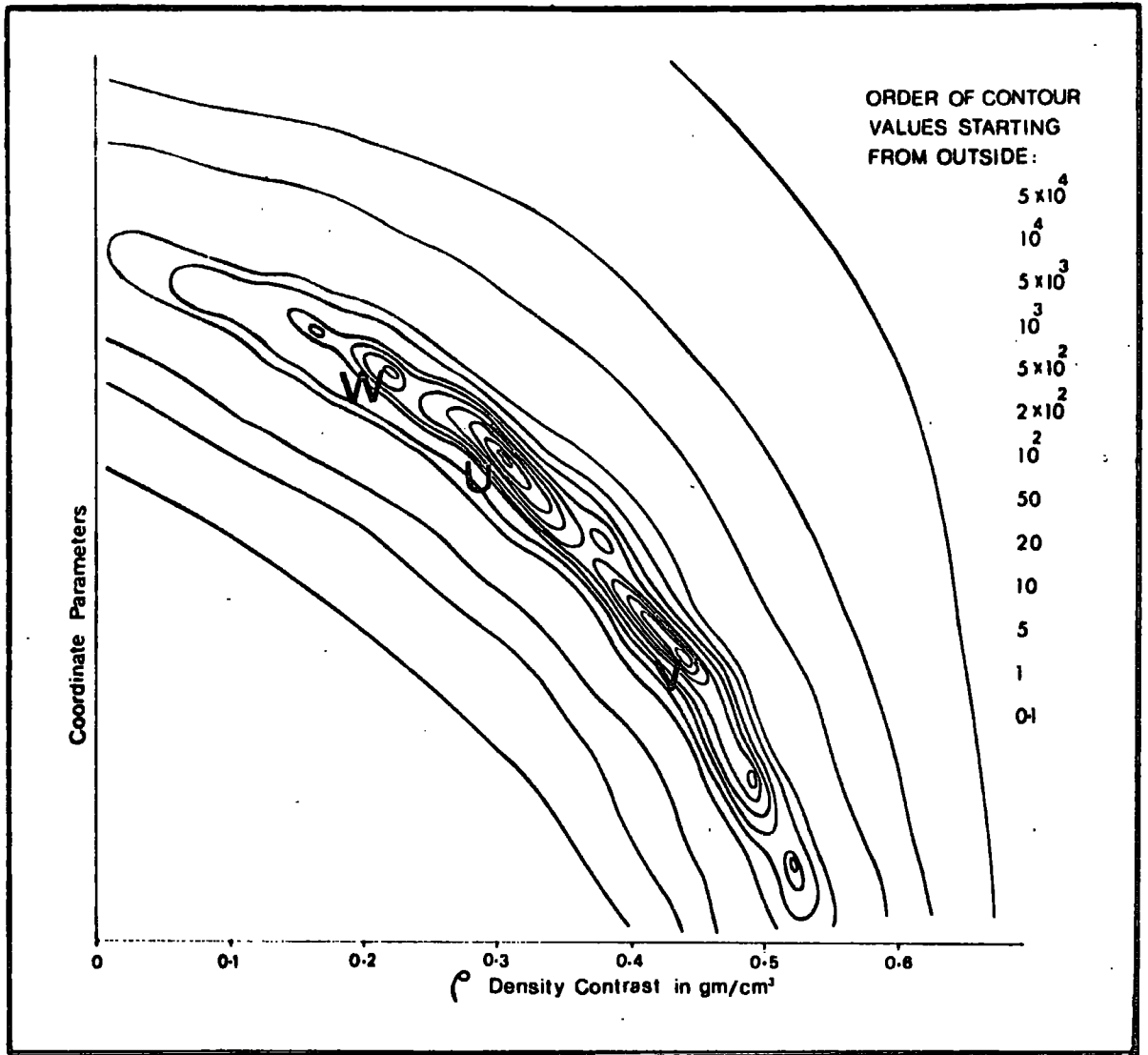


Fig. 4.8. The same cross-section as in Fig. 4.6 when a tolerance of 1.5 mgal is introduced.

large number of local minima and the rapid expansion of the limiting ranges of parameters. Non-representative solutions may therefore appear even if  $e_{\max}$  were quite small. The expansion is most appreciable in the direction of elongation of the objective function. This point implies that if the trend of the objective function bears some parallelism to certain parameters, these parameters will suffer the most increase in ambiguity. The details of this remark will be discussed in section 4.7.

In extreme cases, where  $e_{\max}$  is very large, the region containing permitted solutions becomes so vast that it may occupy a large portion of the geologically feasible hyperspace and the validity of any solution would not be accepted without extensive external control or assumption.

#### 4.6. The Regional Background

A limited amount of theoretical and experimental work has shown that the conclusions reached about the density (or magnetisation) contrast apply, in a general way, to a horizontal regional background, i.e. that which can be represented by a zero order polynomial. Higher order terms cause extensive ambiguity unless their coefficients are specified.

Despite this ambiguity, Corbato (1965) and Johnson (1969) have successfully used higher order polynomials in various interpretations. For the purpose of the present work, however, problems involving the regional background as an additional unknown have been restricted to determining

the zero order term.

#### 4.7. The Question of Uniqueness

Various authors have been able to establish conditions which would ensure, at least in theory, a unique solution (e.g. Sretenskii, 1954; Smith, 1961; Roy, 1962). Although these authors have usually dealt with factor I only, their theoretical considerations have provided us with a strong foundation for uniqueness. Hence, in complying with these conditions, the usual present-day practice is to assume the density contrast of the anomalous feature and one or more depth parameters and to solve for the other parameters (e.g. Bott, 1960; Corbato, 1965). The significance of these conditions can be judged by investigating the behaviour of the objective function in the parameter hyperspace.

Broadly speaking, the parameters defining a model fall into two categories. Firstly, some parameters describe the general properties of the model such as its density contrast, the depth to its top, in the case of a basin-like model, and the depth to its bottom, in the case of a batholith-like model. The regional background is also an important parameter. We shall call these the basic parameters. Fig. 4.9 shows the behaviour of the objective function of the anomaly due to the basin shown in Fig. 4.4. The section is parallel to the axis representing the depth to the top of the basin and is inclined to the axes of the other parameters. Secondly, all other coordinate points describe the details of the model and could therefore emphasise one aspect of the anomalous body or another. The presence of these coordinate points as

a whole is essential to the model but the deletion or creation of individual ones will not cause a loss of generality. These are, therefore, secondary parameters. Intuition, experience and experiments suggest that the objective function bears much more parallelism to the axes of the basic parameters than to those of the secondary parameters. It is difficult to demonstrate parallelism on cross-sections since it is highly dependent upon the orientation of the section. However, if we consider a particular contour whose value is determined by the tolerance of the problem then parallelism to a given parameter, in the hyperspace, may be thought of in terms of the extent of this contour in the direction of the parameter. Figs. 4.6 and 4.9 may, in this way, be used to give some indication of the parallelism to the density contrast and depth parameters, respectively. Fig 4.9 also illustrates the idea of maximum depth estimation, within the realm of the factors discussed so far.

It follows from this parallelism that two anomalies similar to within a small value of  $\sigma$  or  $E$  are not necessarily produced by bodies that are approximately similar. By specifying the basic parameters, the search for a solution is confined to a hyperspace in which the objective function bears little parallelism to any axis and in which the domain containing acceptable solutions is very limited. Thus, by reducing the dimensionality of the problem, in this manner, a vast ambiguous region is avoided and a relatively unique solution may be expected. However, absolute uniqueness is still unobtainable (iv, section 4.4).

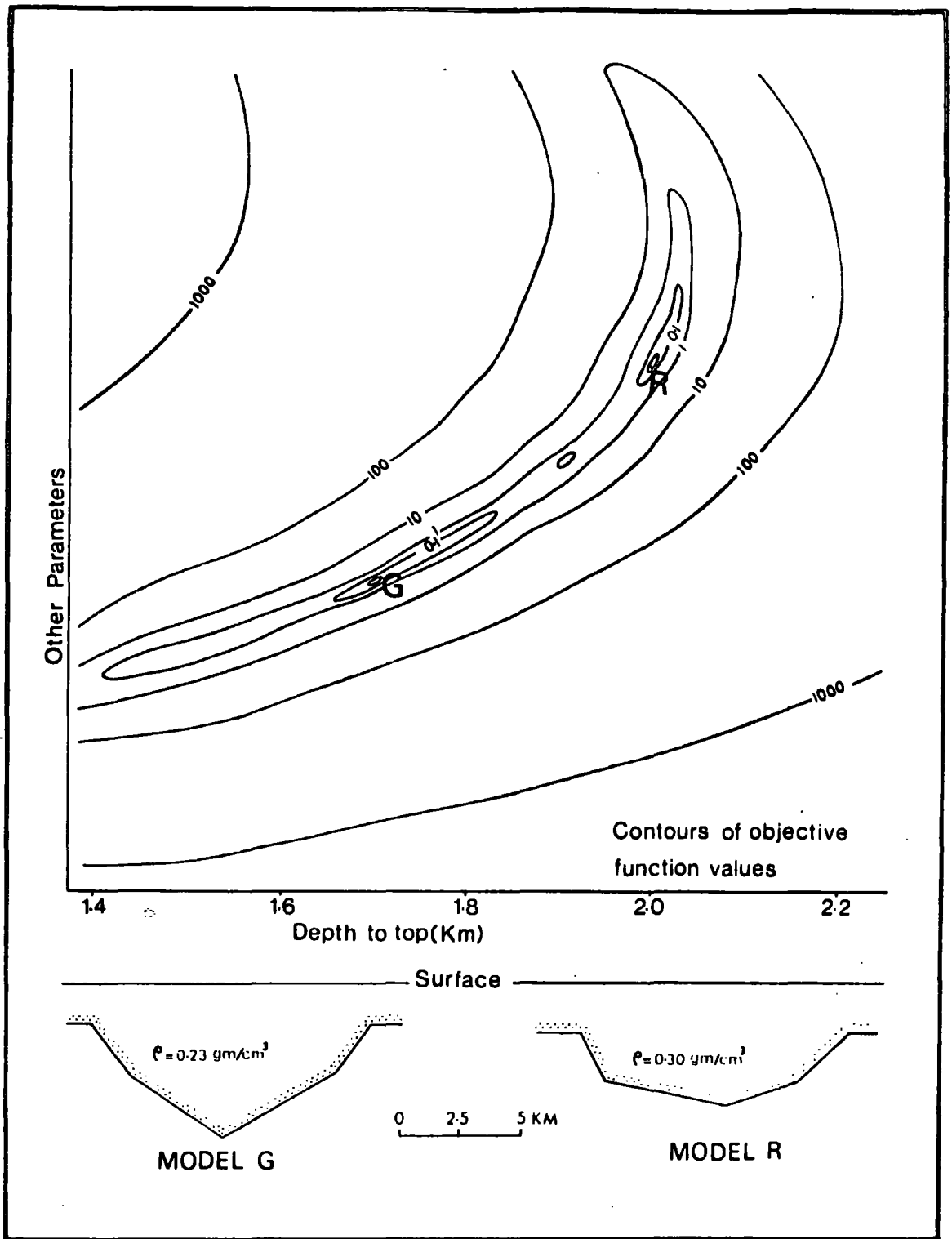


Fig. 4.9. A cross-section, parallel to the axis representing the depth to the top of the model, in the hyperspace of an objective function corresponding to a gravity anomaly caused by a basin. The section gives some indication of the 'parallelism' which the function bears to the axis representing the depth to the top of the model. The back-swing of the function is an indication of the maximum depth which the model can have and which increases with increased tolerance.



The extent of parallelism to any parameter varies according to individual problems. When the factors causing ambiguity are limited, the tolerance is very low and only little parallelism will be possible. Starting from a good initial point and without assuming any parameter, solutions thus obtained will be of the correct order of magnitude. This is especially useful when the basic parameters cannot be established with accuracy e.g. when interpreting basement features. An underestimation of 10% of the density contrast in the problem of Fig 4.5, for example, leads to a solution (not in the plane of the diagram) which is far less satisfactory than would have been obtained had the density contrast not been specified.

In general, the adherence to the 'order of magnitude' depends on the presence and interaction of the various factors causing ambiguity. In many cases, when these factors are not small but also not extensive, a satisfactory solution may be still obtainable by specifying one of the basic parameters only. However, when the presence of ambiguity factors is more conspicuous so that possible solutions are scattered in a vast region, it is obvious that the usual procedure of obtaining a number of solutions, by specifying the basic parameters at a set of intervals, is both desirable and necessary.

#### 4.8. Discussion of Some Examples

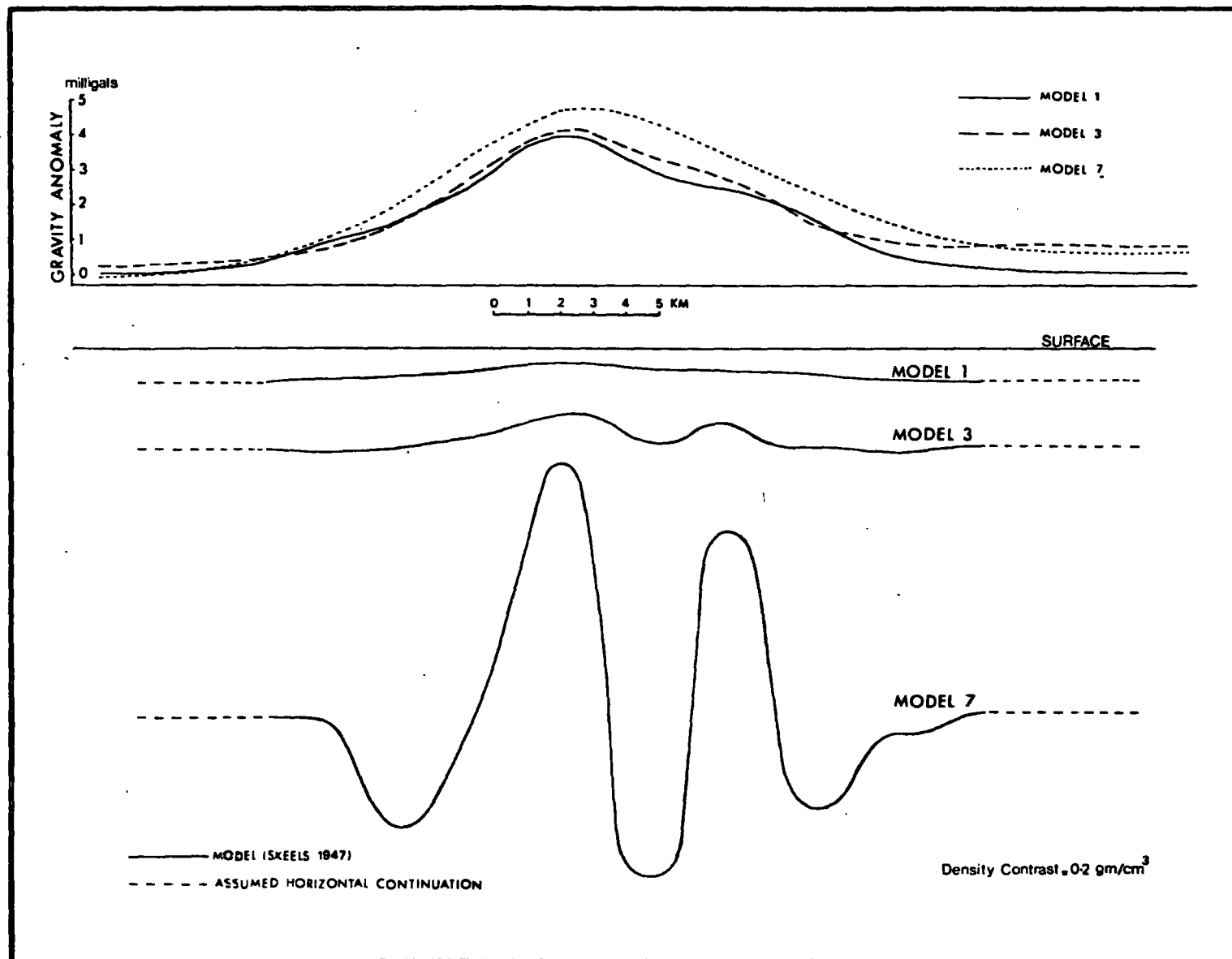
In attempting to warn against the dangers of ambiguity, past work has tended to over-emphasise these dangers. We

shall use the classical example of Skeels (1947, Fig. 1) for illustration. The example presents a gravity anomaly of a maximum amplitude of 4 milligals and shows seven different models which should satisfy the anomaly within 0.1 milligal.

The main source of ambiguity in the example is the decrease in the resolving power of the gravity method when the width of successive anomalous features becomes small compared with their depth (e.g. Bullard and Cooper, 1948). This source, which is related to the ill-conditioning of the problem, is not representative of the major factors in ambiguity and is a drawback shared with almost all other geophysical methods. It is true that extensive ambiguity is present but, if one has even a rough idea about the anomalous feature, a good choice of the initial search point would be possible. The ambiguity is then largely reduced (v, section 4.4).

Moreover, a re-computation of the anomalies caused by three of the seven models was made (Fig 4.10). These models were approximated by open polygons which did not differ from them by more than the thickness of the line representing each model. Equation 4.1 was used in the calculation. It is clear that, despite occasional agreement, the three anomalies are essentially different. Adherence to Skeel's suggestion is not verified and discrepancies of up to 13 times the claimed limit are present. The situation will not be remedied by assuming a different density contrast or changing the background anomaly.

Fig. 4.10  
A re-computation of  
the anomalies caused  
by three of the  
seven models presented  
by Skeels (Fig.  
1, 1947).



Other points must also be considered. The amplitude of the anomaly is quite low and, therefore, tends to attenuate the discrepancies in absolute terms. Also, had a fuller length of the profile been considered, relative disagreement between the anomalies would have been more apparent, particularly as the deeper models would cause longer anomalies.

It is conceivable that better agreement may be obtained if certain modifications to the model were made. Such modifications, however, will fall within the realm of the factors discussed already.

The above-mentioned discrepancies would not have escaped detection had better computing facilities been available. Hence, while this example has served the excellent purpose of showing that an absolutely unique solution is unrealisable in practice, the lack of computing facilities appears to have led to overlooking the existence of situations where ambiguity could be extremely limited.

Let us now consider an example solved in the light of the facts presented in this work. A negative gravity anomaly across the Pennines is attributed to the Weardale Granite which a centrally placed borehole encountered at a depth of 400 metres. The density contrast with the country rock is estimated to be  $-0.11$  to  $-0.15$  gm/cm<sup>3</sup> (Bott, 1967a) whereas the regional background could range from 9 to 14 milligals. End corrections (Nettleton, p.117) were applied to reduce the anomaly to a two-dimensional case and the accuracy of each point is about 0.5 milligal.

The anomaly was interpreted using the method of rotating

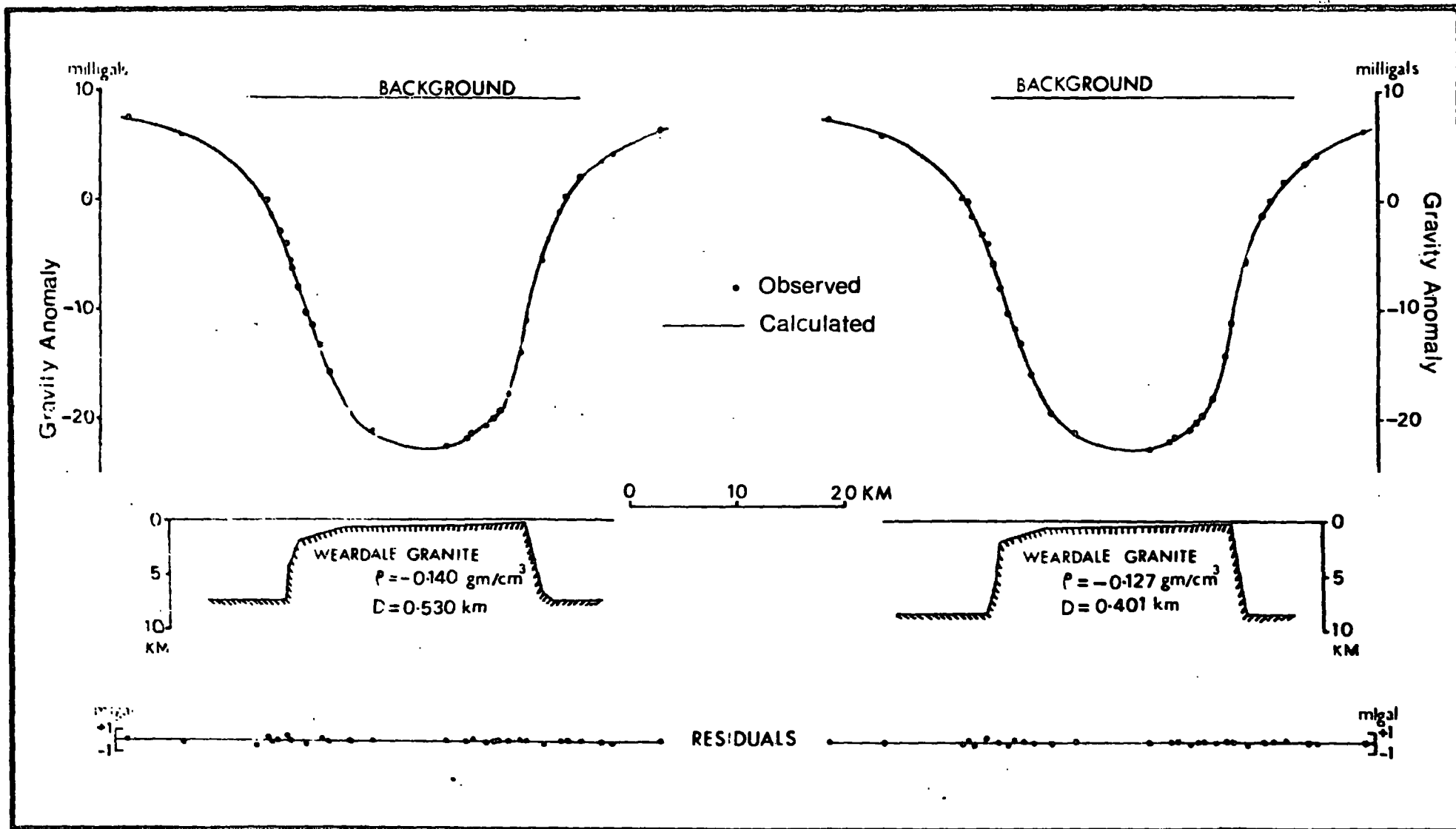


Fig.4.11 Two interpretations of a gravity anomaly across the Weardale Granite. No parameters were fixed and the resulting parameters are of the correct order of magnitude.  $D$  = the resulting depth to the top of the borehole position.  $\rho$  = density contrast.

coordinates (section 3.4.3.1). and assuming a polygonal model of a uniform density contrast with the surrounding country rock. All parameters (including the density contrast and the regional) were left unspecified and, virtually, no limit was imposed on the range in which each parameter could vary except that the model should be geologically feasible.

Two interpretations, each starting from a different initial point, are shown in Fig.4.11. These two models are representative of a large number of other solutions all of which show a remarkable agreement between themselves as well as with the geological occurrence. The depth to the top, the density contrast and the regional background fall well within the expected order of magnitude. The depth to the bottom varies within an estimated range obtained independently by an interpretation procedure based on specifying the density contrast, the regional and the depth to the top (Bott, 1967a; Tanner, 1967).

#### 4.9. Conclusions

A gravity or magnetic anomaly caused by a two-dimensional polygonal model has a unique solution in theory. In practice, ambiguity arises from the presence of observational errors, lack of adherence to the ideal conditions assumed by the model, inadequate definition of the anomaly over its entire length and other factors. The resulting ambiguity takes the form of a scatter of local minima or an elongated 'valley of ambiguity'. Possible solutions will agree between themselves to an order of magnitude determined by the extent

of the region(s) they occupy and, therefore, by the tolerance of the problem. The agreement between these solutions, i.e. the degree of uniqueness in the general solution to the problem, increase as the effect of the factors causing ambiguity decreases and as more basic parameters are specified. The position of the initial point in the hyperspace determines the particular solution to which the search will converge.

Absolute uniqueness is not generally obtainable because there are usually other solutions which would emphasise different aspects of the anomalous feature. A high degree of relative uniqueness is only obtainable within specified basic parameters. However, if some or all of the basic parameters are unspecified, the outcome of the search in the hyperspace is not unpredictable.<sup>1</sup> In these cases, the role of specifying the basic parameters is substituted by the position of the initial point while uniqueness is replaced by the concept of the 'order of magnitude'. Under favourable conditions, solutions may agree between themselves to a close 'order of magnitude'. However, conditions are not usually favourable so that specifying some or all of the basic parameters becomes necessary.

---

1. Search by sequential or random methods is an obvious exception.

## C H A P T E R 5

### GRAVITY INTERPRETATION

#### 5.1. Introduction

The common methods of interpreting gravity anomalies are based on the "forward" approach, i.e. given a model simulating a geological feature it is required to calculate its gravity anomaly. The calculated anomaly is then compared with the observed one and the model's parameters are re-adjusted until a satisfactory fit is obtained. This is an indirect procedure.

There are several direct procedures. They include transforming the anomaly by upward or downward continuation (e.g. Peters, 1949; Dean, 1958). The first and second derivatives of the anomaly may be obtained using other transformations (e.g. Baranov, 1953; Evjen, 1936; Rosenbach, 1953). The purposes of these transformations are usually qualitative. The  $\sin x/x$  method (Tomado and Aki, 1955) and methods which use certain estimators on the anomaly (e.g. Jung, 1953; Smith, 1959) are of more quantitative objective. However, direct methods of interpretation are not of immediate concern to us here and will not be discussed further.

When computing facilities were limited, dot charts and graticules (Levine, 1941; Hubbert, 1948) provided suitable means for calculating the anomaly caused by a model. Mechanical integrators (Siegert, 1942)



were also in use. The increased availability of computers caused two major changes. Firstly, faster and more accurate methods for calculating the anomaly were introduced (e.g. Talwani et al, 1959; Bott, 1969a). Secondly, it became possible to perform the process of adjusting the model parameters automatically using some iterative procedure (e.g. Bott, 1960; La Porte, 1963; Tanner, 1967). These procedures attempt to determine the geometrical details of the anomalous feature, the density contrast(s) being specified. The inverse problem involved is, therefore, basically non-linear (Bott, 1967b).

Non-linear optimisation techniques offer an immediate advantage by being especially designed to treat non-linear problems. Their use in interpreting gravity anomalies was introduced by Stacey (1965) but only limited progress was made because of difficulties with local convergence and low speed of available computers. The present attempt has largely overcome these difficulties. The techniques have been developed to apply to a two-dimensional polygonal model (open or closed) having a uniform density contrast with the surrounding medium. Provisions are also made for cases requiring a number of density contrasts within the model.

Applicability to three-dimensional problems follows in the same way by employing a suitable computational method (e.g. Talwani and Ewing, 1960). However, three-dimensional models usually involve a large number of anomaly points and unknown parameters. Therefore, the required computer time may not be practical. Approximation to a two dimensional

model using end corrections (Nettleton, 1940, p.117) can be used when appropriate. Alternatively, some apparently successful iterative procedures for interpreting three-dimensional models (e.g. La Porte, 1963; Cordell and Henderson, 1968) may be used.

## 5.2. The Auxiliary Procedure

The auxiliary procedure consists of two main parts. In the first part, the gravity anomaly due to the polygonal model is calculated. In the second part, the objective function is calculated. Its value is then returned to the calling optimisation procedure.

### 5.2.1. Calculating the anomaly

The adjustable parameters of the model are passed from the optimisation subroutine. The model is then defined by a series of instructions which allocate the adjustable parameters to the appropriate corners of the model and specify those parameters which are unadjustable. The instructions also define other details of the model, e.g. models requiring a horizontal side are defined by specifying two successive points to be at the same depth, etc.

After defining the model, its gravity anomaly is computed. We adopt a two-dimensional Cartesian system with the anomaly profile taken along the horizontal  $\xi$  - axis perpendicular to the strike of the anomaly and with the  $\zeta$  - axis pointing vertically downwards. Fig. 5.1 illustrates the symbols and adopted convention. Using a formula by Heiland (1940, p.153) and following the familiar method of summing up the effect of

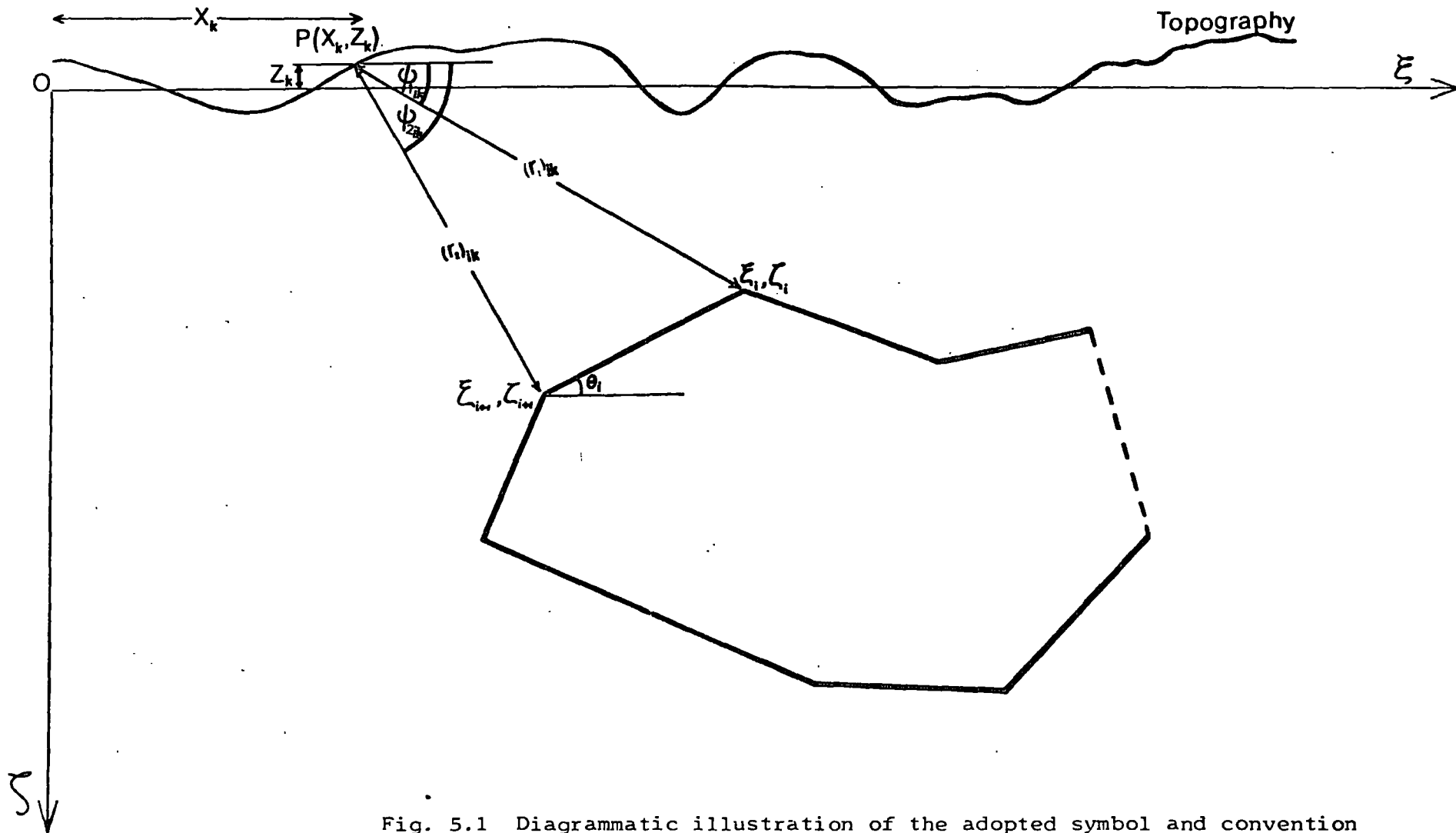


Fig. 5.1 Diagrammatic illustration of the adopted symbol and convention used for the gravity formula at point  $P(X_k, Z_k)$  due to a two-dimensional polygon.

M semi-infinite horizontal step models (Talwani. et al, 1959; Bott, 1969a), the gravity anomaly at the  $k^{\text{th}}$  observation point P ( $X_k, Z_k$ ), due to the resulting M - sided polygon, is given by

$$C_k = 2G \sum_{i=1}^M \rho_i S_{ik} \quad (5.1)$$

where G is the gravitational constant multiplied by a scaling factor appropriate to the units of length being employed,  $\rho_i$  is the density contrast across the  $i^{\text{th}}$  side and

$$S_{ik} = \zeta_{i+1} \phi_{2ik} - \zeta_i \phi_{1ik} - [\zeta_i \sin \theta_i + \zeta_i \cos \theta_i] [\sin \theta_i \log(r_2/r_1) + \cos \theta_i (\phi_{2ik} - \phi_{1ik})] \quad (5.2)$$

For convenience of representation we shall include in  $C_k$  the regional background, B, after reducing it to a horizontal one (see section 4.6). Hence, assuming a uniform density contrast for the model,

$$\begin{aligned} C_k &= B + 2G\rho \sum_{i=1}^M S_{ik} \\ &= B + 2G\rho T_k \\ \text{where } T_k &= \sum_{i=1}^M S_{ik} \end{aligned} \quad (5.3)$$

Equations (5.2) and (5.3) show that  $C_k$  is linear in  $\rho$  and B and non-linear in the coordinate parameters defining

the model. We shall refer to these as the linear and non-linear parameters, respectively. For the purpose of obtaining an optimum solution any of these parameters may be specified at some fixed value or left as an adjustable parameter. However, whether or not to specify a certain parameter must be subject to the considerations discussed in Chapter 4.

### 5.2.2. The Objective function

A number of objective functions are presented below, each being suitable for treating a certain type of problem. The simplest form is given by

$$f(\underline{x}) = \sum_{k=1}^n (A_k - B - 2G\rho T_k)^2 \quad (5.4)$$

where  $\underline{x}$  is an  $m$ -dimensional vector representing the unknown parameters,  $A_k$  is the observed gravity anomaly at  $P(X_k, Z_k)$  and  $n$  is the number of observation points. Equation (5.4) is most suitable when the linear parameters are specified.

As was shown in Chapter 4, there are situations where it may be desirable to obtain a solution without specifying the density contrast. This is obtained by working with a normalised anomaly. Normalisation is achieved by comparing each anomaly value with that at the  $q^{\text{th}}$  point. Hence,

$$f(\underline{x}) = \sum_{k=1}^n (A'_k - T'_k)^2 \quad (5.5)$$

where

$$A'_k = (A_k - B) / (A_q - B)$$

and

$$T'_k = T_k / T_q$$

After an optimum solution is obtained, the density contrast may be recovered from the relation given in equation (5.7).

Alternatively, use may be made of the linear relationships between C and  $\rho$ . Thus, using equation (5.4), we have at the optimum

$$\frac{\partial f}{\partial \rho} = 0 = -2 \sum_{k=1}^n (A_k - B - 2G\rho T_k) (2GT_k) \quad (5.6)$$

$$\therefore \rho = \left[ \sum_{k=1}^n T_k (A_k - B) \right] / \left[ 2G \sum_{k=1}^n T_k^2 \right] \quad (5.7)$$

The objective function is therefore given by

$$f(\underline{x}) = \sum_{k=1}^n \left[ A_k - B - 2G\rho(A, T, B) T_k \right]^2 \quad (5.8)$$

The procedure may be extended to include situations where the two linear parameters are unspecified. Thus, at the optimum

$$\frac{\partial f}{\partial B} = 0 = -2 \sum_{k=1}^n (A_k - B - 2G\rho T_k) \quad (5.9)$$

Equations (5.6) and (5.9) are linear in  $\rho$  and B giving

$$\rho = \left[ n \sum_{k=1}^n A_k T_k - \left( \sum_{k=1}^n A_k \right) \left( \sum_{k=1}^n T_k \right) \right] / 2G \left[ n \sum_{k=1}^n (T_k^2) - \left( \sum_{k=1}^n T_k \right)^2 \right] \quad (5.10)$$

$$B = \frac{1}{n} \left[ \sum_{k=1}^n (A_k) - 2G\rho \sum_{k=1}^n (T_k) \right] \quad (5.11)$$

The objective function is then given by

$$f(\underline{x}) = \sum_{k=1}^n \left[ A_k - B(A, T) - 2G\rho(A, T) T_k \right]^2 \quad (5.12)$$

The objective functions defined by (5.8) and (5.12) both reduce the problem to obtaining a solution by adjusting the model coordinates only. Besides reducing the number of variables, this procedure improves the conditioning of the problem for treatment by non-linear methods because it

involves only those parameters which are properly non-linear. The main disadvantage is the difficulty in obtaining the derivatives with respect to the variable parameters, analytically. Equations (5.8) and (5.12) are, therefore, unsuitable for use in a gradient method.

The general procedure in obtaining equation (5.12) may be extended to problems involving two density contrasts and a regional background, none of which is specified. The solution will probably be ambiguous and will not qualify for the considerations presented in Chapter 4. However, this procedure may be useful in rare cases when several body coordinates are known and it is required to show that the gravity evidence is not against a certain pattern of density distribution.

### 5.3. Available Programmes

The programmes listed below are available in PL/1 F-level. They vary according to the auxiliary procedure which each one incorporates. GAD is for use with P306 (section 3.3.1.3). The other programmes are for use in conjunction with a direct search method and are adapted for P300 (section 3.4.3.1), P301 (section 3.4.2.4) and P303 (section 3.2.3.6). In all programmes, any coordinate parameter defining the polygonal model can be specified or left as an adjustable parameter.

#### 1. GRANOP: Programme specification no. 3a.

The auxiliary procedure is based on equation (5.4). It is most suitable for problems in which the regional background and the density contrast are specified. However the procedure can also handle either or both of them as variable parameters.

As presented, the programme will only accept one density contrast. It may be modified to accept  $m$  density contrasts ( $m \leq$  number of sides) by declaring the density contrast as an array of  $m$  elements, each of which is assigned.

to the appropriate side(s).

2 - GAD: Programme specification no.4.

The auxiliary procedure is based on equation (5.4). In addition to the objective function, the procedure provides the first partial derivatives of the objective function with respect to the variable parameters. The method of obtaining these derivatives is given in Appendix 2.

Either or both of the linear parameters may be specified. The auxiliary procedure can also be modified, on the bases of equation (5.1), to accept a number of density contrasts all of which must be specified.

3. GREGNOP: Programme specification no.3b.

The auxiliary procedure is based on equation (5.8). It is most suitable for problems in which the density contrast is unknown and the regional background is specified. However, it is unsuitable for problems which specify the density contrast.

4. GRAVOP: Programme specification no.3c.

The auxiliary procedure is based on equation (5.12). It is specifically designed for problems involving unspecified linear parameters and is unsuitable when either of them is specified.

5. GRATIOP: Programme specification no. 3d.

The auxiliary procedure is based on equation (5.5). Its other details are similar to GREGNOP.

A summary of the use of these programmes is given in Table 5.1.



	Specified Parameters		
	C and B	B	None
GRANOP	X	0	0
GREGNOP		X	0
GRAVOP			X
GRATIOP		X	0
GAD	X	0	0

Table 5.1. A summary of the use of available programmes. X denotes appropriate programmes. 0 denotes possible alternatives.

#### 5.4. Nature of the Objective Function

Understanding the general behaviour of the objective function in gravity problems is essential for a correct application of optimisation techniques. In Chapter 4, the behaviour was investigated using, mainly, theoretical models. Our present investigation illustrates the practical aspects of the problem using an actual field example.

The behaviour of all the objective functions enlisted in section (5.2) is basically similar. For convenience, the objective function given by equation (5.12) has been chosen for illustration.

The field example is a negative anomaly in the Northern Pennines which was interpreted by Bott (1967a) as being caused by a granitic batholith, the 'Wensleydale Granite'. We chose a different profile and adopted a slightly different gradient on the regional background. Two-dimensionality was assumed throughout.

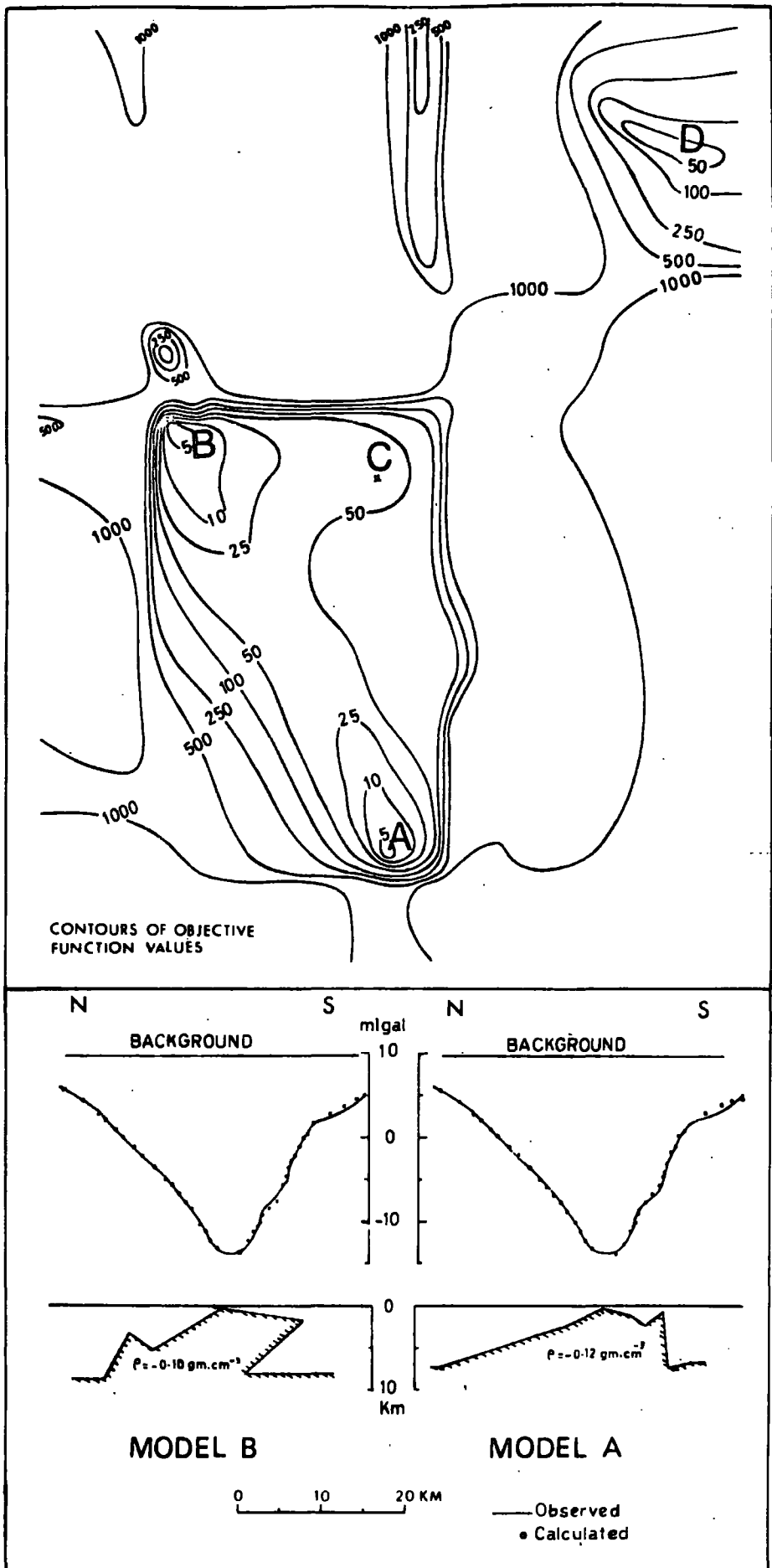


Fig. 5.2. An oblique section in the  $x$  hyperspace of the objective function corresponding to the Wenslydale Granite. The section illustrates the multi-modality of the objective function. Model B is geologically unreasonable.

The first cross-section (Fig. 5.2) is taken across a relatively large portion of the  $\underline{x}$  hyperspace. It clearly reveals the complexity and multi-modality of the function. Points which represent slight undulations in the function, such as C, or ill-defined local minima, such as D, can trap the search and cause local convergence. These difficulties may be overcome by choosing an appropriate optimisation method. Other minima are quite well-defined. Minimum A gives a reasonable model. Minimum B, however, gives a geologically impossible model. Both minima possess a very low function value and illustrate the necessity to use constraints in order to confine the search to a feasible region.

Within a feasible region, the second section (Fig. 5.3) shows a 'valley of ambiguity'. Considering the possible magnitude of observational errors, a tolerance in  $f(\underline{x})$  of 6 is reasonable. Therefore, points within a domain bounded by a contour of value 6 produce possible solutions. The model produced by point E is shown. The gradation from A to E is accompanied by a general reduction in the size of the model and an increase in the density contrast.

The parameters defining models A and E are of the same order of magnitude. However, Fig 5.3 clearly shows that the basic parameters must be specified in order to obtain any form of uniqueness. Such conditions are closely approximated in the third cross-section (Fig. 5.4) where the basic parameters of solutions A and G are almost identical. The general dimensions of the two models are similar. However,

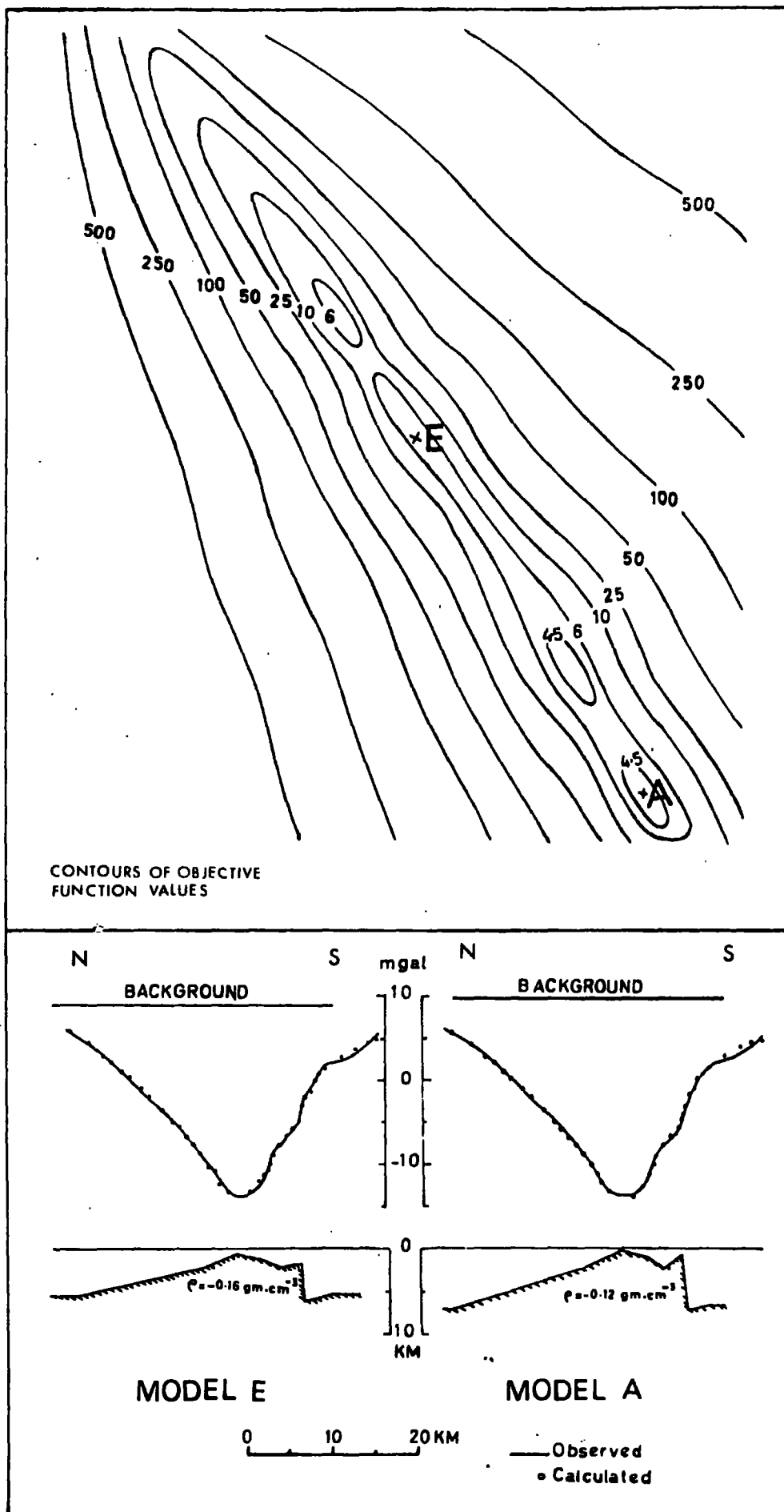


Fig. 5.3. An oblique section in the same hyperspace as Fig. 5.2 showing a 'valley of ambiguity'.

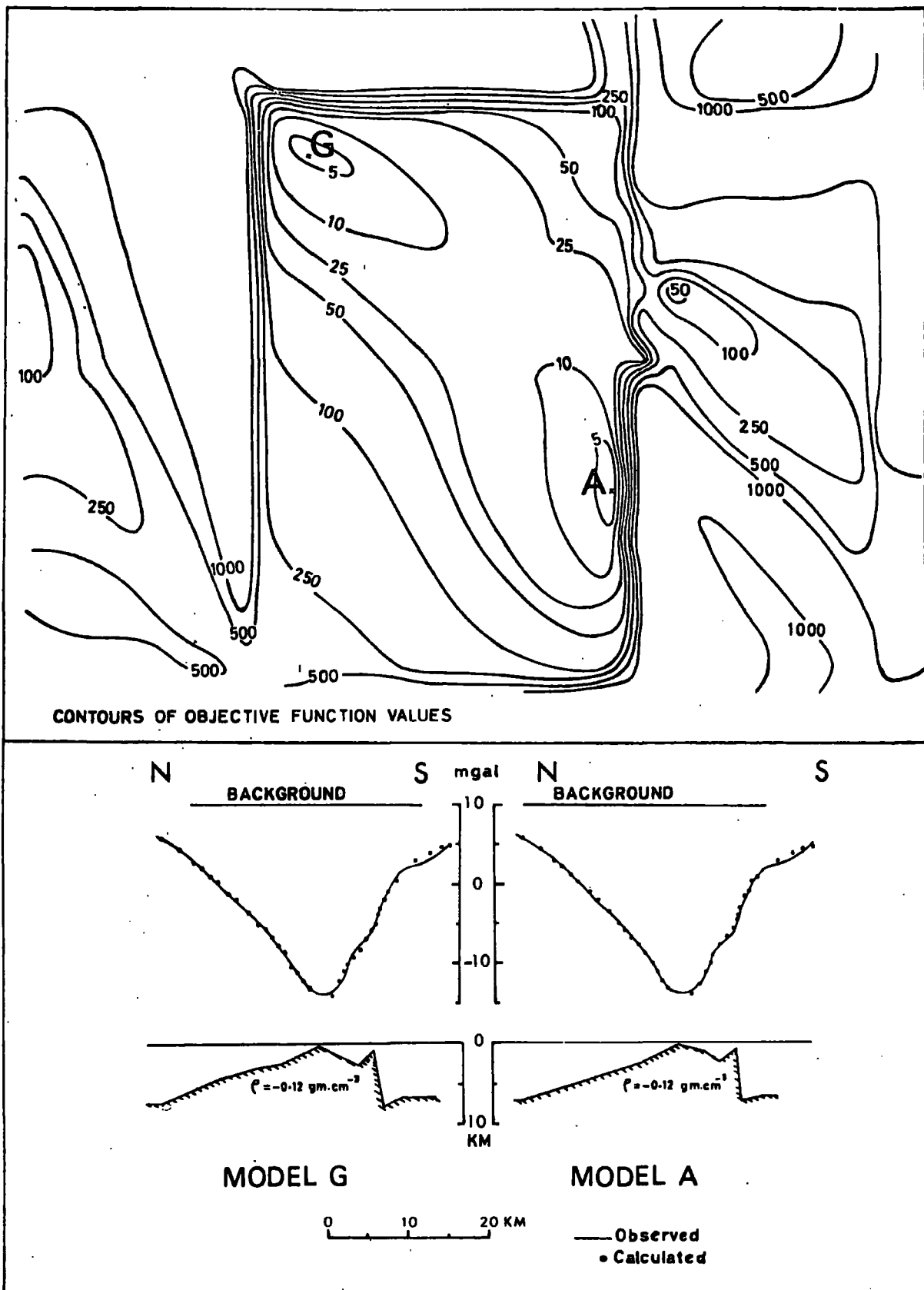


Fig. 5.4. A section in the same hyperspace as Fig. 5.2. Solution A emphasises features on the top of the batholith while solution G emphasises features on its northern side.

solution A emphasises features on the top of the batholith while solution G emphasises features on its northern side.

### 5.5. Method of Application

In view of the nature of the objective function in gravity problems described in Chapter 4 and in section 5.4, the application of non-linear optimisation techniques in interpreting gravity anomalies requires usually the following stages:

1. The problem is assessed, as a whole. All parameters that are known or could be estimated reasonably accurately are specified. The magnitude of factors causing ambiguity and / or the ultimate aim of the interpretation influences the choice of whether to specify all, some or none of the basic parameters (Chapter 4).

Time considerations may also be important. The time taken to produce a solution varies according to the optimisation method used, the closeness of the initial point to a solution, the number of variable parameters, the number of sides defining the model, the number of observation points, the accuracy to which the solution is sought, and the behaviour of the particular objective function being considered. An example of execution times is given in section 5.7.

2. The initial polygonal model is chosen according to available information. Methods of depth estimation (e.g. Smith, 1960) may be used for this purpose. When such information is lacking, the immediate task becomes that of selecting an initial point in a region which contains a

correct solution. This is particularly important when the problem is badly conditioned. For example, in the problem of Fig. 4.4, a basin-like initial model will generally produce a basin-like optimum model and a batholith-like initial model will produce a batholith-like optimum model.

The number of sides used in the model must be carefully chosen. Too many sides increase the computation time and the possibility of ill-conditioning the problem. A small number of sides does not represent the feature adequately. For an isolated anomaly, between 4 and 8 sides provide usually a convenient compromise.

The initial point can be made to emphasise a certain aspect of the anomalous feature so that the optimum solution would be biased towards that aspect. This may involve the need to use additional coordinate points in the emphasised parts of the model.

3. Constraints are inserted to ensure geological feasibility. In order to achieve this, it is usually sufficient to prevent neighbouring points from overlapping in the  $\xi$ -direction. Other constraints may also be inserted to ensure the adherence of the solution to known information about the anomalous feature.

4. An auxiliary procedure is chosen according to the requirements of the problem.

5. An appropriate optimisation method is chosen. The initial choice is usually restricted to direct search methods. The method of rotating coordinates is recommended. The

'Complex' method or the method of conjugate directions may be more suitable in a number of problems (see Chapter 3).

In general, about 100-200 iterations per variable are sufficient to locate the minimum. However, the first 50 iterations usually achieve a rapid progress so that the search converges to a region which is suitable for using a gradient method. Davidon's method is recommended.

6. The procedure may be repeated according to the requirements of the problem. For example, in problems solved by specifying all basic parameters, the interpretation process is usually repeated at a set of intervals of these parameters. Even in problems which arrive at a solution without specifying the basic parameters, it is frequently desirable, in the next stage, to obtain solutions at a set of specified intervals of these parameters.

7. After the basic solution or group of solutions are obtained, a certain amount of detailing may be required. We recommend starting from the basic model as an initial point; the extra coordinate points are placed on the relevant sides of the model.

A gradient method should normally be used for detailing the model. This usually involves no risks since the initial point (the basic model) is already in the vicinity of a solution in the new hyperspace.

Detailing reduces the residuals especially at observation points vertically above those parts being detailed. It should, therefore, be preferred below those parts with high residuals. However, detailing is unjustified when the residuals are



already smaller than the magnitude of observational errors.

### 5.6. Advantages and Limitations of Optimisation Methods in Gravity Interpretation

In the following account, we mean by optimisation methods those which were recommended for use in gravity interpretations, e.g. the method of rotating coordinates. A comparison with other iterative methods is implied in this account so that an assessment of optimisation methods, as interpretational means in gravity problems, may be made.

#### 5.6.1. Advantages

1. Optimisation methods are at least as efficient as any other method in terms of obtaining a satisfactory model with a satisfactory fit between the observed and the calculated data.

2. Any parameter defining the model may or may not be specified. It is also possible to constrain or inter-relate these parameters, e.g. a vertical fault may be established in the model by specifying two successive points to have the same  $\xi$  - coordinate. This flexibility makes it possible to use all available information about the anomalous feature. In other iterative methods, it is necessary to specify certain parameters but it is not usually possible to specify any of the others.

3. The model is of a general polygonal shape which is completely unrestricted. This is a desirable feature which other iterative methods lack.

4. Any number of observation points may be used on the

profile being interpreted, c.f. methods which employ a completely determined system (e.g. Allerton, 1968).

5. The position of the initial point may be used to bias the interpretation towards a certain aspect of the anomalous feature (sections 4.4 and 5.5).

#### 5.6.2. Limitations

1. Direct search methods are, generally, slower than other iterative methods. This limitation may be largely reduced by careful programming and good choice of the initial model.

2. Difficulties in optimisation techniques such as local convergence and convergence at an undesirable local minimum are possible. These difficulties are not important and can be readily avoided by considering the facts discussed in Chapters 2,3, and 4.

#### 5.7. Examples

Three examples are described below, each one presenting rather different problems from the others. The first example is described in slightly more detail.

##### 5.7.1. The Weardale anomaly

Details of the anomaly were given in Chapter 4. Two models obtained without specifying any parameter were shown in Fig. 4.11.

The general dimensions of the batholith for a set of density contrasts were obtained by specifying the depth of a point on the upper surface of the batholith from

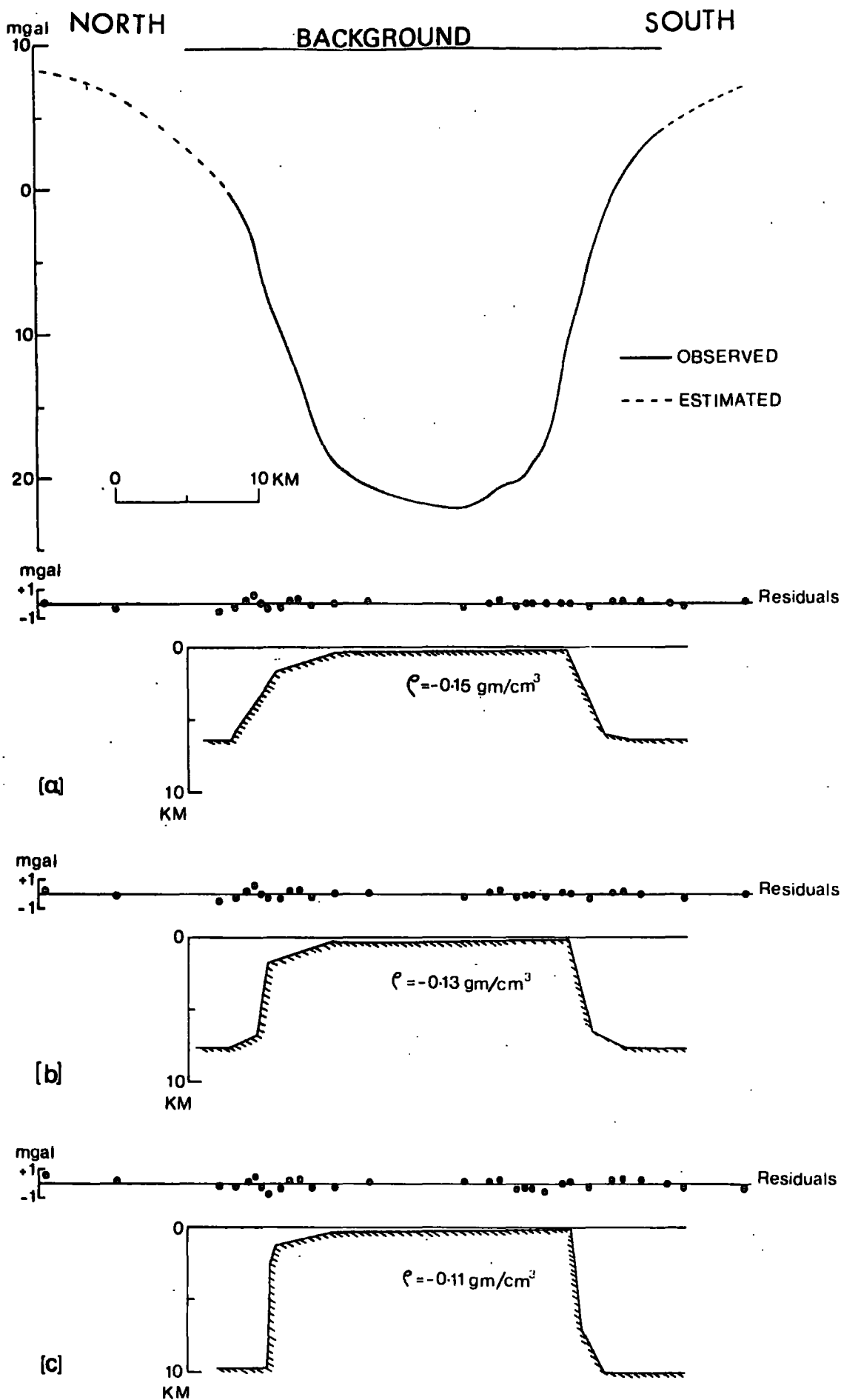


Fig. 5.5. An interpretation of the Weardale anomaly for an assumed density contrast of  $-0.11$ ,  $-0.13$  and  $-0.15 \text{ gm/cm}^3$ . The depth to the top and the regional background are specified.

information obtained from the borehole. The regional background was also specified. Models for density contrasts of  $-0.11$ ,  $-0.13$  and  $-0.15 \text{ gm/cm}^3$  are shown in Fig. 5.5. They all represent satisfactory solutions with a good agreement between the calculated and the observed anomaly.

Using equation (2.18) estimates of the possible error in the coordinate parameters of the model of density contrast  $-0.13 \text{ gm/cm}^3$  were obtained. They are given in Table 5.2. The limited significance of these estimates was discussed in section 2.8. They are, therefore, expected to give only a very rough idea on the accuracy of the parameters.

	Horizontal distance from origin	Error	Depth below datum	Error
Point no. 1	40.6	0.1	7.8	0.1
2	38.4	0.2	6.5	0.3
3	36.7	0.2	0.1	0.4
4	21.3	0.4	Specified	
5	20.1	0.6	0.3	0.4
6	15.6	0.1	1.8	0.1
7	14.8	0.4	6.8	0.2
8	12.9	0.1	7.6	0.4

Table 5.2. Estimates of possible error in the coordinate parameters of Fig. 5.5b. The figures are in kilometers.

Typical times required to produce a satisfactory solution such as the models shown in Fig. 4.11, using IBM 360/67 computer are:

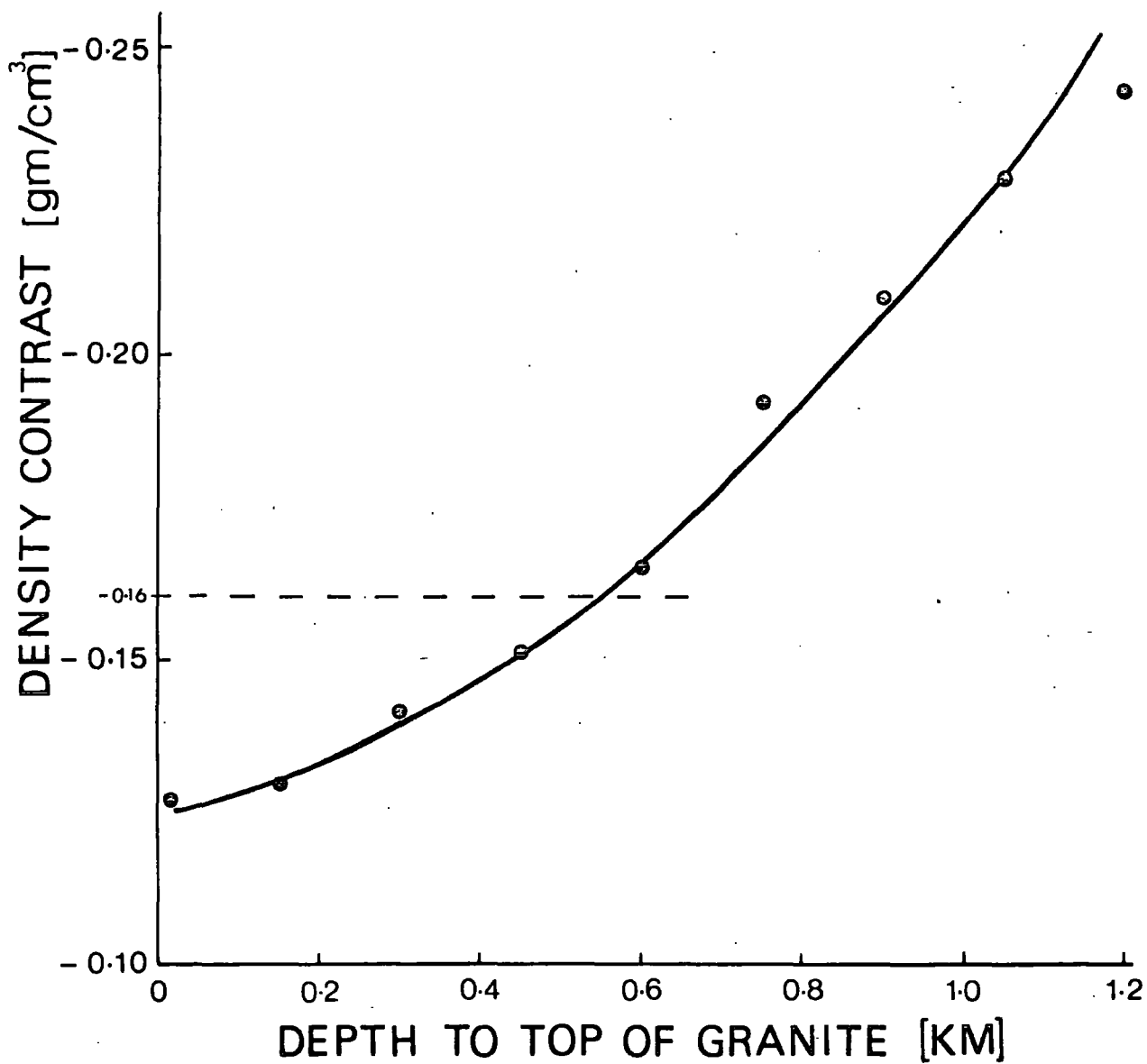


Fig. 5.6. Variation of the optimum density contrast with the assumed depth to the top of the Weardale Granite. The regional background is 10.2 mgal.

Method of rotating coordinates (P300)	7 minutes
Method of conjugate directions (P303)	6 minutes
The 'Complex' method (P301)	14 minutes
Davidon's method (P306)	30 seconds

Davidon's method was employed here only for comparison. The models obtained from the direct search methods were sufficiently detailed so that further detailing by a gradient method was unnecessary.

The Weardale anomaly was also used to demonstrate the use of optimisation techniques for maximum depth estimation (section 4.4). This was done by specifying the depth to the top of the batholith at a set of intervals for which the optimum density contrast was computed using GREGNOP. The regional background was specified at 10.2 milligals. Fig. 5.6 shows the variation of the density contrast vs. the depth to the top. Assuming that a density contrast in excess of  $-0.16 \text{ gm/cm}^3$  is unreasonable, the maximum depth to the top of the batholith becomes about 550 metres.

### 5.7.2. Gravity "low" C - North of Scotland

This negative anomaly was outlined in a marine geophysical survey conducted by the University of Durham during the 1968 cruise of RRS John Murray. It was interpreted by Bott and Watts (1970a) as a sedimentary basin having a lower density than the adjacent crystalline basement. The presence of the basin was supported by magnetic and seismic evidence. Geological and other considerations suggest the following:

1. The basement is probably Lewisian while the sediments are probably post-Devonian.
2. The depth to the bottom of the basin is at least 2.5 km but is unlikely to exceed 6 km.
3. The density contrast may range from  $-0.25$  to  $-0.50 \text{ gm/cm}^3$ .
4. The majority of observations are accurate to within 4 mgal.

(A.B. Watts, private communication).

The regional background was reduced to a horizontal one by subtracting a gradient of  $0.14 \text{ mgal/km}$ , increasing towards the N.W.

The first interpretation was made without specifying any parameter (Fig. 5.7a). The fit between the observed and the calculated anomalies is well inside the amplitude of observational errors and is, therefore, not significant. The parameters defining the model are of comparable magnitudes to the probable values. However, the depth to the bottom of the basin is outside the predicted range, the density contrast is lower than expected and the top of the basin is about 400 metres deeper than values predicted from geological evidence. This emphasises the importance of specifying the basic parameters when observational errors are large. The models of Fig. 5.8 are obtained in this manner. A reasonable solution (Fig 5.7b) was also obtained by constraining the depth to the bottom as an alternative to specifying the density contrast.

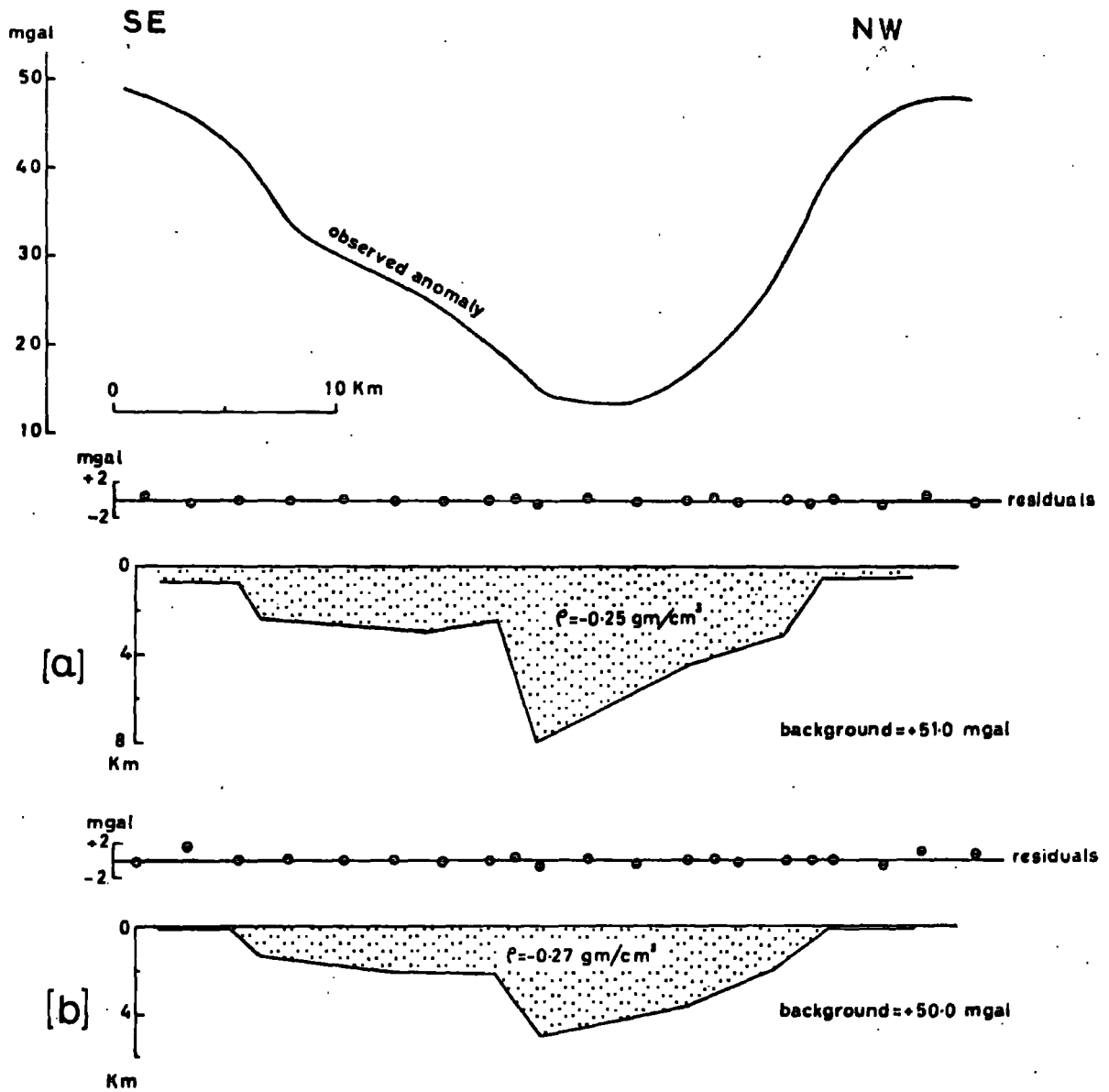


Fig. 5.7. An interpretation of gravity "low" C.

(a) Model obtained without specifying any parameter.

(b) Model obtained by specifying the depth to the top and constraining the depth to the bottom.



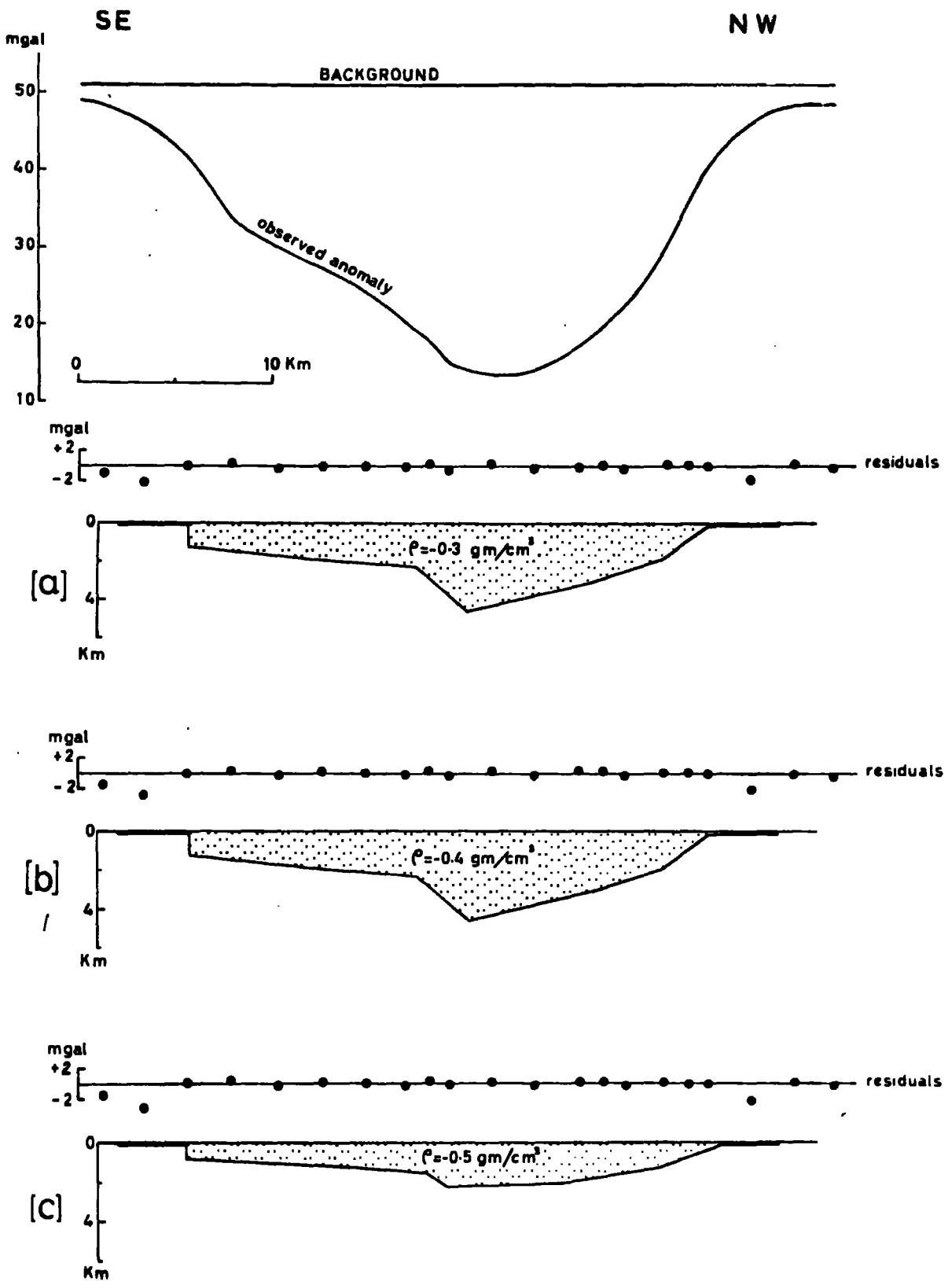


Fig. 5.8. Interpretation of gravity "low" C by specifying the depth to the top (70 m in SE and 140 m in NW) and the regional background (51 mgal after reducing it to a horizontal one) for a set of specified density contrasts.

The general dimensions of the basin were obtained by fixing the top of the model and the regional background for a range of density contrasts between  $-0.3$  and  $-0.5 \text{ gm/cm}^3$ . The model with  $-0.5 \text{ gm/cm}^3$  is probably too shallow. Otherwise, the resulting solutions were reasonable geologically with good agreement between the observed and the calculated anomalies (Fig. 5.8).

The persistent feature in all solutions was the probable faulting which bounds the basin on the southeastern side. Geologic and seismic evidence support the presence of this fault (A.B. Watts, private communication).

### 5.7.3. The gravity high in southeastern Minnesota

Craddock et al (1963) describe a southward trending major gravity high in southeastern Minnesota and western Wisconsin, U.S.A. which locally reaches 130 mgal and which is attributed to a belt of Pre-Cambrian basic igneous rocks. We have chosen traverse no.9 of this survey for interpretation by optimisation methods.

Craddock et al (1963, Fig. 8) interpret the anomaly on this traverse as being caused by a feature with inward sloping sides, extending to a depth of about 24 km and having a density contrast of  $+0.2 \text{ gm/cm}^3$  with the basement rocks. The supposed thickening of the overlying rocks to about 2 miles below the gravity maximum appears to account for the shape of the chosen regional background. The agreement between the observed and the calculated anomalies is within 7 mgal. This is justified in view of

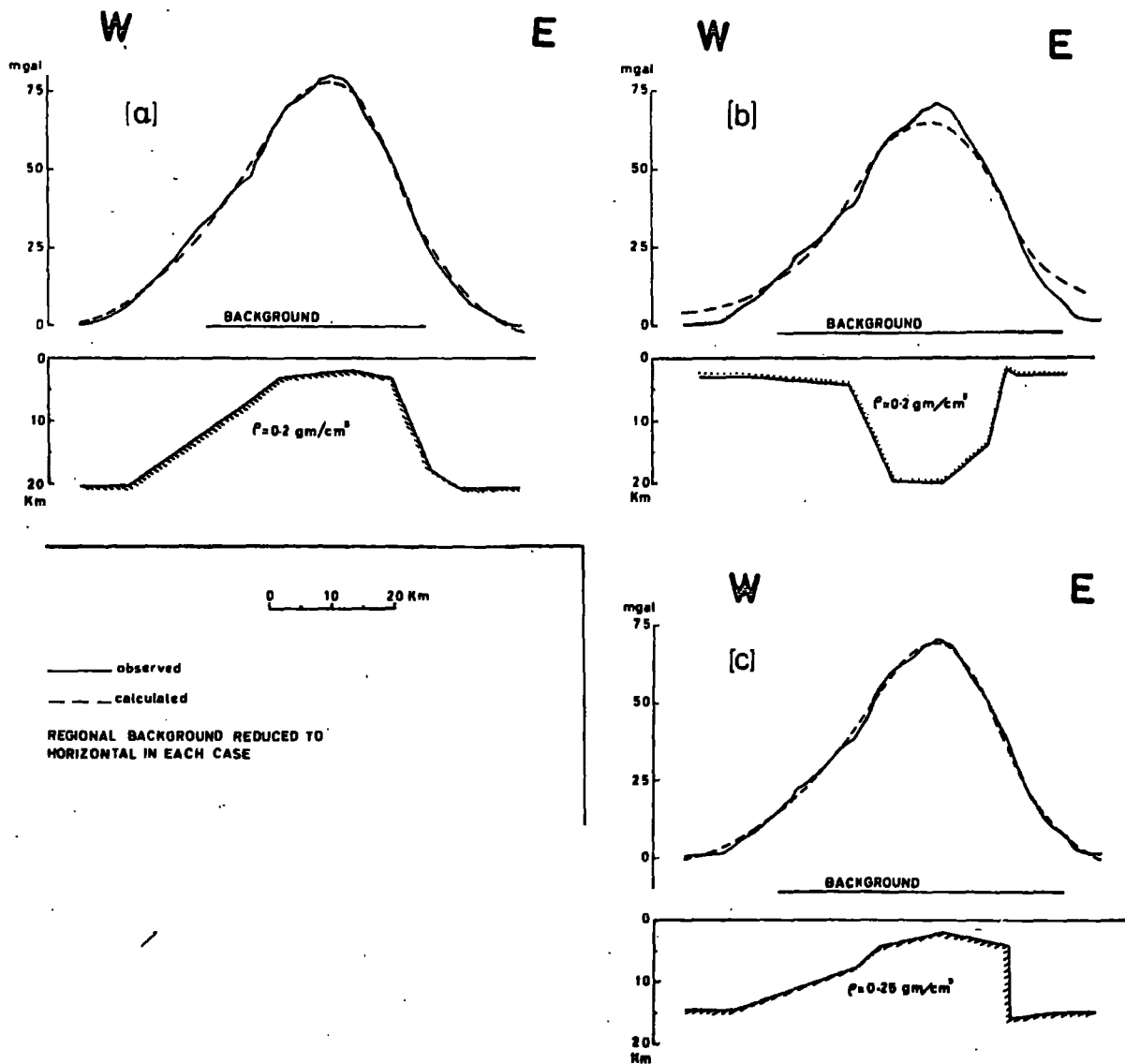


Fig. 5.9. Interpretation of the gravity high in southeastern Minnesota.

(a) Model obtained by specifying the basic parameters close to those of Craddock et al (1963).

(b) Model obtained with specified basic parameters. Other models are also possible.

(c) Model obtained without specifying any parameter.

A linear regional background was assumed in models (b) and (c).

the large magnitude of reduction errors. The ambiguity is further enhanced by the lack of good geologic control. Therefore, the model of Craddock et al (1963, Fig 8) is probably correct in a general manner but the details may be incorrect. For example, specifying the basic parameters at values close to those assumed by Craddock et al, we obtained a model with outward sloping sides (Fig. 5.9 a).

The anomaly was also re-interpreted assuming a linear regional background which increases eastwards by 0.16 mgal/km. The contact with the overlaying rocks was assumed horizontal in the investigated part of the traverse (Fig. 5.9b and c).

An interpretation based on specifying the density contrast and the top of the model at appropriate values yielded a similar model to that of Craddock et al (Fig 5.9b). Many other models were also possible.

Interpreting the anomaly without specifying any parameter also produced several possibilities. A model with outward sloping sides is shown in Fig. 5.9c. In fact, models with outward or inward sloping sides were obtainable whether the basic parameters were fixed or not.

This traverse demonstrates the high degree of indeterminacy arising in problems where observational errors are large and geologic control is lacking; specifying the basic parameters does not improve the situation. The fact that optimisation methods have achieved a much better agreement between the observed and the calculated anomalies is of no importance owing to the magnitude of observational errors.

## CHAPTER 6

## MAGNETIC INTERPRETATION

6.1. Introduction

The problems involved in interpreting magnetic anomalies are broadly similar to those met in gravity interpretation but there are some differences which render magnetic anomalies more difficult to treat. The magnetisation contrast is a vector quantity which does not necessarily lie in the direction of the ambient field because of the presence of remanent components. The ambient field, which is usually the earth's magnetic field, varies in direction according to geographical position. In magnetic methods one may, therefore, encounter vertical field anomalies, horizontal field anomalies or total field anomalies. Further difference from the gravity problem is caused by the nature of the features being interpreted; in magnetic problems these features are usually ore veins, dykes or some basement features which are quite deep. Because of these problems, progress in developing interpretational techniques was quite slow and assumed rather a different trend from that in gravity methods.

Direct methods of interpretation were quite useful. Depth and width estimation using certain estimators from the anomaly curve received wide attention (e.g. Vacquier et al, 1951; Smith, 1959; Bruckshaw and Kunaratnam, 1963). Transforming the anomaly so that it would acquire the simple

form usually exhibited by a gravity anomaly was introduced by Baranov (1957). The transformation was further extended to two-dimensional models and to models with a different direction of magnetisation from the ambient field (Bott et al, 1966). Transformation by upward or downward continuation (e.g. Peters, 1949; Henderson and Zeitz, 1949a; Dean, 1958) and methods for obtaining first and second derivatives (e.g. Baranov, 1953; Henderson and Zeitz, 1949b; Danes, 1962) were developed parallel to those in gravity methods.

There is also a variety of indirect methods of interpretation. The normalised anomaly of a dyke-like structure may be matched with a set of master curves to obtain various parameters (e.g. Hutchinson, 1958; Gay, 1963). The anomaly of less regular models may be calculated using special graticules (e.g. Pirson, 1942; Henderson and Wilson, 1967; Grant and West, 1965, p.342). However, the use of graticules is now superseded by computer methods for calculating the anomaly due to polygonal models (e.g. Talwani and Heirtzler, 1964; Bott, 1969b). Automated iterative adjustment of the model parameters is basically more attractive than processes of trial and error involving human judgement. Optimisation techniques were used by Stacey (1965) to interpret magnetic anomalies with limited progress as described in Chapter 1. Later, Bott and Butler (Butler, 1968) employing an equivalent technique to that used in deriving equation (6.13) succeeded in using optimisation techniques to interpret magnetic anomalies due to dykes. Johnson (1969) was able to

solve some linear and non-linear magnetic problems using a procedure based on Marquardt method (section 3.3.1.)

The work described in this Chapter applies to any two-dimensional model of a polygonal cross-section, open or closed. The magnetisation contrast vector,  $\underline{J}$ , is assumed uniform but cases requiring a limited number of magnetisation contrasts can be easily dealt with.

Applicability to three-dimensional problems involves a straight-forward extension of the general procedure presented below. Calculation of the anomaly due to the model may be made using any convenient method (e.g. Bott, 1963). However, as in gravity methods, it is expected that the large number of parameters and observation points will limit a routine use of optimisation techniques.

## 6.2. The Auxiliary Procedure

The magnetic model is defined within the auxiliary procedure by the adjustable parameters which are passed from the optimisation procedure and by the unadjustable parameters which are specified in the procedure. The magnetic anomaly due to the model is then calculated and used to provide the value of the objective function.

### 6.2.1. Calculating the anomaly

We adopt a two-dimensional Cartesian system with the anomaly profile taken along the horizontal  $\xi$  - axis, perpendicular to the strike of the anomaly and with the  $\zeta$  - axis, pointing vertically downwards. To unify the system

of reference we further assume that the  $\xi$ - axis points towards a northerly direction, i.e. S-N, SE-NW or SW-NE.

The magnetic anomaly at point  $P(X_k, Z_k)$  due to an  $m$ -sided polygon formed by the addition of  $m$  semi-infinite horizontal step-models is given by

$$C_k = \sum_{i=1}^m (J_{s_i} u_{ik} + J_{c_i} v_{ik}) \quad (6.1)$$

where  $J_{c_i}$  and  $J_{s_i}$  represent, respectively, the horizontal component, resolved in the direction of the profile and the vertical component of the magnetisation contrast vector across the  $i^{\text{th}}$  side. If  $C_k$  refers to the anomaly in the direction of the earth's magnetic field then

$$u_{ik} = 2 \sin \theta_i (R_{ik} \cos I \sin d - S_{ik} \sin I) \quad (6.2)$$

$$v_{ik} = 2 \sin \theta_i (S_{ik} \cos I \sin d + R_{ik} \sin I) \quad (6.3)$$

where

$$R_{ik} = \phi_{ik} \cos \theta_i + \log (r_2/r_1)_{ik} \sin \theta_i$$

$$S_{ik} = \phi_{ik} \sin \theta_i - \log (r_2/r_1)_{ik} \cos \theta_i$$

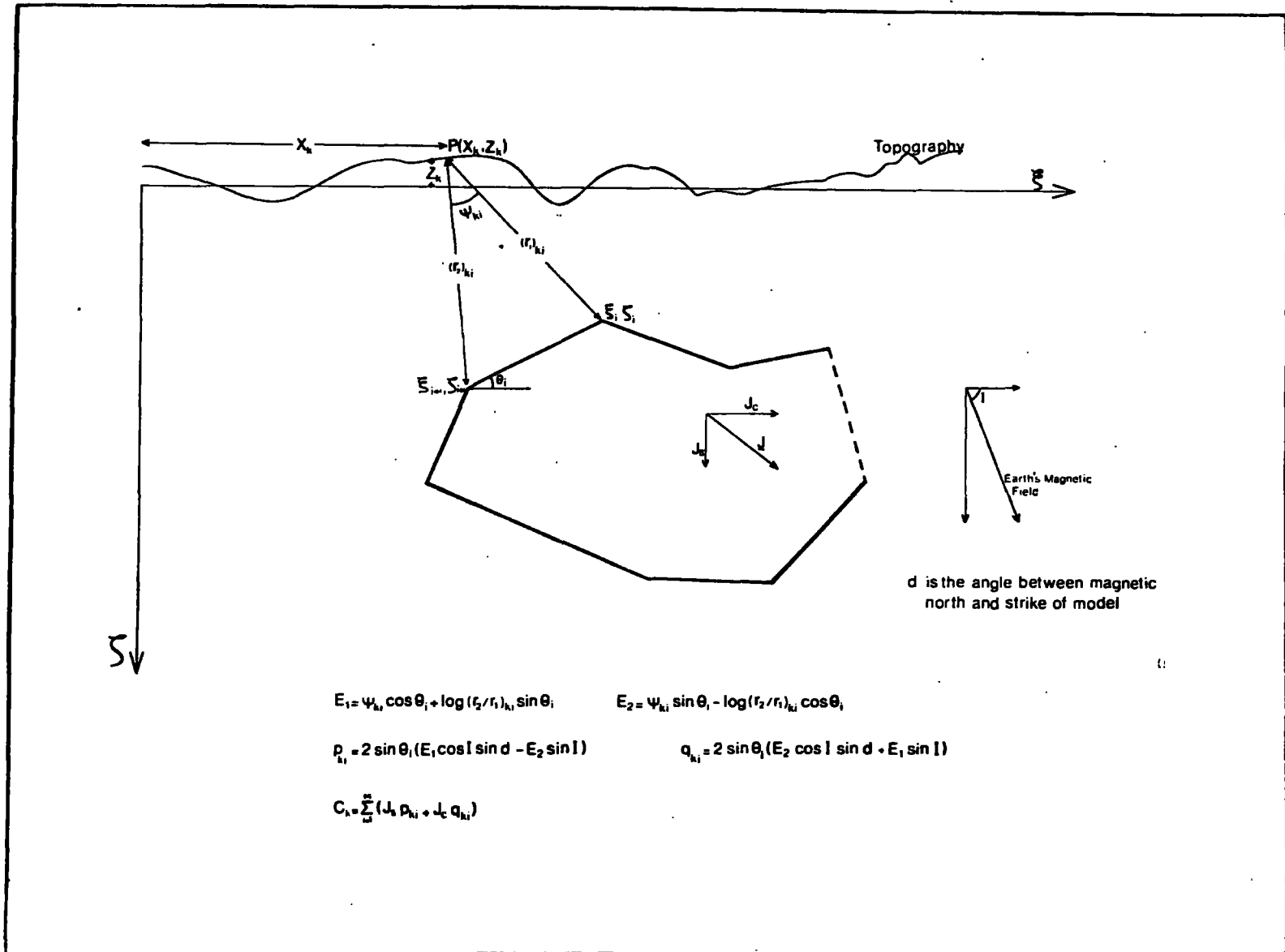
(Bott, 1969b).

Fig. 6.1 illustrates the symbols and the adopted convention.

We assume that  $\underline{J}$  is constant in magnitude and direction throughout the model unless otherwise stated. For convenience, we include in  $C_k$  the regional background,  $B$ , after reducing it to a horizontal one. Hence,



Fig. 6.1  
 Diagrammatic illustration of the adopted symbols and convention used in deriving a formula for the magnetic anomaly at a given point  $P(X,Z)$  due to a two-dimensional polygon.



$$C_k = B + J_s U_k + J_c V_k \quad (6.4)$$

where

$$U_k = \sum_{i=1}^m u_{ik} \quad \text{and} \quad V_k = \sum_{i=1}^m v_{ik} \quad (6.5)$$

We refer to  $J_s$ ,  $J_c$  and  $B$  as the linear parameters and to the coordinates defining the polygonal model as the non-linear parameters, according to their relationship to  $C_k$  (Bott, 1967b). Any of these parameters may be specified or treated as an adjustable parameter.

The present work is devoted to anomalies measured in the direction of the total field because these are currently the most common type of measured anomalies. Anomalies measured in a horizontal direction, a vertical direction or any other direction may be treated in a similar way as this will entail only slight modifications in the objective function.

### 6.2.2. The objective function

A simple form of the objective function is given by

$$f(\underline{x}) = \sum_{k=1}^n (A_k - B - J_s U_k - J_c V_k)^2 \quad (6.6)$$

where  $\underline{x}$  is an  $m$ -dimensional vector representing the adjustable parameters, and  $n$  is the number of observation points and  $A_k$  is the observed anomaly at the  $k^{\text{th}}$  observation point.

Equation (6.6) is most useful when the linear parameters are specified or when using a gradient method.

In situations where it is desirable to interpret the

anomaly without specifying  $\underline{J}$  (Chapter 4), use can be made of the linear relationship between  $C$  and  $\underline{J}$ . Hence, at the optimum

$$\frac{\partial f}{\partial J_s} = 0 = -2 \sum_{k=1}^n (A_k - J_s U_k - J_c V_k - B) U_k \quad (6.7)$$

$$\frac{\partial f}{\partial J_c} = 0 = -2 \sum_{k=1}^n (A_k - J_s U_k - J_c V_k - B) V_k \quad (6.8)$$

The two equations are linear in  $J_s$  and  $J_c$  giving,

$$J_s = (Q_v D - Q_u G) / (D^2 - GH) \quad (6.9)$$

$$J_c = (Q_u D - Q_v H) / (D^2 - GH) \quad (6.10)$$

where

$$Q_u = \sum_{k=1}^n (A_k - B) U_k, \quad Q_v = \sum_{k=1}^n (A_k - B) V_k,$$

$$D = \sum_{k=1}^n U_k V_k,$$

$$G = \sum_{k=1}^n U_k^2, \quad H = \sum_{k=1}^n V_k^2$$

Details of the derivation are given in Appendix 4. The objective function is now given by

$$f(\underline{x}) = \sum_{k=1}^n [A_k - B - U_k J_s(A, B, U, V) - V_k J_c(A, B, U, V)]^2 \quad (6.11)$$

For obtaining a solution without specifying any of the linear parameters, the same procedure is followed. Thus, at the optimum,

$$\frac{\partial f}{\partial B} = 0 = -2 \sum_{k=1}^n (A_k - B - J_s U_k - J_c V_k) \quad (6.12)$$



Equations (6.7), (6.8) and (6.12) can be solved for  $J_s$ ,  $J_c$  and  $B$ . The final expressions are too large to be listed here. They are given in Appendix 5 together with the method of their derivation. The objective function in this case is given by

$$f(\underline{x}) = \sum_{k=1}^n \left[ A_k - B(A, U, V) - U_k J_s(A, U, V) - V_k J_c(A, U, V) \right]^2 \tag{6.13}$$

Equations (6.11) and (6.13) reduce the problem to obtaining a solution by adjusting the model coordinates only. As in gravity methods, this approach reduces the number of unknowns by three and renders the method more suitable for treatment by non-linear techniques. Similarly, these functions are unsuitable for use in conjunction with a gradient method because of the difficulty of providing the derivatives of the function.

By analogy with the normalisation procedure of equation (5.5) the optimisation may be carried out independently of the intensity of magnetisation  $|\underline{J}|$ . This approach is less useful here since the direction of magnetisation will still have to be defined.

When more than one magnetisation contrast are present, we use the objective function

$$f(\underline{x}) = \sum_{k=1}^n (A_k - C_k - B)^2 \tag{6.14}$$

where  $C_k$  is defined by equation (6.1). If no ambiguity is tolerable in the solution these contrasts must be specified.

### 6.3. Available Programmes

The computer programmes are constructed on similar bases to those used in gravity methods. They are written in PL/1 F-level. MAGD is for use with P306 (section 3.3.1.3). The others are adapted for use with the direct search procedures P300 (section 3.4.3.1), P301 (section 3.4.2.4) and P303 (section 3.2.3.6). They are constructed such that it should be possible to specify or leave unspecified any coordinate parameter defining the polygonal model.

1. MANOP: Programme specification no. 5a.

The auxiliary procedure is based on equation (6.6). It is most suitable for problems in which the linear parameters are specified but can also handle any or all of them as variable parameters.

2. MAGD: Programme specification no. 6

The auxiliary procedure is based on equation (6.6). It is designed for use with P306. It provides the objective function and its first partial derivatives with respect to the variable parameters. The variable parameters may include none, some or all of the linear parameters. The method of obtaining the partial derivatives is given in Appendix 3.

The procedure may be modified on the bases of equation (6.14) to accept a number of magnetisation contrasts appropriate to each side of the model, all of which must be specified.

3. MREGNOP: Programme specification no. 5b.

The auxiliary procedure is based on equation (6.11). It is designed for problems in which  $B$  is specified and  $\underline{J}$  is

unspecified. B can also be a variable parameter but the procedure is unsuitable for problems which specify  $\underline{J}$ .

4. MAGOP: Programme specification no.5c.

The auxiliary procedure is based on equation (6.13). It is specifically designed for problems which do not specify the linear parameters and is unsuitable when any of them is specified.

5. MULTIJ: Programme specification no.5d.

The auxiliary procedure is based on equation (6.14). It is similar to MANOP but more than one  $\underline{J}$  may be used. Specifying these contrasts is an option but it is unusual in practice to leave more than one or two contrasts unspecified in view of the extensive ambiguity that would arise.

A summary of the use of these programmes is given in table 6.1.

	Specified Parameters		
	$\underline{J}$ and B	B	None
MANOP	X	0	0
MREGNOP		X	0
MAGOP			X
MULTIJ	X	0	0
MAGD	X	0	0

Table 6.1. A summary of the use of available programmes. X denotes appropriate programmes. 0 denotes possible alternatives.

#### 6.4. Nature of the Objective Function

The emphasis in Chapter 4 was on gravity problems.

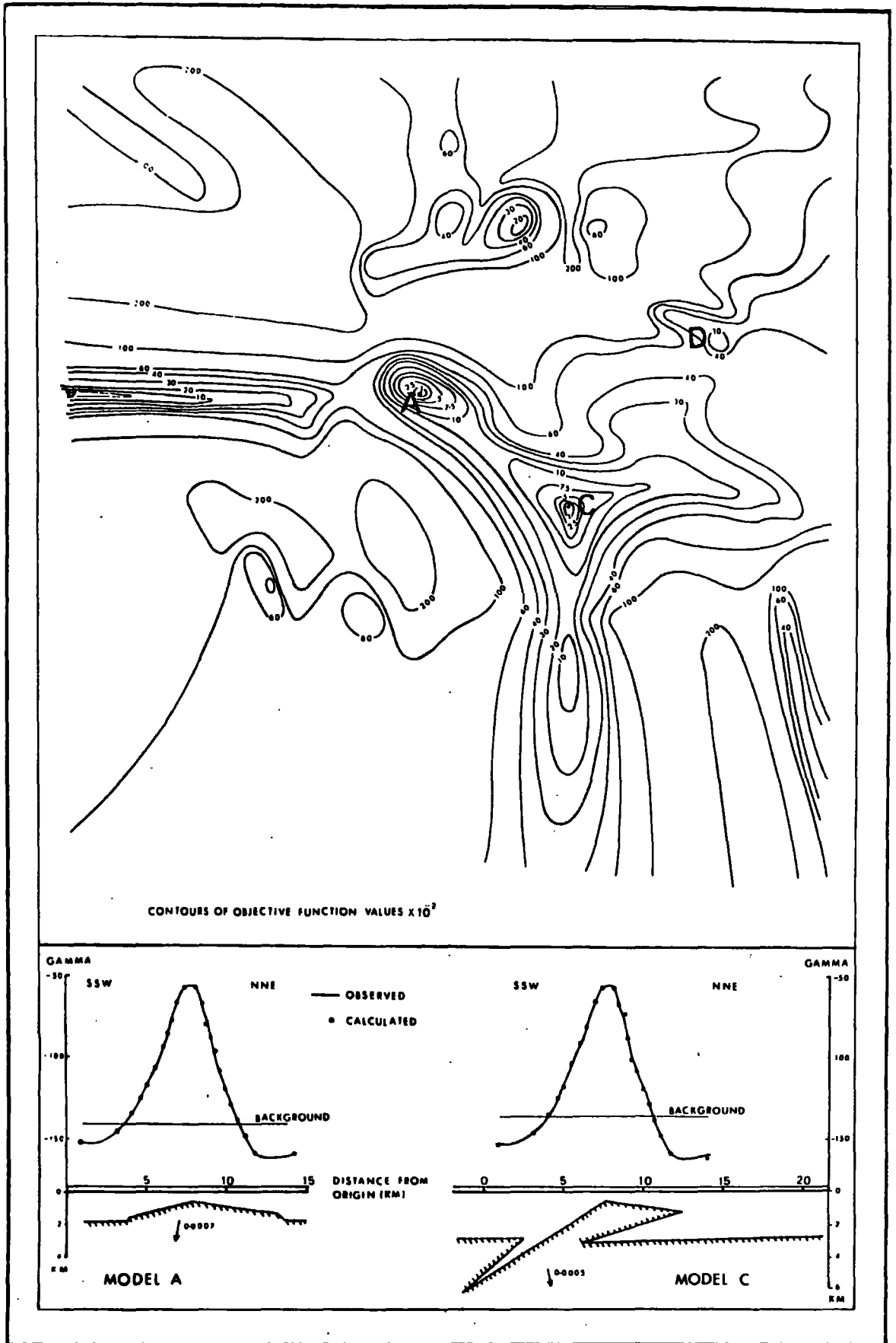


Fig. 6.2. An oblique section in the  $x$  hyperspace of the objective function corresponding to a magnetic anomaly in the English Channel. The section illustrates the multi-modality of the objective function. Model C is geologically unreasonable and may be isolated using constraints.  $|J|$  is in e.m.u./cm<sup>3</sup>.

The general behaviour of the objective functions in magnetic problems is almost identical. We shall assert the practical aspects of these features using an actual field anomaly.

The objective functions given in section 6.2 are similar in general behaviour to each other. Each of the illustrations used below shows an objective function appropriate to the particular aspect being discussed. However, the discussion applies to all of the objective functions of section 6.2 in a general way.

The field example is an aeromagnetic anomaly south of the Isle of Wight between National Grid Coordinates SZ 080367 and SZ 120493. Three sections constructed obliquely through the  $x$  hyperspace are used for illustration.

The first cross-section (Fig. 6.2) covers a large range of each parameter and illustrates the complexity and multimodality of the objective function. Minima A and C are well-defined and have low function values which qualify them as solutions. Both solutions are physically possible but solution C is geologically unreasonable. In applying optimisation techniques all such minima are isolated by constraints.

Tests on other local minima, such as D, show them to be ill-defined. It is difficult to determine how many of the minima shown in the section close in all directions but it is probable that most of them do not.

In the second section (Fig. 6.3), solutions A and E are both feasible. In fact, the valley A-E is a 'valley of ambiguity' with all the points in the domain bounded by a



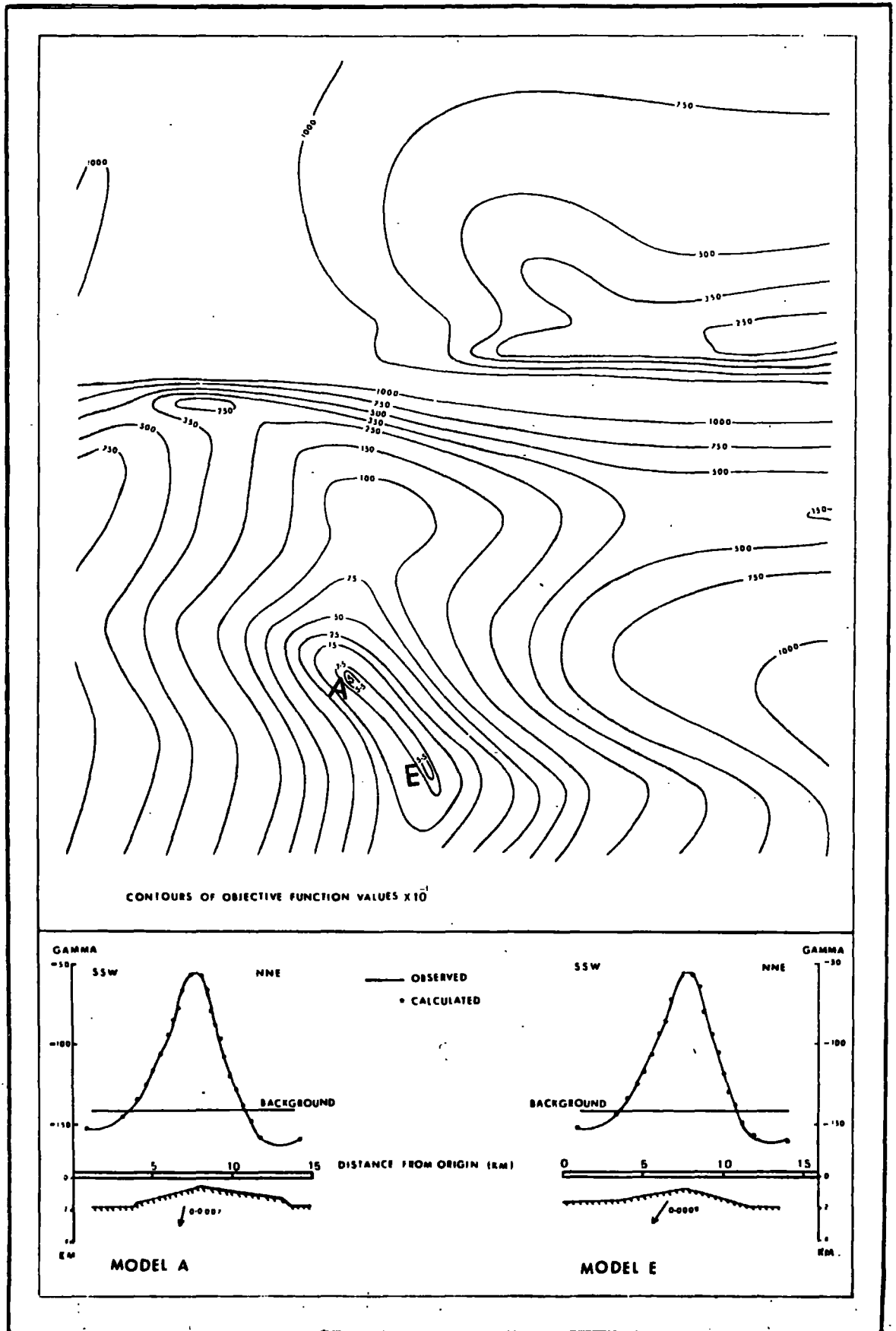


Fig. 6.3. An oblique section through the same hyperspace as Fig. 6.2 showing a 'valley of ambiguity'.

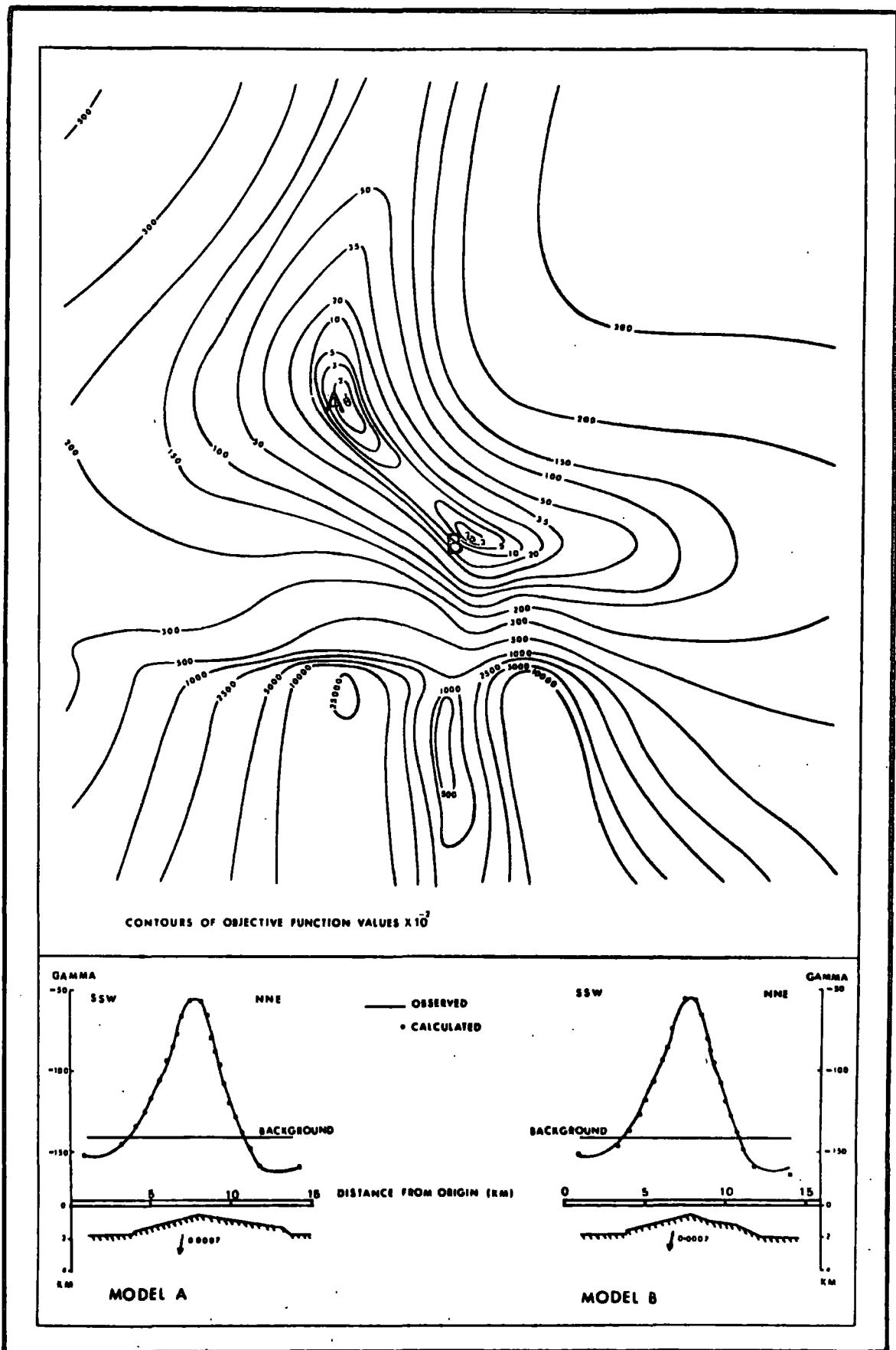


Fig. 6.4. A section in the same hyperspace as Fig. 6.2. Solution B emphasises the details of the NNE part of the body. Solution A gives an even emphasis to the body.  $|J|$  is in e.m.u./cm<sup>3</sup>.

contour of value 75 qualifying as solutions. The gradation from A to E is accompanied by a change in the size of the model and the magnetisation contrast vector. However, the parameters defining the model are of the same order of magnitude.

The third section (Fig. 6.4) shows the behaviour of the objective function in a hyperspace which is orthogonal to the axes of the magnetisation contrast vector, the depth coordinates of the bottom of the model and the regional background. This is, therefore, a problem in which the basic parameters are specified. Multi-modality is caused by emphasising different aspects of the anomalous body (iv, section 4.4). Solution B, for example, brings out features on the northern part of the body while solution A gives even emphases to the body as a whole. Usually, all such solutions are similar in the general outline.

Within the assumptions made about the model we may view the whole complex of 'valley of ambiguity' and valleys or regions containing solutions with various emphases, as constituting the "global solution" of the problem.

#### 6.5. Method of Application

The stages followed in using optimisation techniques to interpret magnetic anomalies are usually similar to those followed in gravity problems with a step-by-step correspondance. We shall not, therefore, go into the details of the application. However, two differences require pointing out.

Firstly, magnetic interpretation often deal with

basement features. The basic parameters in these problems are difficult to establish particularly as the remanent component of the magnetisation contrast vector may be quite significant (see for example Girdler and Peter, 1960).

There will, therefore, be more temptation to overlook stages in which the basic parameters are specified. It is difficult to recommend any kind of decision to be taken in this respect; whether fixing the basic parameters will produce a better solution depends on the particular problem at hand.

Secondly, when the model is being detailed the anomaly points most influenced by the addition of new sides are not necessarily those situated vertically above these sides. Detailing cannot therefore be preferred vertically below points where residuals are high.

#### 6.6. Advantages and Limitations of Optimisation Methods in Magnetic Interpretation

Optimisation techniques are the only available automated iterative procedures for interpreting magnetic anomalies. The role which they play in magnetic interpretation is, therefore, in itself an important advantage. They also enjoy all the general advantages discussed in gravity interpretation (section 5.6); efficiency and flexibility are the most important features. The possibility of obtaining a solution, without the necessity to specify the basic parameters, is an important asset because information about these parameters is often lacking in basement

interpretation problems. In particular, no restrictive assumption about the direction of magnetisation is required. This overcomes a common difficulty in currently used interpretation techniques.

The limitations are again similar to those mentioned in gravity interpretation. We may add here that occasional difficulties arise when interpreting very steep-sided anomalies caused by shallow features. These difficulties are probably caused by the invalidity, at shallow depth, of the approximation that the anomalous feature is effectively homogeneous. Furthermore, the steep gradient on such anomalies causes high residuals between the observed and the calculated anomalies for small errors in positioning. These high residuals often confuse the search for a solution. The difficulties would be probably overcome by minimising an objective function in the form of area of discrepancy between the calculated and the observed anomalies (equation 2.2). Moreover, if certain assumptions about the shape of the feature can be made, the solution may be sought in terms of the variation in the magnetisation distribution within the feature. The latter problem is linear. It is soluble by matrix algebra (e.g. Hutton, 1970) and is outside the scope of the present work.

### 6.7. Examples

A number of examples are chosen from the aeromagnetic map of Great Britain to illustrate the applicability of optimisation techniques. The techniques have also had equal success in interpreting land and ship-borne data (e.g.

Dobinson, 1970).

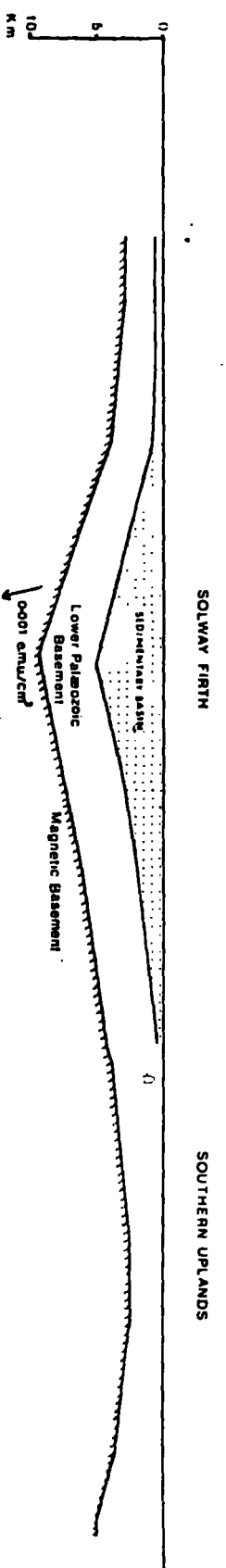
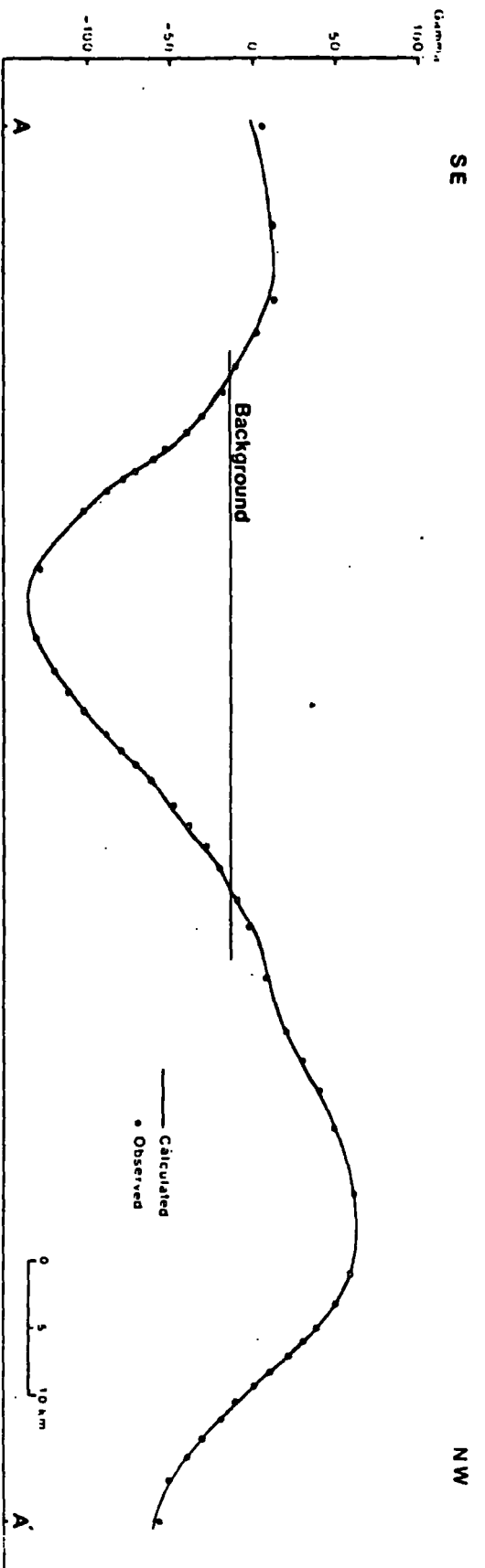
The first example is described in detail to show the general method of approach.

#### 6.7.1. The Solway Firth and Southern Uplands anomaly

This anomaly extends over the Solway Firth and, on land, occupies a small part of the Southern Uplands. Within the Solway Firth, the anomaly is negative and the region is occupied by a sedimentary basin which is mainly of Carboniferous and younger rocks. This basin was deduced from gravity measurements by Bott (1965) who also demonstrated that the magnetic negative cannot be attributed to a magnetisation contrast between the basin and the Lower Palaeozoic rocks immediately below it. In the Southern Uplands the anomaly is positive and the area is complicated by strong folding of the Lower Palaeozoic rocks. In both areas the general structural trend is Caledonian.

MAGOP in conjunction with the method of rotating coordinates was used to obtain the model shown in Fig 6.5. The fit between the observed and the calculated anomalies is very satisfactory. The model indicates that the anomaly is caused by a contrast within the basement; a magnetic basement underlies a layer of less magnetic rocks.

The trough causing the anomaly at the Solway Firth is in remarkable parallelism with the sedimentary basin suggesting that the two structures are closely associated. However, the rise in the Southern Uplands seems to represent a general rise of the magnetic basement underneath the complex tectonics of the region. The apparent smoothness of



the contact may have well been enhanced by the comparatively large depth to the magnetic basement.

The magnetisation contrast vector is shown in a plane parallel to the profile. Assuming that the true vector lies in a plane parallel to the geographical north the vector would have a magnitude of  $0.001 \text{ e.m.u./cm}^3$  and would be inclined at  $77^\circ$ . These values, together with a regional of  $-12$  gammas are well within the expected range and indicate quite a good solution.

The procedure was repeated using the method of conjugate directions, for comparison purposes. Convergence to the minimum was usually faster than in the method of rotating coordinates. However, the procedure has no provision for constraining the parameters and there was occasional tendency for converging to geologically unfeasible minima.

The residuals obtained with the model of Fig. 6.5, compared with the accuracy of observations, did not justify further detailing on the model. However, for the purpose of illustration, a detailed model was attempted using Davidon's procedure. The extra coordinates in the new model defined points that were already on straight segments between the original coordinates indicating the relative straightness of the contrast plane.

Other possibilities were also surveyed. A closed body within the basement was assumed and the model was optimised starting from various initial points. However, all solutions gave models that were geologically unreasonable and the model shown in Fig. 6.5 was regarded as the best available



approximation to the true geological picture.

The volcanic activity during Lower Ordovician might appear to provide reasonable grounds for attributing the anomaly to a contrast between such volcanic rocks and overlying non-magnetic Lower Palaeozoic and younger rocks. However, the basic nature of these volcanic rocks is not persistent even within the Southern Uplands. Furthermore, the postulated depth to the contrast plane is not compatible with the known depth of Lower Ordovician rocks in the interpreted part of the Southern Uplands (Pringle, 1948). It would, therefore, seem probable that the magnetic basement is Pre-Cambrian; the contribution from the Lower Ordovician is probably not significant.

Interpretation of the anomaly corresponding to the Solway Firth alone is shown in Fig. 6.6b. The parameters defining the model are similar to those of Fig. 6.5. Two more models were produced by specifying the direction of the contrast vector, the depth to the top of the basin and the regional background at values similar to those of Fig. 6.6b. The magnitude of the magnetisation contrast was specified at half and twice that of Fig. 6.6b, respectively (Figs. 6.6a and 6.6c). The three models are reasonable geologically. However, the high residuals associated with model (a) suggest that the magnetisation contrast is probably much larger or that the basic parameters had not been specified correctly.

Table 6.2 gives estimates of the accuracy in the coordinate parameters of the model of Fig. 6.6b., using

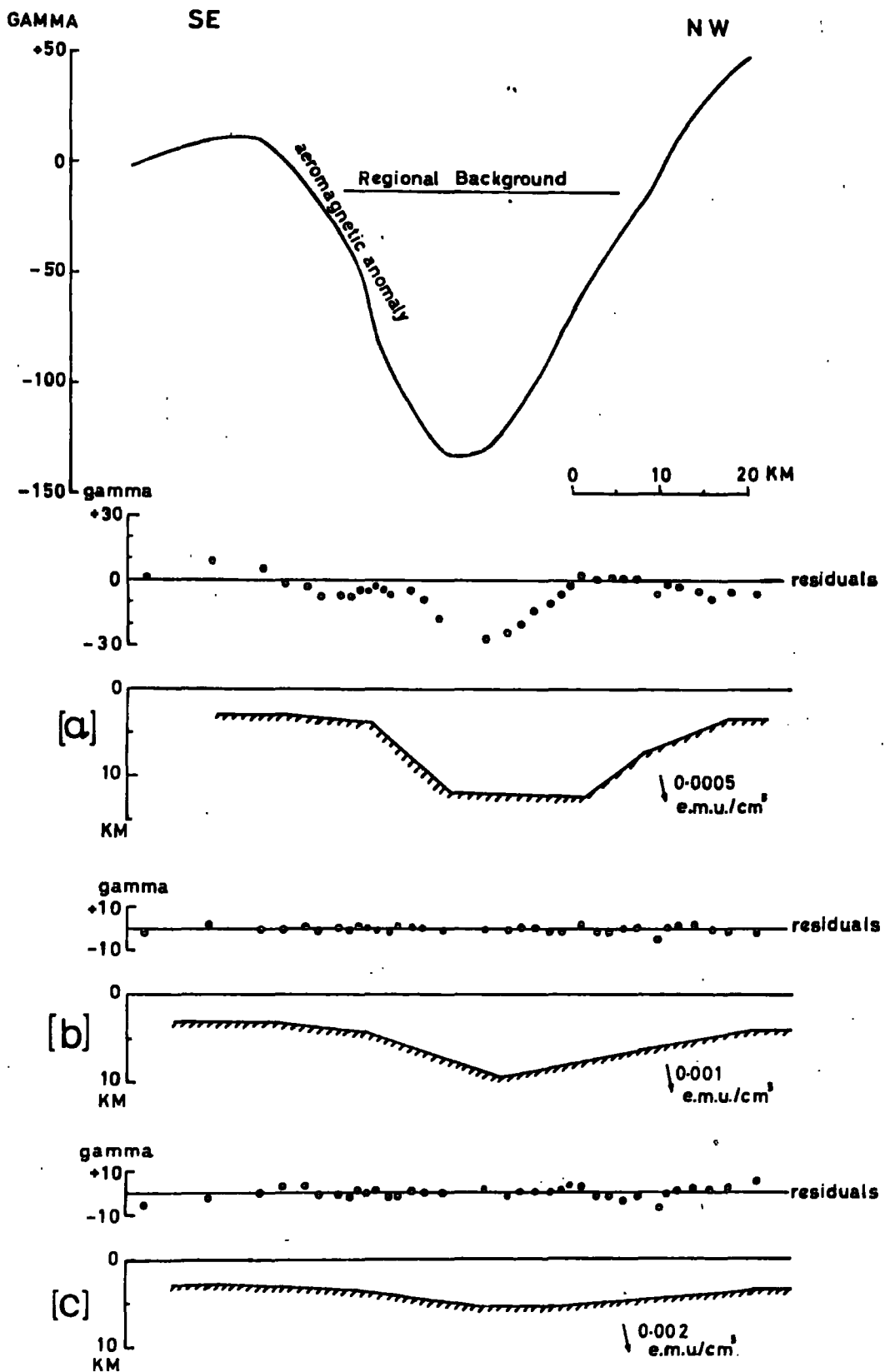


Fig. 6.6. Interpretation of the aeromagnetic anomaly across the Solway Firth by specifying the depth to the top of the model and the regional background for a set of specified magnetisation contrasts. The high residuals of model (a) would be eliminated if the basin was allowed to extend to 24 km.

equation (2.18). As in the gravity models these estimates have a limited significance. They serve to give only a rough idea on the possible error in the "dummy" parameters within the simplifications assumed by the model.

	Horizontal distance from origin	Error	Depth below flight level	Error
Point no. 1	31.3	0.8	3.1	0.5
2	41.6	0.5	4.0	0.6
3	57.3	1.1	9.4	1.3
4	74.5	3.1	6.0	0.7
5	85.9	0.7	3.7	0.5

Table 6.2. Estimates of possible error in the coordinate parameters of Fig. 6.6b. The figures are in kilometers.

The time taken to obtain a solution in magnetic interpretation depends upon the same factors as in gravity methods (section 5.5). As an example we quote typical times required to obtain the model of Fig. 6.5 using an IBM 360/67 computer:

Method of rotating coordinates (P300)	8 minutes
Method of conjugate directions (P303)	6 minutes
The 'Complex' method (P301)	15 minutes
Davidon's method (P306)	50 seconds

### 6.7.2. The English Channel anomalies

Four moderately isolated anomalies in the English Channel were chosen to demonstrate the efficiency of optimisation techniques in magnetic interpretation (Figs 6.7 and 6.8).

All models were obtained using a direct search method,

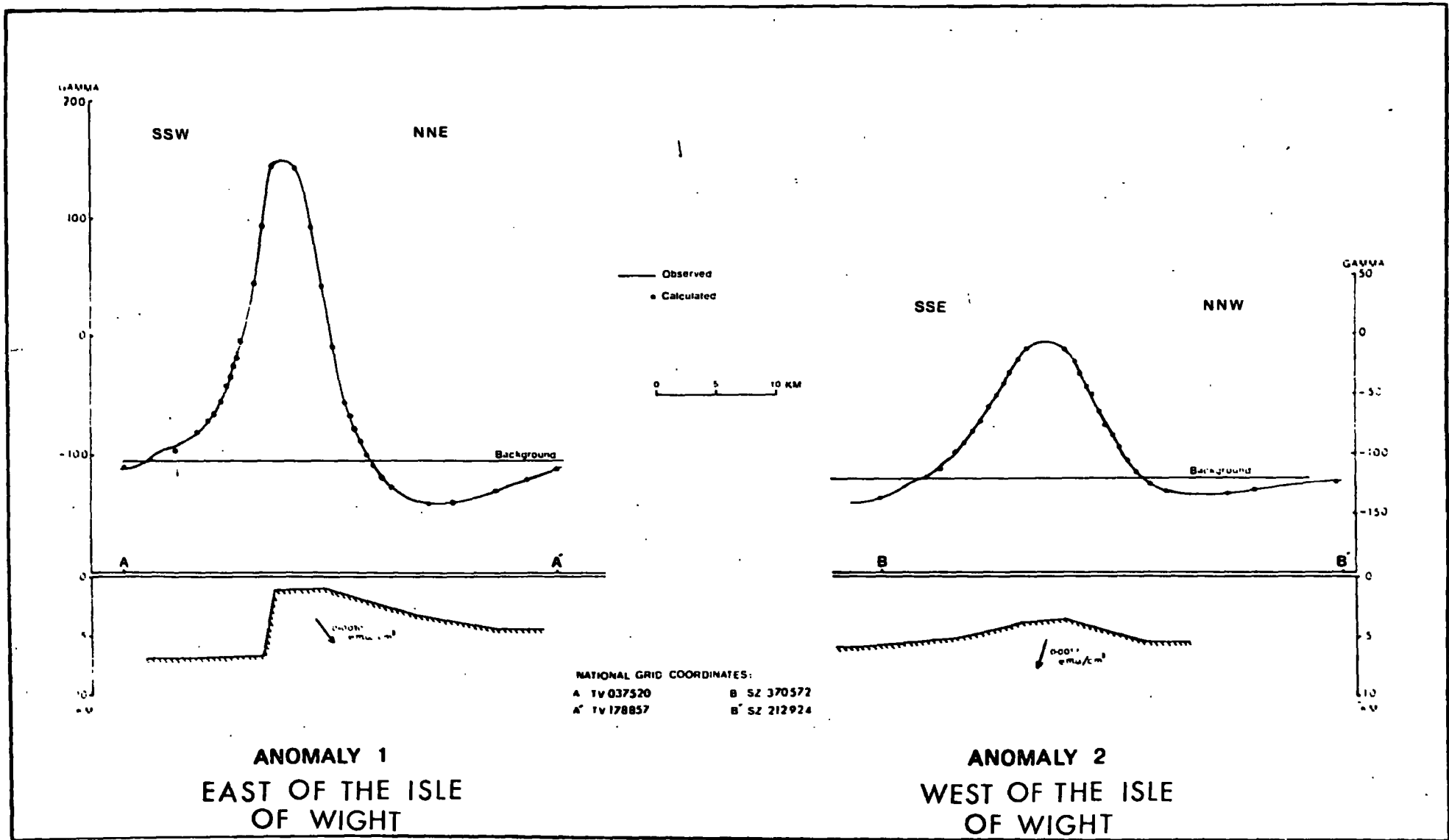
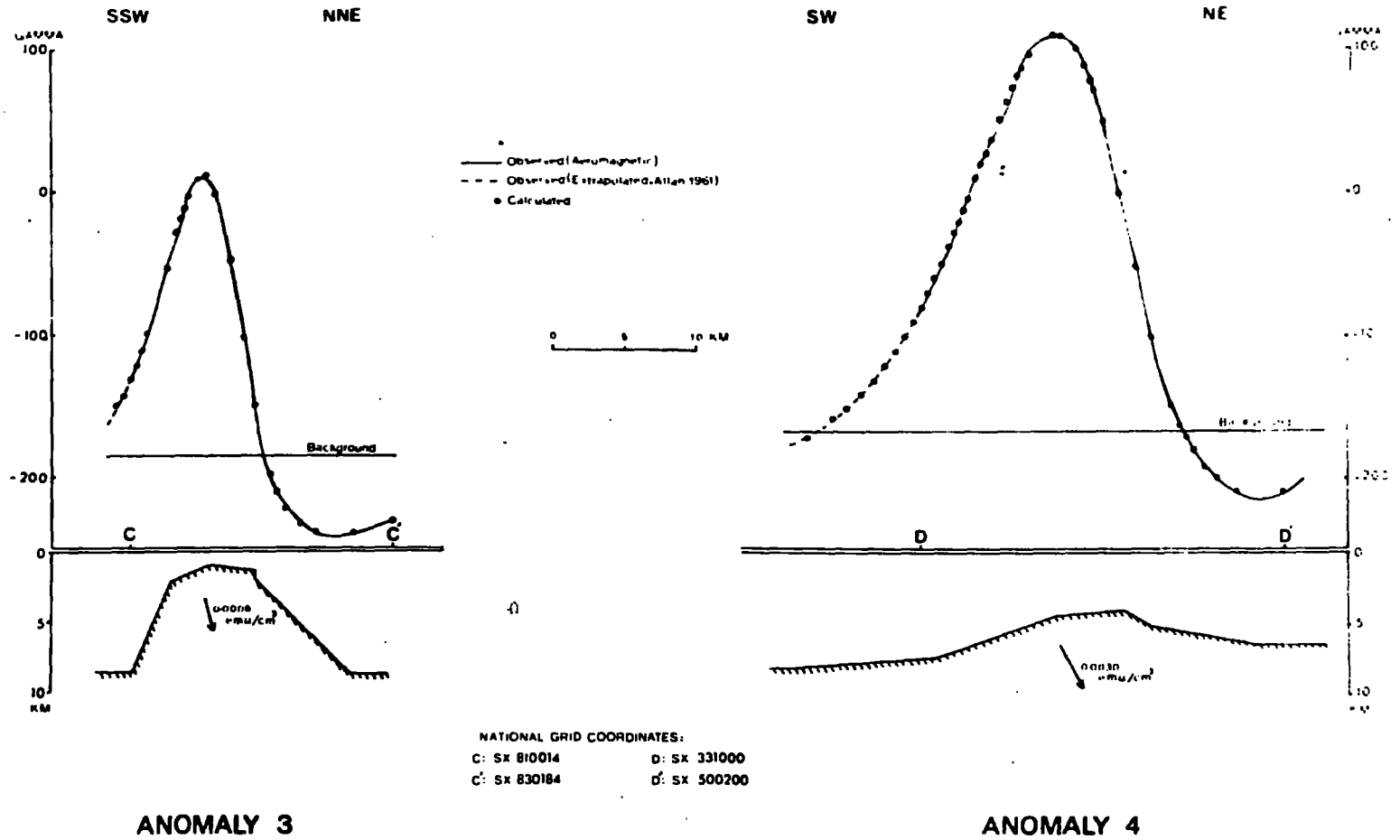


FIG. 6.7.

Fig. 6.8  
 Anomalies 3 and 4  
 lie to the south-  
 east and south  
 of Plymouth respect-  
 ively. Beyond the  
 edge of the aero-  
 magnetic map an  
 extrapolation  
 based on data pro-  
 duced by Allan  
 (1961) was used.



usually the method of rotating coordinates. They are all interpreted as features, within the basement, owing their origin partly to faulting and perhaps partly to igneous or metamorphic activities.

The interpretation of anomalies 1 and 2 (and solution A in Figs. 6.2, 6.3 and 6.4) is in good agreement with the structural features of the overlying Mesozoic and Tertiary rocks in this area (R. Dingwall, private communication).

The anomaly no. 4 was interpreted by Allan (1961) as being a basic intrusion which has been subject to some thrusting. Whilst the model of Fig. 6.8 would support such a proposition the depth to the top, suggested by Allan to be 1-1.5 miles, is about one mile shallower than that given by this model.

### 6.7.3. The Moray Firth

Two profiles were chosen across the Moray Firth at approximately right angles to the predominantly Caledonian trend. The method of rotating coordinates was used to obtain a general model and was followed by Davidon's method to obtain the required detail.

The two profiles (Fig. 6.9) show the presence of two important high features in the basement with the development of a basin-like structure between them. The 'high' in the north-west is bounded on the south-east by a fault which appears to be a continuation of the Helmsdale fault. The 'high' in the south-east is separated from the basin-like structure by a fault which appears as an extension of the

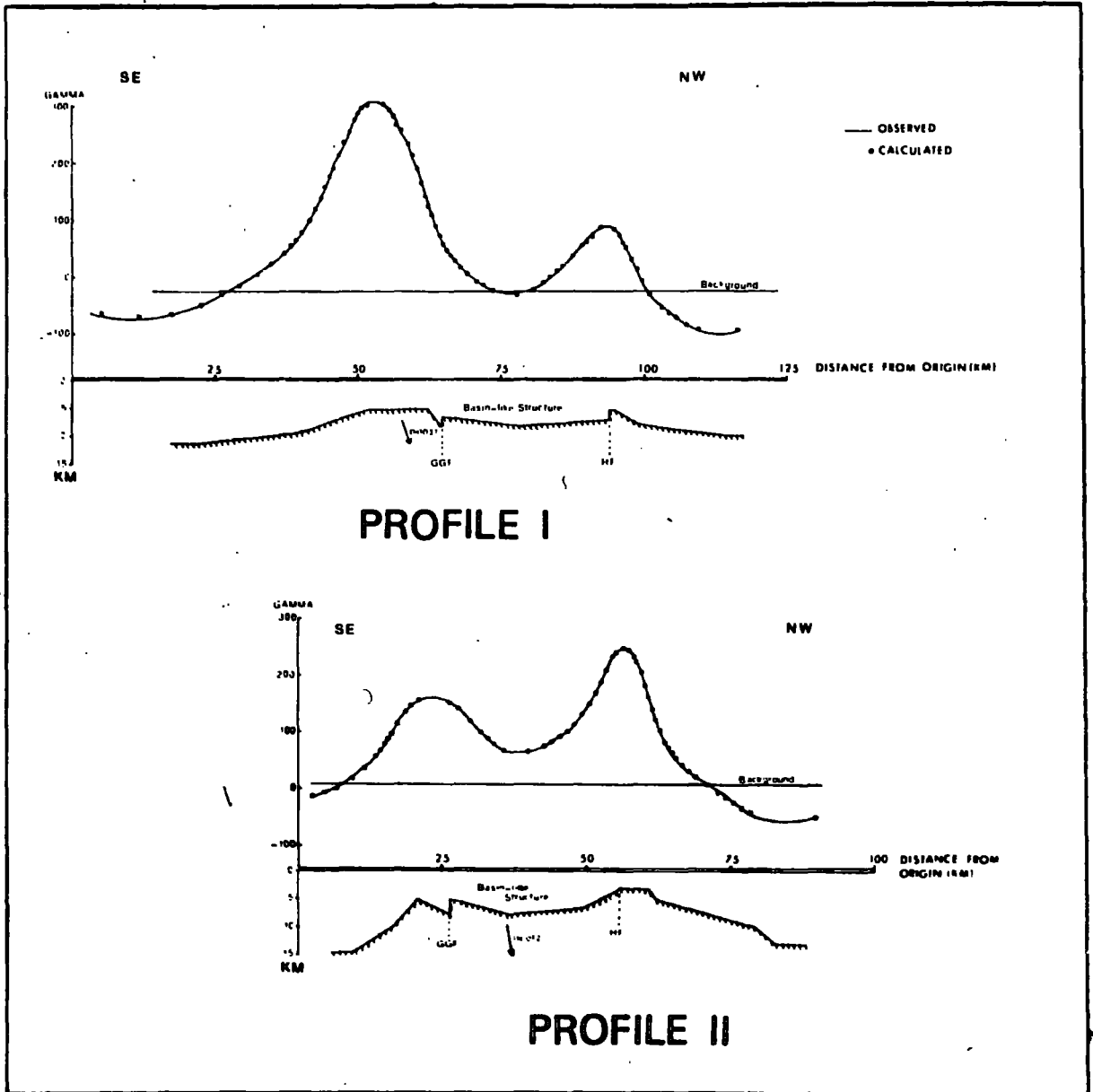


Fig. 6.9. The interpretation of two aeromagnetic anomalies across the Moray Firth. The magnetisation contrast (in e.m.u./cm) is assumed uniform in both models.

GGF = Great Glen Fault

HF = Helmsdale Fault

Great Glen Fault. Fig. 6.10 represents a likely conclusion from such interpretation.

The solutions are not unique. In particular, profile II may be interpreted using different magnetisation contrasts; an appropriate value would be a contrast similar to that obtained from profile I. Such assumptions tend to influence the depth coordinates mainly while the general picture remains basically unaltered.

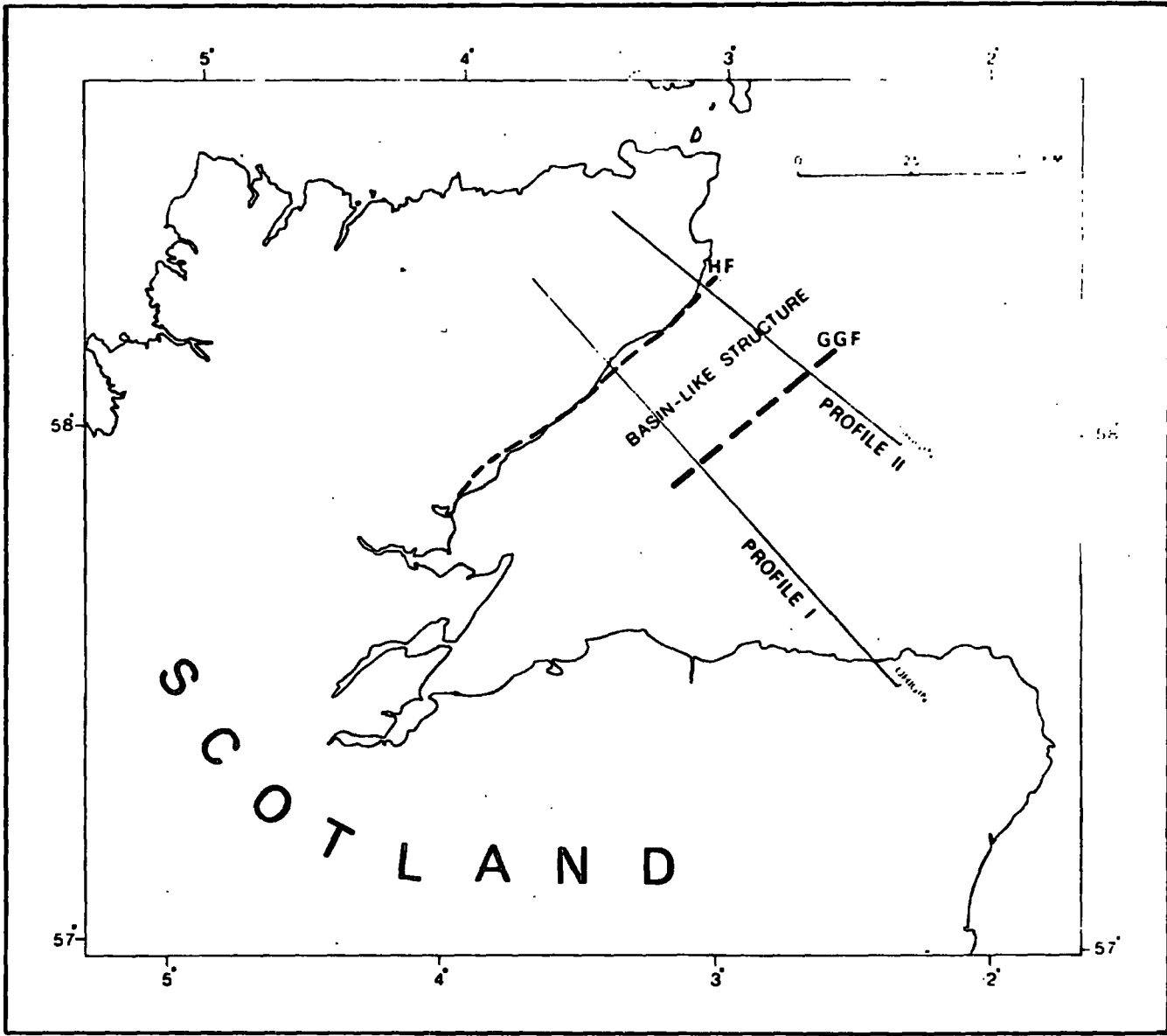
If the displacement along the Great Glen Fault was predominantly of lateral nature it would be expected to bring masses of contrasting magnetisations in contact. The assumption of uniform magnetisation of Fig. 6.9 would no longer be valid and the apparently good fit would be a normal consequence of ambiguity. The two profiles were, therefore, re-interpreted using **MULTIJ** programme with contrasting magnetisations across the supposed transcurrent fault. The optimisation process showed a tendency to bring the magnetisations, on either side of the fault, closer together. A good fit was actually only obtainable when the two magnetisations were not significantly different.

The results of this limited investigation are inconclusive. They suggest that the displacement along the Great Glen Fault is predominantly vertical. The whole interpretation is in favour of the following hypothesis. The Great Glen Fault is not a single fault but is a complex fault system involving a wide region on either side (including the Helmsdale fault). The faults are not always detectable in the magnetic basement owing to its large depth. The



Fig. 6.10 A map of the Moray Firth area showing the two profiles and a possible interpretation based on the models of Fig. 6.9

GGF = Great Glen Fault  
HF = Helmsdale Fault



fault system culminates in the development of a 'trough' along the middle of the basin-like structure. The Loch Ness 'trough' is its inland extension. The fault marked GGF in Fig. 6.9 is a major fault in the fault complex. The general structure is then similar to a 'rift system'.

The regional structural picture is not against this hypothesis. However, the hypothesis is difficult to reconcile with the increasing evidence in favour of the displacement along the Fault being predominantly lateral (e.g. Kennedy, 1946; Holgate, 1969).

Further details of this matter are not central to our present topic and a lot of work is obviously needed before the structural aspects of the area are fully understood.

## CHAPTER 7

## SEISMIC AND ELECTRICAL RESISTIVITY EXAMPLES

## PART I

INTERPRETATION OF  
SURFACE WAVE DISPERSION7.1. Introduction

The velocity of propagation of surface waves in layered media is frequency dependant. This is a consequence of the attenuation of particle displacement with depth, which increases rapidly as the frequency increases. For a given wave train, the relationship between the phase velocity,  $C(\omega)$  and the frequency,  $\omega$ , varies according to the  $\alpha, \beta, \rho$  and  $t$  parameters of the layers through which the waves are propagated, where

$\alpha$  = velocity of propagation of dilatational waves,

$\beta$  = velocity of propagation of rotational waves,

$\rho$  = density,

$t$  = thickness.

The relationship between  $C(\omega)$  and  $\omega$  is conveniently represented by a curve known as the phase velocity dispersion curve.

Those Fourier components which are momentarily in phase travel coherently as a group. The group velocity  $U(\omega)$  is directly obtainable from

$$U(\omega) = C(\omega) \left[ 1 - \frac{\omega}{C(\omega)} \frac{dC}{d\omega} \right]^{-1} \quad (7.1)$$

Interpreting the phase and group velocity curves in terms of  $\alpha$ ,  $\beta$ ,  $\rho$  and  $t$  can provide important information on the physical properties of the layers being traversed. The method is widely used in seismology to study the broad crustal and upper mantle structure of the earth.

Haskell (1953), modifying an older version by Thomson (1950), formulated the basic method for computing the phase velocity dispersion curve for a model of  $n$  horizontal layers. The formulation is applicable to Rayleigh and Love waves. The final expression which involves  $C(k)$  as a function of  $k$  ( $k$  being the wave number) is too complicated to enable obtaining  $C(k)$  directly from  $k$ . A univariate search procedure is used as an alternative.

Dorman et al (1960) adapted Haskell's formulation for carrying out the computation by digital computer. Harkrider and Anderson (1962) introduced other modifications to increase the range of frequency which the procedure can handle accurately.

The simplest interpretation of phase and group velocity curves is by trial and error. There are also procedures based on the method of steepest descent (e.g. Dorman and Ewing, 1962) etc. Matching the dispersion curve with a set of standard curves is also sometimes employed (e.g. Raju, 1968).

The problem is non-linear and invites a full utilisation of non-linear optimisation techniques.

## 7.2. Interpretation Using Optimisation Techniques

A simple objective function is given by

$$f(\underline{x}) = \left[ \frac{1}{n} \sum_{i=1}^n (A_i - D_i)^2 \right]^{\frac{1}{2}} \quad (7.2)$$

where  $A_i$  is the observed phase or group velocity value at the  $i^{\text{th}}$  frequency (or period) and  $D_i$  is the corresponding calculated value. The  $m$  variable parameters  $\underline{x}$  can include the  $\alpha, \beta, \rho$  and  $t$  of all the layers involved. The number of variables may be reduced by expressing  $\alpha$  in terms of  $\beta$  through the appropriate relationship.

The immediate choice of optimisation method is restricted to a direct search method for two reasons. Firstly, the relation between  $D$  and  $\underline{x}$  is complicated so that an explicit expression for  $\frac{\partial f}{\partial x_j}$  ( $j = 1, 2, \dots, m$ ) is difficult to provide. Secondly, the behaviour of  $f(\underline{x})$  in the  $\underline{x}$  hyperspace is apparently very complicated so that the use of a gradient method is unjustified until the final stages of the search.

To ensure the feasibility of the variable parameters simple constraints of the form given in equation (3.36) are sufficient. The method of conjugate directions can, therefore, be used. However, the method of rotating coordinates would probably be at least as efficient. The latter method was only available in PL/1. It could not be used in the investigation owing to problems arising from language compatibility with the auxiliary procedure which was only available in Fortran IV.

The investigation was started by interpreting a Rayleigh phase velocity curve computed for a theoretical

2-layer model. The  $\alpha, \beta, \rho$  and  $t$  parameters of the layers were not specified. Using the objective function defined by equation (7.2), the search was started from a reasonably distant initial point. The progress was quite slow and terminated without locating the original model.

The phase and group velocity curves were then combined using

$$f(\underline{x}) = \left[ \frac{1}{n} \sum_{i=1}^n (A_i - D_i)^2 \right]^{\frac{1}{2}} + \left[ \frac{1}{n} \sum_{i=1}^n (A'_i - D'_i)^2 \right]^{\frac{1}{2}} \quad (7.3)$$

where the prime denotes group velocity. The search, in this case, terminated at the true solution after achieving a very rapid progress.

These experiments were substantiated by a number of other trials from different initial points. The results tentatively suggest that the inverse solution for a theoretical problem is probably unique. The incorporation of group velocity data cannot be the cause of this uniqueness since the group velocity is directly obtainable from the phase velocity. The original model could not be recovered by using phase velocity alone probably because the points with very low function value lie in a narrow trough (Fig. 7.1) causing the search to terminate by local convergence. The incorporation of group velocity data has probably improved the conditioning of the problem.

The conditioning of the problem can be further improved by incorporating the Love dispersion curve, the latter being an independent observation of the Rayleigh dispersion curve.

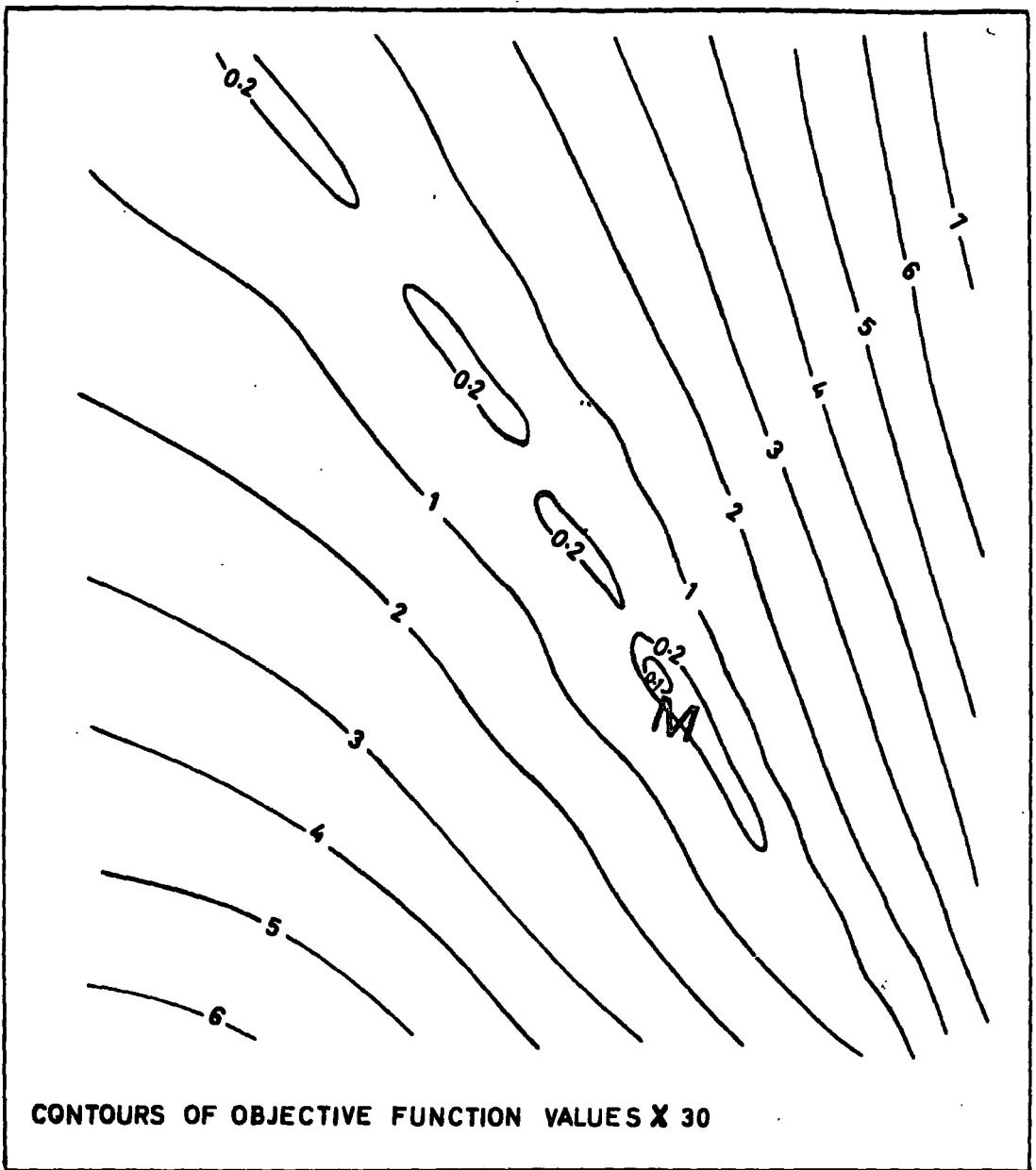


Fig. 7.1. An oblique section through the  $x$  hyperspace of the objective function corresponding to a Raleigh phase velocity dispersion curve of a two-layer model. Point M represents the true solution. Points with low function values occupy a long narrow region (not wholly in the plane of the section).

This was supported by a limited amount of experimentation.

From a practical point of view, the indeterminacy of the inverse solutions seems to be more pronounced than in the case of gravity and magnetic problems. Any combination of phase and group velocity curves of Rayleigh and Love waves would, therefore, be highly desirable. However, not all these data are usually available. The accuracy of the data may also impose a limitation. The best practical approach is to specify as many parameters as possible.

A test on actual field data was carried out using phase and group velocity of Rayleigh waves to investigate the crustal and upper mantle structure in the East African rift area.<sup>1</sup>

The model was divided into fourteen different layers (Fig. 7.2). To limit the indeterminacy, the  $\alpha$ ,  $\rho$  and  $t$  parameters of all layers were specified; Dorman and Ewing (1962) suggest that these conditions are sufficient to ensure the uniqueness of the solution within the limitation of observational errors.

Results of the interpretation (Fig. 7.2) do not appear to be realistic. The oscillation in the values of  $\beta$  is probably due to the decrease of the resolving power of the method with increased depth. Some of the layers were therefore combined and the resulting model consisted of

---

1. This test was carried out by Mr. K. Sundaralingam.



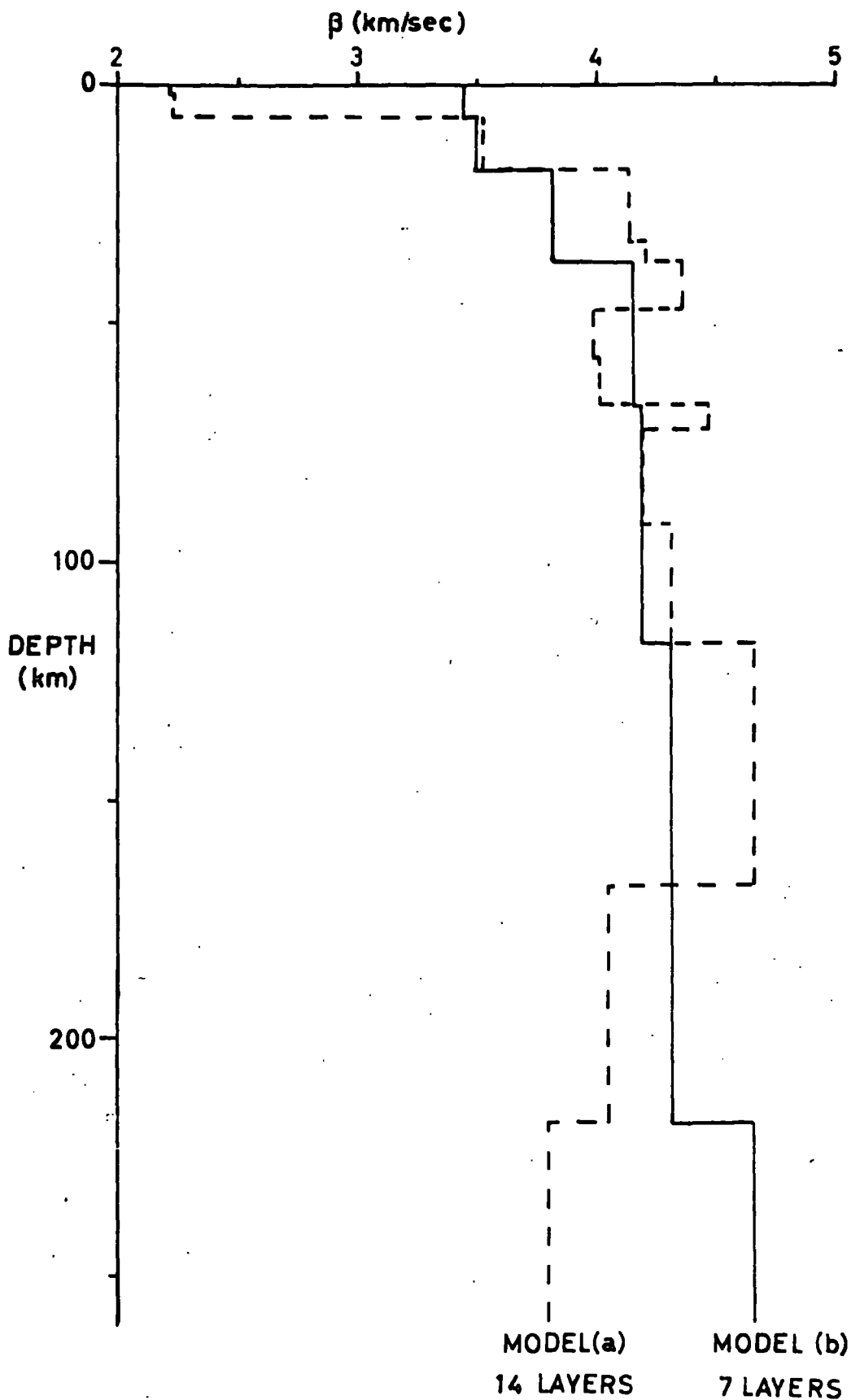


Fig. 7.2. An interpretation of a combined Raleigh phase and group velocity dispersion curves for the variation of the velocity of rotational waves with depth in the East African rift area. The velocity of the top and bottom layers of model (b) are specified.

seven layers only. The  $\beta$  values of the top two layers and of the bottom layer were also specified. The solution was quite satisfactory in this case (Fig. 7.2). Although the R.M.S. deviation (= 0.9) was higher than that of the first model, the agreement between the observed and the calculated data was still inside the range of observational errors.

However, in view of the limited amount of experimentation, the results given above must be subject to further testing.

## PART II

INTERPRETATION OF APPARENT RESISTIVITY CURVES OVER  
LAYERED MEDIA7.3. Introduction

The variation of electrical resistivity with depth is usually studied by interpreting a plot of apparent resistivity vs. electrode spacing known as the apparent resistivity curve. Most methods of interpretation are based on the assumption that the ground consists of  $n$  horizontally stratified layers of infinite extent and which are uniform and, usually, isotropic. These methods are usually based on a formulation by Stefanescu (1930) for the potential  $V$  at a distance  $r$  from a point source of current  $I$  on the surface of the ground. This is given by

$$V(r) = \frac{I \rho_1}{2\pi r} \left[ 1 + 2r \int_0^{\infty} K(t) J_0(rt) dt \right] \quad (7.4)$$

where

$\rho_1$  = resistivity of the top layer

$J_0$  = Bessel function of first kind and zero order

$t$  = parameter of integration

$K$  = the kernel function determined by layer depths and resistivities.

A common method of interpretation is to compare the apparent resistivity curve with a set of standard curves (e.g. La Compagnie Générale de Géophysique, 1955; Mooney and Wetzel, 1956). Vosoff (1958) works with the kernel function and uses the methods of Newton and steepest descent

(section 3.3) to determine the parameters of the layers. Other methods treat the observed curve directly. Koefoed (1968) decomposes the curve into a number of partial apparent resistivity curves and uses a 'raised kernel function' at the final stages to determine the depths and resistivities of the layers.

However, most methods require lengthy calculations or tedious operations. Moreover, although the solution to the inverse problem in electric resistivity is, theoretically, unique (Langer, 1933), a large number of widely contrasting models can usually produce apparent resistivity curves which agree closely between themselves. This phenomenon is known as the "principle of equivalence". These difficulties are further increased by deviations from the theoretical conditions assumed by the model, by the presence of observational errors and by the decrease in the resolving power of the resistivity method with depth. Optimisation techniques do not overcome these difficulties. A careful application of the techniques, however, can substantially reduce the limitations and increase the reliability of the interpretation.

#### 7.4. Interpretation Using Optimisation Techniques

An iterative procedure based on minimising the discrepancy between an observed and a calculated apparent resistivity curve requires very unreasonable computer time. Even under favourable circumstances and using efficient methods (e.g. Van Dam, 1965; Mooney et al, 1966), the

computation of a single curve due to a four-layer model would require about 10 seconds on IBM 360/67 Computer. Gradient methods would require at least 20 iterations and are not expected to perform efficiently in the earlier stages of the search, as was indicated in parts of the work of Vosoff (1958). Sequential and linear direct search methods would require some 100 or more iterations per variable. In all cases, the computer time involved is quite considerable on an industrial scale.

To overcome the question of computer time, a curve matching process is adopted to provide a value for the objective function, with minimum computation. This process constitutes the auxiliary procedure. The main optimisation procedure is based on a modification of grid tabulation techniques (section 3.2.1.). The method consists of the following stages:

1. A set of standard curves, referring to a specific number of layers (four in our case) and covering a wide range of resistivity and depth ratios, are digitised. Each curve is identified by a unique number denoting its depth and resistivity ratios.

2. The number of variable parameters is reduced to two, namely the depth ratio and the resistivity ratio of the layers. In the resulting two-dimensional space, the objective function will be known only at points for which standard curves exist. Since these curves are computed for discrete intervals in the two parameters, there results a two-dimensional grid in which the objective function is known at the nodes only.

3. The observed curve is digitised at the same intervals as the standard curves. The observed curve is compared systematically with all standard curves in the required range of depth and resistivity ratios. The objective function at each node is represented by the sum of squares (or absolute values) of residuals between the observed curve and the standard curve corresponding to the particular node.

4. The best fitting standard curve, i.e. the node with the lowest function value, does not generally represent a true solution, partly because of equivalence and partly because the ground being tested does not usually consist of layers in the same ratios of depth and resistivity as any of the standard curves. However, this 'optimum' fit can give a rough estimate of the depths involved; the depth ratios being converted to actual values by using the appropriate conversion parameters.

5. The value of each objective function is output near or at the corresponding node on the grid. A convenient representation of these values is to use alphameric characters denoting the range in which each value falls. An example of such output is shown in Fig. 7.3.

6. Those standard curves producing a reasonable fit are determined by visual inspection of the grid. The general scatter of these curves, throughout the grid, makes it possible to determine those depth and resistivity ratios which are more likely than others.

7. Using external control, all ratios which do not

```

.H .H .G .G .G .G .G .G .F .F .F .G .G .F .G .G .G .G .G .G
.G .G .G .F .F .F .D .D .C .B .B .C .D .D .F .F .D .F .G .G
.G .G .G .F .F .F .D .D .C .C .D .C .D .C .D .F .D .F .G .J
.G .G .G .F .F .F .D .D .D .D .D .D .D .D .D .F .D .F .G .G
.H .G .K .J .H .K .K .K .J .G .G .G .G .F .F .F .F .C .F .G
.F .G .G .F .F .F .F .D .F .F .H .F .C .F .D .F .D .F .G .G
.J .H .H .G .L .K .K .M .L .M .M .M .M .L .L .K .J .J .H .H
.H .H .G .K .K .L .L .K .K .K .K .K .K .J .J .J .H .G .G .G
.F .G .F .F .G .H .H .H .H .H .J .H .H .G .G .G .F .D .F .D
.B .C .C .C .C .C .C .D .D .D .D .D .C .C .B .F .A .B .B .C
.F .F .F .F .F .F .F .F .F .F .B .B .A .B .A .A .B .C .C .C
.G .H .H .H .H .H .H .H .H .H .H .H .H .H .H .H .H .H .H .H
.G .F .F .G .H .H .H .H .H .H .H .H .N .N .J .H .H .H .H .H
.D .C .D .F .F .F .F .G .G .F .F .F .F .F .F .G .G .F .F .F .G
.O * .A .C .C .A .A .F .B .C .B .B .C .C .D .D .B .C .C .F
.G .F .F .F .H .H .H .H .H .J .J .J .J .H .H .H .G .G .G .G
.J .H .G .G .K .K .J .K .K .K .L .L .S .K .K .K .J .J .J .J
.K .J .J .H .L .L .K .M .L .M .M .M .M .M .M .M .L .L .L .L

```

Fig. 7.3. An example of a grid output. The alphameric characters indicate the degree of fit with each standard curve in ascending order so that a fit of degree A is better than a fit of degree B. The asterisk denotes the standard curve with the best fit. The O indicates the standard curve with the next best fit.

conform with available informations can be discarded and a final interpretation may then be made.

The method has many advantages. Firstly, it is extremely fast; the average computer time per curve is just over half a second on an IBM 360/67 computer. Secondly, the "principle of equivalence" is overcome appreciably by outputting a whole series of possible solutions rather than a single one. Thirdly, no tedious operations or calculations are involved.

The method has also a number of limitations. Firstly, it is only applicable to a specific number of layers. Secondly, it requires the provision of a set of standard curves which may have to be constructed if the desired depth or resistivity ratio intervals are unavailable. The standard curves usually also require a very large storage space in the computer. Thirdly, it is only possible to provide the solution at discrete intervals.

The applicability of the method to field data was tested by interpreting a number of apparent resistivity curves obtained over glacial drift. A borehole log was available close to the position of each of the resistivity probes so that a direct assessment of the solution was possible.

The depth to the lowest interface obtained from the optimum fit, in each of the interpretations, was used as a reference to convert the depth ratios to actual values. The probable interpretation was then generally worked out in the manner described above. Some of these interpretations are



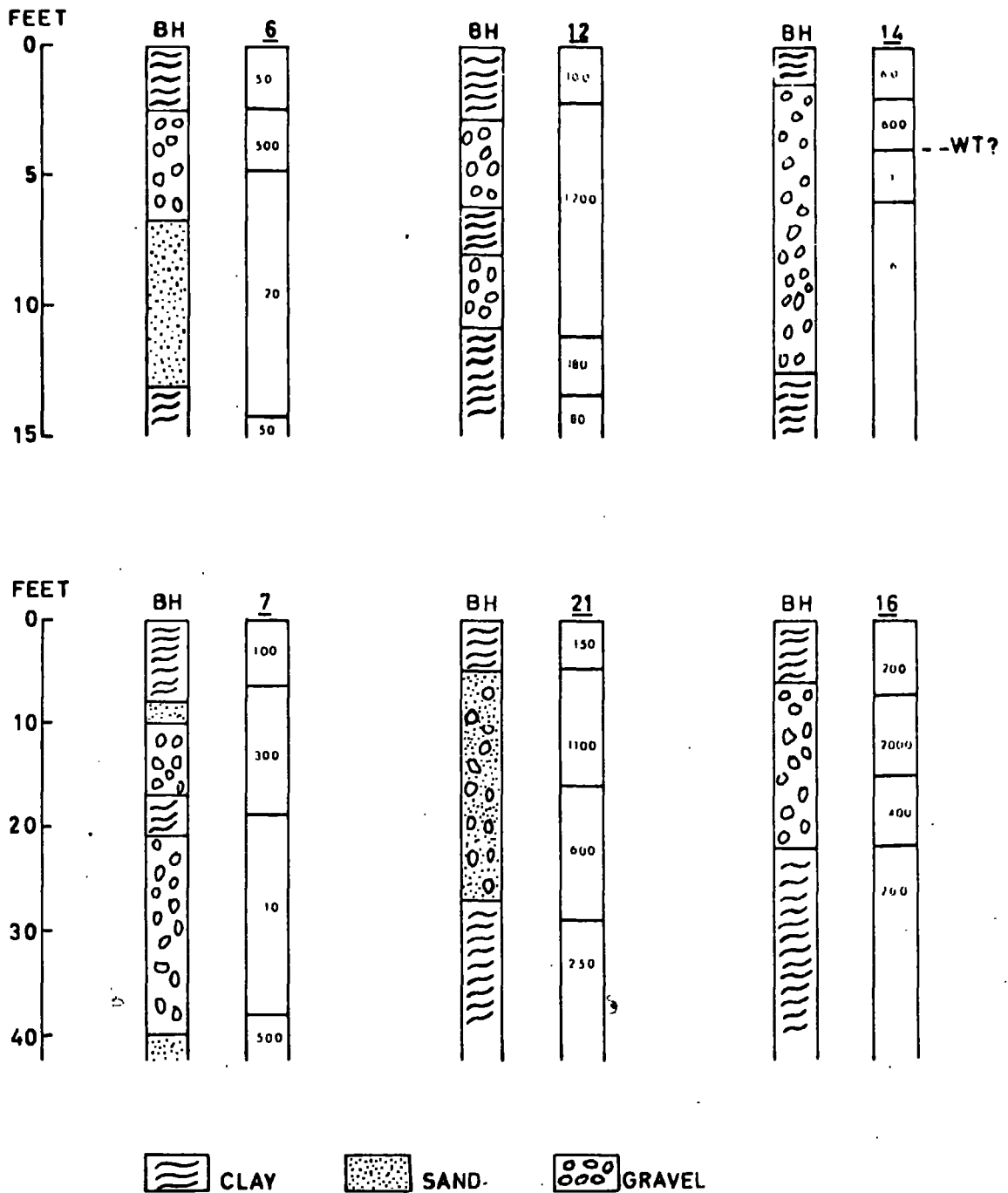


Fig. 7.4. Comparison of interpretation of apparent resistivity curves with borehole results drilled in the vicinity of each depth probe.

Underlined figures represent the code number of the depth probe. Figures inside the columns represent resistivity in ohm. ft. estimated very roughly.

BH = Borehole log

WT = Water table

shown in Fig. 7.4. Most of them show quite a good agreement with the borehole log indicating that the method is, probably, at least as efficient as most other methods.

## CHAPTER 8

## THE FITTING OF CONTINENTAL EDGES

8.1. Evolution of the Concept of Continental Drift

The first serious attempts to establish continental drift were those made by Taylor and, more significantly, by Wegener, more than fifty years ago (Holmes, 1965 p.1199). However, due to the lack of a plausible mechanism for the drift, this early work was subjected to sharp criticisms which checked further advances. Thus, the concept of continental drift remained no more than an embarrassing possibility. Most palaeontologists had still to make do with some unreasonable land bridges to ferry the various migrating species across both sides of the Atlantic while paleo-climatic findings were being explained away by polar-wandering speculations.

Early in the fifties, however, a vast amount of palaeomagnetic data began to furnish fresh and powerful evidence for continental drift, exemplified by the works of Blackett, Creer, Irving, and Runcorn, among many others. With the support of this new and independent evidence, all major geological and palaeo-climatic results were integrated to provide grounds for the rapidly evolving concept of ocean-floor spreading by the injection of new material along oceanic ridges (Dietz, 1961; Hess, 1962). The significance of magnetic lineations was being rapidly realised (Vine and Matthews, 1963; Pitman and Heirtzler, 1966) and the role of

transform faults in the growth of ocean-floor, and hence in continental drift, was becoming more apparent (Wilson, 1965). The continuous flow of data and the gradual elaboration of ideas led to the collection of all the evidence under yet another new concept, now popularly known as "plate tectonics".

According to the new concept, the outer part of the globe is formed by the lithosphere, a relatively rigid material about 100 kms. thick (and therefore includes the crust and the uppermost part of the mantle) resting on a layer, about 700 kms. thick, of effectively no strength, called the asthenosphere. The lithosphere consists of a number of blocks (e.g. McKenzie and Parker, 1967; Morgan, 1968); each block is relatively aseismic and is defined by seismically active boundaries (Sykes, 1967; Isacks, Oliver and Sykes, 1968). The relative movement between the blocks is associated with the creation and destruction of the lithosphere and is consistent and interrelated on a global scale (Le Pichon, 1968). The boundaries of each block do not in general coincide with continental boundaries but continental drift is implicit in these relative motions. The mechanism for the motion is usually sought in terms of convective processes. However, regardless of whether the concept of plate tectonics and the mechanisms behind it continue to be supported by fresh evidence, we shall assume continental drift to be a real geologic process. The actual mechanism causing the drift is not an essential part of the present work.

## 8.2. The Significance of the Fit

Restoring the original position of continents by fitting corresponding lines along which fracturing and separation is supposed to have taken place was the most tempting method to demonstrate continental drift. Except in very special cases, the irrelevance of the actual coast line for the fitting process is quite obvious. Continents are usually delimited by the continental slope which is usually quite steep. Any isobath between 500 and 1000 fathoms will normally represent the edge of the continent, adequately. However, it cannot be assumed that the initial break up was effected at a uniform depth nor can the passage into oceanic crust be expected to take place at the same level. No single isobath, therefore, can define the original break up. This is further complicated by the deformation that may accompany fracturing and drifting and by the depositional and erosional processes subsequent to separation. Therefore, for a given fit, the presence of gaps and overlaps is not always serious. They can be the result of any of the factors mentioned above. Therefore, these factors can become important in asserting the plausibility of a given fit. However, they can also shed extensive doubt on the validity of the position of the pole of rotation obtained on the bases of minimising the misfit between the edges being matched (section 8.5).

Occasionally, it may become impossible to employ the continental slope in the fitting procedure. Depositional or extrusive activities may reach such an extent that they

could completely obscure the continental slope, e.g. the Red Sea. Separation may also have not progressed sufficiently far for a continental slope to develop, e.g. The East African rift system. The continental edges in these cases, are approximated by methods appropriate to each individual case. For these reasons, we shall use the term 'edge' in a general way to denote the sides of continents being fitted, regardless of whether these sides represent a coastline, a continental slope or any other feature.

The reality of the fit must also be translated geologically since the shape fit is merely the first criterion. This was well discussed by Westoll (1965) who also points out that a detailed matching of structures is difficult although the correlation may be improved by drilling, sample dredging, etc. Examples of the use of geological criteria, in restoring continents to their pre-drift relative position will be given later.

### 8.3. Fitting Procedures

#### 8.3.1. General remarks

Continents may be restored to their original relative position by making use of a theorem due to Euler, namely that any displacement of a rigid shell on the surface of a sphere is equivalent to a rotation about an axis through the centre of the sphere (Bullard et al, 1965). This axis meets the surface of the sphere at two points known as the centres or poles of rotation. The geographical position of one of the two centres of rotation is sufficient to define

the axis on the surface of the earth assuming that the earth is practically a sphere.

Continental drift may be envisaged as the rotation of one continent relative to the other about a given centre of rotation. Determination of the geographical position of the centre and the amount of rotation are sufficient to restore the two continents to their pre-drift relative position.

The rotation at various stages could have been achieved about successively different centres (see for example Fox et al, 1969). It is the resultant relative displacement that must be determined in these cases.

The position of the centre of rotation may be determined using transform faults or other data from ocean-floor spreading (e.g. Morgan, 1968; Le Pichon, 1968). Palaeomagnetic evidence may also be used for the purpose (Frencheteau and Sclater, 1969). However, these methods are usually concerned with the movement between plates at various stages of their geological history rather than with establishing original relative position of continents. Our present topic is concerned with determining the centre of rotation directly from the fit between the two continental edges regardless of what paths these continents followed in acquiring their present position

### 8.3.2. Bases of the method

The edge of a continent can be defined by the latitudes and longitudes of a series of points placed sufficiently close for the form of the continental edge to be interpolated between them. We can consider the centre of rotation as a

geographical pole and convert the latitudes and longitudes of all these points to correspond to the new pole, using the following equations (Young and Douglas, 1968):

$$t = \sin^{-1} (\sin T \sin a + \cos T \cos a \cos B) \quad (8.1)$$

$$e = \tan^{-1} \left[ \cos T \sin B / (\cos T \sin a \cos B - \sin T \cos a) \right] \quad (8.2)$$

where

T = latitude of any point

E = east longitude of any point

a = latitude of new pole (centre of rotation)

b = east longitude of new pole

t = latitude of point with respect to new pole

e = east longitude of point with respect to new pole

B = E - b.

The problem is then to find the position of a centre of rotation which would give an optimum fit between the two edges being matched.

There are several possible criteria for the optimum fit. Bullard et al (1965) use the function

$$Q^2 = \frac{1}{2N} \left[ \sum_{n=1}^N (s_n - s_o)^2 + (s'_n - s_o)^2 \right] \quad (8.3)$$

where

N = the number of points on each side,

$s_n$  = the longitude difference between the  $n^{\text{th}}$  point on the first edge and its interpolated equivalent (on the same latitude) on the second edge.



$S_n$  = the longitude difference between the  $n^{\text{th}}$  point on the second edge and its interpolated equivalent on the first edge.

$$S_o = \frac{1}{2N} \sum_{n=1}^N (S_n + S'_n).$$

All measurements refer to the centre of rotation as the new pole.

$a$  and  $b$  are the only variable parameters of  $Q$ . Bullard et al (1965) use the method of alternating variables (section 3.2.3) to minimise  $Q(a,b)$ . The values of  $a$  and  $b$  at the optimum give the required position of the centre of rotation while  $S_o$  is numerically equal to the amount of rotation necessary to bring the two edges in contact. However, although the procedure of Bullard et al is very sound in principle it suffers from the drawbacks of the method of alternating variables and from the possibility of converging at a local minimum.

Our method is based on the same principle but the optimisation is carried out differently in order to avoid the drawbacks mentioned above and to gain certain advantages.

We define an objective function  $Q$  by

$$Q = \frac{1}{M+N} \left[ \left( \sum_{n=1}^N (S_n - S_o)^2 H_n W_n \right)^{\frac{1}{2}} + \left( \sum_{m=1}^M (S_m - S_o)^2 H_m W_m \right)^{\frac{1}{2}} \right] \quad (8.4)$$

where

$N$  = number of points on the first edge

$M$  = number of points on the second edge

$H = \cos^2(t)$ . Appropriate factor to allow for longitude difference at different latitudes, i.e. to emphasise the actual distance of misfit.

$W$  = appropriate weighting function according to the reliability of the part of the edge involved.

If

$$S_u = \frac{1}{N} \sum_{n=1}^N S_n \quad , \quad S_v = \frac{1}{M} \sum_{m=1}^M S_m$$

then

$$S_o = \frac{1}{2} (S_u + S_v)$$

The fact that  $Q$  is function of two variables only is of fundamental importance. We make use of this by mapping  $Q$  in the two dimensional space of  $a$  and  $b$ . This has the advantage of providing a complete description of the behaviour of  $Q$  within the range being mapped. The presence of any local minima becomes, therefore, readily detectable. More important is the possibility of asserting how well defined is the global minimum and, therefore, its validity when compared with other points in its neighbourhood. The importance of this feature will become evident when the significance of the position of the pole of rotation is discussed.

To map the function we use the grid tabulation method (section 3.2.1). Each node of the grid is defined by its appropriate  $(a,b)$  value.  $Q$  is thus evaluated for a range of values of  $a$  and  $b$  sufficient to cover all possible solutions, at intervals determined by the required accuracy. According to the grid method the node possessing the lowest

value of  $Q$  is considered the required minimum. However, such a solution does not achieve any of the advantages mentioned above. We therefore print out the whole grid. The printed values of  $Q$  are arranged in such a manner that the  $b$  - axis is the horizontal axis of the grid and the  $a$ -axis is the vertical one. Each node has the corresponding  $Q$  value printed on it. The resulting grid is then contoured for equal values of  $Q$  and a map of  $Q$  for the specified range of  $a$  and  $b$  is produced.

In practice, the numerical values of  $Q$  are not output. Instead, an alphameric character denoting the range in which  $Q$  falls, is output at each node, similarly to the method of section 7.4. This renders the contouring process easy without much loss in accuracy.

The recommended procedure is to cover a wide range of  $a$  and  $b$  values on an initial map, using a coarse interval. Once the solution is localised, a high resolution may be achieved by mapping the appropriate range of  $a$  and  $b$  at a much smaller interval; the accuracy to which a solution may be obtained by this method has no limit. However, a high resolution is often unnecessary in view of the large possible variation in the position of the optimum pole of rotation for a given tolerance. Usually, this tolerance depends upon the density and accuracy of the digitised points. It also depends upon how well do the fitted edges represent the original continental edges.

#### 8.4. Description of Programme

The essential features of the computer programme are shown by means of a flow chart (Fig. 8.1). The blocks marked by broken lines constitute the auxiliary part of the optimisation programme. This auxiliary part may also be used with any other optimisation method when an alternative to mapping  $Q$  is sought.

The procedure works with each point  $(a,b)$ , in turn. The current point is assumed to be the new pole so that all the coordinates are converted with respect to it. For each of the digitised points,  $u_n$ , on edge  $U$ , an equivalent point,  $v_n$ , on edge  $V$  is then located i.e. a point which falls on the same latitude as  $u_n$  with respect to the new pole. The process is then repeated for all the digitised points,  $v_m$ , on edge  $V$ .

The equivalent of  $u_n$  is found by a linear interpolation between two successive points  $v_m$  and  $v_{m+1}$  on edge  $V$  where

$$T_{v_m} < T_{u_n} < T_{v_{m+1}} \quad \text{or} \quad T_{v_m} > T_{u_n} > T_{v_{m+1}}$$

Since  $T_{v_n} = T_{u_n}$ , it is sufficient to determine  $E_{v_n}$  in order

to define  $v_n$ . The linear interpolation gives

$$E_{v_n} = (E_{v_m} - E_{v_{m+1}}) \frac{T_{v_n} - T_{v_m}}{T_{v_{m+1}} - T_{v_m}} + E_{v_m} \quad (8.5)$$

The actual relationship in spherical trigonometry is more complicated and entails several cumbersome evaluations. However, if the difference between  $v_m$  and  $v_{m+1}$  is less than

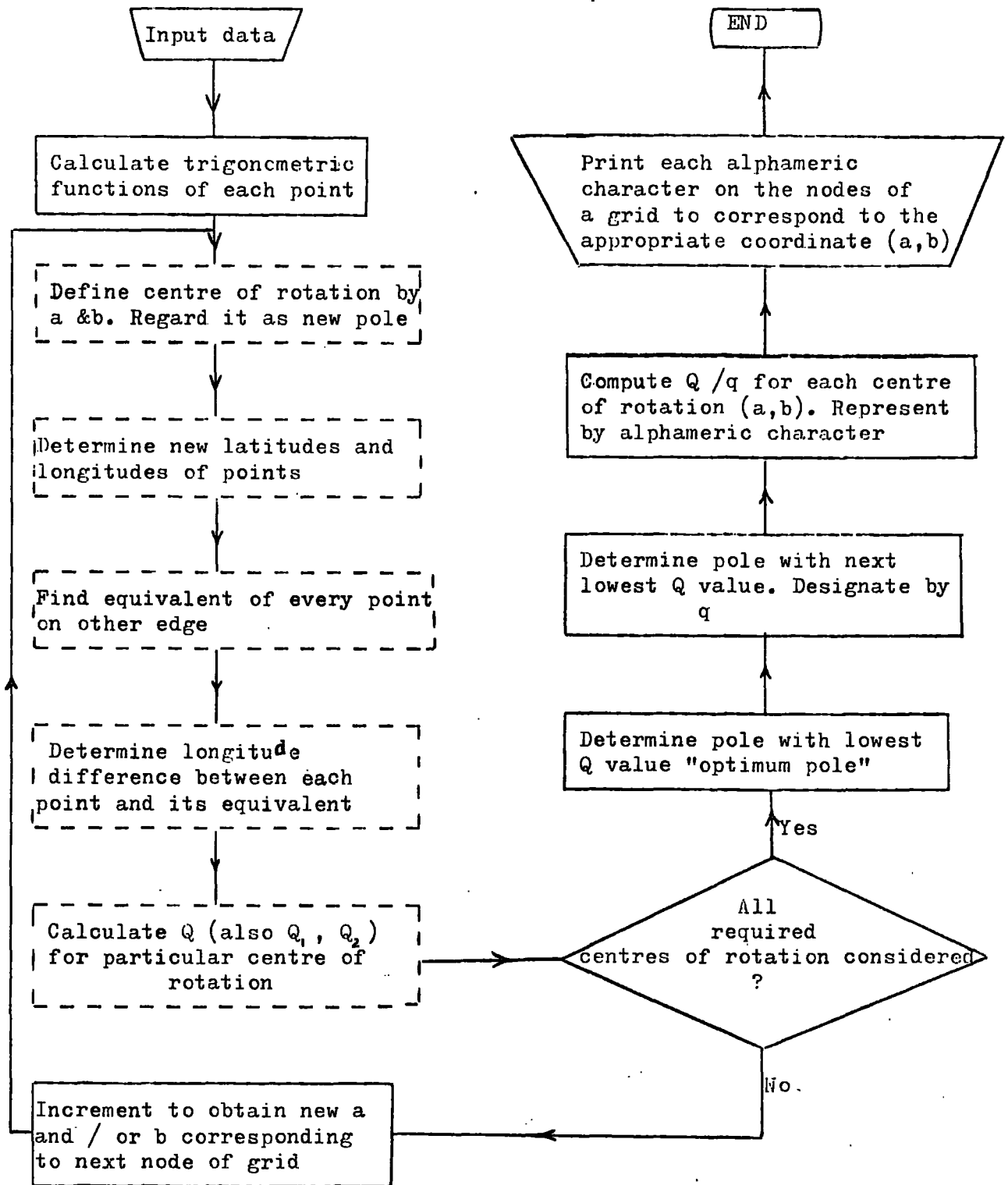


Fig. 8.1. A flow chart outlining the basic method of obtaining grids for the objective functions  $Q_1$ ,  $Q_2$  and  $Q$ . Blocks of the auxiliary part are marked by broken lines.

$2^\circ$  the error in  $E_{v_n}$  is less than  $0.002^\circ$ , which is adequate for practical purposes.

Three kinds of objective function are computed simultaneously so that three maps corresponding to  $Q_1$ ,  $Q_2$  and  $Q$  are produced, where

$$Q_1 = \frac{1}{N} \left[ \sum_{n=1}^N (s_n - s_u)^2 \cdot H_n \cdot W_n \right]^{\frac{1}{2}} \quad (8.6)$$

$$Q_2 = \frac{1}{M} \left[ \sum_{m=1}^M (s_m - s_v)^2 \cdot H_m \cdot W_m \right]^{\frac{1}{2}} \quad (8.7)$$

The maps of  $Q_1$  and  $Q_2$  serve as a qualitative criterion for assessing the validity of the solution; when the minimum is well-defined, agreement between the three maps is quite strong.

The execution time depends upon the number of grid points, the number of points defining each edge and somewhat upon the shape of the edges being matched. If individual parts of the edges are given different weights, the computation time is increased further. For 30 latitude values and 30 longitude values (900 nodes) on each of the grids of  $Q_1$ ,  $Q_2$  and  $Q$ , and with 60 points defining each of the two edges, a typical time required on an IBM 360/67 computer is about 6 minutes. Although this time is quite practical, it is somewhat large and constitutes a drawback in the method. Only 10 seconds will probably be sufficient for the same problem if another optimisation method (the

pattern search method for example) was used. However, this would mean the loss of the advantages of mapping Q.

The second drawback arises in the presence of special types of infolds on the fitted edges. If an infold is present on edge V then a given point,  $u_k$ , on edge U may have two equivalent points on V: While our method of finding an equivalent will deal with most types of infolds properly, there are certain situations when the method will fail. However, such situations are very rare; should they arise, the programme could be appropriately modified to deal with them. McKenzie et al (1970) attempt to overcome difficulties with turns and infolds by minimising the total area of misfit. However, it is necessary with such an objective function to use the angle of rotation as a third variable.

The third drawback concerns the need for a large storage space in the computer; at least 120 K bytes are required in most problems.

#### 8.5. Significance of the Position of the Pole of Rotation

The method of restoring continents to their pre-drift position by regarding their relative displacement as a rigid rotation about a given pole, has received wide attention since its introduction by Bullard et al (1965). However, although the pole position and the angle of rotation completely define the displacement, the inverse problem, i.e. the determination of the pole position and the amount of rotation, is not unambiguous in practice.

Most methods determine this pole by assuming it to produce minimum gaps and overlaps, i.e. the 'best fit' between the edges being matched. This is probably the best available criterion but the pole determined in this manner is only correct in as far as saying that the 'best fit' determines the original relative juxtaposition of the continents concerned. This is far from being rigorous. We have already seen that the presence of gaps and overlaps is not always critical because the original 'line' of break up can rarely be defined with precision. It follows that the possible positions of the pole of rotation spread geographically over an area determined by the tolerance of the particular problem. In terms of the objective function, this area is defined by a contour whose value is equal to the tolerance. When the minimum is bounded by steep sides, the solution may be localised within a small area even for very large tolerance. However, such well-defined problems are rare. Only a slight deviation from the 'best fit' is usually sufficient to cause the area of possible solutions to extend over many degrees of latitude and longitude.

The actual position of an optimum pole of rotation is, therefore, not significant. A meaningful solution must refer to an area which is defined by the permitted tolerance. Methods which 'home' onto a solution are, therefore, inadequate for the purpose. A procedure based on mapping the objective function, such as the one presented in this Chapter, must be used.



External control is very important. Any available geological informations must be used to reduce the ambiguity. Data obtained from transform faults, palaeomagnetic work, etc., are similarly useful although, by their very nature, such data exhibit a comparable ambiguity. However, being independant criteria, they may be used by superimposing the contour of maximum tolerance, given by each of these methods, on the contour of maximum tolerance of  $Q$  to obtain an area common to all of them. The solution may thus be localised further and its 'accuracy' increased.

## 8.6. Examples

The examples presented below demonstrate the use of the general procedure and the problems associated with the position of the pole of rotation.

### 8.6.1. The fit of Greenland to Northern Europe

The continental edges of Greenland and Northern Europe were mainly represented by the 500 fathom line. The fitted segments were approximately the same as those used by Bullard et al (1965) for a similar purpose.

Iceland and the ridges joining it to Greenland were assumed to be post-drift in origin. The continental edge in the vicinity of these ridges was defined by a number of widely separated points.

On the European side, a plateau (marked N, Fig. 8.3)

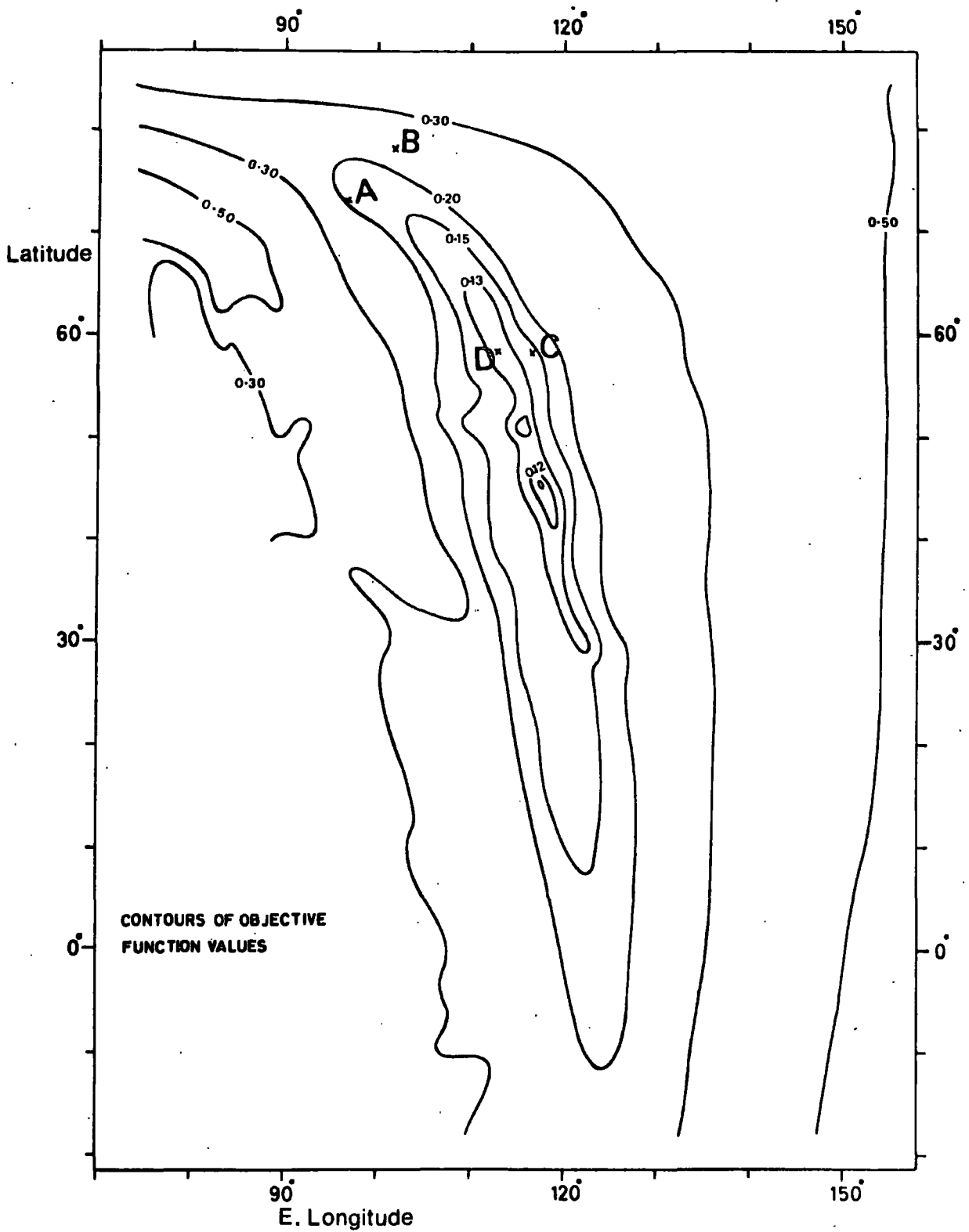


Fig. 8.2. Contours of  $Q$  values for the fit between Greenland and Northern Europe. Poles of rotation indicated are:

- A = Bullard et al (1965)
- B = Le Pichon (1968)
- C = Bott and Watts (1970b)
- D = Pole used to obtain the fit of Fig. 8.3.

formed by young sediments fans out in the Norwegian Sea. The continental edge across this plateau was estimated by assuming it to be parallel to the magnetic lineations in the neighbouring oceanic crust. Near the Faroe Islands, an assumed deviation of the edge from the 500 fathom line was also necessary in order to follow the boundary suggested for the continental crust from gravity data (Bott and Watts, 1970b).

In the fitting process, various parts of both edges were weighted according to the confidence attached to each part. A map of  $Q$  for a range of  $90^{\circ}\text{N}$  to  $18^{\circ}\text{S}$  and  $65^{\circ}\text{E}$  to  $155^{\circ}\text{E}$ , is shown in Fig. 8.2. The map of  $Q_1$  and  $Q_2$  are roughly similar to this map. Details of the optimum pole of rotation from the three maps are indicated below (in degrees)

		latitude (N)	longitude (E)	Rotatio
Fit on Europe	$Q_1 = 0.13$	42.0	119.0	9.9
Fit on Greenland	$Q_2 = 0.10$	65.0	110.0	13.5
Combined fit	$Q = 0.12$	45.0	117.5	10.3

The pole positions are widely different but they all fall within the axis of the trough in Fig. 8.2, indicating the validity of the map as a whole and the insignificance of the individual pole positions. In fact, Fig. 8.2 shows that if the tolerated value of  $Q$  is only 10% higher than that at the optimum the possible positions of the pole of rotation would occupy a zone about  $3^{\circ}$  wide and extending for  $32^{\circ}$ .

When no weights are placed on the function, an increase of 10% corresponds to an extent of  $20^{\circ}$ . In both cases, the range is large and illustrates the practical difficulty in assessing the validity of a given pole without reference to some other criteria.

A close resolution of the main trough in Fig. 8.2 indicates the presence of many ill-defined local minima. This illustrates how search by 'homing' techniques could terminate erroneously. Fig. 8.2 also shows the optimum poles of rotation adopted by Bullard et al (1965), A, Le Pichon (1968), B, and Bott and Watts (1970b), C. All of these poles fall within the main trough.

The maps of  $Q_1$ ,  $Q_2$  and  $Q$ , when no weighting functions were used, were similar to the map of Fig. 8.2. The optimum poles in the three maps were in good agreement between themselves. Greenland was fitted to Europe (Fig. 8.3) using the optimum pole of  $Q$ , at  $58.3^{\circ}\text{N}$ ,  $113.0^{\circ}\text{E}$  with a rotation angle of  $12.4^{\circ}$ . This pole is indicated by point D in Fig. 8.2. It was used instead of the corresponding pole of the weighted function merely for convenience, being a point on the axis of the trough in Fig. 8.2 and because of its agreement with the optimum poles of  $Q_2$  and  $Q$ .

The fit (Fig. 8.3) is quite satisfactory and produces no unreasonable gaps or overlaps. The overlap of plateau N suggests that the extent of the continental edge is even less than was indicated from following the magnetic lineations. The overlap which includes the Faroes is probably caused by

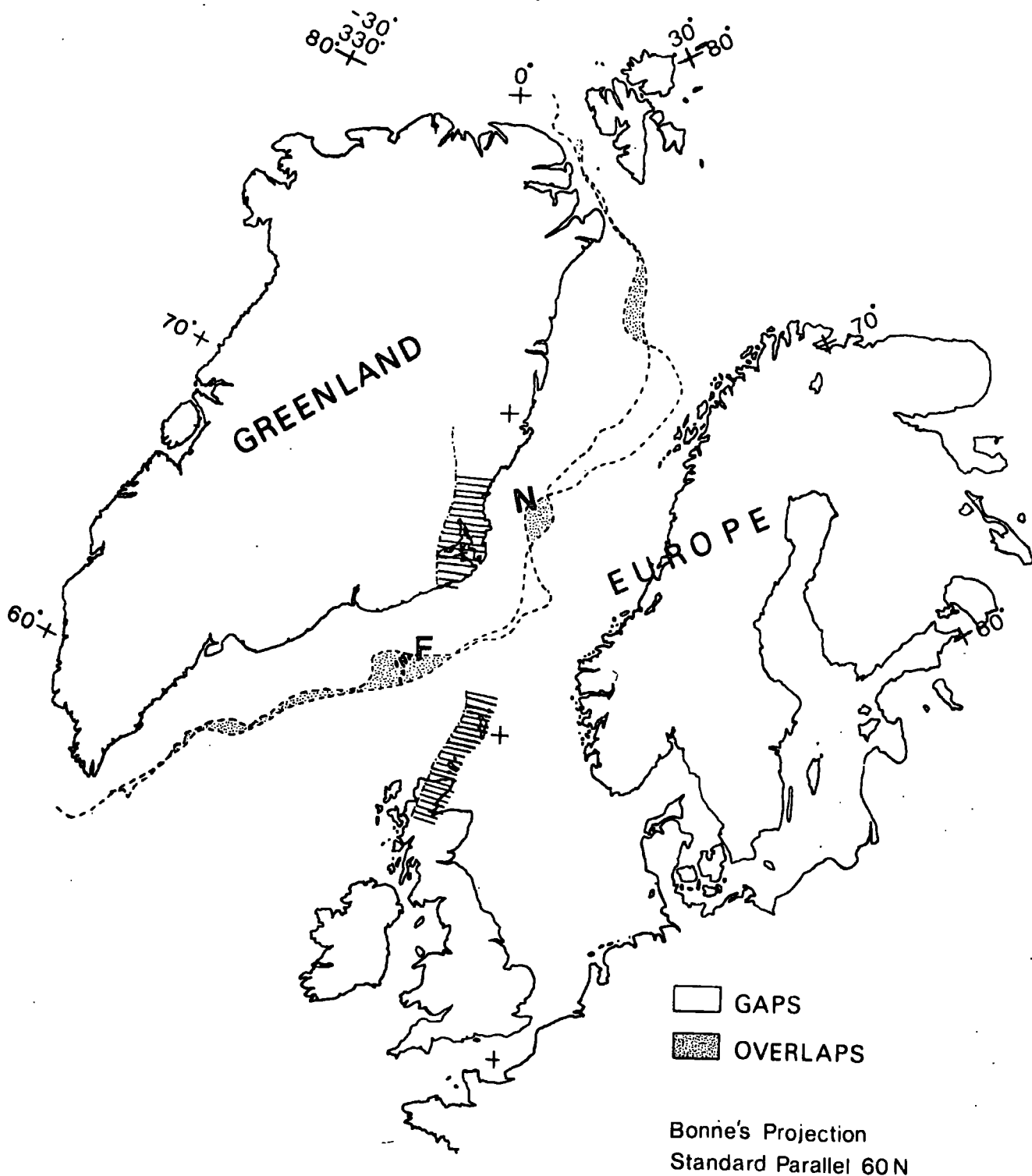


Fig. 8.3. A fit of the Greenland and the NW European assumed continental edges (marked by broken lines). The fit is obtained by rotating the Greenland shelf  $12.4^\circ$  about a pole of rotation at  $58.3^\circ$  N,  $113.0^\circ$  E. The shaded area indicates the relative position of the western side of the Caledonian fold belt reconstructed similarly to Bott and Watts (1970b).

an overestimation of the extent of the continent on the Greenland side, which was badly defined in this part.

The relative position of the Caledonian fold belt boundary on the Greenland side is in agreement with that on the European side. This match was indicated by Bott and Watts (1970b) who obtained a similar result using the pole indicated in Fig. 8.2. This geologic control is an example of an external criterion which may be used to localise the possible solutions. Poles which produce a good fit between the two ~~sides~~ but do not match the fold belts are rejected on these bases.

## 8.6.2. Movement between the Arabian, Nubian and Somalian plates

### 8.6.2.1. Introduction

Through a vast amount of geological and geophysical work, it is now generally recognised that the crustal structure of the Red Sea and the Gulf of Aden is essentially oceanic and that the Arabian plate is moving away from the African continent at an average rate of about 2cm/year (Girdler, 1958; Vine, 1966; Laughton, 1966, inter alia). The relative movement across the Red Sea is slightly different from that across the Gulf of Aden. This difference is allowed for by the relative movement between the Somalian and the Nubian plates across the East African rift. McKenzie et al (1970) have studied the relative movement between the three plates. They deduced the pole of rotation Nubia - Somalia from the difference between the rotations Arabia - Nubia and Arabia

- Somalia. This pole was approximately located at  $8.5^{\circ}\text{S}$ ,  $31.0^{\circ}\text{E}$  with a rotation angle of  $1.9^{\circ}$  indicating an opening of the rift by 65 km in northern Ethiopia and 30 km in Kenya.<sup>1</sup>

#### 8.6.2.2. The Red Sea

The actual coastlines were assumed to represent the continental edges and were used in the fitting process. This has been justified by McKenzie et al (1970) on the grounds that the marginal seas are complicated by thick evaporite deposits.

A map of  $Q$  (Fig. 8.4) shows a well-defined minimum with an optimum pole of rotation at  $37.1^{\circ}\text{N}$ ,  $18.5^{\circ}\text{E}$  corresponding to a rotation angle of  $6.1^{\circ}$ . This position ( $M$ ) is close to that obtained by McKenzie et al ( $K$ ). It was used to construct the fit between the Nubian and the Arabian plates (Fig. 8.5). The maps of  $Q_1$  and  $Q_2$  are very similar to that of  $Q$  with the respective optimum poles in close agreement with that given above.

#### 8.6.2.3. The Gulf of Aden

The continental edges on both sides of the Gulf of Aden were represented by the 500 fathom line. Another representation was also possible by assuming the break in the continental slope to represent the passage from continental to oceanic crust. The anaglyph map of Laughton et al (1970) was used for the purpose. However, the results obtained from both representations were very

---

1. A re-computation based on the same data showed that the figures for the opening are underestimated by at least 10%

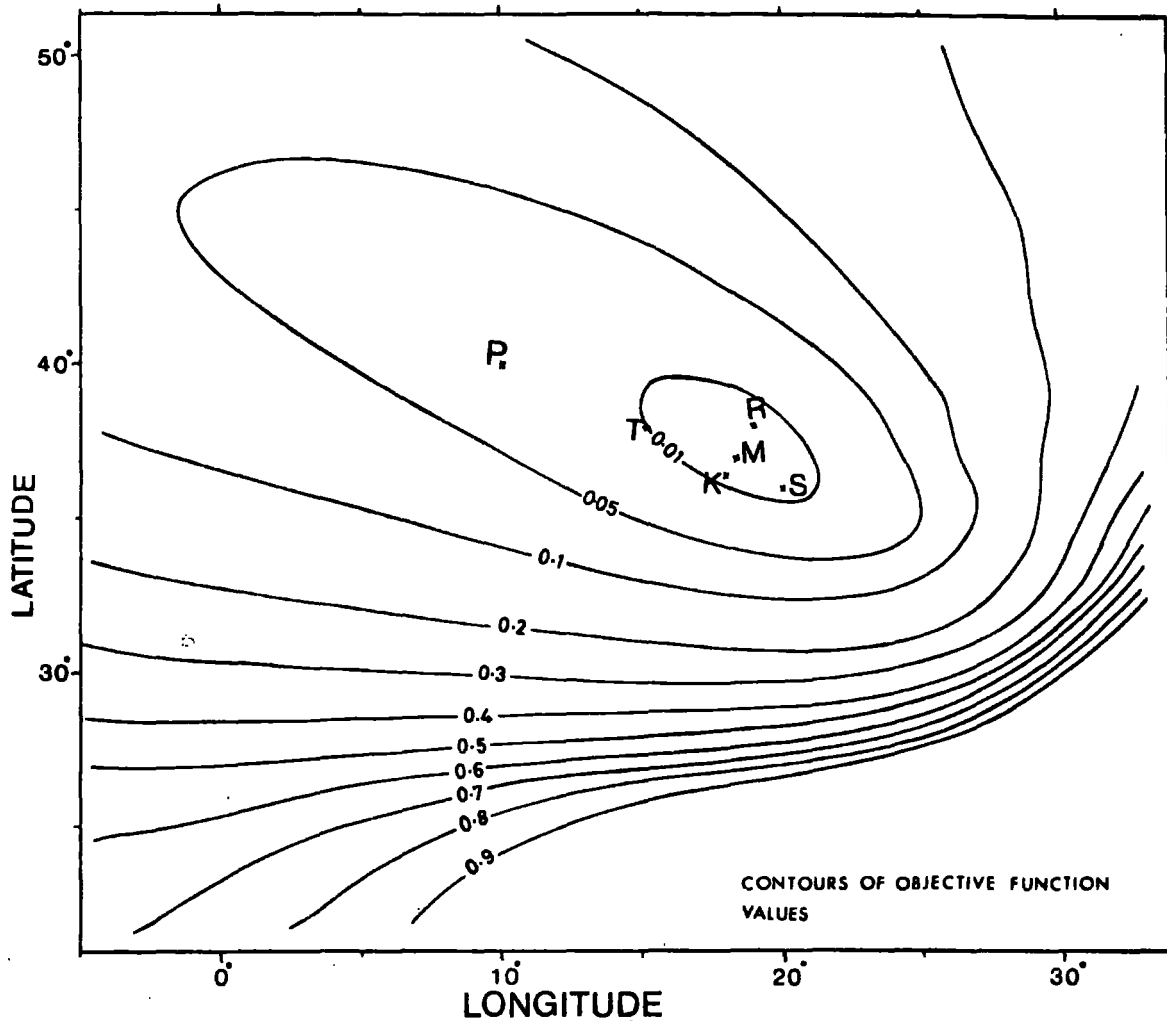


Fig. 8.4. Contours of  $Q$  values for the opening across the Red sea.

M = The pole position with minimum misfit

K = The pole position suggested by Mckenzie et al (1970).

Other arbitrary points used in Table 8.1 are also shown.



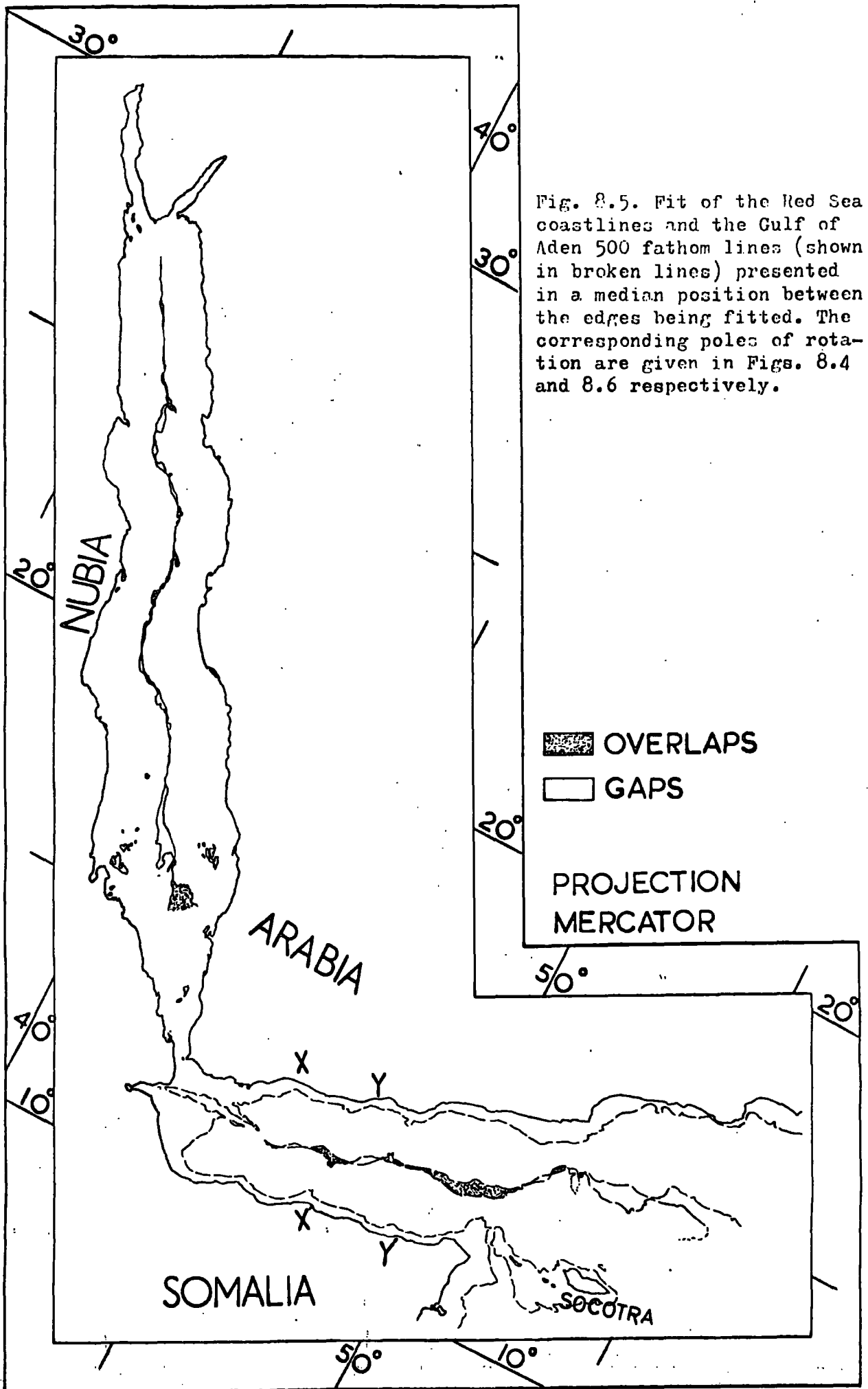


Fig. 8.5. Fit of the Red Sea coastlines and the Gulf of Aden 500 fathom lines (shown in broken lines) presented in a median position between the edges being fitted. The corresponding poles of rotation are given in Figs. 8.4 and 8.6 respectively.

similar; most discussion will be limited to the 500 fathom line representation.

In fitting the two edges of the Gulf, the Socotra shelf was first included as part of the Somalian plate in its true relative position. Results of mapping Q are shown in Fig. 8.6. Minimum A is locally an optimum solution with coordinates  $22.9^{\circ}\text{N}$ ,  $31.6^{\circ}\text{E}$  and a rotation angle of  $12.0^{\circ}$ . This pole position was used to produce the fit between the two plates as shown in Fig. 8.5. The fit is not as spectacular as in the case of the Red Sea. A better fit would be obtained if the Socotra shelf was excluded, in the same way as was suggested by Laughton (1966) and by McKenzie et al (1970).

Q was mapped with the Socotra shelf excluded, giving another locally optimum minimum at  $23.4^{\circ}\text{N}$ ,  $28.2^{\circ}\text{E}$ , with a rotation angle of  $9.5^{\circ}$ . The resulting fit is shown in Fig. 8.7 and indicates a definite improvement over the first fit. However, the first fit has three important features. Firstly, it does not require a displacement of the Socotra shelf as an independent 'fragment'. Secondly, it suggests even better geological continuity across the fitted edges than was originally demonstrated by Laughton (1966). Thirdly, it is consistent with the Island of Socotra being originally close to the Kuria Muria islands. The gaps and overlaps are nowhere excessive and, therefore, cannot be used as an evidence against the fit.

Therefore, despite the better fit obtained by excluding

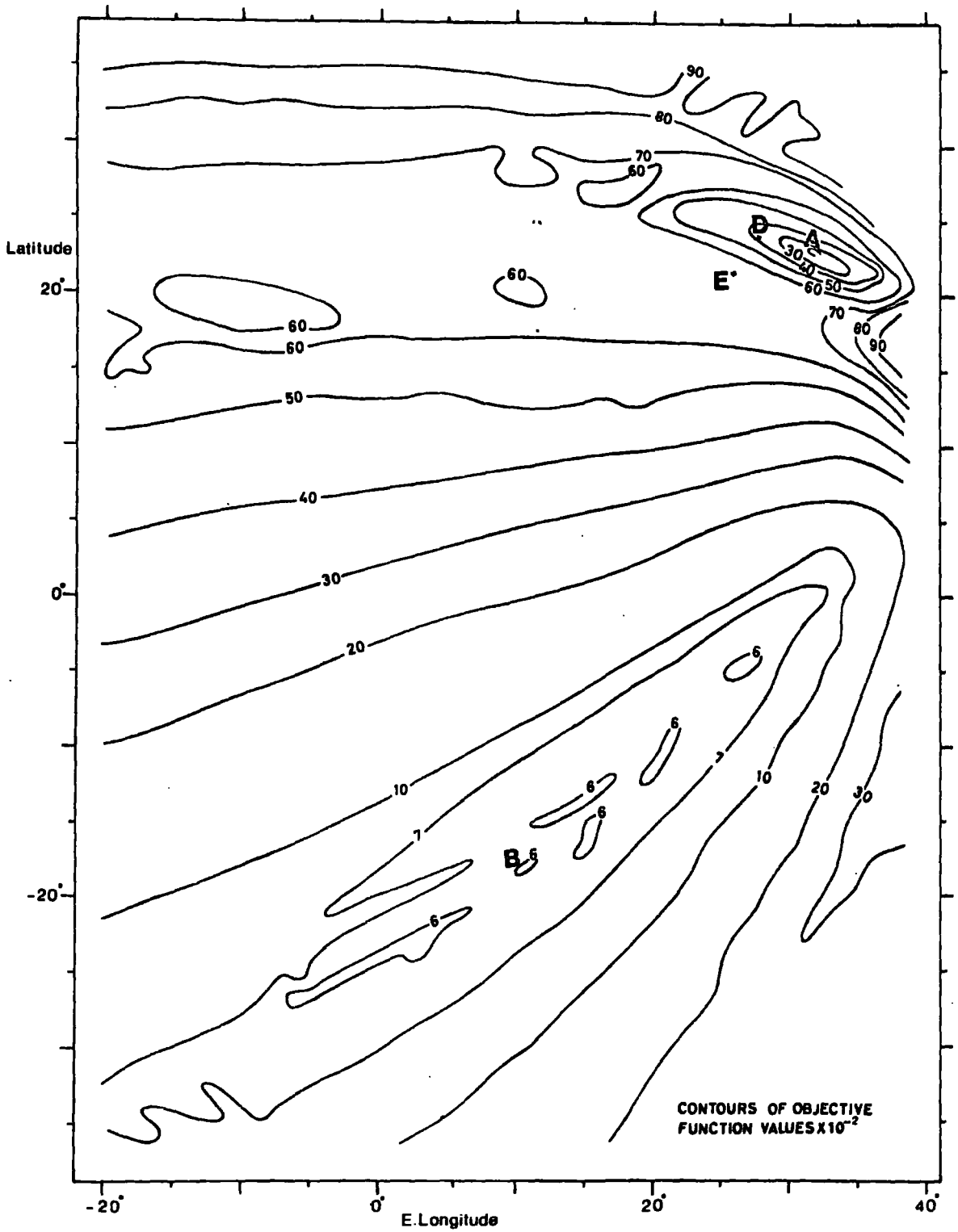
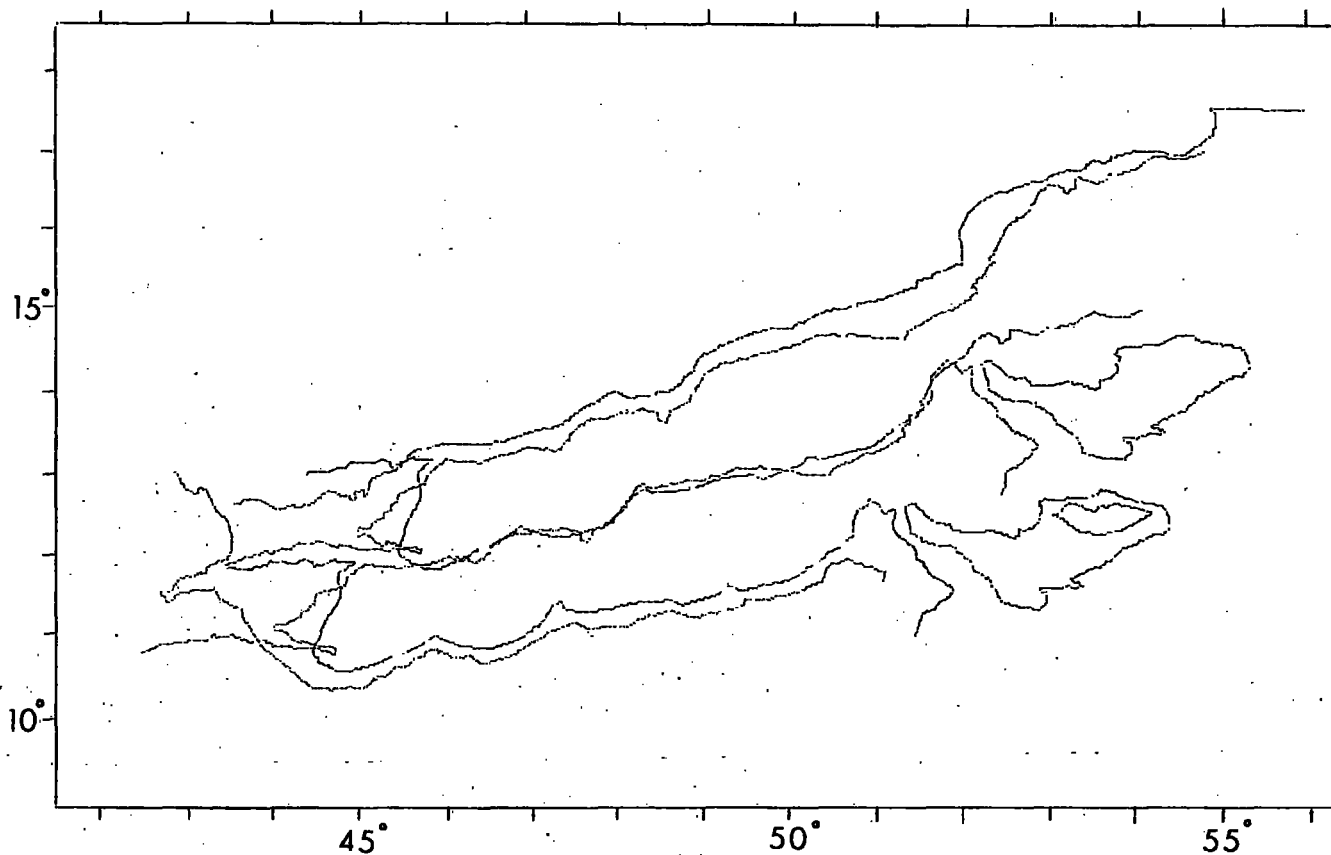


Fig. 8.6. Contours of  $Q$  values for the opening across the Gulf of Aden when the Socotra shelf is included as part of the Somalian plate.

A = The pole used to obtain the fit of Fig. 8.5.

D = The optimum pole position when the Socotra shelf is excluded.

E = The pole position of McKenzie et al (1970).



Projection: Mercator

Fig. 8.7. A fit between the Arabian and the Somali plates, using a pole of rotation at  $23.4^{\circ}$  N,  $28.2^{\circ}$  E and a rotation angle of  $9.5^{\circ}$ . This pole is obtained by excluding the Socotra shelf. The 500 fathom line is marked red on the Arabian side and green on the Somali side.

Plotting programme after A. G. McKay.

Socotra, the overall evidence is in better agreement with the fit shown in Fig. 8.5. This again shows the vulnerability of the 'best fit' as a criterion for establishing the original relative position of continents.

Fig. 8.6, in fact, suggests that a better fit is obtainable from a solution like B at  $18.5^{\circ}\text{S}$ ,  $10.0^{\circ}\text{E}$ , with a rotation angle of  $3.4^{\circ}$ . A similar local minimum also appears when the Socotra shelf is not included.

Solution B corresponds to a fit correlating points X and Y on Arabia with points X' and Y' on Somalia, respectively (Fig. 8.5). However, such fit is difficult to reconcile with the geological features on land and the magnetic lineations in the Gulf (Laughton, 1966; Laughton et al, 1970). Thus, the better fit of solution B is also eliminated in favour of the more definite criteria suggested by using the pole at A.

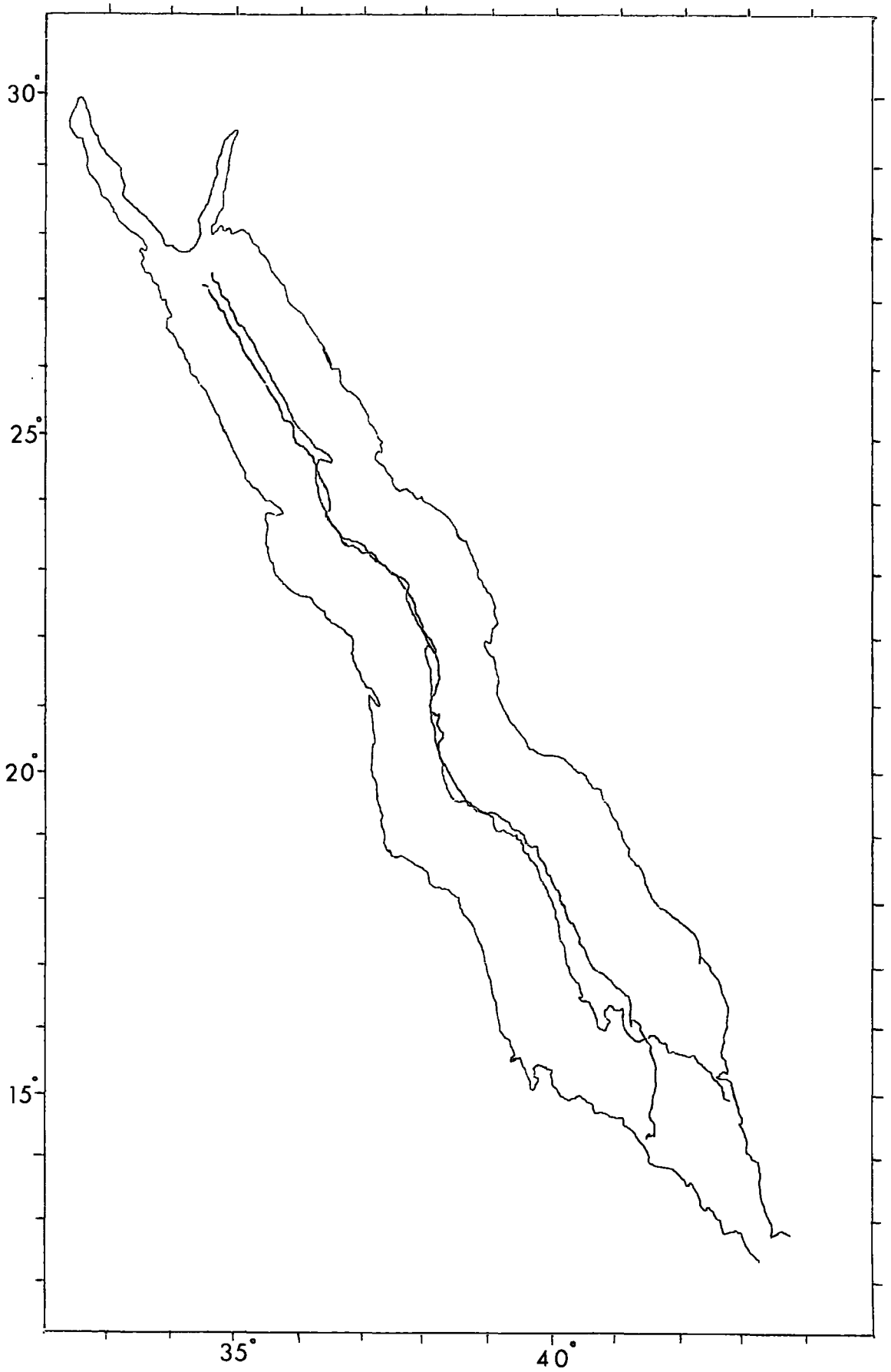
#### 8.6.2.4. Determination of the movement across the East African rift.

The ambiguity in the position of the pole of rotation invalidates its use in processes involving accurate quantitative determinations. We use, as an example, the attempt of McKenzie et al (1970) to determine the movement across the East African rift by a vectorial addition of the movement across the Gulf of Aden and that across the Red Sea. Clearly, the fit of the edges across the Red Sea is so good that, even if the area of misfit is increased by 30%, the resulting fit would still be inside the tolerable limit. For the data presented by McKenzie et al

(1970, Fig. 2), this is equivalent to a range of  $4^{\circ}$  in latitude and  $7^{\circ}$  in longitude. For illustration, we used the point P (Fig. 8.4) to produce a fit of the two edges of the Red Sea (Fig. 8.8). Despite a shift from the pole of the 'best fit' by  $3^{\circ}$  latitude and  $8.5^{\circ}$  longitude, the resulting fit is quite satisfactory. In the same way, a large number of other points may be shown to provide a possible pole of rotation for the displacement across the Red Sea. Each of these poles, when added vectorially to the pole for the movement across the Gulf of Aden, will produce a different pole for the movement across the East African rift. Results of the vectorial addition of some of these poles are given in table 8.1. For the movement across the Gulf of Aden, the pole of McKenzie et al was used to simplify comparison

Pole for the Red Sea (Fig. 8.4)	Pole for the rift (degrees)			Displacement (km)		
	Lat.(N)	Long.(E)	Rotation	Central Ethiopia	Kenya	
M	-8.0	28.9	2.0	65	35	
P	5.8	34.1	3.3	(45)	(-45)	
T	0.3	32.6	2.6	55	(20)	
R	-7.1	27.0	2.2	80	40	
S	-16.9	26.8	1.6	90	60	

Table 8.1. Variation of the resultant movement across the East African rift according to the pole adopted for the Red Sea. This is always larger than the displacement in a direction perpendicular to the sides of the rift. Figures in brackets indicate displacements which are more than twice the apparent displacement perpendicular to the sides. The minus sign indicates compressional movement.



Projection: Mercator

Fig. 6.8. A fit between the Arabian and the Nubian plates using an arbitrary pole of rotation. The Arabian side is marked red and the Nubian side is marked green.

The displacements in Table 8.1 are significantly different. Displacements, obtained by using the same poles as Figs. 8.5 or 8.7 to represent the movement across the Gulf, are similarly varied but are more suggestive of compressional movements in Kenya and tensional movements in Ethiopia. The pole obtained using the anaglyph map of Laughton et al (1970) produces displacements similar to those of Table 8.1 but of smaller magnitudes. None of these results is intended to indicate the actual movement across the East African rift. They are used to demonstrate the difficulty of obtaining meaningful quantitative results from a pole position estimated on the grounds of 'best fit'. Had all possible pole positions for the movement across the Gulf of Aden been considered the results would have been even more varied. Although a large number of the resulting poles for the movement across the East African rift could be discarded as being geologically unreasonable the basic indeterminacy remains unresolved.

Qualitative deductions are generally easier. Within the tolerance of each problem it is usually possible to establish relative movements in a general manner. For instance, the contours of  $Q$  for the Red Sea do not overlap with those of  $Q$  for the Gulf of Aden for any reasonably large tolerance. This establishes a displacement across the East African rift. The nature of this displacement can only be given as a broad range of possibilities. Geological and other relevant information may decide which of these possibilities are more likely.



## SUMMARY AND CONCLUSIONS

1. In applying optimisation techniques to a given geophysical problem the procedure would usually consist of the following stages:

(a) The behaviour of the objective function is studied, preferably by means of cross-sections. This is important in establishing the modality of the function, the degree of ambiguity expected in the solution, the nature and scaling of the function and any other special features.

(b) The constraints of the problem are worked out so as to ensure the physical or geological feasibility of the optimum model. The term "constraints" may be extended to denote the specification of some parameters at certain values in order to improve the validity or uniqueness of the solution.

(c) An auxiliary subroutine is constructed to provide the objective function for a given set of model parameters. A suitable optimisation subroutine is then chosen. The choice depends on the problem. For example, the method of rotating coordinates is well suited for curved and complicated functions; the simplex method is suitable for problems with many isolated local minima, etc. Generally, gradient methods are fast but tend to break down when the current point is remote from a solution or when the function has many ill-defined local minima. Direct search methods are slow but do not usually have the disadvantages of gradient methods. A good strategy is to use direct search methods at the early

stages of the search and to change to a gradient method when the solution is approached.

2. In all of the investigated cases, a unique solution to the problem appears to exist in theory but a high degree of non-uniqueness arises in practice. The non-uniqueness is primarily due to observational errors and to the lack of adherence to the ideal conditions assumed by the model. The tolerance of the problem is usually determined by the magnitude of observational errors. In the parameter hyperspace, this gives rise to a 'valley of ambiguity' where all points bounded by a contour of value equal to the tolerance qualify as possible solutions.

3. In gravity and magnetic problems, uniqueness in practice is only obtainable within specified basic parameters. However, if some or all of the basic parameters are unspecified the outcome of the search in the hyperspace is not unpredictable; the position of the initial point will generally decide the solution to which the search will converge. The optimum parameters will be usually of the correct order of magnitude.

4. Optimisation techniques may be used to interpret a two-dimensional gravity anomaly in terms of a polygonal model. The method is formulated such that any of the parameters defining the model can be specified or treated as an unknown. The use of optimisation techniques renders the interpretation

more flexible and efficient than is generally obtained using other methods. The disadvantage of requiring long computing time may be largely overcome by careful programming.

5. The use of optimisation techniques in interpreting two-dimensional magnetic anomalies has the same general features as those of gravity interpretation. It has the additional advantage that efficient iterative methods for interpreting magnetic anomalies are generally lacking.

6. Surface wave dispersion data may be interpreted by optimisation techniques. However, it seems necessary to specify a large number of parameters in order to overcome the high degree of non-uniqueness which arises in practice.

7. A fast method for interpreting apparent resistivity curves is based on transforming the problem so that there are only two variable parameters. The observed curve is then matched with a set of standard curves and the results are printed on the corresponding two-dimensional grid. The solutions seem to be satisfactory and problems associated with equivalence are substantially reduced.

8. A modified two-dimensional grid method can be used to locate a pole of rotation for the relative displacement between two continents. External control may reduce the ambiguity in the solution. The use of the 'optimum' pole position for quantitative determinations is unjustified.

9. There is a very wide scope for applying optimisation techniques to solving non-linear geophysical problems. Specific problems of interest arising from the present work are the interpretation of three-dimensional gravity and magnetic anomalies and a fuller investigation of the problem of surface wave dispersion.

Appendix 1

Calculation of the Accuracy of Optimum Parameters.

In the vicinity of the optimum, the hyper-surface of a non-linear function behaves asymptotically as a hyper-plane so that an approximation to the linear case, at the optimum, is quite justified.

If a multi-variate regression is fitted by minimising

$$s^2 = \sum_{k=1}^n (y_k - g - b_{1k} x_1 - b_{2k} x_2 - \dots - b_{mk} x_m)^2 \tag{A1.1}$$

then the parameters  $x_j$  have variances and covariances given by the elements of the matrix  $\sigma^2 L^{-1}$  where

$$L = \begin{bmatrix} \sum_{k=1}^n b_{1k}^2 & \sum b_{1k} b_{2k} & \dots & \sum b_{1k} b_{mk} \\ \sum b_{mk} b_{1k} & \cdot & \cdot & \sum b_{mk}^2 \end{bmatrix} \tag{A1.2}$$

Each of the elements of L may be derived from

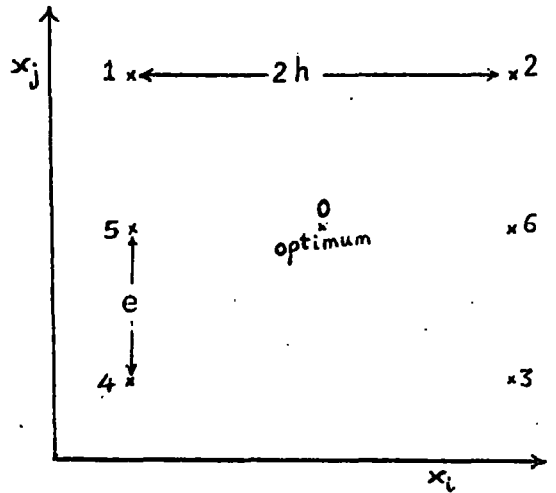
$$\frac{\partial^2 s^2}{\partial x_i^2} = 2 \sum b_{ik}^2, \quad \frac{\partial^2 s^2}{\partial x_i \partial x_j} = 2 \sum b_{ik} b_{jk} \tag{A1.3}$$

The general non-linear case is represented by

$$s^2 = \sum_{k=1}^n (A_k - C_k(x_1, x_2, \dots, x_m))^2 \tag{A1.4}$$

By approximation to the linear case, the elements of the matrix Q, which is the equivalent of L in the linear case, are also given by equations(3).

The computation of the second partial derivatives may be carried out numerically by perturbing from the optimum parallel to each of  $x_i$  and  $x_j$  as in the diagram. A perturbation in the order of 1% of the value at the optimum is probably adequate. The derivatives are then given by



$$\frac{\partial^2 s^2}{\partial x_i^2} = \frac{s_6^2 + s_5^2 - 2s_0^2}{h^2} \tag{A1.5}$$

and 
$$\frac{\partial^2 s^2}{\partial x_i \partial x_j} = \frac{s_4^2 - s_3^2 + s_2^2 - s_1^2}{4 h e} \tag{A1.6}$$

The symmetric matrix Q is then inverted to obtain the matrix P.  $\bar{\sigma}^2$ , the estimate of residual variance is calculated from

$$\bar{\sigma}^2 = \frac{s^2}{n-m} \tag{A1.7}$$

$\bar{\sigma}^2$  and the diagonal elements of P may then be used in equation (2.18) to estimate the possible error in parameter  $x_i$ .

## Appendix 2

Method of obtaining the Partial Derivations of the Objective Function in Equation (5.4).

The variable parameters include all unknown coordinate parameters defining the polygon and the linear parameters when unspecified.

The derivatives with respect to the coordinate parameters may be obtained in the following manner.

Equation (5.4) may be re-written as

$$f(\underline{x}) = \sum_{k=1}^n (A_k - B - 2G \rho \sum_{i=1}^m S_{ik})^2 \quad (A2.1)$$

where  $S_{ik}$  is the geometrical term of the  $i$ th slab at the  $k$ th observation point as defined by equation (5.2).

If a coordinate parameter of the  $i$ th slab is referred to by  $p_i$  then

$$\frac{\partial f}{\partial p_i} = -4 G \rho \sum_{k=1}^n [(A_k - B - 2G \rho \sum_{i=1}^m S_{ik}) \frac{\partial}{\partial p_i} S_{ik}] \quad (A2.2)$$

Hence, the problem is reduced to obtaining a general expression for the derivatives of the objective function with respect to the four coordinate parameters defining the  $i$ th slab.

For convenience, the symbols used in the text are replaced by the following:

$$u = x_{1i}, \quad v = x_{2i}, \quad w = z_{1i}, \quad t = z_{2i},$$

$$\theta = \theta_i, \quad \phi_1 = \phi_{1ik}, \quad \phi_2 = \phi_{2ik}, \quad \phi = \phi_2 - \phi_1,$$

$$R_1 = 1/r_{1ik}^2, \quad R_2 = 1/r_{2ik}^2, \quad R = \log(R_1/R_2)$$

$$b = [(u-v)^2 + (w-t)^2]^{-1/2}$$

Equation (5.2) may hence be re-written as

$$S_{ik} = t \phi_2 - w \phi_1 - (u \sin \theta + w \cos \theta) \left( \frac{1}{2} R \sin \theta + \phi \cos \theta \right) \quad (\text{A2.3})$$

$$= t \phi_2 - w \phi_1 - WH \quad (\text{A2.4})$$

where

$$W = u \sin \theta + w \cos \theta$$

and

$$H = \frac{1}{2} R \sin \theta + \phi \cos \theta$$

Expressions for the derivatives of individual factors in equation (A2.3) are given as follows:

$$\frac{\partial \sin \theta}{\partial u} = -b \cos \theta \sin \theta,$$

$$\frac{\partial \sin \theta}{\partial v} = b \cos \theta \sin \theta$$

$$\frac{\partial \sin \theta}{\partial w} = -b \cos^2 \theta,$$

$$\frac{\partial \sin \theta}{\partial t} = b \cos^2 \theta$$



$$\frac{\partial \cos \theta}{\partial u} = b \sin^2 \theta \quad , \quad \frac{\partial \cos \theta}{\partial v} = -b \sin^2 \theta$$

$$\frac{\partial \cos \theta}{\partial w} = b \cos \theta \sin \theta \quad , \quad \frac{\partial \cos \theta}{\partial t} = -b \cos \theta \sin \theta$$

$$\frac{\partial R}{\partial u} = -2R_1(u-X_k) \quad , \quad \frac{\partial R}{\partial v} = 2R_2(v-X_k)$$

$$\frac{\partial R}{\partial w} = 2R_1(w-Z_k) \quad , \quad \frac{\partial R}{\partial t} = -2R_2(t-Z_k)$$

$$\frac{\partial \Phi}{\partial u} = -\frac{\partial}{\partial u} \Phi_1 = R_1(w-Z_k) \quad , \quad \frac{\partial \Phi}{\partial v} = \frac{\partial}{\partial v} \Phi_2 = -R_2(t-Z_k)$$

$$\frac{\partial \Phi}{\partial w} = -\frac{\partial}{\partial w} \Phi_1 = -R(u-X_k) \quad , \quad \frac{\partial \Phi}{\partial t} = \frac{\partial}{\partial t} \Phi_2 = R_2(v-X_k)$$

It therefore follows that

$$W'_u = \frac{\partial W}{\partial u} = \sin \theta (1 - bu \cos \theta + bw \sin \theta)$$

$$W'_v = \frac{\partial W}{\partial v} = \sin \theta (bu \cos \theta - bw \sin \theta)$$

$$W'_w = \frac{\partial W}{\partial w} = \cos \theta (1 - bu \cos \theta + bw \sin \theta)$$

$$W'_t = \frac{\partial W}{\partial t} = \cos \theta (bu \cos \theta - bw \sin \theta)$$

$$H'_u = \frac{\partial H}{\partial u} = b \sin \theta (\Phi \sin \theta - \frac{1}{2} R \cos \theta) + R_1 [(u-X_k) \sin \theta + (w-Z_k) \cos \theta]$$

$$= b (\Phi - H \cos \theta) + R_1 [(u-X_k) \sin \theta + (w-Z_k) \cos \theta]$$

$$H'_v = \frac{\partial H}{\partial v} = b (H \cos \theta - \Phi) - R_2 [(v-X_k) \sin \theta + (t-Z_k) \cos \theta]$$

$$H'_w = \frac{\partial H}{\partial w} = b (H \sin \theta - \frac{1}{2} R) + R_1 [(u-X_k) \cos \theta - (w-Z_k) \sin \theta]$$

$$H'_t = \frac{\partial H}{\partial t} = b (\frac{1}{2} R - H \sin \theta) - R_2 [(v-X_k) \cos \theta - (t-Z_k) \sin \theta]$$

The above expressions are very similar, causing considerable saving in computing time. They can be used directly to obtain:

$$\frac{\partial}{\partial u} S_{ik} = -wR_1(w-Z_k) - HW'_u - WH'_u \quad (A2.5)$$

$$\frac{\partial}{\partial v} S_{ik} = -tR_2(t-Z_k) - HW'_v - WH'_u \quad (A2.6)$$

$$\frac{\partial}{\partial w} S_{ik} = wR_1(u-X_k) - HW'_w - WH'_w - \Phi \quad (A2.7)$$

$$\frac{\partial}{\partial t} S_{ik} = tR_2(v-X_k) - HW'_t - WH'_t + \Phi \quad (A2.8)$$

Substituting in equation (A2.2), the required derivatives are obtained.

Since, in general, the coordinate parameter  $x_j$  of the polygon is the parameter  $v_i$  of the  $i$ th slab and is also the parameter  $u_{i+1}$  of the  $i+1$ th slab, the derivative with respect to the parameter  $x_j$  is obtained from

$$\frac{\partial f}{\partial x_j} = \frac{\partial f}{\partial v_i} + \frac{\partial f}{\partial u_{i+1}}$$

The same is also true for  $t_i$  and  $w_{i+1}$ .

However, the first and the last points of an open polygon are used only once. Also, polygons with vertical or horizontal sides have some parameters common to more than two slabs. For all such cases, appropriate definitions must be made in the gradient specification part of the programme (see programme specification no. 4).

The derivatives with respect to the density contrast and the regional background follow directly from equation (A2.1). Hence,

$$\frac{\partial f}{\partial \rho} = -4G \sum_{k=1}^n [(A_k - B - 2G\rho \sum_{i=1}^m S_{ik}) \sum_{i=1}^m S_{ik}] \quad (\text{A2.9})$$

$$\frac{\partial f}{\partial B} = -2 \sum_{k=1}^n (A_k - B - 2G\rho \sum_{i=1}^m S_{ik}) \quad (\text{A2.10})$$

## Appendix 3

## Method of Obtaining the Partial Derivatives of the Objective Function in Equation (6.6)

The variable parameters include all unknown coordinate parameters defining the polygon and the linear parameters when unspecified.

The derivatives with respect to the coordinate parameters may be obtained following a procedure similar to that used in Appendix 2.

Equation (6.1) may be re-written as

$$f(\underline{x}) = \sum_{k=1}^n (A_k - B - J_s \sum_{i=1}^m P_{ik} - J_c \sum_{i=1}^m Q_{ik})^2 \quad (A3.1)$$

where  $P_{ik}$  and  $Q_{ik}$  replace  $u_{ik}$  and  $v_{ik}$  in equations (6.2) and (6.3) respectively.

If we again define a coordinate parameter on the  $i$ th slab by  $p_i$ , it follows that

$$\frac{\partial f}{\partial p_i} = -2 \sum_{k=1}^n [A_k - B - J_s \sum_{i=1}^m P_{ik} - J_c \sum_{i=1}^m Q_{ik}] (J_s \frac{\partial}{\partial p_i} P_{ik} + J_c \frac{\partial}{\partial p_i} Q_{ik}) \quad (A3.2)$$

Therefore, the method depends on determining the derivatives of  $P_{ik}$  and  $Q_{ik}$  with respect to each of the four parameters defining the two corners of the  $i$ th slab.

We use the same symbols as in Appendix 2 so that equations (6.2) and (6.3) may be re-written as

$$P_{ik} = 2 \sin \theta (H \cos I \sin d - G \sin I)$$

$$Q_{ik} = 2 \sin \theta (G \cos I \sin d - H \sin I)$$

where  $G = \Phi \sin \theta - \frac{1}{2} R \cos \theta$

Derivatives of  $\theta$ ,  $R$ ,  $\phi$  and  $H$  were also presented in Appendix 2.

Derivatives of  $G$  are given by the following:

$$\begin{aligned} G'_u &= \frac{\partial G}{\partial u} = -b \sin \theta \left( \phi \cos \theta + \frac{1}{2} R \sin \theta \right) + R_1 [(u-X_k) \cos \theta + (w-Z_k) \sin \theta] \\ &= -b H \sin \theta + R_1 [(u-X_k) \cos \theta + (w-Z_k) \sin \theta] \end{aligned}$$

$$G'_v = \frac{\partial G}{\partial v} = bH \sin \theta - R_2 [(v-X_k) \cos \theta + (t-Z_k) \sin \theta]$$

$$G'_w = \frac{\partial G}{\partial w} = -bH \cos \theta - R_1 [(u-X_k) \sin \theta + (w-Z_k) \cos \theta]$$

$$G'_t = \frac{\partial G}{\partial t} = bH \cos \theta + R_2 [(v-X_k) \sin \theta + (t-Z_k) \cos \theta]$$

The derivatives of  $P_{ik}$  and  $Q_{ik}$  may now be obtained directly. Thus,

$$\begin{aligned} \frac{\partial}{\partial u} P_{ik} &= 2 \sin \theta (H'_u \cos I \sin d - G'_u \sin I) - 2b \cos \theta \sin \theta (H \cos I \\ &\quad \sin d - G \sin I) \\ &= 2 \sin \theta (H'_u \cos I \sin d - G'_u \sin I) - b P_{ik} \cos \theta \end{aligned} \quad (A3.3)$$

$$\frac{\partial}{\partial v} P_{ik} = 2 \sin \theta (H'_v \cos I \sin d - G'_v \sin I) + b P_{ik} \cos \theta \quad (A3.4)$$

$$\frac{\partial}{\partial w} P_{ik} = 2 \sin \theta (H'_w \cos I \sin d - G'_w \sin I) - b P_{ik} \cos \theta \tan \theta \quad (A3.5)$$

$$\frac{\partial}{\partial t} P_{ik} = 2 \sin \theta (H'_t \cos I \sin d - G'_t \sin I) + b P_{ik} \cos \theta \tan \theta \quad (A3.6)$$

$$\frac{\partial}{\partial u} Q_{ik} = 2 \sin \theta (G'_u \cos I \sin d - H'_u \sin I) - b Q_{ik} \cos \theta \quad (A3.7)$$

$$\frac{\partial}{\partial v} Q_{ik} = 2 \sin \theta (G'_v \cos I \sin d - H'_v \sin I) + b Q_{ik} \cos \theta \quad (A3.8)$$

$$\frac{\partial}{\partial w} Q_{ik} = 2 \sin \theta (G'_w \cos I \sin d - H'_w \sin I) - b Q_{ik} \cos \theta \tan \theta \quad (A3.9)$$

$$\frac{\partial}{\partial t} Q_{ik} = 2 \sin \theta (G'_t \cos I \sin d - H'_t \sin I) + b Q_{ik} \cos \theta \tan \theta \quad (A3.10)$$

Substituting in equation (A3.2), the required derivatives are obtained.

As in the gravity case, a given coordinate parameter  $x_j$  of the polygon may be common to one, two or more slabs. Appropriate specifications must, therefore, be made in the gradient specification part of the programme in order to obtain  $\frac{\partial f}{\partial x_j}$ .

The derivatives with respect to the linear parameters are directly obtainable from equation (A3.1). Hence

$$\frac{\partial f}{\partial J_s} = -2 \sum_{k=1}^n [(A_k - B - J_s \sum_{i=1}^m P_{ik} - J_c \sum_{i=1}^m Q_{ik}) (\sum_{i=1}^m P_{ik})] \quad (A3.11)$$

$$\frac{\partial f}{\partial J_c} = -2 \sum_{k=1}^n [(A_k - B - J_s \sum_{i=1}^m P_{ik} - J_c \sum_{i=1}^m Q_{ik}) (\sum_{i=1}^m Q_{ik})] \quad (A3.12)$$

$$\frac{\partial f}{\partial B} = -2 \sum_{k=1}^n [(A_k - B - J_s \sum_{i=1}^m P_{ik} - J_c \sum_{i=1}^m Q_{ik})] \quad (A3.13)$$

## Appendix 4

Derivation of Equations (6.9) and (6.10)

Equations (6.7) and (6.8) give, respectively

$$\sum_{k=1}^n (A_k - J_s U_k - J_c V_k - B) U_k = 0 \quad (A4.1)$$

$$\sum_{k=1}^n (A_k - J_s U_k - J_c V_k - B) V_k = 0 \quad (A4.2)$$

Hence,

$$\sum G_k U_k - J_s \sum U_k^2 - J_c \sum U_k V_k = 0 \quad (A4.3)$$

$$\sum G_k V_k - J_s \sum U_k V_k - J_c \sum V_k^2 = 0 \quad (A4.4)$$

where the summation is taken over the range 1 to n and

$$G_k = A_k - B$$

Multiplying equation (A4.3) by  $\sum V_k^2$  and equation (A4.4) by

$\sum U_k V_k$ , we obtain

$$\left( \sum G_k U_k \right) \left( \sum V_k^2 \right) - J_s \left( \sum U_k^2 \right) \left( \sum V_k^2 \right) - J_c \left( \sum U_k V_k \right) \left( \sum V_k^2 \right) = 0 \quad (A4.5)$$

$$\left( \sum G_k V_k \right) \left( \sum U_k V_k \right) - J_s \left( \sum U_k V_k \right)^2 - J_c \left( \sum U_k V_k \right) \left( \sum V_k^2 \right) = 0 \quad (A4.6)$$

By solving equations (A4.5) and (A4.6) for  $J_s$ , equation (6.9) follows directly.

Similarly, by multiplying equation (A4.3) by  $\sum U_k V_k$  and equation (A4.4) by  $\sum U_k^2$ , and solving the resulting equations for  $J_c$ , equation (6.10) follows directly.

## Appendix 5

Derivation of An Expression for Equation (6.13)

Equations (6.7), (6.8) and (6.12) give, respectively

$$\sum_{k=1}^n (A_k - J_s U_k - J_c V_k - B) U_k = 0 \quad (A5.1)$$

$$\sum_{k=1}^n (A_k - J_s U_k - J_c V_k - B) V_k = 0 \quad (A5.2)$$

$$\sum_{k=1}^n (A_k - J_s U_k - J_c V_k - B) = 0 \quad (A5.3)$$

Hence,

$$\sum A_k U_k - B \sum U_k - J_s \sum U_k^2 - J_c \sum U_k V_k = 0 \quad (A5.4)$$

$$\sum A_k V_k - B \sum V_k - J_s \sum U_k V_k - J_c \sum V_k^2 = 0 \quad (A5.5)$$

$$\sum A_k - nB - J_s \sum U_k - J_c \sum V_k = 0 \quad (A5.6)$$

where the summation is taken over the range 1 to n.

Multiplying equation (A5.4) by n and (A5.6) by  $U_k$ , we obtain the pair of equations

$$n \sum A_k U_k - nB \sum U_k - nJ_s \sum U_k^2 - nJ_c \sum U_k V_k = 0 \quad (A5.7)$$

$$\left( \sum A_k \right) \left( \sum U_k \right) - nB \sum U_k - J_s \left( \sum U_k \right)^2 - J_c \left( \sum U_k \right) \left( \sum V_k \right) = 0 \quad (A5.8)$$

Subtracting, we get

$$P - J_s R - J_c W = 0 \quad (A5.9)$$



where,

$$P = n \sum A_k U_k - \left( \sum A_k \right) \left( \sum U_k \right)$$

$$R = n \sum U_k^2 - \left( \sum U_k \right)^2$$

$$W = n \sum U_k V_k - \left( \sum U_k \right) \left( \sum V_k \right)$$

Similarly, by multiplying equation (A5.5) by  $n$  and equation (5.6) by  $\sum V_k$  and subtracting we get

$$Q - J_s W - J_c S = 0 \quad (\text{A5.10})$$

where

$$Q = n \sum A_k V_k - \left( \sum A_k \right) \left( \sum V_k \right)$$

$$S = n \sum V_k^2 - \left( \sum V_k \right)^2$$

Solving (A4.9) and (A4.10) for  $J_s$  and  $J_c$ , we have

$$J_s = D(WQ - SP) \quad (\text{A5.11})$$

$$J_c = D(WP - RQ) \quad (\text{A5.12})$$

where

$$D = 1/(W^2 - RS).$$

$B$  may now be obtained from (A5.3),

$$B = \frac{1}{n} \left( \sum A_k - J_s \sum U_k - J_c \sum V_k \right) \quad (\text{A5.13})$$

where  $J_s$  and  $J_c$  are defined by equations (A5.11) and (A5.12), respectively.

Equation (6.13) follows directly from equations (A5.11), (A5.12) and (A5.13).

## PROGRAMME SPECIFICATIONS

Programmes number 3a, 3b, 3c, 3d, 5a, 5b, 5c, and 5d are compatible with the method of rotating coordinates, P300 (Rosenbrock, 1960), the 'Complex' method, P301 (Box, 1965) and the method of conjugate directions, P303 (Powell, 1964). Only the P300 version is given in each of the corresponding print-outs. To adapt the programmes to either P301 or P303, the steps indicated in the print-out of GRANOP (specification no. 3a) must be followed.

Programmes 3-6 are constructed such that any of the coordinate parameters defining the polygonal model can be specified or treated as a variable parameter.

All programmes have been written in PL/1 for use on the NUMAC IBM 360/67 computer. Data items other than integers and strings may be written in any of the valid forms appropriate to PL/1, but will normally be written as fixed point decimal data items.

Procedures P300, P301, P303 and P306 have been kindly lent by I.C.I. Ltd. on the condition that their use must be confined to the Department of Geology, University of Durham.

Specification No. 3a

Title: GRANOP

Purpose: This programme progressively modifies the parameters defining a two-dimensional polygonal model in order to minimise the discrepancy between an observed gravity anomaly and the calculated anomaly due to the model. The resulting parameters define an 'optimum' model.

Use: The programme is most suitable for problems in which the regional background and the density contrast are specified but can also handle either or both of them as variable parameters. As presented, it will only accept one density contrast. It may be modified to accept  $m$  density contrasts ( $m \leq$  number of sides) by declaring the density contrast to be an array of  $m$  elements each of which is assigned to the appropriate side(s).

Description: The main programme deals with inputting, outputting and editing of the data. The optimisation procedure is called by a suitable CALL statement in which the initial estimates are passed. The optimisation procedure passes the current values of the variable parameters to the auxiliary procedure AG. The auxiliary procedure then calculates the anomaly in a manner similar to that of GRAVN (specification no. 1, Bott, 1969a) so that the addition of the step-models is carried out in an anticlockwise order. The objective function is then calculated according to equation (5.4) and its value is returned to the optimisation procedure. The process is iterated.

The details of the model are specified in the model definition part in the auxiliary procedure by a series of instructions. These include allocating the variable parameters to the appropriate coordinates of the model and assigning values to the coordinates required to be fixed. The density contrast and the regional background are also defined. In the print-out for GRANOP, an example is given where all the coordinates are defined as adjustable parameters, the density contrast is specified at  $+0.15 \text{ gm/cm}^3$  and the regional background is specified at 5.5 mgal.

Input data: The data are input in the following order:

<u>data</u>	<u>notes</u>
'NAME'	3.1
nsta nx mx	3.2
data;	3.3
wtf	3.4
zs	3.5
xs obs	3.6
g x h	3.7
lmg	3.8

Data notes:

3.1. Each new set of data must commence with a name consisting of up to 80 characters enclosed in single quotation marks.

## 3.2.

nsta = Number of observation points

nx = Total number of variable parameters

mx = Total number of coordinates. If the polygon has  
v corners then

mx =  $2v$  for an open polygon and

mx =  $2(v+1)$  for a closed polygon.

3.3. The following are integers which may be altered by the  
GET DATA statement.

sc: A scaling factor appropriate to the measurement  
units. The default units are kilometers. For  
other units, sc must be set equal to

unit of measurement  $\div$  1 kilometer.

iter: Number of required iterations per variable. Between  
100-200 iterations are usually adequate. The  
default value is 200.

zaza: If set to 1 the effect of change in the height  
of the observation point from the datum plane  
will be considered. The default value is 0.

lp: If set to 1 it indicates that after the specified  
number of iterations, the optimisation procedure  
is to be called again with  $1/5$  the original  
number of iterations. This occasionally helps  
re-setting the search directions more favourably.  
The default value is 0.

wt: If set to 1, weighting functions will be used. The  
default value is zero.

lmg: see note 3.8

An example is  $SC = 0.001$ ,  $ZAZA = 1$ ;

The semi-colon should be punched even if no data items were needed.

3.4.  $wtf$  is an array of  $nsta$  elements. Each element contains a weighting function appropriate to the observation point so that the  $i^{th}$  observation is weighted by a factor  $WTF(I)$ .

The input command is only activated by setting  $WT = 1$ .

Otherwise, no data are required.

3.5  $zs$  is an array of  $nsta$  elements. The  $i^{th}$  element denotes the difference in the height of observation of the  $i^{th}$  point from a reference datum passing through the origin (see note 3.6). This allows for changes in topography, etc. along the profile. The measurement is +ve downwards so that points higher than the datum are assigned -ve  $zs$  and vice versa. The input command is only activated by setting  $ZAZA = 1$ . Otherwise, no data are required.

3.6.  $xs$  is an array of  $nsta$  elements. The  $i^{th}$  element denotes the horizontal distance of the  $i^{th}$  observation point from the origin. The origin is chosen arbitrarily and is retained for reference throughout the problem.

$obs$  is an array of  $nsta$  elements. The  $i^{th}$  element denotes the anomaly value at the  $i^{th}$  observation point in milligals. The complete  $xs$  data list must be input before inputting  $obs$ .

3.7.  $g$  is an array of  $nx$  elements. The  $j^{th}$  element denotes the lower bound (constraint) on the  $j^{th}$  variable parameter.

$x$  is an array of  $nx$  elements representing the initial

point in the hyperspace. The  $j^{\text{th}}$  element denotes the initial estimate of the  $j^{\text{th}}$  variable parameter.

$h$  is an array of  $nx$  elements. The  $j^{\text{th}}$  element denotes the upper bound on the  $j^{\text{th}}$  variable parameter.

The data are input in the order: all  $g$ , all  $x$ , all  $h$ .

3.8.  $lmg$  is an integer controlling the re-entry into the main programme after the optimisation process has terminated. This allows using the programme for different problems in the same run or for the same problem under different conditions or assumptions. Every time the optimisation process is activated, the integer  $II$  is incremented by 1 from an initial value of 0.

#### Model definition:

The polygonal outline of the body is defined by the coordinates of the corner  $(x_1, z_1)$  with reference to the arbitrary origin (note 3.6). In the model definition part of the auxiliary procedure these are defined by the elements of the array  $xa$ . They are defined in an anticlockwise direction in the order  $x_1, z_1, x_2, \dots, x_m, z_m$ . Hence the  $(2j-1)^{\text{th}}$  and the  $2j^{\text{th}}$  elements of  $xa$  refer to the  $x$  and  $z$  coordinates of the  $j^{\text{th}}$  corner, respectively. A closed polygon has the first and last corners coincident. This is specified by

$$XA(MX-1) = XA(1); \quad XA(MX) = XA(2);$$

The array  $xx$  consists of  $nx$  elements. It passes the current value of the variable parameters to the auxiliary

procedure. Adjustable xa elements are assigned the appropriate xx elements. Unadjustable xa elements are assigned the required value. Therefore:

```
XA(1)=XX(1); XA(2)=3.4; XA(3)=XA(1);
XA(4)=XA(2)-XX(2)**2; DO J=5 TO MX;
XA(J)=XX(J-2); END: RHO=0.25; REG=7.0;
```

defines a model where the first corner is 3.4 units deep with an adjustable x-coordinate, the second corner is vertically above the first one. All of the other corners have adjustable coordinates. rho refers to the density contrast in gm/cm<sup>3</sup> reg refers to the regional background in milligals.

Output: The output data list consists of

- (1) The name
- (2) The number of observation points, the number of variable parameters and the number of body coordinates.
- (3) Three columns representing the lower bounds, the initial estimates and the upper bounds, respectively.
- (4) A print out of the current objective function value and parameter values at the beginning of each search stage.
- (5) The values of variable parameters at the 'optimum'.
- (6) The values of the coordinate points at the 'optimum'.
- (7) The values of the regional background and the density contrast at the 'optimum'.
- (8) Four columns representing xs (note 3.6), obs (note 3.6), the calculated anomaly due to the 'optimum' model and the residuals.
- (9) The 'optimum' function value.
- (10) The number of iterations per variable.



Specification No. 3b

Title: GREGNOP

Purpose: As in specification No. 3a

Use: The programme is most suitable for problems in which the regional background is specified and the density contrast is unspecified. It can also handle the regional background as a variable parameter.  $\rho$  must not appear in the body definition part.

Description: The objective function is calculated according to equation (5.8).

All the remaining details are as in specification No. 3a.

Specification No. 3c

Title: GRAVOP

Purpose: As in specification No. 3a.

Use: The programme is only suitable for problems in which the density contrast and the regional background are unspecified. Neither  $\rho$  nor  $\text{reg}$  must appear in the body definition part.

Description: The objective function is calculated according to equation (5.12).

All the remaining details are as in specification No. 3a.

Specification No. 3d

Title: GRATIOP

Purpose: As in specification No. 3a.

Use: As in specification No. 3b.

Description: The objective function is calculated according to equation (5.5).

All the remaining details are as in specification No. 3a.



```

    /** FOR P303 REPLACE STATEMENTS 32-35 BY THE FOLLOWING **
L4: GET LIST(X,BAC,EEC);
    **
    THE ITH ELEMENT OF THE BAC ARRAY SHOULD CONTAIN THE
    REQUIRED ACCURACY FOR THE ITH PARAMETER X(I). EEC IS THE
    INITIAL STEP-LENGTH FACTOR. BAC(I)*EEC GIVES THE ITH STEP.
    * * * * *
L5: CALL P300(AG,NX,NX,-1,ITER,1,G,X,H,FM,F,I);
    IF LP=1 THEN DO;          ITER=ITER/5;
    CALL P300(AG,NX,NX,-1,ITER,1,G,X,H,FM,F,I);
    END;
    /* * * * * *
    /*
    /* FCR P301 REPLACE CALL STATEMENTS BY:
L5: CALL P301(AG,NX,NX,-1,ITER,1,G,X,H,RES1,RES2,RES3);
    /*
    /* FCR P303 REPLACE CALL STATEMENTS BY:
L5: CALL P303(AG,NX,-1,ITER,EEC,1,1,X,BAC,FF,0,I);
    * * * * *
    /*
    PUT PAGE EDIT(NAME)(X(20),A);
    PUT EDIT('OPTIMUM VARIABLE VALUES')(SKIP(2),A);
    PUT SKIP;
    PUT EDIT((X(J) CO J=1 TO NX))(F(15,5));
    PUT SKIP(8);
    CALL AG(NX,MX,G,X,H,F);
    PUT EDIT('BODY COORDINATES AT OPTIMUM')(A); PUT SKIP;
    PUT EDIT((XA(J) CO J=1 TO MX))(F(15,5)); PUT SKIP(5);
    PUT EDIT('REGIONAL','DENSITY CONTRAST')(SKIP(2),X(10),A,
    X(15),A);
    PUT EDIT(REG,RHO)(SKIP,X(10),F(12,5),X(10),F(8,4));
    PUT EDIT('COMPARISON OF ANOMALIES AT OPTIMUM')(SKIP(3),A);
    PUT EDIT('XS','OBS','AN','RESIDUAL')(SKIP,X(6),A,
    X(10),A,X(10),A,X(9),A);
    DO K=1 TC NSTA;
    RESIDL(K)=OBS(K)-(AN(K)+REG);
    PUT EDIT(XS(K),OBS(K),AN(K),RESIDL(K))(SKIP,4 F(12,2));
    END;
    PUT EDIT('OPTIMUM FUNCTION VALUE',F,'NUMBER OF ITERATIONS PER
    VARIABLE',ITER)(SKIP,A,E(23,5),SKIP,A,F(8));
    IF LMG=0 THEN GO TO FIN;
    IF LMG=9 THEN GET DATA;
    II=II+1;
    PUT PAGE;
    GET LIST(LMG);
    IF LMG=1 THEN GO TO L1; ELSE IF LMG=2 THEN GO TO L2;
    IF LMG=3 THEN GO TO L3; ELSE IF LMG=4 THEN GO TO L4;
    ELSE IF LMG=5 THEN GO TO L5; ELSE GO TO FIN;
    /* * * * * *
    /*
    /* AUXILIARY PART
    /*
    /* * * * * *
AG: PROC(N,M,GG,XX,HH,R);

```



```

GREGNCP:PROC OPTIONS (MAIN); /* M.AL-CHALABI MARCH 1969 */
ON ENDFILE(SYSIN) GO TO FIN;
DCL NAME CHARACTER(80);
DCL (NSTA,NX,MX,MSIDE)FIXED BIN;
DCL II FIXED BIN INITIAL(0);
L1:GET LIST(NAME);
GET LIST(NSTA,NX,MX);
MSIDE=MX-3;
PUT PAGE EDIT(NAME)(X(30),A);
PUT EDIT('THERE ARE',NSTA,'OBSERVATION POINTS,',NX,
'UNKNOWNS AND',MX,'COORDINATE PARAMETERS')(SKIP(4),A,
3(F(3),X(1),A));
BEGIN;
DCL((G,X,H)(NX),FM,F)FLOAT(16),I FIXED BIN,
P3CC ENTRY(ENTRY,FIXED BIN,FIXED BIN,FIXED BIN,FIXED BIN,
FIXED BIN,(*)FLOAT(16),(*)FLCAT(16),(*)FLOAT(16),FLCAT(16),
FLOAT(16),FIXED BIN)EXT,AG ENTRY(FIXED BIN,FIXED BIN,
(*)FLCAT(16),(*)FLCAT(16),(*)FLCAT(16),FLOAT(16));
DCL((XS,OBS,AN,AR,RESIDL,WTF)(NSTA),XA(MX),RHO,REG,SC,GSC,
SOBS,SAQ,SOA)FLOAT(16),(ITER,ZAZA,LP,WT)FIXED BIN;
DCL(V,Y,Z,T,FI1,FI2,R1,R2,HA,W,(S,C)(MSIDE))FLOAT(16);
DCL ZS(1:NSTA)FLCAT(16) INITIAL((NSTA)0);
DCL LMG FIXED BIN INITIAL(C);
SC=1; ITER=200; ZAZA=0; LP=0; WT=0;
L2:GET DATA;
GSC=2*6.667*SC;
IF WT=1 THEN GET COPY LIST(WTF);
IF ZAZA=1 THEN DO;
GET LIST(ZS); PUT LIST(ZS);
END;
L3:GET LIST(XS,OBS);
L4:GET LIST(G,X,H);
PUT SKIP(2);
DO I=1 TO NX; PUT EDIT(G(I),X(I),H(I))(SKIP,3 F(15,5));END;
PUT SKIP(2);
SOBS=SUM(OBS);
L5:CALL P300(AG,NX,NX,-1,ITER,1,G,X,H,FM,F,I);
IF LP=1 THEN DO; ITER=ITER/5;
CALL P3CC(AG,NX,NX,-1,ITER,1,G,X,H,FM,F,I);
END;
PUT PAGE EDIT(NAME)(X(20),A);
PUT EDIT('OPTIMUM VARIABLE VALUES')(SKIP(2),A);
PUT SKIP;
PUT EDIT((X(J) DO J=1 TO NX))(F(15,5));
PUT SKIP(5);
CALL AG(NX,NX,G,X,H,F);
PUT EDIT('OPTIMUM BODY COORDINATES')(SKIP,X(5),A,SKIP);
PUT SKIP;
PUT EDIT((XA(K) DO K=1 TO MX))(F(15,5));
PUT SKIP(5);
PUT EDIT('REGIONAL','DENSITY CONTRAST')(SKIP(2),X(10),A,
X(15),A);
PUT EDIT(REG,RHO)(SKIP,X(10),F(12,5),X(10),F(8,4));
PUT EDIT('COMPARISON OF ANOMALIES AT OPTIMUM')(SKIP(3),A);
PUT EDIT('XS','OBS','AN','RESIDUAL')(SKIP,X(6),A,
X(10),A,X(10),A,X(9),A);

```



```

GRAVOP:PROC OPTICNS (MAIN); /* M.AL-CHALABI FEB.1969 */
ON ENDFILE(SYSIN) GO TO FIN;
DCL NAME CHARACTER(80);
DCL (NSTA,NX,MX,MSIDE)FIXED BIN;
DCL II FIXED BIN INITIAL(0);
L1:GET LIST(NAME);
GET LIST(NSTA,NX,MX);
MSIDE=MX-3;
PUT PAGE EDIT(NAME)(X(30),A);
PUT EDIT('THERE ARE',NSTA,'OBSERVATION POINTS,',NX,
'UNKNCWNS AND',MX,'CCORDINATE PARAMETERS')(SKIP(4),A,
3(F(3),X(1),A));
BEGIN;
DCL((G,X,H)(NX),FM,F)FLCAT(16),I FIXED BIN,
P3CC ENTRY(ENTRY,FIXED BIN,FIXED BIN,FIXED BIN,FIXED BIN,
FIXED BIN,(*)FLOAT(16),(*)FLOAT(16),(*)FLOAT(16),FLOAT(16),
FLCAT(16),FIXED BIN)EXT,AG ENTRY(FIXED BIN,FIXED BIN,
(*)FLOAT(16),(*)FLOAT(16),(*)FLCAT(16),FLOAT(16));
DCL((XS,OBS,AN,AR,RESIDL,WTF)(NSTA),XA(MX),RHO,REG,SC,GSC,
SAR,SOBS,SAQ,SOA)FLOAT(16),(ITER,ZAZA,LP,WT)FIXED BIN;
DCL(V,Y,Z,T,FI1,FI2,R1,R2,HA,W,(S,C)(MSIDE))FLOAT(16);
DCL ZS(1:NSTA)FLOAT(16) INITIAL((NSTA)0);
DCL LMC FIXED BIN INITIAL(0);
SC=1; ITER=200; ZAZA,LP,WT=0;
L2:GET DATA;
GSC=2*6.667*SC;
IF WT=1 THEN GET COPY LIST(WTF);
IF ZAZA=1 THEN DO;
GET LIST(ZS); PUT LIST(ZS);
END;
L3:GET LIST(XS,GBS);
L4:GET LIST(G,X,H);
PUT SKIP(2);
DO I=1 TO NX;
PUT EDIT(G(I),X(I),H(I))(SKIP,3 F(15,5)); END;
PUT SKIP(2);
SOBS=SUM(OBS);
L5:CALL P300(AG,NX,NX,-1,ITER,1,G,X,H,FM,F,I);
IF LP=1 THEN DO; ITER=ITER/5;
CALL P300(AG,NX,NX,-1,ITER,1,G,X,H,FM,F,I);
END;
PUT PAGE EDIT(NAME)(X(20),A);
PUT EDIT('OPTIMUM VARIABLE VALUES')(SKIP(2),A);
PUT SKIP;
PUT EDIT((X(J) DC J=1 TO NX))(F(15,5));
PUT SKIP(5);
CALL AG(NX,MX,G,X,H,F);
PUT EDIT('BCDY CCCORDINATES AT OPTIMUM')(X(15),A);
PUT SKIP;PUT EDIT((XA(J) DO J=1 TO MX))(F(15,5));
PUT SKIP(5);
PUT EDIT('REGIONAL','DENSITY CCNTRAST')(SKIP(2),X(10),A,
X(15),A);
PUT EDIT(REG,RHO)(SKIP,X(10),F(12,5),X(10),F(8,4));
PUT EDIT('COMPARISON OF ANOMALIES AT OPTIMUM')(SKIP(3),A);
PUT EDIT('XS','GBS','AN','RESICUAL')(SKIP,X(6),A,
X(10),A,X(10),A,X(9),A);

```





```

GRATIOP:PROC OPTIONS (MAIN); /* M.AL-CHALABI FEB.1969 */
CN ENDFILE(SYSIN) GO TO FIN;
DCL NAME CHARACTER(80);
DCL (NSTA,NX,MX,MSIDE,MSTA)FIXED BIN;
DCL II FIXED BIN INITIAL(0);
L1:GET LIST(NAME);
GET LIST(NSTA,NX,MX);
MSIDE=MX-3; MSTA=(NSTA/2)+1;
PUT PAGE EDIT(NAME)(X(30),A);
PUT EDIT('THERE ARE',NSTA,'OBSERVATION POINTS,',NX,
'UNKNOWN AND',MX,'COORDINATE PARAMETERS')(SKIP(4),A,
3(F(3),X(1),A));
BEGIN;
DCL((G,X,H)(NX),FM,F)FLOAT(16),I FIXED BIN,
P300 ENTRY(ENTRY,FIXED BIN,FIXED BIN,FIXED BIN,FIXED BIN,
FIXED BIN,*)FLCAT(16),(*)FLCAT(16),(*)FLOAT(16),FLOAT(16),
FLOAT(16),FIXED BIN)EXT,AG ENTRY(FIXED BIN,FIXED BIN,
(*)FLCAT(16),(*)FLOAT(16),(*)FLOAT(16),FLOAT(16));
DCL((XS,OBS,AN,AR,RESIDL,RCB,RAN,WTF)(NSTA),XA(MX),RHO,RR,
REG,SC,GSC,SAR,SOBS)FLOAT(16),(ITER,ZAZA,LP,WT)FIXED BIN;
DCL(V,Y,Z,T,FI1,FI2,R1,R2,HA,W,(S,C)(MSIDE))FLOAT(16);
DCL ZS(1:NSTA)FLCAT(16) INITIAL((NSTA)0);
DCL LMG FIXED BIN INITIAL(0);
SC=1; ITER=200; ZAZA,LP,WT=0;
L2:GET DATA;
GSC=2*6.667*SC;
IF WT=1 THEN GET COPY LIST(WTF);
IF ZAZA=1 THEN DO;
GET LIST(ZS); PUT LIST(ZS);
END;
L3:GET LIST(XS,OBS);
L4:GET LIST(G,X,H);
PUT SKIP(2);
DO I=1 TO NX; PUT EDIT(G(I),X(I),H(I))(SKIP,3 F(15,5));END;
PUT SKIP(2);
SOBS=SLM(OBS);
L5:CALL P300(AG,NX,NX,-1,ITER,1,G,X,H,FM,F,I);
IF LP=1 THEN DO; ITER=ITER/5;
CALL P300(AG,NX,NX,-1,ITER,1,G,X,H,FM,F,I);
END;
PUT PAGE EDIT(NAME)(X(20),A);
PUT EDIT('OPTIMUM VARIABLE VALUES')(SKIP(2),A);
PUT SKIP;
PUT EDIT((X(J) DO J=1 TO NX))(F(15,5));
PUT SKIP(5);
CALL AG(NX,NX,G,X,H,F);
PUT EDIT('OPTIMUM BODY COORDINATES')(SKIP,X(5),A,SKIP);
PUT SKIP;
PUT EDIT((XA(K) DO K=1 TO MX))(F(15,5));
PUT SKIP(5);
SAR=SUM(AR);
RHO=(SCBS-REG*NSTA)/SAR;
PUT EDIT('REGIONAL','DENSITY CONTRAST')(SKIP(2),X(10),A,
X(15),A);
PUT EDIT(REG,RHO)(SKIP,X(10),F(12,5),X(10),F(8,4));
PUT EDIT('COMPARISON OF ANOMALIES AT OPTIMUM')(SKIP(3),A);

```



Specification No. 4.Title: GADPurpose: As in specification No. 3a.

Use: The programme is most suitable for problems in which the regional background and the density contrast are specified but can handle either or both of them as variable parameters. It may be modified to accept  $m$  density contrasts ( $m \leq$  number of sides) all of which must be specified.

Description: The programme is specifically constructed for use in conjunction with Davidon's procedure, P306 (Fletcher and Powell, 1963). Expressions for the first order partial derivatives of the objective function with respect to the variable parameters are provided in the auxiliary procedure. These derivatives are allocated to the appropriate variable parameters in the gradient definition part of the auxiliary procedure. The example given in the print out defines an 8-sided polygon (18 coordinate parameters) with five specified coordinate parameters.

The remaining details are similar to specification No. 3a.

Input data: The data are input in the following order:

<u>data</u>	<u>notes</u>
'NAME'	3.1
nsta nx mx nxa	4.1
data;	4.2
zs	3.5
xs obs	3.6
x opt bac	4.3
lmg	3.8

Data notes:

## 4.1

nsta = Number of observation points

nx = Total number of variable parameters

mx = Total number of coordinates

nxa = Number of variable coordinate parameters.

4.2. The following are integers which may be altered by the GET DATA statement.

sc: As in note 3.3

zaza: As in note 3.3

lmg: As in note 3.3

jd: If set to 1 will cause exploration about the optimum after the termination of the search.

## 4.3.

x = As in note 3.7.

opt = An estimate of the value of the objective function at the optimum.

bac = The required accuracy in each parameter.

0.001 is an adequate order of magnitude.

Model definition: When either or both of rho and reg are required as variable parameters, rho must be defined as the  $(nxa+1)^{th}$  element of xx and reg as the  $nx^{th}$  element of xx.

The remaining details are as in specification No. 3a.

Gradient definition: The gradient is computed in four two-dimensional arrays each of which is mside X nsta large where m side = mx-3. gv and gz define the derivatives with respect to the x and z coordinate parameters of the first corner of the appropriate side while gy and gt define those

of the second corner respectively. Therefore,

$$GV(I,J)$$

represents the derivative with respect to the x coordinate of the first corner of the  $i^{\text{th}}$  side at the  $j^{\text{th}}$  observation point. The sides are numbered 1,3,5,..., mside in an anticlockwise direction.

Each coordinate parameter defining the polygon (except the first and the last corners of an open polygon) is common to at least two sides. gx is an array of nxa elements. The  $k^{\text{th}}$  element denotes the derivative of the objective function with respect to the  $k^{\text{th}}$  coordinate parameter at the  $j^{\text{th}}$  observation point. Its value is obtained by summing up the contribution of all the sides in which the  $k^{\text{th}}$  parameter occurs. lx is an array of nxa elements, which follow the same order as the gx elements. The example given in the print-out illustrates the allocation of the derivatives to the appropriate parameters for the model defined in the first part of the auxiliary procedure.

The derivatives with respect to the density contrast and the regional background are given by

$$GG(NXA+1) \text{ and } GG(NX),$$

respectively. When either or both parameters are specified, the pertinent card(s) is reserved in the space allocated for reserving suspended cards at the end of the auxiliary procedure.

Output: This is similar to specification No. 3a but instead of the lower and upper bounds, the values of opt and bac are printed.

PROC OPTIONS (MAIN); /\* M.AL-CHALABI MAY 1969 \*/

```
GAD:PROC OPTIONS (MAIN); /* M.AL-CHALABI MAY 1969 */
CN ENDFILE(SYSIN) GO TO FIN;
DCL NAME CHARACTER(80);
DCL (NSTA,NX,MX,MSIDE,NXA)FIXED BIN;
DCL II FIXED BIN INITIAL(0);
L1:GET LIST(NAME);
GET LIST(NSTA,NX,MX,NXA);
MSIDE=NX-3;
PUT PAGE EDIT(NAME)(X(30),A);
PUT EDIT('THERE ARE',NSTA,'OBSERVATION POINTS,',NX,
'UNKNOWN AND',MX,'COORDINATE PARAMETERS')(SKIP(4),A,
3(F(3),X(1),A));
BEGIN;
DCL ((X,G)(NX))FLOAT(16);
DCL (GPT,BAC,F)FLOAT(16);
DCL P306 ENTRY(ENTRY,FIXED BIN,FIXED BIN,FIXED BIN,FLOAT(16),
FLOAT(16),FIXED BIN,(*)FLOAT(16),(*)FLOAT(16),FLOAT(16),
FIXED BIN)EXT;
DCL AG ENTRY(FIXED BIN,(*)FLCAT(16),(*)FLOAT(16),FLOAT(16));
DCL ((XS,OBS,AR,AN,RES,RESIDL)(NSTA),XA(MX),(P,S,C)(MSIDE),GN,
GX(NXA),(GV,GY,GZ,GT)(MSIDE,NSTA),RHO,REG,SC,GSC,V,Y,Z,T,FI1,FI2,
PW,R1,R2,FI,W,WM,TW,SW,WW,VV,BW,TR,CW)FLOAT(16);
DCL (DSV,DSY,DSZ,DST,DCV,DCY,DCZ,DCT,DLGV,DLGY,
DLGZ,DLGT,DFIV,DFIY,DFIZ,DFIT,DFI1V,DFI2Y,DFI1Z,DFI2T,
DMV,DMY,DMZ,DMT,CWV,CWY,CWZ,DWT)FLOAT(16);
DCL (JD,JJD,ZAZA)FIXED BIN;
DCL ZS(1:NSTA)FLOAT(16) INITIAL((NSTA)0);
SC=1; ZAZA=0; JD=0;
L2:GET DATA;
GSC=2*6.667*SC;
IF ZAZA=1 THEN DO;
GET LIST(ZS); PUT LIST(ZS);
END;
L3:GET LIST(XS,OBS);
L4:GET LIST(X,GPT,BAC);
PUT EDIT('ESTIMATED FUNCTION VALUE AT OPTIMUM(OPT)',
OPT)(SKIP(2),A,E(12,3));
PUT EDIT('PARAMETER ACCURACY',BAC)(SKIP,A,E(12,3));
/*** IF CHANGE IN EACH PARAMETER IS L.T. BAC SEARCH
WILL TERMINATE *****/
PUT EDIT('INITIAL ESTIMATES')(SKIP,A);
PUT EDIT((X(J) CO J=1 TO NX))(F(15,5));
PUT SKIP(2);
L5:CALL P306(AG,NX,-1,1,OPT,BAC,JD,X,G,F,JJD);
PUT PAGE EDIT(NAME)(X(20),A);
PUT EDIT('OPTIMUM VARIABLE VALUES')(SKIP(2),A);
PUT SKIP;
PUT EDIT((X(J) DO J=1 TO NX))(F(15,5));
PUT SKIP(8);
CALL AG(NX,X,G,F);
PUT EDIT('BODY COORDINATES AT OPTIMUM')(A); PUT SKIP;
PUT EDIT((XA(J) CO J=1 TO MX))(F(15,5)); PUT SKIP(5);
PUT EDIT('REGIONAL','DENSITY CONTRAST')(SKIP(2),X(10),A,
X(15),A);
PUT EDIT(REG,RHO)(SKIP,X(10),F(12,5),X(10),F(8,4));
PUT EDIT('COMPARISON OF ANOMALIES AT OPTIMUM')(SKIP(3),A);
```





```

DSV=-DSY;DSZ=-DST;
CCY=-DCV;DCZ=DSY;DCT=DSV;
DLGV=-V/R1;DLGY=Y/R2;
DLGZ=-Z/R1;DLGT=T/R2;
DFIV=-CLGZ;DFIY=-DLGT;
DFIZ=DLGV;DFIT=CLGY;
DFI1V=-DFIV;DFI2Y=DFIY;
DFI1Z=-DFIZ;DFI2T=DFIT;
DMV=V*CSV+S(I)+Z*DCV;
DMY=V*DSY+Z*DCY;
DMZ=V*DSZ+C(I)+Z*DCZ;
DMT=V*CST+Z*DCT;
DWW=GN*DSV+S(I)*DLGV+FI*CCV+C(I)*DFIV;
DWW=GN*DSY+S(I)*DLGY+FI*DCY+C(I)*DFIY;
DWW=GN*DSZ+S(I)*DLGZ+FI*DCZ+C(I)*DFIZ;
DWT=GN*DST+S(I)*DLGT+FI*DCT+C(I)*DFIT;
GV(I,J)=-Z*DFI1V-W*DMV-DWV*WM;
GY(I,J)=T*DFI2Y-W*DMY-DWY*WM;
GZ(I,J)=-FI1-Z*DFI1Z-W*DMZ-DWZ*WM;
GT(I,J)=FI2+T*DFI2T-W*DMT-DWT*WM;

```

```

END;
END;

```

```

DO J=1 TO NSTA;
AN(J)=GSC*RHO*AR(J);
RES(J)=(OBS(J)-REG-AN(J))*2;
R=R+(0.5*RES(J))**2;
END;
DO K=1 TO NXA; DO J=1 TO NSTA;
GO TO LX(K);

```

```

/*****
/***** GRADIENT DEFINITION PART *****/
/*****

```

```

LX(1):GX(1)=GV(1,J);
GOTO TOT;
LX(2):GX(2)=GZ(1,J)+GT(15,J);
GOTO TOT;
LX(3):GX(3)=GV(3,J)+GY(1,J);
GOTO TOT;
LX(4):GX(4)=GZ(3,J)+GT(1,J);
GOTO TOT;
LX(5):GX(5)=GV(5,J)+GY(3,J);
GOTO TOT;
LX(6):GX(6)=GZ(5,J)+GT(3,J);
GOTO TOT;
LX(7):GX(7)=GZ(7,J)+GT(5,J);
GOTO TOT;
LX(8):GX(8)=GZ(11,J)+GT(9,J);
GOTO TOT;
LX(9):GX(9)=GV(13,J)+GY(11,J);
GOTO TOT;
LX(10):GX(10)=GZ(13,J)+GT(11,J);
GOTO TOT;
LX(11):GX(11)=GV(15,J)+GY(13,J);
GOTO TOT;

```

```
LX(12):GX(12)=GZ(15,J)+GT(13,J);
      GOTO TOT;
LX(13):GX(13)=GY(15,J);
      TOT:GG(K)=GG(K)-RES(J)*GSC*RFO*GX(K);
      END; END;
      GG(NX)=0-SUM(RES);
      /*****
      /*****
      /**** THIS PART IS FOR RESERVING SUSPENDED CARDS *****/
      *****/
      DO J=1 TO NSTA; GG(NXA+1)=GG(NXA+1)-RES(J)*AR(J)*GSC; END;
      *****/
      /*****/
      END AG;
      END; /*END OF BEGIN */
      FIN:END GAD;
```

Specification No. 5aTitle: MANOP

Purpose: This programme progressively modifies the parameters defining a two-dimensional polygonal model in order to minimise the discrepancy between an observed magnetic anomaly and the calculated anomaly due to the model. The resulting parameters define an 'optimum' model.

Use: The programme is most suitable for problems in which the linear parameters are specified but can also handle any or all of them as variable parameters.

Description: The auxiliary procedure AM calculates the anomaly in a manner similar to that of MAGN (specification No. 2, Bott, 1969b) so that the addition of the step-models is carried out in an anticlockwise order. The objective function is calculated according to equation (6.6). All remaining details are similar to specification No. 3a. The print-out shows an example where the second side of the polygon is horizontal and the regional background is  $-12$  gammas. The vertical and horizontal components of the magnetisation contrast vector resolved in the direction of the profile are specified at 200 and 40 in  $(\text{e.m.u./cm}^3) \times 10^5$ .

Input data: The data are input in the following order:

<u>data</u>	<u>notes</u>
'NAME'	3.1
nsta nx mx	3.2
data;	5.1
fi fa	5.2
wtf	3.4
zs	3.5
xs obs	5.3
g x h	3.7
lmg	3.8

Data notes

5.1. The integers which may be altered by the GET DATA statement are the same as those of specification No. 3a except that sc does not exist here.

5.2. fi and fa are the values of the dip and azimuth of the Earth's field, in degrees. The azimuth is measured from the strike towards the positive horizontal axis. The dip is measured from the azimuth direction downwards towards the positive vertical axis.

5.3 xs is an array of nsta elements. The  $i^{\text{th}}$  element denotes the horizontal distance of the  $i^{\text{th}}$  observation point from the origin. The origin is chosen arbitrarily and is retained for reference throughout the problem. The horizontal axis must increase towards a northerly direction, i.e. S-N, SE-NW or SW-NE.

obs is an array of nsta elements. The  $i^{\text{th}}$  element denotes the anomaly value at the  $i^{\text{th}}$  observation point in gammas. The complete xs data list must be input before inputting obs.

Model definition: The coordinate parameters of the polygonal model are defined in the same way as in specification No. 3a. reg, ajs and ajc must be defined in the auxiliary procedure. ajs and ajc denote the vertical and horizontal components of the magnetisation contrast vector resolved into the direction of the profile. They are measured in  $10^5 \times \text{e.m.u./cm}^3$ . If aj denotes the intensity of magnetisation in  $\text{e.m.u./cm}^3$

then

$$ajs = 10^5 \times sj \times \sin bi$$

$$ajc = 10^5 \times sj \times \cos bi \times \sin ba$$

where bi and ba are the dip and azimuth of the magnetisation contrast vector in degrees measured in the same sense as fi and fa. ajs and ajc may be defined by fixed values, variable parameters or any combination of these, e.g.

$$(a) \quad AJS = 120; \quad AJC = XX(NX);$$

$$(b) \quad AJS = 150 * SINDI: (XX(NX));$$

$$AJC = 150. * COSDI: (XX(NX)) * 0.5;$$

etc.

reg denotes the regional background measured in gammas.

Output: The output data list is similar to specification no. 3a except that ajs and ajc are printed instead of the density contrast. The values of fi and fa are also printed.

Specification No. 5b

Title: MREGNOP

Purpose: As in specification no. 5a.

Use: The programme is most suitable for problems in which the regional background is specified and the two components of the magnetisation contrast vector are unspecified. It can also handle the regional background as a variable parameter. Neither of ajs or ajc may appear in the model definition part.

Description: The objective function is calculated according to equation (6.11).

All the remaining details are as in specification no. 5a.

Specification No. 5c

Title: MAGOP

Purpose: As in specification No. 5a.

Use: The programme is only suitable for problems in which the linear parameters are unspecified. None of  $a_{js}$ ,  $a_{jc}$  or  $reg$  may appear in the model definition part.

Description: The objective function is calculated according to equation (6.13).

All the remaining details are as in specification No. 5a.

Specification No. 5d

Title: As in specification No. 5a.

Purpose: As in specification No. 5a.

Use: The programme is most suitable for problems involving more than one magnetisation contrast. Only one magnetisation contrast can be used across each side. Any of the contrasts may be specified or treated as a variable parameter. Two is the maximum recommended number of unspecified magnetisation contrasts.

Description:  $a_{js}$  and  $a_{jc}$  are declared as arrays, each consisting of  $n_{mside}$  elements ( $n_{mside} = mx-3$ ). The  $k^{th}$  element of each array denotes the magnetisation contrast component appropriate to the  $k^{th}$  side. The sides are numbered 1,3,5,...,  $n_{mside}$  in an anticlockwise direction. The numbering of the elements of  $a_{js}$  and  $a_{jc}$  therefore increments from 1 by steps of 2 (see example in the print-out). All of these elements must be defined in the model definition part. The objective function is calculated according to equation (6.14). All the remaining details are as in

OP:PROC OPTIONS (MAIN); /\* M.AL-CHALABI FEB. 1969 \*/

```
MANOP:PROC OPTIGNS (MAIN); /* M.AL-CHALABI FEB. 1969 */
ON ENDFILE(SYSIN) GO TO FIN;
DCL NAME CHARACTER(80);
DCL(NSTA,NX,MX,MSIDE)FIXED BIN;
DCL II FIXED BIN INITIAL(0);
L1:GET LIST(NAME);
GET LIST(NSTA,NX,MX);
MSIDE=MX-3;
PUT PAGE EDIT(NAME)(X(30),A);
PUT EDIT('THERE ARE',NSTA,'OBSERVATION POINTS,',NX,
'UNKNOWNNS AND',MX,'COORDINATE PARAMETERS')(SKIP(4),A,
3(F(3),X(1),A));
BEGIN;
DCL((G,X,H)(NX),FM,F)FLCAT(16),I FIXED BIN,
P3CC ENTRY(ENTRY,FIXED BIN,FIXED BIN,FIXED BIN,FIXED BIN,
FIXED BIN,(*)FLOAT(16),(*)FLOAT(16),(*)FLOAT(16),FLOAT(16),
FLOAT(16),FIXED BIN)EXT,AM ENTRY(FIXED BIN,FIXED BIN,
(*)FLOAT(16),(*)FLOAT(16),(*)FLCAT(16),FLOAT(16));
DCL((XS,OBS,AN,RESIDL,WTF)(NSTA),XA(MX),(S,C)(MSIDE),PXE,PZE,
HA,REG,AJS,AJC,EA,EB,V,Y,Z,T,R1,R2,AB,AD,UP,UN,ANG,GN,
E1,E2)FLOAT(16),
(FI,FA)FIXED DECIMAL,(ITER,ZAZA,LP,WT)FIXED BIN;
DCL LMG FIXED BIN INITIAL(0);
DCL ZS(1:NSTA)FLCAT(16) INITIAL((NSTA)0);
ITER=200; ZAZA,LP,WT=0;
L2:GET DATA;
GET LIST(FI,FA); PUT EDIT('FIELD DIP & AZIMUTH',
FI,FA)(SKIP,A,X(2),2 F(6,1));
IF WT=1 THEN GET COPY LIST(WTF);
IF ZAZA=1 THEN DO;
GET LIST(ZS); PUT LIST(ZS);
END;
L3:GET LIST(XS,OBS);
L4:GET LIST(G,X,H);
PUT SKIP(2);
DO I=1 TO NX; PUT EDIT(G(I),X(I),H(I))(SKIP,3 F(15,5));END;
PUT SKIP(2);
PXE=COSD(FI)*SIND(FA); PZE=SIND(FI);
L5:CALL P300(AM,NX,NX,-1,ITER,1,G,X,H,FM,F,I);
IF LP=1 THEN DO; ITER=ITER/5;
CALL P300(AM,NX,NX,-1,ITER,1,G,X,H,FM,F,I);
END;
PUT PAGE EDIT(NAME)(X(20),A);
PUT EDIT('OPTIMUM VARIABLE VALUES')(SKIP(2),A);
PUT SKIP;
PUT EDIT((X(J) DO J=1 TO NX))(F(15,5));
PUT EDIT('BCDY COORDINATES')(SKIP(2),A); PUT SKIP(2);
CALL AM(NX,NX,G,X,H,F);
PUT EDIT((XA(K) DO K=1 TO MX))(F(15,5)); PUT SKIP(2);
PUT EDIT('JS','JC','REGIONAL')(SKIP(2),3(X(10),A));
PUT EDIT(AJS,AJC,REG)(SKIP,3(F(12,3)));
PUT EDIT('COMPARISON OF ANOMALIES AT OPTIMUM')(SKIP(3),A);
PUT EDIT('XS','OBS','AN','RESIDUAL')(SKIP,X(6),A,
X(10),A,X(10),A,X(9),A);
DO K=1 TO NSTA;
RESIDL(K)=OBS(K)-(AN(K)+REG);
```

```

PUT EDIT(XS(K),OBS(K),AN(K),RESIDL(K))(SKIP,4 F(12,2));
END;
PUT EDIT('OPTIMUM FUNCTION VALUE',F,'NUMBER OF ITERATIONS PER
VARIABLE',ITER)(SKIP,A,E(23,5),SKIP,A,F(8));
IF LMG=0 THEN GO TO FIN;
PUT PAGE;
II=II+1;
GET LIST(LMG);
IF LMG=1 THEN GO TO L1;
IF LMG=2 THEN GO TO L2;
IF LMG=3 THEN GET DATA;
IF LMG=3 THEN GO TO L3;
ELSE IF LMG=4 THEN GO TO L4;
ELSE IF LMG=5 THEN GO TO L5;
ELSE GO TO FIN;
/* * * * * * * * * * * * * * * * * * * * * * * * * * * */
/*                                                                 */
/*          AUXILIARY PART                                         */
/*                                                                 */
/* * * * * * * * * * * * * * * * * * * * * * * * * * * */
AM:PROC(N,M,GG,XX,HH,R);
DCL(N,M)FIXED BIN,((GG,XX,HH)(*),R)FLOAT(16);
/* * * * * * * * * * * * * * * * * * * * * * * * * * * */
/*          MODEL DEFINITION PART                                  */
/* * * * * * * * * * * * * * * * * * * * * * * * * * * */
XA(1)=XX(1);XA(2)=XX(2);XA(3)=XX(3);XA(4)=XX(4);XA(5)=XX(5);
DO I=7 TO MX; XA(I)=XA(I-1); END;
XA(6)=XA(4);
AJS=200;  AJC=40;  REG=-12;
/*                                                                 */
/* * * * * * * * * * * * * * * * * * * * * * * * * * * */
      DO I=1 BY 2 TO MSIDE;
        HA=SQRT((XA(I)-XA(I+2))**2+(XA(I+1)-XA(I+3))**2);
        C(I)=(XA(I)-XA(I+2))/HA;
        S(I)=(XA(I+3)-XA(I+1))/HA;
      END;
      R=0.00;
      DO J=1 TO NSTA;
AN(J)=0.00;
        DO I=1 BY 2 TO MSIDE;
          IF S(I)~=0 THEN DO;
V=XA(I)-XS(J);
Y=XA(I+2)-XS(J);
Z=XA(I+1)-XS(J);  T=XA(I+3)-XS(J);
R1=V**2+Z**2; R2=Y**2+T**2;
AB=V/Z; AC=Y/T; UP=AB-AC; UN=1+AB*AC; ANG=ATAN(UP,UN);
GN=0.5*LOG(R2/R1);
E1=ANG*S(I)-GN*C(I);
E2=GN*S(I)+ANG*C(I);
EA=2*S(I)*(PXE*E2-PZE*E1);
EB=2*S(I)*(PXE*E1+PZE*E2);
AN(J)=AN(J)+AJS*EA+AJC*EB;
          END;
        END;
      END;
      IF WT=1 THEN DO I=1 TO NSTA;
R=R+((OBS(I)-REG-AN(I))*WTF(I))**2;  END;
      ELSE DO I=1 TO NSTA;
R=R+(OBS(I)-REG-AN(I))**2;
      END;
      END AM;
END; /* END OF BEGIN * * * */
FIN:END MANOP;

```



NOP:PRCC OPTICNS (MAIN); /\* M.AL-CHALABI MARCH 1969 \*/

```
MREGNOP:PROC OPTIONS (MAIN); /* M.AL-CHALABI MARCH 1969 */
ON ENDFILE(SYSIN) GO TO FIN;
DCL NAME CHARACTER(80);
DCL (NSTA,NX,MX,MSIDE)FIXED BIN;
DCL II FIXED BIN INITIAL(0);
L1:GET LIST(NAME);
GET LIST(NSTA,NX,MX);
MSIDE=MX-3;
PUT PAGE EDIT(NAME)(X(30),A);
PUT EDIT('THERE ARE',NSTA,'OBSERVATION POINTS',NX,
'UNKNOWN AND',MX,'COORDINATE PARAMETERS')(SKIP(4),A,
3(F(3),X(1),A));
BEGIN;
DCL((G,X,H)(NX),FM,F)FLOAT(16),I FIXED BIN,
P300 ENTRY(ENTRY,FIXED BIN,FIXED BIN,FIXED BIN,FIXED BIN,
FIXED BIN,(*)FLOAT(16),(*)FLOAT(16),(*)FLOAT(16),FLOAT(16),
FLOAT(16),FIXED BIN)EXT,AM ENTRY(FIXED BIN,FIXED BIN,
(*)FLOAT(16),(*)FLOAT(16),(*)FLOAT(16),FLOAT(16));
DCL((CBS,AN,XS,EA,EB,RESIDL,WTF)(NSTA),PXE,PZE,
ALPHA,BETA,GAMMA,PI,
DELTA,SIGMA,EAS,EBSS,OBSS,AJS,AJC,REG,XA(MX),(S,C)(MSIDE),
HA,V,Y,Z,T,R1,R2,AB,AD,UP,UN,ANG,GN,E1,E2)FLOAT(16),
(FI,FA)FIXED DECIMAL,(ITER,ZAZA,LP,WT)FIXED BIN;
DCL LMG FIXED BIN INITIAL(0);
DCL ZS(1:NSTA)FLOAT(16) INITIAL((NSTA)0);
ITER=200; ZAZA,WT,LP=0;
L2:GET DATA;
GET LIST(FI,FA); PUT EDIT('FIELD DIP & AZIMUTH',
FI,FA)(SKIP,A,X(2),2 F(6,1));
IF WT=1 THEN GET CCPY LIST(WTF);
IF ZAZA=1 THEN DO;
GET LIST(ZS); PUT LIST(ZS);
END;
L3:GET LIST(XS,OBSS);
L4:GET LIST(G,X,H);
PUT SKIP(2);
DO I=1 TO NX; PUT EDIT(G(I),X(I),F(I))(SKIP,3 F(15,5));END;
PUT SKIP(2);
PXE=COSC(FI)*SINC(FA); PZE=SINC(FI);
L5:CALL P300(AM,NX,NX,-1,ITER,1,G,X,H,FM,F,I);
IF LP=1 THEN DO; ITER=ITER/5;
CALL P300(AM,NX,NX,-1,ITER,1,G,X,H,FM,F,I);
END;
PUT PAGE EDIT(NAME)(X(20),A);
PUT EDIT('OPTIMUM VARIABLE VALUES')(SKIP(2),A);
PUT SKIP;
PUT EDIT((X(J) DO J=1 TO NX))(F(15,5));
PUT EDIT('BODY COORDINATES')(SKIP(2),A); PUT SKIP(2);
CALL AM(NX,NX,G,X,H,F);
PUT EDIT((XA(K) DO K=1 TO MX))(F(15,5)); PUT SKIP(2);
PUT EDIT('JS','JC','REGIONAL')(SKIP(2),3(X(10),A));
PUT EDIT(AJS,AJC,REG)(SKIP,3(F(12,3)));
PUT EDIT('COMPARISON OF ANOMALIES AT OPTIMUM')(SKIP(3),A);
PUT EDIT('XS','OBS','AN','RESIDUAL')(SKIP,X(6),A,
X(10),A,X(10),A,X(9),A);
DO K=1 TO NSTA;
```

```

RESIDL(K)=OBS(K)-(AN(K)+REG);
PUT EDIT(XS(K),OBS(K),AN(K),RESIDL(K))(SKIP,4 F(12,2));
END;
PUT EDIT('OPTIMUM FUNCTION VALUE',F,'NUMBER OF ITERATIONS PER
VARIABLE',ITER)(SKIP,A,E(23,5),SKIP,A,F(8));
IF LMG=C THEN GO TO FIN;
PUT PAGE;
II=II+1;
GET LIST(LMG);
IF LMG=1 THEN GO TO L1;
IF LMG=2 THEN GO TO L2;
IF LMG=3 THEN GET DATA;
IF LMG=3 THEN GO TO L3;
ELSE IF LMG=4 THEN GO TO L4;
ELSE IF LMG=5 THEN GOTO L5;
ELSE GO TO FIN;
/* * * * * * * * * * * * * * * * * * * * * * * * * * * */
/*                                                                 */
/*              AUXILIARY PART                                     */
/*                                                                 */
/* * * * * * * * * * * * * * * * * * * * * * * * * * * */
AM:PROC(N,M,GG,XX,HH,R);
DCL(N,M)FIXED BIN,((GG,XX,HH)(*),R)FLOAT(16);
/* * * * * * * * * * * * * * * * * * * * * * * * * * * */
/*              MODEL DEFINITION PART                             */
/* * * * * * * * * * * * * * * * * * * * * * * * * * * */
XA(1)=XX(1);XA(2)=XX(2);XA(3)=XX(3);XA(4)=XX(4);XA(5)=XX(5);
XA(6)=XA(4);
DO I=7 TO MX; XA(I)=XX(I-1); END;
REG=-12;
/*                                                                 */
/* * * * * * * * * * * * * * * * * * * * * * * * * * * */
DO I=1 BY 2 TO MSIDE;
HA=SQRT((XA(I)-XA(I+2))**2+(XA(I+1)-XA(I+3))**2);
S(I)=(XA(I+3)-XA(I+1))/HA;
C(I)=(XA(I)-XA(I+2))/HA;
END;
R,ALPHA,BETA,GAMMA,DELTA,SIGMA=0;
DO J=1 TO NSTA;
EA(J),EB(J)=C;
DO I=1 BY 2 TO MSIDE;
IF S(I)~=0 THEN CO;
V=XA(I)-XS(J);
Y=XA(I+2)-XS(J);
Z=XA(I+1)-ZS(J); T=XA(I+3)-ZS(J);
R1=V**2+Z**2; R2=Y**2+T**2;
AB=V/Z; AD=Y/T; UP=AB-AD; UN=1+AB*AD; ANG=ATAN(UP,UN);
GN=0.5*LOG(R2/R1);
E1=ANG*S(I)-GN*C(I);
E2=GN*S(I)+ANG*C(I);
EA(J)=EA(J)+2*S(I)*(PXE*E2-PZE*E1);
EB(J)=EB(J)+2*S(I)*(PXE*E1+PZE*E2);
END;
END;

```

```
ALPHA=ALPHA+EA(J)*(OBS(J)-REG);
BETA=BETA+EB(J)*(OBS(J)-REG);
GAMMA=GAMMA+EA(J)**2;
DELTA=DELTA+EA(J)*EB(J);
SIGMA=SIGMA+EB(J)**2;
END;
PI=DELTA**2-GAMMA*SIGMA;
AJS=(BETA*DELTA-ALPHA*SIGMA)/PI;
AJC=(ALPHA*DELTA-BETA*GAMMA)/PI;
IF WT=1 THEN DO I=1 TO NSTA;
AN(I)=AJS*EA(I)+AJC*EB(I);
R=R+((OBS(I)-REG-AN(I))*WT(I))**2;
END;
ELSE DO I=1 TO NSTA;
AN(I)=AJS*EA(I)+AJC*EB(I);
R=R+(OBS(I)-REG-AN(I))**2;
END;
END AM;
END; /***** END THE BEGIN BLOCK *****/
FIN:END MREGNOP;
```

P:PROC OPTIONS (MAIN); /\* M.AL-CHALABI FEB. 1969 \*/

```
MAGOP:PROC OPTIONS (MAIN); /* M.AL-CHALABI FEB. 1969 */
ON ENCFILE(SYSIN) GO TO FIN;
DCL NAME CHARACTER(80);
DCL (NSTA,NX,MX,MSIDE)FIXED BIN;
DCL II FIXED BIN INITIAL(0);
L1:GET LIST(NAME);
GET LIST(NSTA,NX,MX);
MSIDE=MX-3;
PUT PAGE EDIT(NAME)(X(30),A);
PUT EDIT('THERE ARE',NSTA,'OBSERVATION POINTS,',NX,
'UNKNOWN AND',MX,'COORDINATE PARAMETERS')(SKIP(4),A,
3(F(3),X(1),A));
BEGIN;
DCL((G,X,H)(NX),FM,F)FLOAT(16),I FIXED BIN,
P300 ENTRY(ENTRY,FIXED BIN,FIXED BIN,FIXED BIN,FIXED BIN,
FIXED BIN,(*)FLOAT(16),(*)FLOAT(16),(*)FLOAT(16),FLOAT(16),
FLOAT(16),FIXED BIN)EXT,AM ENTRY(FIXED BIN,FIXED BIN,
(*)FLOAT(16),(*)FLOAT(16),(*)FLOAT(16),FLOAT(16));
DCL((OBS,AN,XS,EA,EB,RESIDL,WTF)(NSTA),PXE,PZE,
ALPHA,BETA,GAMMA,
DELTA,SIGMA,EAS,EBS,OBSS,AJS,AJC,REG,XA(MX),(S,C)(MSIDE),
XM,XN,ZM,YM,YN,YZ,
HA,V,Y,Z,T,R1,R2,AB,AC,UP,UN,ANG,GN,E1,E2)FLOAT(16),
(FI,FA)FIXED DECIMAL,(ITER,ZAZA,LP,WT)FIXED BIN;
DCL LMG FIXED BIN INITIAL(0);
DCL ZS(1:NSTA)FLOAT(16) INITIAL((NSTA)0);
ITER=200; ZAZA,LP,WT=0;
L2:GET DATA;
GET LIST(FI,FA); PUT EDIT('FIELD DIP & AZIMUTH',
FI,FA)(SKIP,A,X(2),2 F(6,1));
IF WT=1 THEN GET COPY LIST(WTF);
IF ZAZA=1 THEN DO;
GET LIST(ZS); PUT LIST(ZS);
END;
L3:GET LIST(XS,OBS);
L4:GET LIST(G,X,H);
PUT SKIP(2);
DO I=1 TO NX; PUT EDIT(G(I),X(I),H(I))(SKIP,3 F(15,5));END;
PUT SKIP(2);
SOBS=SLM(OBS);
PXE=COSD(FI)*SIND(FA); PZE=SIND(FI);
L5:CALL P300(AM,NX,NX,-1,ITER,1,G,X,H,FM,F,I);
IF LP=1 THEN DO; ITER=ITER/5;
CALL P3CC(AM,NX,NX,-1,ITER,1,G,X,H,FM,F,I);
END;
PUT PAGE EDIT(NAME)(X(20),A);
PUT EDIT('OPTIMUM VARIABLE VALUES')(SKIP(2),A);
PUT SKIP;
PUT EDIT((X(J) DO J=1 TO NX))(F(15,5));
PUT EDIT('BODY COORDINATES')(SKIP(2),A); PUT SKIP(2);
CALL AM(NX,NX,G,X,H,F);
PUT EDIT((XA(K) DO K=1 TO MX))(F(15,5)); PUT SKIP(2);
PUT EDIT('JS','JC','REGIONAL')(SKIP(2),3(X(10),A));
PUT EDIT(AJS,AJC,REG)(SKIP,3(F(12,3)));
PUT EDIT('COMPARISON OF ANOMALIES AT OPTIMUM')(SKIP(3),A);
PUT EDIT('XS','OBS','AN','RESIDUAL')(SKIP,X(6),A,
```

```

X(10),A,X(10),A,X(9),A);
DO K=1 TO NSTA;
RESIDL(K)=OBS(K)-(AN(K)+REG);
PUT EDIT(XS(K),OBS(K),AN(K),RESIDL(K))(SKIP,4 F(12,2));
END;
PUT EDIT('OPTIMUM FUNCTION VALUE',F,'NUMBER OF ITERATIONS PER
VARIABLE',ITER)(SKIP,A,E(23,5),SKIP,A,F(8));
IF LMG=0 THEN GO TO FIN;
PUT PAGE;
II=II+1;
GET LIST(LMG);
IF LMG=1 THEN GO TO L1;
IF LMG=2 THEN GO TO L2;
IF LMG=3 THEN GET DATA;
IF LMG=3 THEN GO TO L3;
ELSE IF LMG=4 THEN GO TO L4;
ELSE IF LMG=5 THEN GOTO L5;
ELSE GO TO FIN;
/* * * * * * * * * * * * * * * * * * * * * * * * * * * * */
/*
/*          >          AUXILIARY PART
/*
/* * * * * * * * * * * * * * * * * * * * * * * * * * * * */
AM:PROC(N,M,GG,XX,HH,R);
DCL(N,M)FIXED BIN,((GG,XX,HH)(*),R)FLOAT(16);
/* * * * * * * * * * * * * * * * * * * * * * * * * * * * */
/*
/*          MODEL DEFINITION PART
/* * * * * * * * * * * * * * * * * * * * * * * * * * * * */
XA(1)=XX(1);XA(2)=XX(2);XA(3)=XX(3);XA(4)=XX(4);XA(5)=XX(5);
XA(6)=XA(4);
DO I=7 TO MX; XA(I)=XX(I-1); END;
/*
/* * * * * * * * * * * * * * * * * * * * * * * * * * * * */
DO I=1 BY 2 TO MSIDE;
HA=SQRT((XA(I)-XA(I+2))**2+(XA(I+1)-XA(I+3))**2);
S(I)=(XA(I+3)-XA(I+1))/HA;
C(I)=(XA(I)-XA(I+2))/HA;
END;
R,ALPHA,BETA,GAMMA,DELTA,SIGMA=0;
DO J=1 TO NSTA;
EA(J),EB(J)=0;
DO I=1 BY 2 TO MSIDE;
IF S(I)~=0 THEN DO;
V=XA(I)-XS(J);
Y=XA(I+2)-XS(J);
Z=XA(I+1)-ZS(J); T=XA(I+3)-ZS(J);
R1=V**2+Z**2; R2=Y**2+T**2;
AB=V/Z; AC=Y/T; UP=AB-AD; UN=1+AB*AD; ANG=ATAN(UP,UN);
GN=0.5*LCC(R2/R1);
E1=ANG*S(I)-GN*C(I);
E2=GN*S(I)+ANG*C(I);
EA(J)=EA(J)+2*S(I)*(PXE*E2-PZE*E1);
EB(J)=EB(J)+2*S(I)*(PXE*E1+PZE*E2);
END;

```

```

END;
ALPHA=ALPHA+EA(J)*OBS(J);
BETA=BETA+EB(J)*CBS(J);
GAMMA=GAMMA+EA(J)**2;
DELTA=DELTA+EA(J)*EB(J);
SIGMA=SIGMA+EB(J)**2;
END;
EAS=SUM(EA); EBS=SUM(EB);
XM=NSTA*ALPHA-SOBS*EAS; XN=NSTA*BETA-SOBS*EBS;
ZM=NSTA*DELTA-EAS*EBS; YM=NSTA*GAMMA-EAS**2;
YN=NSTA*SIGMA-EBS**2;
YZ=YM*YN-ZM**2;
AJS=(XM*YN-XN*ZM)/YZ;
AJC=(XN*YM-XM*ZM)/YZ;
REG=(SOBS-AJS*EAS-AJC*EBS)/NSTA;
IF WT=1 THEN DO J=1 TO NSTA; AN(J)=AJS*EA(J)+AJC*EB(J);
R=R+((OBS(J)-REG-AN(J))*WTF(J))**2; END;
ELSE DO I=1 TO NSTA; AN(I)=AJS*EA(I)+AJC*EB(I);
R=R+(OBS(I)-REG-AN(I))**2; END;
END AM;
END; /* END OF BEGIN * * * */
FIN:ENC MAGOP;

```

```

MULTIJ:PROC OPTIONS(MAIN);          /* M.AL-CHALABI JULY 1969 */
CN ENDFILE(SYSIN) GO TO FIN;
DCL NAME CHARACTER(80);
CCL(NSTA,NX,MX,MSIDE)FIXED BIN;
DCL II FIXED BIN INITIAL(0);
L1:GET LIST(NAME);
GET LIST(NSTA,NX,MX);
MSIDE=MX-3;
PUT PAGE EDIT(NAME)(X(30),A);
PUT EDIT('THERE ARE',NSTA,'OBSERVATION POINTS',NX,
'UNKNOWN AND',MX,'COORDINATE PARAMETERS')(SKIP(4),A,
3(F(3),X(1),A));
BEGIN;
DCL((G,X,H)(NX),FM,F)FLOAT(16),I FIXED BIN,
P300 ENTRY(ENTRY,FIXED BIN,FIXED BIN,FIXED BIN,FIXED BIN,
FIXED BIN,*)FLCAT(16),(*)FLCAT(16),(*)FLOAT(16),FLOAT(16),
FLOAT(16),FIXED BIN)EXT,AM ENTRY(FIXED BIN,FIXED BIN,
(*)FLCAT(16),(*)FLOAT(16),(*)FLOAT(16),FLOAT(16));
DCL((XS,ORS,AN,RESIDL,WTF)(NSTA),XA(MX),
(S,C,AJS,AJC)(MSIDE),
HA,REG,PXE,PZE,EA,EB,V,Y,Z,T,R1,R2,AB,AD,UP,UN,ANG,GN,
E1,E2)FLOAT(16),
(FI,FA)FIXED DECIMAL,(ITER,ZAZA,LP,WT)FIXED BIN;
DCL LMG FIXED BIN INITIAL(0);
CCL ZS(1:NSTA)FLOAT(16) INITIAL((NSTA)0);
ITER=200; ZAZA,LP,WT=0;
L2:GET DATA;
GET LIST(FI,FA); PUT EDIT('FIELD DIP & AZIMUTH',
FI,FA)(SKIP,A,X(2),2 F(6,1));
IF WT=1 THEN GET COPY LIST(WTF);
IF ZAZA=1 THEN DO;
GET LIST(ZS); PUT LIST(ZS);
END;
L3:GET LIST(XS,ORS);
L4:GET LIST(G,X,H);
PUT SKIP(2);
DO I=1 TO NX; PUT EDIT(G(I),X(I),H(I))(SKIP,3 F(15,5));END;
PUT SKIP(2);
PXE=COSEC(FI)*SINC(FA); PZE=SINC(FI);
L5:CALL P300(AM,NX,NX,-1,ITER,1,G,X,H,FM,F,I);
IF LP=1 THEN DO; ITER=ITER/5;
CALL P300(AM,NX,NX,-1,ITER,1,G,X,H,FM,F,I);
END;
PUT PAGE EDIT(NAME)(X(20),A);
PUT EDIT('OPTIMUM VARIABLE VALUES')(SKIP(2),A);
PUT SKIP;
PUT EDIT((X(J) DO J=1 TO NX))(F(15,5));
PUT EDIT('BODY COORDINATES')(SKIP(2),A); PUT SKIP(2);
CALL AM(NX,NX,G,X,H,F);
PUT EDIT((XA(K) DO K=1 TO MX))(F(15,5)); PUT SKIP(2);
PUT EDIT('REGIONAL',REG)(SKIP(2),X(5),A,X(2),F(8,4));
PUT EDIT('COMPARISON OF ANOMALIES AT OPTIMUM')(SKIP(3),A);
PUT EDIT('XS','CBS','AN','RESIDUAL')(SKIP,X(6),A,
X(10),A,X(10),A,X(9),A);
DO K=1 TO NSTA;
RESIDL(K)=ORS(K)-(AN(K)+REG);

```





Specification No. 6.Title: MAGDPurpose: As in specification No. 5a.

Use: The programme is most suitable for problems in which the linear parameters are specified but can also handle any of them as a variable parameter. It may be modified to accept  $m$  magnetisation contrasts ( $m \leq$  number of sides) all of which must be specified

Description: As in specification No. 4.Input data: The data are input in the following order:

<u>data</u>	<u>notes</u>
'NAME'	3.1
nsta, nx, mx, nxa	4.1
data;	6.1
fi fa	5.2
zs	3.5
xs obs	5.3
x opt bac	4.3
lmg	3.8

Data notes:

6.1 The integers which may be altered by the GET DATA statement are the same as in specification No. 4 except that sc does not exist here.

Model definition: The same as in specification No. 5a.

Gradient definition: The principle of defining the derivatives is given in Appendix 3. The procedure has been formulated here on the same bases as in GAD (specification No. 4). The derivative with respect to each coordinate parameter consists of two terms corresponding to P and Q in Appendix 3. Each term is calculated separately resulting in eight two-dimensional arrays, eav, eaz, eay, eat, ebv, ebz, eby, and ebt. The two terms corresponding to the x coordinate of the first point of the  $i^{\text{th}}$  side at the  $j^{\text{th}}$  observation point are

$$EAV(I,J) \quad \text{and} \quad EBV(I,J)$$

and so on. The process of defining the derivatives consists of the same steps as in GAD, each step being repeated to account for the second term. The first term is computed in the array gxa and the second in the array gxb. The definition of each element of these arrays is similar to that of the array gx in GAD. An example is given in the print-out illustrating the definition of these derivatives. All of the coordinate parameters have been treated as variable parameters.

The derivatives with respect to ajs, ajc and reg are respectively given by

$$GG(NXA+1), \quad GG(NXA+2) \quad \text{and} \quad GG(NX).$$

When any of these parameters is specified the pertinent card(s) is reserved in the space allocated for reserving suspended cards the end of the auxiliary procedure.

Output: This is similar to specification No. 5a but instead of the lower and upper bounds, the values of opt and bac are printed

0: PROC OPTIONS (MAIN); /\* M.AL-CHALABI MAY 1969 \*/

```
MAGD:PRCC OPTIONS (MAIN); /* M.AL-CHALABI MAY 1969 */
ON ENDFILE(SYSIN) GO TO FIN;
DCL NAME CHARACTER(80);
DCL(NSTA,NX,MX,MSIDE,NXA)FIXED BIN;
DCL II FIXED BIN INITIAL(0);
L1:GET LIST(NAME);
GET LIST(NSTA,NX,MX,NXA);
MSIDE=MX-3;
PUT PAGE EDIT(NAME)(X(30),A);
PUT EDIT('THERE ARE',NSTA,'OBSERVATION POINTS,',NX,
'UNKNOWNNS AND',MX,'COORDINATE PARAMETERS')(SKIP(4),A,
3(F(3),X(1),A));
BEGIN;
DCL((X,G)(NX))FLCAT(16);
DCL(OPT,BAC,F)FLOAT(16);
DCL P306 ENTRY(ENTRY,FIXED BIN,FIXED BIN,FIXED BIN,FLOAT(16),
FLOAT(16),FIXED BIN,(*)FLCAT(16),(*)FLOAT(16),FLOAT(16),
FIXED BIN)EXT;
DCL AM ENTRY(FIXED BIN,(*)FLOAT(16),(*)FLOAT(16),FLOAT(16));
DCL((XS,CBS,RESICL,RES,AN,SEA,SEB)(NSTA),XA(MX),(P,S,C)(MSIDE),
(EAV,EBV,EAY,EBY,EAZ,EBZ,EAT,EPT)(MSIDE,NSTA),(GXA,GXB)(NXA),
V,Y,Z,T,PXE,PZE,AJC,AJS,R1,R2,AB,AD,UP,UN,ANG,GN,REG,
E1,E2,EA,EB,XI1,XI2)FLOAT(16);
DCL(DSV,DSY,DSZ,DST,DCV,DCY,CCZ,CCT,DLGV,DLGY,DLGZ,DLGT,
DFIV,DFIY,DFIZ,DFIT,DE1V,DE1Y,DE1Z,DE1T,DE2V,DE2Y,DE2Z,DE2T,
CXI1V,CXI1Y,CXI1Z,CXI1T,CXI2V,CXI2Y,CXI2Z,CXI2T)FLOAT(16);
DCL(FI,FA)FIXED DECIMAL,(JD,JJD,ZAZA)FIXED BIN;
DCL ZS(1:NSTA)FLOAT(16) INITIAL((NSTA)0);
CCL LMG FIXED BIN INITIAL(0);
ZAZA=0; JD=0;
L2:GET DATA;
GET LIST(FI,FA); PUT EDIT('FIELD DIP & AZIMUTH',
FI,FA)(SKIP,A,X(2),2 F(6,1));
IF ZAZA=1 THEN DC;
GET LIST(ZS); PUT LIST(ZS);
END;
L3:GET LIST(XS,OBS);
L4:GET LIST(X,CPT,BAC);
PUT EDIT('ESTIMATED FUNCTION VALUE AT OPTIMUM(OPT)',
CPT)(SKIP(2),A,E(12,3));
PUT EDIT('PARAMETER ACCURACY',BAC)(SKIP,A,E(12,3));
/**** IF CHANGE IN EACH PARAMETER IS L.T. BAC SEARCH
WILL TERMINATE *****/
PUT EDIT('INITIAL ESTIMATES')(SKIP,A);
PUT EDIT((X(J) DO J=1 TO NX))(F(15,5));
PUT SKIP(2);
PXE=COSD(FI)*SINC(FA); PZE=SINC(FI);
L5:CALL P306(AM,NX,-1,1,OPT,BAC,JD,X,G,F,JJD);
PUT PAGE EDIT(NAME)(X(20),A);
PUT EDIT('OPTIMUM VARIABLE VALUES')(SKIP(2),A);
PUT SKIP;
PUT EDIT((X(J) DO J=1 TO NX))(F(15,5));
PUT ECIT('BODY COORDINATES')(SKIP(2),A); PUT SKIP(2);
CALL AM(NX,X,G,F);
PUT EDIT((XA(K) DO K=1 TO MX))(F(15,5)); PUT SKIP(2);
PUT EDIT('JS','JC','REGIONAL')(SKIP(2),3(X(10),A));
```



```

SEB(J)=SEB(J)+EB;
DSY=C(I)*S(I)/P(I);
CST=C(I)*C(I)/P(I);
DCV=S(I)*S(I)/P(I);
DSV=-DSY;DSZ=-DST;
DCY=-DCV;DCZ=DSY;DCT=DSV;
CLGV=-V/R1;CLGY=Y/R2;
DLGZ=-Z/R1;DLGT=T/R2;
DFIV=-DLGZ;DFIY=-DLGT;
CFIZ=CLGV;DFIT=DLGY;
DE1V=ANG*DSV+S(I)*CFIV-GN*DCV-C(I)*DLGV;
DE1Y=ANG*DSY+S(I)*DFIY-GN*DCY-C(I)*DLGY;
DE1Z=ANG*DSZ+S(I)*DFIZ-GN*DCZ-C(I)*DLGZ;
DE1T=ANG*DST+S(I)*DFIT-GN*DCT-C(I)*DLGT;
DE2V=GN*DSV+S(I)*DLGV+ANG*DCV+C(I)*DFIV;
DE2Y=GN*DSY+S(I)*DLGY+ANG*DCY+C(I)*DFIY;
DE2Z=GN*DSZ+S(I)*DLGZ+ANG*DCZ+C(I)*DFIZ;
DE2T=GN*DST+S(I)*DLGT+ANG*DCT+C(I)*DFIT;
DXI1V=2*(PXE*DE2V-PZE*DE1V);
CXI1Y=2*(PXE*DE2Y-PZE*DE1Y);
DXI1Z=2*(PXE*DE2Z-PZE*DE1Z);
DXI1T=2*(PXE*DE2T-PZE*DE1T);
DXI2V=2*(PXE*DE1V+PZE*DE2V);
DXI2Y=2*(PXE*DE1Y+PZE*DE2Y);
DXI2Z=2*(PXE*DE1Z+PZE*DE2Z);
DXI2T=2*(PXE*DE1T+PZE*DE2T);
EAV(I,J)=S(I)*DXI1V+XI1*DSV;
EAY(I,J)=S(I)*CXI1Y+XI1*DSY;
EAZ(I,J)=S(I)*DXI1Z+XI1*DSZ;
EAT(I,J)=S(I)*DXI1T+XI1*DST;
EBV(I,J)=S(I)*DXI2V+XI2*DSV;
EBY(I,J)=S(I)*DXI2Y+XI2*DSY;
EBZ(I,J)=S(I)*DXI2Z+XI2*DSZ;
EBT(I,J)=S(I)*DXI2T+XI2*DST;
END;
END;
DO K=1 TO NSTA;
RES(K)=2*(OBS(K)-REG-AN(K));
R=R+(0.5*RES(K))**2;
ENC;
DO K=1 TO NXA;
DO J=1 TO NSTA;
GO TO LX(K);
/*****
/***** GRADIENT DEFINITION PART *****/
/*****
LX(1):GXA(1)=EAV(1,J); GXB(1)=EBV(1,J);
GOTC TCT;
LX(2):GXA(2)=EAZ(1,J); GXB(2)=EBZ(1,J);
GOTO TOT;
LX(3):GXA(3)=EAV(3,J)+EAY(1,J);
GXB(3)=EBV(3,J)+EBY(1,J);
GOTO TOT;
LX(4):GXA(4)=EAZ(3,J)+EAT(1,J); GXB(4)=EBZ(3,J)+EBT(1,J);

```

```

GOTO TOT;
LX(5):GXA(5)=EAV(5,J)+EAY(3,J);    GXB(5)=EBV(5,J)+EBY(3,J);
GOTO TOT;
LX(6):GXA(6)=EAZ(5,J)+EAT(3,J);    GXB(6)=EBZ(5,J)+EBT(3,J);
GOTC TCT;
LX(7):GXA(7)=EAV(7,J)+EAY(5,J);    GXB(7)=EBV(7,J)+EBY(5,J);
GOTO TOT;
LX(8):GXA(8)=EAZ(7,J)+EAT(5,J);    GXB(8)=EBZ(7,J)+EBT(5,J);
GOTO TCT;
LX(9):GXA(9)=EBV(9,J)+EAY(7,J);    GXB(9)=EBV(9,J)+EBY(7,J);
GOTO TOT;
LX(10):GXA(10)=EAZ(9,J)+EAT(7,J);   GXB(10)=EBZ(9,J)+EBT(7,J);
GOTO TOT;
LX(11):GXA(11)=EAV(11,J)+EAY(9,J);  GXB(11)=EBV(11,J)+EBY(9,J);
GOTC TCT;
LX(12):GXA(12)=EAZ(11,J)+EAT(9,J);  GXB(12)=EBZ(11,J)+EBT(9,J);
GOTO TOT;
LX(13):GXA(13)=EAY(11,J);   GXB(13)=EBY(11,J);
GOTO TCT;
LX(14):GXA(14)=EAT(11,J);   GXB(14)=EBT(11,J);
TOT:GG(K)=GG(K)-RES(J)*(AJS*GXA(K)+AJC*GXB(K));
END;  END;
T DO J=1 TO NSTA; GG(NXA+1)=GG(NXA+1)-RES(J)*SEA(J);
GG(NXA+2)=GG(NXA+2)-RES(J)*SEB(J);  END;
/*****
/*****
/**** THIS PART IS FOR RESERVING SUSPENDED CARCS *****/
*****
GO TO TCT;
GO TO TOT;
GG(NX)=0-SUM(RES);
*****
/*****
END AM;
END; /*END OF BEGIN */
FIN:END MAGD;

```

Specification No. 7Title CONFIT

Purpose: This programme uses a set of geographical positions for the pole of rotation for the relative movement between two continental edges and determines the misfit between the two edges when brought in contact by rotating about each pole position. The pole position giving a minimum misfit is determined and a grid is printed out of the values of the misfit at each pole position.

Use: To determine a possible pole of rotation for restoring two continents to their pre-drift relative position.

Description: see section 8.4 in the text.

Input data: The data are input in the following order:

<u>data</u>	<u>notes</u>
nsta msta ns ne ms me	7.1
data;	7.2
ctl cgl	7.3
ct2 cg2	7.4
wtn wtm wt1 wt2	7.5
ft <sub>1</sub> fit fg <sub>1</sub> fig	7.6
'NAME'	3.1
le	7.7

Data notes:

7.1 If we denote the first edge by N and the second edge by M then

nsta = Number of digitised points on edge N.

msta = Number of digitised points on edge M.

ns and ne = All points between the ns<sup>th</sup> point and the ne<sup>th</sup> point on edge N are the active points in the matching process. An equivalent to each of these points is found on edge M by interpolating between any of the msta points.

ms and me define the first and the last active points on edge M.

7.2. The following programme parameters may be altered by the GET DATA statement:

nt = Number of the required latitude intervals for the pole of rotation.

ng = Number of the required longitude intervals for the pole of rotation.

The default value of NT and NG is 30.

saz = If the ratio of the total number of active points to the difference between the number of active points on both edges is smaller than saz a grid of Q, equation (8.4), will not be constructed. The grids of Q<sub>1</sub> and Q<sub>2</sub> will be constructed as usual. The default value is 3.0.

fsn and fsm = For a given position of the pole of rotation it may happen that the j<sup>th</sup> point on edge N does not have an equivalent point on edge M. If the ratio of the number of points on edge N which have an equivalent to



the total number of active points on edge N is less than  $f_{sn}$ , the  $Q_1$  value for that particular pole position will be assigned a very large value ( $10^{20}$ ).  $f_{sm}$  is the corresponding factor on edge M. The default value of both factors is 0.66.

wt = If set to any value different from zero weighting functions will be used (note 7.5). The default value is zero.

mints = If set to 1, the figures after the decimal point in the input latitude and longitude data will be regarded as minutes. Otherwise, they are regarded as decimal fractions of a degree. The default value is 1.

7.3  $ctl$  is an array of  $nsta$  elements. The  $i^{th}$  element denotes the latitude of the  $i^{th}$  point on edge N.  $cgl$  is a similar array with the  $i^{th}$  element denoting the east longitude of the  $i^{th}$  point on edge N. The data are given in degrees with the decimal point followed by either minutes or decimal fractions of a degree. The data are input in the order:

$CT1(1)$ ,  $CG1(1)$ ,  $CT1(2)$ ,  $CG1(2)$ , etc.

The latitudes vary from  $90^\circ$  to  $-90^\circ$ . The east longitudes vary from  $0^\circ$  to  $360^\circ$ .

7.4  $ct2$  and  $cg2$  are the corresponding arrays on edge M.

7.5.  $wtn$  is an array of  $nsta-1$  elements. The  $k^{th}$  element denotes the weight on the segment between the  $k^{th}$  and the  $k+1^{th}$  points of edge N.  $wtm$  is the corresponding array for the segments on edge M.

$wtl$  is an array of  $ne-ns+1$  elements. The  $j^{th}$  element

denotes the weight on the  $j^{\text{th}}$  active point on edge N.  
 wt2 is the corresponding array for the active points on  
 edge M.

The data are input in the order: all wtn elements,  
 all wtm elements, all wtl elements, all wt2 elements.

$ft_1$  = The latitude value of the first position of the  
 pole of rotation.

fit = The increment by which the latitude is decreased  
 (the co-latitude increased) at each interval of  
 latitude.

$fg_1$  = The east longitude of the first position of the  
 pole of rotation

fig = The increment by which the east longitude is  
 increased at each interval of longitude.

fit and fig are given in degrees and a decimal  
 fraction of a degree.  $ft_1$  and  $fg_1$  are given in degrees with  
 the decimal point followed by either minutes or decimal  
 fractions of a degree according to the option MINTS.  $ft_1$   
 can assume values from  $90^\circ$  to  $-90^\circ$ .  $fg_1$  can assume values  
 from  $0^\circ$  to  $360^\circ$ .

7.7. le is an integer controlling the re-entry into the  
 main programme after all grids have been printed. This  
 allows using the programme for different problems in the  
 same run or for the same problem under different conditions  
 or assumptions.

Output: The output data list consists of

- (1) nsta, msta, ng, nt, ns, ne, ms, me (notes 7.1 and 7.2).
- (2)  $ft_1$ ,  $fg_1$ , fit, fig (note 7.6).

- (3) Latitudes and longitudes of points on first edge.
- (4) Latitudes and longitudes of points on second edge.
- (5) 'NAME'.
- (6) Results of the fit on the first edge. They consist of the pole position giving the least misfit (the 'optimum' pole), the value of  $Q_1$  at that position, the value of  $Q_1$  at the position with the next least misfit and the angle of rotation required to close the continents about the 'optimum' pole.
- (7) A grid of the  $Q_1$  values at each of the assumed pole positions. The values are printed as alphabetic characters (see section 8.4) in ascending order so that a point of value C has a lower  $Q_1$  value than a point of value D. The 'optimum' pole is marked with an asterisk. The alphabetic characters can be converted to absolute values using the assignments in the block labelled MAP.
- (8) The output (6) and (7) is repeated for  $Q_2$  and  $Q$ . If the number of active points on one of the edges is much larger than on the second edge,  $sax$  becomes relatively small and a grid of  $Q$  will not be constructed.
- (9) The rotation angle for each pole position for the grid of  $Q$  is printed in degrees and decimal fractions. If a grid for  $Q$  is not constructed these angles will not be printed.

```

CONFIT:PROC OPTIONS(MAIN);
  ON ENCFILE(SYSIN) GOTO FIN;
  DCL(NSTA,MSTA,NG,NT,NS,NE,MS,ME)FIXED BIN;
  DCL(FIG,FIT,CP,SP,SC,AM,BM,SN,SM,GT,DIF1,DIF2,AK,UP,UN,
  UNP,UPP,UPK,PP,PQ,PQ1,PQ2,Q1,Q2,QA,QB,C1,C2,D1,D2,
  SAZ,FSN,FSM,CSN,CSM)FLOAT(16);
  DCL ZZ(C:23) CHAR(2);
  ZZ(0)='.A'; ZZ(1)='.B'; ZZ(2)='.C'; ZZ(3)='.D'; ZZ(4)='.F';
  ZZ(5)='.G'; ZZ(6)='.H'; ZZ(7)='.J'; ZZ(8)='.K'; ZZ(9)='.L';
  ZZ(10)='.M'; ZZ(11)='.N'; ZZ(12)='.P'; ZZ(13)='.Q'; ZZ(14)='.R';
  ZZ(15)='.S'; ZZ(16)='.T'; ZZ(17)='.U'; ZZ(18)='.V'; ZZ(19)='.W';
  ZZ(20)='.X'; ZZ(21)='.Y'; ZZ(22)='.Z'; ZZ(23)='.E';
L1:GET LIST(NSTA,MSTA,NS,NE,MS,ME);
  NST=NSTA-1; MST=MSTA-1;
  NT,NG=30; SAZ=3; FSN,FSM=0.66; WT=0; MINTS=1; GET DATA;
  /** * * MINTS=1 WHEN LATS & LONGS ARE GIVEN IN DEGS & MINUTES **/
  PUT EDIT(NSTA,MSTA,NG,NT,NS,NE,MS,ME)(SKIP,X(10),
  F(4),F(5),6 F(3));
  SN=NE-NS+1;
  SM=ME-MS+1;
  QT=(SN+SM)/SAZ-ABS(SN-SM);
  CSN=FSN*SN; /* DS.. IS THE LOWER LIMIT FOR *
  DSM=FSM*SM; /* THE NO. OF CORRELATED POINTS *
  BEGIN;
  DCL(FG(NG),(FT,CA,SA)(NT),
  (CG1,CT1,PG1,PT1,CTH1,STH1)(NSTA),(PEG2,PN,F,FX)(NS:NE),
  (CG2,CT2,PG2,PT2,CTH2,STH2)(MSTA),(PEG1,PM,G,GX)(MS:ME),
  (CL1,CL2,CL)(NG,NT),
  (VA1,VA2,VA3,VA)(NG,NT))FLOAT(16),LB(2) LABEL INITIAL(LC,LD),
  CT(NT,NG)CHAR(2),NAME CHAR(80);
  DCL(WTN(NST),WTM(MST),(WT1,WT2,WT3)(NS:NE),(WT4,WT5,WT6)
  (MS:ME))FLOAT(16);
L3:DO I=1 TO NSTA; GET LIST(CT1(I),CG1(I)); END;
L4:DO I=1 TO MSTA; GET LIST(CT2(I),CG2(I)); END;
  IF WT=0 THEN GET LIST(WTN,WTM,WT1,WT2);
  /*READING CCORDS. AND CALC. TRIG. VALUES OF PTS. ON EACH COAST*/
  PUT PAGE;
  PUT EDIT('LATITUDES AND LONGITUDES OF POINTS ON FIRST COAST')
  (X(30),A); PUT SKIP(2);
  DO J=1 TO NSTA;
  PUT EDIT(CT1(J),CG1(J))(SKIP,6(F(15,3)));
  IF MINTS=1 THEN DO; ICT=CT1(J); ICG=CG1(J);
  CT1(J)=90-((CT1(J)-ICT)/0.6+ICT);
  CG1(J)=(CG1(J)-ICG)/0.6+ICG;
  END;
  ELSE CT1(J)=90-CT1(J);
  STH1(J)=SIND(CT1(J));CTH1(J)=CCSC(CT1(J));
  END;
  PUT SKIP;
  PUT EDIT('LATITUDES AND LONGITUDES OF POINTS ON SECOND COAST')
  (X(30),A); PUT SKIP(2);
  DO J=1 TO MSTA;
  PUT EDIT(CT2(J),CG2(J))(SKIP,6(F(15,3)));
  IF MINTS=1 THEN DO; ICT=CT2(J); ICG=CG2(J);
  CT2(J)=90-((CT2(J)-ICT)/0.6+ICT);
  CG2(J)=(CG2(J)-ICG)/0.6+ICG;

```

```

END;
ELSE CT2(J)=90-CT2(J);
STH2(J)=SIND(CT2(J));CTH2(J)=CCSD(CT2(J));
END;
L2:GET LIST(FT(1),FIT,FG(1),FIG);
PUT EDIT ('PCLE POSITICNS:LATS AND LONGS OF FIRST POINT
AND INCREMENTS')(SKIP(4),X(1C),A);
PUT EDIT(FT(1),FG(1),FIT,FIG)(SKIP,4(F(10,2)));
IF MINTS=1 THEN DC; IFT=FT(1);IFG=FG(1);
FT(1)=(FT(1)-IFT)/0.6+IFT;
FG(1)=(FG(1)-IFG)/0.6+IFG;
END;
/*****
/*WORKING OUT POLE POSITIONS AND TRIGON. VALUES */
*****/
GLONG=FG(1);
TLAT=90-FT(1);
DO I=1 TO NG;
AI=I-1;
FG(I)=GLONG+FIG*AI;
IF FG(I)>360 THEN FG(I)=FG(I)-360;
/** TO ALLOW CROSSING ZERO LONGITUDE FROM LARGER ANGLES *****/
END;
DO I=1 TO NT;
AI=I-1;
FT(I)=TLAT+FIT*AI;
IF FT(I)<0 THEN FT(I)=-FT(I);/* TO ALLOW GOING OVER NTH POLE &
DOWN THE OTHER SIDE *****/
CA(I)=CCSD(FT(I)); SA(I)=SINC(FT(I));
END;
/*****
*****/
DO IG=1 TO NG;
DO IT=1 TO NT;
PEG1=800; PEG2=800;
WTA=0; WTB=0;
ASN=SN; ASM=SM;
/*****
/****** CONVERSION TO NEW POLE *****/
*****/
DO IA=1 TO NSTA;
PP=CG1(IA)-FG(IG); IF PP<0 THEN PP=PP+360;
CP=CCSD(PP); SP=SIND(PP);
SC=CP*STH1(IA);
AK=CTH1(IA)*CA(IT)+SC*SA(IT);
UP=STH1(IA)*SP; UN=SC*CA(IT)-CTH1(IA)*SA(IT);
IF UN=C THEN UN=1E-20;
IF AK=0 THEN AK=1E-15;
UNP=UP/UN;
PG1(IA)=ATAND(UNP);
PG1(IA)=PG1(IA)+180*((PG1(IA)<0)+(SP<0)+((PG1(IA)=0)*(FT(IT)>
CT1(IA)))); /**PLACING ANGLE AT CORRECT QUADRANT *****/
UPP=SQRT(1-AK**2); UPK=UPP/AK;
PT1(IA)=ATAND(UPK);

```

PRCC OPTIONS(MAIN);

```
IF PT1(IA)<C THEN PT1(IA)=PT1(IA)+180;
ENC;
CO IB=1 TO MSTA;
PP=CG2(IB)-FG(IG); IF PP<0 THEN PP=PP+360;
CP=COSD(PP); SP=SIND(PP);
SC=CP*STH2(IB);
AK=CTH2(IB)*CA(IT)+SC*SA(IT);
UP=STH2(IB)*SP; UN=SC*CA(IT)-CTH2(IB)*SA(IT);
IF UN=0 THEN UN=1E-20;
IF AK=0 THEN AK=1E-15;
UNP=UP/UN;
PG2(IB)=ATAN(UNP);
PG2(IB)=PG2(IB)+180*((PG2(IB)<0)+(SP<0)+((PG2(IB)=0)*(FT(IT)>
CT2(IB)))));
UPP=SQRT(1-AK**2); UPK=UPP/AK;
PT2(IB)=ATANC(UPK);
IF PT2(IB)<0 THEN PT2(IB)=PT2(IB)+180;
END;
```

```
/*
**** FINDING EQUIVALENT AND CALCULATING ITS LONG. ****
*/
```

```
K=0;
CO I=NS TO NE;
JM=MSTA-K-1;
DO J=1 TO JM;
JK=J+K;
DIF1=PT1(I)-PT2(JK); IF DIF1=0 THEN DO;
PEG2(I)=PG2(JK); GOTO LA; END;
DIF2=PT1(I)-PT2(JK+1); IF DIF2=C THEN DO;
PEG2(I)=PG2(JK+1);GOTO LA; END;
T=-DIF1/DIF2; IF T>0 THEN CC;
A=PG2(JK); B=PG2(JK+1);
IF A<90 THEN IF B>270 THEN A=A+360;
ELSE IF B<90 THEN IF A>270 THEN B=B+360;
PEG2(I)=(A+B*T)/(T+1); hTA(I)=hTM(JK);
GO TO LA;
END;
END;
IF PEG2(I)=8C0 THEN DO;
PN(I)=0; ASN=ASN-1; IF ASN<DSN THEN GOTO BAL; END;
GOTO AAL;
LA:PN(I)=PG1(I)-PEG2(I);
IF PN(I)<0 THEN PN(I)=PN(I)+360;
K=JK-1;
/*FORMULA WILL NOT WORK IF CCASTS CROSS EACH OTHER,WHICH IS AN
IMPOSSIBLE SITUATION *****/
```

AAL:END;

BAL:K=0;

```
DO I=MS TO ME;
JN=NSTA-K-1;
DO J=1 TO JN;
JK=J+K;
DIF1=PT2(I)-PT1(JK); IF DIF1=0 THEN DO;
PEG1(I)=PG1(JK); GO TO LV; END;
```

```

DIF2=PT2(I)-PT1(JK+1); IF DIF2=0 THEN DO;
PEG1(I)=PG1(JK+1); GC TC LV; ENC;
T=-DIF1/DIF2; IF T>C THEN DC;
A=PG1(JK); B=PG1(JK+1);
IF A<90 THEN IF B>270 THEN A=A+360;
ELSE IF B<90 THEN IF A>270 THEN B=B+360;
PEG1(I)=(A+B*T)/(T+1); WTB(I)=WTN(JK);
GCTC LV;
END;
END;
IF PEG1(I)=800 THEN DO;
PM(I)=0; ASM=ASM-1; IF ASM<DSM THEN GOTO CAL; END;
GOTO CAL;
LV:PM(I)=PG2(I)-PEG1(I);
IF PM(I)<0 THEN PM(I)=PM(I)+360; /* THIS TAKES CARE OF COASTS
WHICH CRSS FROM 1ST TO 4TH QUADRANT OR VISE VERSA */
K=JK-1;
CAL:ENC;
DAL:IF WT=0 THEN DC; DC I=NS TO NE; WTF1(I)=SINC(PT1(I)); END;
DO I=MS TO ME; WTF2(I)=SINC(PT2(I)); END; ENC;
ELSE DO;
DO I=NS TO NE; WTF1(I)=SINC(PT1(I))*WTA(I)*WT1(I); END;
DO I=MS TO ME; WTF2(I)=SINC(PT2(I))*WTB(I)*WT2(I); END; END;
/*****
/****CALCULATING OBJECTIVE FUNCTIONS *****/
/*****
IF ASN<DSN THEN DO; VA1(IG,IT)=1E20; GOTO EAL; ENC;
PQ1=SUM(PN)/ASN;
CL1(IG,IT)=PQ1;
DO L=NS TO NE;
F(L)=((PQ1-PN(L))*(PN(L)~=0))**2*WTF1(L);
END;
Q1=SQRT(SUM(F));
VA1(IG,IT)=Q1/ASN;
EAL:IF ASM<DSM THEN DO; VA2(IG,IT)=1E20; GOTO FAL; END;
PQ2=SUM(PM)/ASM;
CL2(IG,IT)=PQ2;
DO L=MS TO ME;
G(L)=((PQ2-PM(L))*(PM(L)~=0))**2*WTF2(L);
END;
Q2=SQRT(SUM(G));
VA2(IG,IT)=Q2/ASM;
FAL:IF QT>0 THEN DC;
IF(DSN<ASN)&(DSM<ASM) THEN DO;
C1,C1=PQ1; C2,D2=PQ2;
IF C1>C2 THEN C1=360-C1;
ELSE C2=360-C2;
/***** THIS HAS THE EFFECT OF REDUCING MEASUREMENT OF ONE COAST
SAME SENSE & SAME ABSOLUTE VALUE BECAUSE IF PX HAPPENED TO BE -VE
(PX=PN OR PM) THEN FINAL ANGLE IS PX+360 & HENCE 360-(PX+360)=-PX
WHICH IS +VE, I.E. WE ARE MEASURING THE DIFFERENCE IN THE SAME SENSE
BOTH CASES *****/
PQ=(C1+C2)/2;
CL(IG,IT)=PQ;

```

```

IF D1>D2 THEN DO;
CO L=NS TO NE;
FX(L)=((PQ+PN(L)-360)*(PN(L)≠0))*2*WTF1(L);
END;
CO L=MS TO ME;
GX(L)=((PQ-PM(L))*(PM(L)≠0))*2*WTF2(L);
END;
END;
ELSE DO;
DO L=NS TO NE;
FX(L)=((PQ-PN(L))*(PN(L)≠0))*2*WTF1(L);
END;
CO L=MS TO ME;
GX(L)=((PQ+PM(L)-360)*(PM(L)≠0))*2*WTF2(L);
END; END;
QA=SQRT(SUM(FX));
QB=SQRT(SUM(GX));
VA3(IG,IT)=(QA+QB)/(ASN+ASM);
END;
ELSE IF (ASN<DSN)&(ASM<DSM) THEN VA3(IG,IT)=1E20;
ELSE VA3(IG,IT)=VA1(IG,IT)*(DSN<ASN)+VA2(IG,IT)*(DSM<ASM);
/** I.E. VA3=THE FUNCTION OF THE COAST HAVING A SUFFICIENT NUMBER OF
CORRELATING POINTS */
END;
END; END;
GET LIST(NAME); PUT PAGE EDIT(NAME)(X(30),A);
PUT EDIT('FIT ON FIRST EDGE')(SKIP(4),X(45),A);
LK=0;
VA=VA1; GOTO MP;
LC:VA=VA2;
PUT PAGE EDIT('FIT ON SECOND EDGE')(SKIP(4),X(45),A);
GOTO MP;
LD: IF QT>C THEN VA=VA3; ELSE GOTO LL;
PUT PAGE EDIT('COMBINED FIT ON BOTH EDGES')(SKIP(4),X(45),A);
MP:BM=VA(1,1); AM=VA(2,1);
II=1; JJ=1;
DO I=1 TO NG; DO J=1 TO NT;
IF VA(I,J)<BM THEN DC;BM=VA(I,J); II=I; JJ=J; END;
END; END;
PUT SKIP(2);
PUT LIST(II,JJ);
PUT SKIP;
DO I=1 TO NG; DO J=1 TO NT;
IF(VA(I,J)<AM)&(VA(I,J)>BM) THEN AM=VA(I,J);
END; END;
PUT EDIT('OPTIMUM POSITION OF POLE OF ROTATION')(SKIP(3),X(4),A);
PUT EDIT('LONGITUDE',FG(II),'CO-LATITUDE',FT(JJ))(SKIP,X(6),
A,F(6,1),X(4),A,F(6,1));
PUT EDIT('DEGREE OF FIT(BM)',BM)(SKIP(2),X(4),A,E(9,2));
PUT EDIT('DEGREE OF SECOND BEST FIT(AM)',AM)(SKIP,X(4),A,E(9,2));
IF LK=0 THEN
PUT EDIT('LONGITUDE DIFFERENCE',CL1(II,JJ))(SKIP(4),A,F(6,2));
ELSE IF LK=1 THEN

```



```

PUT EDIT('LONGITUDE DIFFERENCE =',CL2(II,JJ))(SKIP(4),A,F(6,2));
ELSE IF LK=2 THEN
PUT EDIT('LONGITUDE DIFFERENCE =',CL(II,JJ))(SKIP(4),A,F(6,2));
/*****
/*****
MAP:DO I=1 TO NG; DC J=1 TO NT;
IF VA(I,J)<AM THEN CT(J,I)='.*';
/**** AM IS THE DEGREE OF SECOND BEST FIT ****/
ELSE IF VA(I,J)=AM THEN CT(J,I)='.0';
ELSE IF VA(I,J)<AM*1.1 THEN CT(J,I)='*E';
ELSE IF VA(I,J)<AM*1.2 THEN CT(J,I)='*G';
ELSE IF VA(I,J)<AM*1.3 THEN CT(J,I)='*H';
ELSE IF VA(I,J)<AM*1.4 THEN CT(J,I)='*P';
ELSE DO;
LAR=2*LCG(VA(I,J)/AM);
IF LAR<24 THEN CT(J,I)=ZZ(LAR); ELSE CT(J,I)='.#';
END;
END; END;
PUT PAGE EDIT(CT)((NG)(A(3)),SKIP(2));
/*****
/*****
LK=LK+1;
IF LK=2 THEN
IF QT>0 THEN DO;
PUT EDIT('ANGLES OF ROTATION FOR ALL Q FITS')(A);
PUT SKIP(3);
DO J=1 TO NT; PUT SKIP(2); DO I=1 TO NG;
PUT EDIT(CL(I,J))(F(6,2));IF I=16 THEN PUT SKIP(2);
END; END;
END;
IF LK>2 THEN GOTO LL;
GOTO LB(LK);
LL:GET LIST(LE); PUT PAGE;
IF LE=1 THEN GOTO L1; ELSE IF LE=2 THEN GOTO L2;
ELSE IF LE=3 THEN GOTO L3; ELSE IF LE=4 THEN GOTO L4;
END;
FIN:END CONFIT;

```

## REFERENCES

- Allan, T.D., 1961. A magnetic survey in the Western English Channel. Q. Jl. geol. Soc. Lond., 117, 157-170.
- Allerton, H. A., 1968. An interpretation of the gravity field of the North Minch. M.Sc. thesis, University of Durham.
- Baranov, V., 1953. Calcul du gradient vertical du champ de gravité ou du champ magnetique mesuré á la surface du sol. Geophys. Prosp., 1, 171.
- Baranov, V., 1957. A new method for interpretation of aeromagnetic maps: Pseudogravimetric anomalies. Geophysics, 22, 359-383.
- Booth, A.D., 1957. Numerical Methods. Butterworths, London.
- Bott, M.H.P., 1960. The use of rapid digital computing methods for direct gravity interpretation of sedimentary basins. Geophys. J. R. astr. Soc., 3, 63-67.
- Bott, M.H.P., 1962. A simple criterion for interpreting negative gravity anomalies. Geophysics, 27, 376-381.
- Bott, M.H.P., 1963. Two methods applicable to computers for evaluating magnetic anomalies due to finite three dimensional bodies. Geophys. Prosp., 11, 292-299.
- Bott, M.H.P., 1965. The deep structure of the Northern Irish Sea - A problem of crustal dynamics. Colston Papers, 17, 179-204. Butterworth, London.
- Bott, M.H.P., 1967a. Geophysical investigation of the Northern Pennine basement rocks. Proc. of the Yorkshire Geol. Soc., 36, 139-168.
- Bott, M.H.P., 1967b. Solution of the linear inverse problem in magnetic interpretation with application to oceanic magnetic anomalies. Geophys. J. R. astr. Soc., 13, 313-323.
- Bott, M.H.P., 1969a. GRAVN. Durham geophysical computer programme specification no. 1.
- Bott, M.H.P., 1969b. MAGN. Durham geophysical computer programme specification no. 2.
- Bott, M.H.P., and Smith, R.A., 1958. The estimation of the limiting depth of gravitating bodies. Geophys. Prosp., 6, 1-10.
- Bott, M.H.P., Smith, R.A., and Stacey, R.A., 1966. Estimation of the direction of magnetisation of a body causing a magnetic anomaly using a pseudo-gravity transformation. Geophysics, 31, 803-811.

- Bott, M.H.P., and Watts, A.B., 1970a. Deep sedimentary basins proved in Shetland-Hebridean continental shelf and margin. *Nature Lond.*, 225, 265-268.
- Bott, M.H.P., and Watts, A.B., 1970b. Deep structure of the continental margin adjacent to the British Isles. In *Geology of the East Atlantic Continental Margin. Symposium, Cambridge* (in press).
- Box, M.J., 1966. A comparison of several current optimisation methods and the use of transformations in constrained problems. *The Computer Journal*, 9, 67-77.
- Box, K.J., Davies, D., and Swann, W.H., 1969. *Non-linear Optimization Techniques. I.C.I. Monograph no. 5.* Oliver and Boyd, Edinburgh and London.
- Bruckshaw, J.M., and Kunaratnam, 1963. The interpretation of magnetic anomalies due to dykes. *Geophys. Prosp.*, 11, 509-522.
- Bullard, E.C., and Cooper, R.I.B., 1948. The determination of the masses necessary to produce a given gravitational field. *Proc. Roy. Soc., A*, 194, 332-347.
- Bullard, E.C., Everett, J.E., and Smith, A.G., 1965. The fit of the continents around the Atlantic. In *A Symposium on Continental Drift. Phil. Trans. Roy. Soc., A*, 258, 41-51.
- Butler, P.F., 1968. The interpretation of magnetic field anomalies over dykes by optimisation procedures. M.Sc. thesis, University of Durham.
- Campey, I.G., and Nicholls, D.G., 1961. Simplex minimisation. Programme specification, I.C.I. Ltd.
- Carroll, C.W., 1961. The created response surface technique for optimizing non-linear restrained systems. *Operations Research*, 9, 169-184.
- Cauchy, A.L., 1847. Méthode Générale pour la resolution des systemes d'equations simultanées. *C.R. Read Sci, Paris*, 25, 536.
- Corbato, E.C., 1965. A least-squares procedure for gravity interpretation. *Geophysics*, 30, 228-233.
- Cordell, L., and Henderson, R.G., 1968. Iterative three-dimensional solution of gravity anomaly data using a digital computer. *Geophysics*, 33, 596-601.
- Craddock, C., Thiel, E.C., and Gross, B., 1963. A gravity investigation of the Precambrian of southeastern Minnesota and western Wisconsin. *J. Geophys. Res.*, 68, 6015-6032.

- Cramer, H., 1946. *Mathematical Methods of Statistics*. Princeton University Press. Princeton.
- Danes, Z.F., 1960. On a successive approximation for interpreting gravity anomalies. *Geophysics*, 25, 1215.
- Davidon, W.C., 1959. Variable metric method for minimization. Argonne National Laboratory, Report no. ANL-5990.
- Davies, D., 1968. The use of Davidon's method in non-linear programming. I.C.I. Ltd., Management Services Report MSDH/68/110.
- Dean, W.C., 1958. Frequency analysis for gravity and magnetic interpretation. *Geophysics*, 23, 97.
- Dietz, R.S., 1961. Continent and ocean basin evolution by spreading of the sea-floor. *Nature Lond.*, 190, 854-857.
- Dobinson, A., 1970. A magnetic survey of the Faroe Bank. Ph.D. thesis, Part II, University of Durham.
- Dorman, J., Ewing, M., and Oliver, J., 1960. Study of shear velocity distribution in the upper mantle by mantle Rayleigh waves. *Bull. Seism. Soc. Am.*, 50, 87-115.
- Dorman, J., and Ewing, M., 1962. Numerical inversion of seismic surface wave dispersion data. *J. Geophys. Res.*, 67, 5227-5241.
- Evjen, H.M., 1936. The place of the vertical gradient in gravitational interpretation. *Geophysics*, 1, 127-136.
- Fleischer, P.E., 1965. Optimisation techniques in system design. In *System Analysis by Digital Computer*, editors F.F. Kuo and J.F. Kaiser. 175-217. Wiley and Sons, London and Sydney.
- Fletcher, R., and Powell, M.J.D., 1963. A rapidly convergent descent method for minimization. *The Computer Journal*, 6, 163-168.
- Fox, P.J., Pitman III, W.C., Shephard, F., 1969. Crustal plates in the central Atlantic: Evidence for at least two poles of rotation. *Science*, 165, 487-489.
- Francheteau, J., and Sclater, J.G., 1969. Palaeomagnetism of the southern continents and plate tectonics. *Earth and Planetary Science Letters*, 6, 93-106.
- Friedman, M., and Savage, L.S., 1947. *Selected Techniques of Statistical Analysis*. McGraw-Hill, New York.
- Gray, S.P., 1963. Standard curves for interpretation of magnetic anomalies over long tabular bodies. *Geophysics*, 28, 161-200.

- Girdler, R.W., 1958. The relationship of the Red Sea to the East African rift system. *Q. Jl. geol. Soc. Lond.*, 114, 79-105.
- Girdler, R.W., and Peter, G., 1960. An example of the importance of natural remanent magnetization in the interpretation of magnetic anomalies. *Geophys. Prosp.*, 8, 474-483.
- Grant, F.S., and West, G.F., 1965. *Interpretation Theory in Applied Geophysics*. McGraw-Hill, New York.
- Harkrider, D.G., and Anderson, D.L., 1962. Computation of surface wave dispersion for multilayered anisotropic media. *Bull. Seism. Soc. Am.*, 52, 321-332.
- Haskell, N.A., 1953. The dispersion of surface waves on multilayer media. *Bull. Seism. Soc. Am.*, 43, 17-34.
- Heiland, C.A., 1940. *Geophysical Exploration*. Prentice-Hall, New York.
- Henderson, R.G., and Wilson, A., 1967. Polar Charts for calculating aeromagnetic anomalies of three-dimensional bodies. In *Mining Geophysics*, Society of Exploration Geophysicists, 554-568.
- Henderson, R.G., and Zeitz, I., 1949a. The upward continuation of anomalies in total intensity fields. *Geophysics*, 14, 517-534.
- Henderson, R.G., and Zeitz, I., 1949b. The computation of second vertical derivatives of geomagnetic fields. *Geophysics*, 14, 508-516.
- Hess, H.H., 1962. History of ocean basins. In *Petrological Studies*, editors A.E.J. Engle, H.L. James and B.L. Leonard, 599-620, Geol. Soc. America, New York.
- Holgate, N., 1969. Palaeozoic and Tertiary transcurrent movements on the Great Glen fault. *Scott. J. Geol.*, 5, 97-130.
- Holmes, A., 1965. *Principles of Physical Geology*. 2nd ed., Nelson and Sons Ltd., London.
- Hooke, R., and Jeeves, T.A., 1961. Direct search solution of numerical and statistical problems. *Jour. Ass. Comp. Mach.*, 8, 212-229.
- Hubbert, M.K., 1948. Line integral method of computing gravity. *Geophysics*, 13, 215-225.
- Hutchinson, R.D., 1958. Magnetic analysis by logarithmic curves. *Geophysics*, 23, 749-769.
- Hutton, M.A., 1970. Ph.D. thesis, University of Durham.

- Isacks, B., Oliver, J., and Sykes, L.R., 1968. Seismology and the new global tectonics. *J. Geophys. Res.*, 73, 5855-5899.
- Johnson, W.W., 1969. A least-squares method of interpreting magnetic anomalies caused by two-dimensional structures. *Geophysics*, 34, 65-74.
- Jung, K., 1953. Some remarks on the interpretation of gravitational and magnetic anomalies. *Geophys. Prosp.*, 1, 29.
- Kennedy, W.Q., 1946. The Great Glen fault. *Q. Jl. geol. Soc. Lond.*, 102, 41-72.
- Klimpel, R.R., 1969. Some recent advances in the use of mathematical optimization in the mineral industries. *Min. Sci. Engng.*, 1, 15-22.
- Koefoed, O., 1968. The application of the kernel function in interpreting geoelectrical resistivity measurements, Gebruder Borntraeger, Berlin and Stuttgart.
- La Compagnie Générale de Géophysique, 1955. Abaque de sondage électrique. *Geophys. Prosp.*, 3, supplement no. 3.
- Langer, R.E., 1933. An inverse problem in differential equations. *Am. Math. Soc. Bull.*, ser. 2, 29, 814-820.
- La Porte, M., 1963. Calcul de la forme d' une structure homogène a partir de son champ gravimétrique. *Geophys. Prosp.*, 11, 276-291.
- Laughton, A.S., 1966. The Gulf of Aden. *Phil. Trans. Roy. Soc., A*, 259, 150-171.
- Laughton, A.S., Whitmarsh, R.B., and Jones, M.T., 1970. The evolution of the Gulf of Aden. *Phil. Trans. Roy. Soc. Lond., A*, 267, 227-266.
- Le Pichon, X., 1968. Sea-floor spreading and continental drift. *J. Geophys. Res.*, 73, 3661-3697.
- Levine, S., 1941. The calculation of gravity anomalies due to bodies of finite extent. *Geophysics*, 6, 180-196.
- Marquandt, D.W., 1963. An algorithm for least-squares estimation of non-linear parameters. *J. Soc. Indust. Appl. Math.*, 11, 431-441.
- McKenzie, D.P., and Parker, R.L., 1967. The north Pacific: An example of tectonics on a sphere. *Nature Lond.*, 216, 1276-1280.
- McKenzie, D.P., Davies, D., and Molnar, P., 1970. Plate tectonics of the Red Sea and East Africa. *Nature Lond.*, 226, 243-248.

- Mooney, H.M., and Wetzel, W.W., 1956. The Potentials About a Point Electrode and Apparent Resistivity Curves for a Two-, Three- and Four-layer Earth. University of Minnesota Press, Mineapolis.
- Mooney, H.M., Orellana, E., Pickett, H., and Tornheim, L., 1966. A resistivity computation method for layered earth models. *Geophysics*, 31, 192-203.
- Morgan, W.J., 1968. Rises, Trenches, great faults and crustal blocks. *J. Geophys. Res.*, 73, 4259.
- Mugele, R.A., 1962. A nonlinear digital optimising program for process control systems. Proc. of Western Joint Computer Conference.
- Nelder, J.A., and Mead, R., 1965. A simplex method for function minimization. *The Computer Journal*, 7, 308-313.
- Nettleton, L.L., 1940. *Geophysical Prospecting for Oil*. McGraw-Hill, New York.
- Parasnis, D.S., 1962. *Principles of Applied Geophysics*. Methuen and Co. Ltd., London.
- Peters, L.J., 1949. The direct approach to magnetic field interpretation and its practical application. *Geophysics*, 14, 290-320.
- Pirson, S.J., 1940. Polar charts for interpreting magnetic anomalies. *A.I.M.E. Trans.*, 138, 173-192.
- Pitman, W.C., and Heirtzler, J.R., 1966. Magnetic anomalies over the Pacific-Antarctic ridge. *Science*, 154, 1164.
- Powell, M.J.D., 1964. An efficient method for finding the minimum of a function of several variables without calculating derivatives. *The Computer Journal*, 7, 155-162.
- Powell, M.J.D., 1968. A survey of numerical methods for unconstrained optimization. S.I.A.M., 1968 National Meeting.
- Press, F., 1968. Density distribution in earth. *Science*, 160, 1218-1221.
- Pringle, J., 1948. *The South of Scotland*. British Regional Geology, H.M. Stationery Office, Edinburgh.
- Raju, C.V., 1968. A seismic study of the Iceland-Faroe ridge. Ph.D. thesis, University of Durham.
- Roberts, S.M., and Lyvers, H.I., 1961. The gradient method in process control. *Ind. Eng. Chem.*, 53, 877-882.

- Rosenbach, O., 1953. A contribution to the computation of the "second Derivative" from gravity data. *Geophysics*, 18, 894.
- Rosenbrock, H.H., 1960. An automatic method for finding the greatest and least value of a function. *The Computer Journal*, 3, 175-184.
- Rosenbrock, H.H., and Storey, C., 1966. *Computational Techniques for Chemical Engineers*. Pergamon Press, Oxford.
- Roy, A., 1962. Ambiguity in geophysical interpretation. *Geophysics*, 27, 90-99.
- Siegert, A.J.F., 1942. A mechanical integrator for the computation of gravity anomalies. *Geophysics*, 7, 354-366.
- Skeels, D.C., 1947. Ambiguity in gravity interpretation. *Geophysics*, 12, 43-56.
- Smith, R.A., 1959. Some depth formulae for local magnetic and gravity anomalies. *Geophys. Prosp.*, 7, 55-63.
- Smith, R.A., 1960. Some formule for interpreting local gravity anomalies. *Geophys. Prosp.*, 8, 607-613.
- Smith, R.A., 1961. A uniqueness theorem concerning gravity fields. *Proc. Camb. Phil. Soc.*, 57, 865-870.
- Spang, H.A., 1962. A review of minimization techniques for non-linear functions. *S.I.A.M. Review*, 4, 343-365.
- Spendley, W., Hext, G.R., and Himsforth, F.R., 1962. Sequential applications of simplex designs in optimization and evolutionary operation. *Technometrics*, 4, 441.
- Sretenskii, L.N., 1954. Concerning the uniqueness of determination of the shape of an attracting body by the value of its external potential. *Dokl. Acad. Nauk SSSR*, 99, 21-22.
- Stacey, R.A., 1965. Computer methods for the interpretation of two-dimensional gravity and magnetic anomalies. Ph.D. thesis, University of Durham.
- Stefanescu, S.S., 1930. Sur la distribution électrique potentielle autour d'une prise de terre ponctuelle dans un terrain a'couches horizontales homogène et isotropes. *Jour. Physique et le Radium*, 1, 132-140.
- Sykes, L.R., 1967. Mechanisms of earthquakes and nature of faulting on the mid-oceanic ridges. *J. Geophys. Res.*, 72, 2131-2153.



- Talwani, M., Worzel, J.L., and Landisman, M., 1959. Rapid gravity computations for two-dimensional bodies with application to the Mendocino submarine fracture zone. *J. Geophys. Res.*, 64, 49-59.
- Talwani, M., and Ewing, M., 1960. Rapid computation of gravitational attraction of three-dimensional bodies of arbitrary shape. *Geophysics*, 25, 203-225.
- Talwani, M., and Heirtzler, J.R., 1964. Computation of magnetic anomalies caused by two dimensional structures of arbitrary shape. In *Computers in the Mineral Industry*, editor G.A. Parks. The School of Earth Sciences, Stanford University.
- Tanner, J.G., 1967. An automated method of gravity interpretation. *Geophys. J. R. astr. Soc.*, 13, 339-347.
- Thomson, W.T., 1950. Transmission of elastic waves through a stratified solid medium. *Jour. Appl. Phys.*, 21, 89.
- Tomado, Y., and Aki, K., 1955. Use of the function  $\sin x/x$  in gravity problems. *Proc. Japan Acad.*, 31, 443-448.
- Vacquier, V., Steenland, N.C., Henderson, R.G., and Zeitz, I., 1951. Interpretation of aeromagnetic maps. Geological Society of America, Memoir 47.
- Van Dam, J.C., 1965. A simple method for the calculation of standard graphs to be used in geoelectrical prospecting. *Geophys. Prosp.*, 13, 37-65.
- Vine, F.J., 1966. Spreading of the ocean floor: New evidence. *Science*, 154, 1405-1415.
- Vine, F.J., and Matthews, D.H., 1963. Magnetic anomalies over oceanic ridges. *Nature Lond.*, 199, 947-949.
- Vosoff, K., 1958. Numerical resistivity analysis: Horizontal layers. *Geophysics*, 23, 536-556.
- Westoll, T.S., 1965. Geological evidence bearing upon continental drift. In *A Symposium on Continental Drift*, *Phil. Trans. Roy. Soc.*, A, 258, 41-51.
- Wilde, D.J., 1964. *Optimum Seeking Methods*. Prentice-Hall, New York.
- Wilde, D.J., and Beightler, C.S., 1967. *Foundations of Optimization*. Prentice-Hall, New York.
- Wilson, J. Tuzo, 1965. A new class of faults and their bearing on continental drift. *Nature*, 207, 343-347.

Wood, C.F., 1962. Recent developments in 'direct search' techniques.  
Westinghouse Research Report 62-159-522-R1.

Young, J.B., and Douglas, A., 1968. A.W.R.E. Report no. 041/68. U.K.A.E.A.

